Downloaded from orbit.dtu.dk on: Dec 17, 2017

Technical University of Denmark

Identification and Quantification of Uncertainties Related to Using Distributed X-band Radar Estimated Precipitation as input in Urban Drainage Models

Pedersen, Lisbeth; Madsen, Henrik; Jensen, Niels Einar

Publication date:
2009

Document Version
Publisher's PDF, also known as Version of record

Link back to DTU Orbit

Citation (APA):
Pedersen, L., Madsen, H., & Jensen, N. E. (2009). Identification and Quantification of Uncertainties Related to Using Distributed X-band Radar Estimated Precipitation as input in Urban Drainage Models. Kgs. Lyngby, Denmark: Technical University of Denmark (DTU). (The PhD is an Industrial PhD and the work has been conducted in a cooperation between DHI Weather Radar Systems, (Chief Engineer, Niels Einar Jensen), and DTU Informatics, the Technical University of Denmark.).

DTU Library
Technical Information Center of Denmark

General rights
Copyright and moral rights for the publications made accessible in the public portal are retained by the authors and/or other copyright owners and it is a condition of accessing publications that users recognise and abide by the legal requirements associated with these rights.

- Users may download and print one copy of any publication from the public portal for the purpose of private study or research.
- You may not further distribute the material or use it for any profit-making activity or commercial gain
- You may freely distribute the URL identifying the publication in the public portal

If you believe that this document breaches copyright please contact us providing details, and we will remove access to the work immediately and investigate your claim.

Identification and Quantification of Uncertainties Related to Using Distributed X-band Radar Estimated Precipitation as input in Urban Drainage Models

Lisbeth Pedersen

Technical University of Denmark
DTU Informatics
Department of Informatics and Mathematical Modelling

DHI
DHI Weather Radar Systems
Department of Urban & Industry

Kongens Lyngby 2009
IMM-PHD-2009-215

DHI
Gustav Wieds Vej 10
DK-8000 Århus C, Denmark
Phone +45 8620 5100
www.dhigroup.com

Technical University of Denmark
Department of Informatics and Mathematical Modelling
Building 321, DK-2800 Lyngby, Denmark
Phone +45 4525 3351
www.imm.dtu.dk

IMM-PhD: ISBN 978-87-643-0534-0
ISSN 0909-3192

Summary

The Local Area Weather Radar (LAWR) is a small scale weather radar providing distributed measurements of rainfall primarily for use as input in hydrological applications. As any other weather radar the LAWR measurement of the rainfall is an indirect measurement since it does not measure the rainfall, but the energy reflected from the raindrops in the atmosphere. As result a calibration from reflectivity to rainfall intensities is required.

This thesis focuses on identifying and estimating uncertainties related to LAWR rainfall estimates. In this connection the calibration procedure is a key element. A LAWR is normally calibrated against a single rain gauge, which is the normal procedure used to calibrate weather radars. Based on a large set of rain gauge data collected during this project, the uncertainties related to assuming a single gauge representative for a whole LAWR pixel are quantified using statistical methods.

Furthermore, the present calibration method is reviewed and a new extended calibration method has been developed and tested resulting in improved rainfall estimates. As part of the calibration analysis a number of elements affecting the LAWR performance were identified and possible improvements suggested.

The LAWR is designed to provide rainfall data, especially for urban drainage applications, and as part of the thesis the integration of LAWR data into the DHI software application MIKE URBAN has been analyzed. The work has resulted in

identification of scaling issues in connection with boundary assignment besides general improved understanding of the benefits and pitfalls in using distributed rainfall data as input to models. In connection with the use of LAWR data in urban drainage context, the potential for using LAWR data for extreme rainfall statistics has been studied revealing interesting new spatial characteristics of extreme rainfall events not earlier observed.

Resume

Local Area Weather Radar (LAWR) er en lokal vejrradar til distribueret måling af nedbør, primært som input til hydrologiske applikationer. LAWR giver en indirekte måling af nedbøren, idet den ikke måler selve nedbøren, men derimod den energi, der reflekteres fra regndråberne i atmosfæren. Derfor er en kalibrering fra reflektivitets værdier til nedbørsintensiteter påkrævet.

Denne afhandling fokusere på at identificere og estimere usikkerheder relateret til nedbørs estimering med LAWR. I forbindelse med estimering af usikkerheder er kalibreringsproceduren et vigtigt element. En LAWR kalibreres normalt med data fra en enkelt regnmåler, som er normalt er fremgangsmåden ved kalibrering af vejrradarer. Baseret på et stort sæt regndata opsamlet i løbet af dette projekt identificeres og kvantificeres ved hjælp af statistiske metoder usikkerhederne relateret til at anvende en enkelt regnmåler og dermed antage målingen er repræsentativ for en hel LAWR pixel.

Den eksisterende kalibreringsmetode er analyseret, og en ny udvidet kalibreringsmetode er udviklet og testet, resulterende i forbedrede nedbørsestimater. Som en del af kalibreringsanalysen blev der identificeret en række elementer, som har indflydelse på kvaliteten af LAWRs nedbørsestimat; hvortil der er fremsat forbedringsforslag.

LAWR er udviklet til at måle nedbør med specielt henblik på urbane applikationer. Som en del af denne afhandling er integrationsprocessen af LAWR data med DHIs software MIKE URBAN blevet testet og analyseret, hvilket har ført til identifikation af problemer i forbindelse med koblingen nedbørs randdata og oplande samt generel bedre forståelse af fordelene og faldgruberne ved at anvende distribueret nedbørsdata som input til urbane afstrømningsmodeller. I forbindelse med anvendelsen af LAWR data i sammenhæng med afstrømningsforhold, er potentialet ved at anvende LAWR til statistik af ekstrem regn blevet undersøgt, hvilket har afsløret interessante ukendte spatiale egenskaber ved ekstremregn-hændelser, som ikke tidligere er observeret.

Preface

This thesis is a part of the fulfillment in completion of the PhD degree in engineering at the Department of Informatics and Mathematical Modelling (IMM) at the Technical University of Denmark (DTU). The PhD is an Industrial PhD and the work has been conducted in a cooperation between DHI and the Technical University of Denmark. The project has been supervised by Professor Henrik Madsen, DTU, and Chief Engineer, Niels Einar Jensen, DHI.

The work was carried out at DHI in Aarhus and at DTU in Lyngby, both Denmark. As part of the project a three months' period was spent with the weather radar group at the Department of Atmospheric and Oceanic at McGill University, Montreal, Canada, under the supervision of Professor Isztar Zawadzki.

The project has been funded by the Danish Ministry for Science, Technology and Innovation through the Industrial PhD program and by DHI.

Århus, February 2009

Lisbeth Pedersen

Papers Included in Thesis

A Lisbeth Pedersen, Niels Einar Jensen, Lasse Engbo Christensen and Henrik Madsen. *Quantification of the Spatial Variability of Rainfall based on a Dense Network of Rain Gaug*es. Submitted to Journal of Atmospheric Research

B Lisbeth Pedersen, Niels Einar Jensen and Henrik Madsen. *Calibration of Local Area Weather Radar – Identifying Significant Factors Affecting the Calibration*. Submitted to Journal of Atmospheric Research

C Lisbeth Pedersen, Niels Einar Jensen and Henrik Madsen. *Estimation of Radar Calibration Uncertainties Related to the Spatial Variability of Rainfall within a Single Radar Pixel - Statistical Analysis of Rainfall Data from a Dense Network of Rain Gauges*. Proceedings of World Environmental & Water Resources Congress 2008 (EWRI 2008), May 12-16, 2008, Honolulu, Hawaii.

D Lisbeth Pedersen, Niels Einar Jensen and Henrik Madsen. *Application of Local Area Weather Radar (LAWR) in Relation to Hydrological Modeling – Identification of the Pitfalls in Using High Resolution Radar Rainfall Data.* Proceedings of Fourth European Conference on Radar in Meteorology and Hydrology (ERAD06), 18-22 September 2006, Barcelona, Spain

E Lisbeth Pedersen, Niels Einar Jensen and Henrik Madsen. *Return Period for Radar Rainfall – Spatial Validity of Return Period*. Proceedings of 7th International Workshop on Precipitation in Urban Areas, 7-10 December 2006, St. Moritz, Switzerland

F Lisbeth Pedersen, Niels Einar Jensen and Henrik Madsen. *Extreme Rainfall Statistics Based on Rain Gauges and Radar*. Proceedings of International Symposium Weather Radar and Hydrology (WRaH 2008), 10-12 March 2008, Grenoble, France

G Lisbeth Pedersen, Niels Einar Jensen and Henrik Madsen. *Assessment of QPE Results from 4 kW X-band Local Area Weather Radar (LAWR) Evaluated with S-band Radar Data.* Proceedings of Fifth European Conference on Radar in Meteorology and Hydrology (ERAD08), June 30 - July 4, 2008, Helsinki, Finland

H Lisbeth Pedersen, Niels Einar Jensen and Henrik Madsen. *Network Architecture for Small X-band Weather Radars – Test Bed for Automatic Inter-Calibration and Nowcasting*. Proceedings of The 33rd Conference on Radar Meteorology, 6 – 10 August 2007, Cairns, Australia

Acknowledgements

A journey of three years is now close to its destination. It has been three years with hard work, new opportunities, challenges and rewarding experiences. Being an Industrial PhD student has provided a unique opportunity to combine academia and business and this has been worth all the hours of train rides between Aalborg - Aarhus and Aalborg - Lyngby. I would like to acknowledge DHI and the Danish Ministry for Science, Technology and Innovation for providing the funding of this project.

First of all, I want to thank my supervisors, Chief Engineer Niels Einar Jensen, DHI, and Professor Henrik Madsen, DTU, for their faith, patience, humor and strong sense of optimism throughout the project. I would also like to express gratitude towards all the people in the statistics group from the Department of Informatics and Mathematical Modelling (IMM) at DTU and my colleagues at DHI for guidance, support, encouragement throughout the project. A special thanks to the people at the DHI office in Aarhus who have celebrated the ups and shared the downs with me all the way along the journey and to Lasse Engbo Christensen, DTU for valuable discussions regarding rainfall statistics.

Without the help from Bo Præstegaard Jensen, Anders Sloth Møller, Ida Rasmussen and Niels Eisum it would not have been possible to carry out the rain gauge field experiment. Special thanks are given to Bo for hammering down the eight huge poles in the seabed standing in a rubber dinghy – a tremendous task for which I am truly grateful. Furthermore I would like to express my gratitude to Signe Nielsen for proofreading this thesis.

During the fall of 2007 I spent three months as a guest in the weather radar group at McGill University, Montreal, Canada under the supervision of Professor Isztar Zawadzki. I would like to express my gratitude to all the people there that helped me and made it a very educational experience, in particular Isztar Zawadzki, Marc Berenguer, and Aldo Bellon. In this connection I would like to thank Paul Joe, Environment Canada, for setting up the visit and having me as a guest for two enlightening days at Environment Canada.

Over the past three years I have encountered upon a large number of motivating people within the radar and hydrological communities who have shown interest in my work. They should be acknowledged for both supporting and challenging my ideas – and thereby forcing me to seek new ways. They have been sources of great inspiration.

Finally, but definitely not least, I would like to thank my family and friends for their support, patience, practical assistance, housing and for enduring me over the past three years. Special dedications to the bravest man of them all – my other half Kristian, for always believing in me.

"Bad weather always looks worse through a window"
- Tom Lehrer

Contents

Part III – Published Papers

PART I

The Theme

CHAPTER 1

Introduction

Globally people are migrating from rural areas to urban areas in their pursuit of a different life and better opportunities. In 2008 a landmark was reached since for the first time in history the urban population matched the size of the rural population and is expected to grow in the future (UN, 2008). This urbanization is putting stress on the infrastructure of already large urban cities and in particular on the water and sanitation infrastructure. Correctly designed and properly operated drainage systems are essential for the survival and well-being of people living in urban areas. In the western part of the world urban drainage systems are considered a fundamental part of the infrastructure, but it is out of sight and out of mind of the general population – unless it is not functioning.

High intense rainfall, also referred to as extreme rainfall events, can result in flooding of streets and buildings due to overload of the urban drainage system. Extreme rainfall events can cause servere damage to infrastructures and personal possessions and this can be extreme costly. In recent years many European cities have experienced flooding as result of high intense rainfall, e.g. the large flood in 2002 causing damage for billion of Euros and casualties in Czech Republic, Austria, Germany, Slovakia, Poland, Hungary, Romania and Croatia.

A frequently used tool in connection with planning design, operation and management is numerical models for simulation of dry and wet weather flow in

drainage systems. A variety of models exists from simplified lumped models to fully distributed models where all structures and catchments are modeled individually. Common for all models disregarding their level of complexity is that they will never perform better than the quality of the input data. In connection with urban drainage modeling the major input is rainfall. Rainfall measurements are most often obtained by rain gauges which register the rain falling over a small surface of a few hundred square centimeters. A single rain gauge cannot provide any information on the spatial properties of the rainfall, and even when observations from a dense network of rain gauges are interpolated by e.g. Krieging, Thiessen polygon or spline interpolation techniques methods, they only provide a simplified and smoothed representation of the spatial variability of rainfall (Sempere-Torres, et al., 1999). This lack of spatial information is problematic in connection with urban drainage modeling since rainfall occurring over the majority of the area of interest may not be observed by a single gauge due to the variability of the rainfall. Even if the rain gauge observes rainfall it is rarely representative for the whole area.

Urban drainage applications today are becoming more and more distributed and detailed, however, the rainfall input is still applied as uniform rainfall over the whole area and thereby a lot of the complexity of the model is lumped. To obtain high resolution distributed rainfall measurements as input to urban drainage models DHI has developed a small scale weather radar capable of providing high resolution rainfall measurements. The radar is denoted Local Area Weather Radar (LAWR) and was designed with the aim of being a cost-efficient weather radar supplement to rain gauges which can be installed and operated by the hydrological services in need of such data for their applications – online in real-time as well as off-line.

Weather radars provide a mean to obtain spatially distributed measurements of rainfall. This type of measurement is an indirect measurement, since the output from the radar is received energy backscattered from rain drops in the atmosphere. The measured energy is converted to rainfall intensities in the calibration process which is normally based on rain gauge observations. The radar performance is usually evaluated by comparing the rainfall estimate to the gauge observations. This approach is problematic since a gauge is a discrete point measurement while the radar is a volume measurement. In order to assess the uncertainties related to weather radar rainfall estimates it is therefore of uttermost importance to identify the scaling properties of rainfall at the extent of the spatial footprint of weather radar observations.

The interest in using weather radar rainfall data in urban drainage applications has increased steadily over the past 5-10 years, but it is still primarily confined to research projects (Einfalt, et al., 2005). One of the barriers is that weather radars are normally operated by meteorological services while drainage modeling is carried out

by hydrological services. These two communities are starting to work together towards the use weather radar data as input to hydrological models including urban applications.

From the hydrologist's point of view it is essential to get radar observations with a temporal and spatial resolution in the same domain as the model to which it is being used as input. The complexity of weather radar data and the sources of errors and uncertainties are manifold compared to those of a single rain gauge. The use of weather radar data as input to urban drainage modeling therefore requires inter-disciplinary skills from the fields of hydrometeorology, radar and hydrology.

This thesis is a compilation of an Industrial PhD project at the Department of Informatics and Mathematical Modelling at the Technical University of Denmark and at DHI, which is an independent, international consulting and research organization. The field of research is hydrometeorology coupled with urban drainage. The overall focus of the research is rainfall estimated with the LAWR. Based on data collected by rain gauges and multiple LAWRs during the PhD project the performance and uncertainties of LAWR rainfall estimates are evaluated by statistical methods. The focal point of the work has been to determine the spatial variability of rainfall within a LAWR pixel of 500x500 meter. This is essential in order to quantify the precision of LAWR rainfall estimates since it depends on the calibration process using a single pixel and a single gauge. Furthermore, the process of integrating LAWR into urban drainage models is analyzed. The findings and results are presented the papers A-H.

1.1 Thesis Outline

This thesis is subdivided into three parts.

Part I – "The Theme" contains a brief introductory to the thesis subject followed by summaries of the included eight published papers or in the process of publishing. Finally, conclusions and discussion are presented based on the research presented in the eight papers.

Part II – "Point of Departure" consists of three chapters, each dealing with one of the main topics of this cross-disciplinary thesis: "Meteorology", "Local Area Weather Radar" and "The Use of Weather Radar Data in Urban Drainage". These chapters are included to provide a common foundation for the work presented here.

Part III – "Published Papers" includes the collection of papers published during this PhD.

CHAPTER 2

Paper Summaries

2.1 Paper A: Quantification of the Spatial Variability of Rainfall Based on a Dense Network of Rain Gauges

The topic in Paper A is quantification of the spatial variability of rainfall event depths. The data used in the analysis presented in this paper comes from a Danish field experiment using nine rain gauges. This experiment was a vital aspect of the PhD project, and a substantial amount of time and effort has been invested in order to ensure good quality data. The nine gauges were originally set up in the exact same locations as in a previous similar experiment conducted in the fall of 2003. The aim of this second setup was to verify the results from 2003 with a more stable type of rain gauge and increase the data foundation to fortify the conclusions. Since most of the gauges were destroyed by farming equipment in the summer of 2006, the nine gauges were relocated in 2007 to the shallow waters of a nearby estuary named Norsminde Fjord. The aim of the experiment was to analyze the variability of rainfall depths within a 500x500 meter area corresponding to the largest pixel size of a Local Area Weather Radar (LAWR).

The spatial variability of rainfall at within a LAWR pixel is of interest since rainfall observed by a single rain gauge is assumed representative for the whole pixel area in connection with calibration of weather radars. Conventional weather radars operates

with pixels (spatial footprint) ranging from 1x1 km to 4x4 km depending on the radar. To quantify the accuracy of LAWR rainfall estimates it is therefore necessary to quantify the variability of the area normally represented by a single gauge, in order to indentify uncertainties related to the scaling properties of rainfall affecting the calibration.

During the first campaign from 13th September - 7th November 2007 a total of 19 events exceeding a threshold depth of 1 mm was observed by minimum three out of the nine gauges resulting in a total rainfall of 71 mm. During the second period from 17th June - 13th November 2008 a total of 55 events exceeding the threshold depth of 1 mm was observed by minimum three out of the nine gauges with a total rainfall of 222 mm. In both seasons malfunctioning gauges occurred – primarily as result of clogging due to bird droppings. The results from the original 2003 experiment were included for comparison (a total of 20 events with a total rainfall of 89 mm). The 2003 data was collected using an optical drop counting gauge with a 0.01 mm resolution, while the 2007 and 2008 data was collected with a standard 0.2 mm tipping bucket gauge.

First the variability was quantified by the coefficient of variation estimated as the ratio of the standard deviation to the arithmetic mean depth. The coefficients of variation were notably larger for the 2003 data than for 2007 and 2008 and were found to be correlated with the rainfall depths as they decreased with increasing rainfall depths. The coefficient of variation was estimated to range from 1-26% in the 2007 and 2008 data, which was considerably lower than the 1-77% range of the 2003 dataset. The large variability of the 2003 data was suspected to be a result of a different and more unstable gauge type. The large variability of 2003 data only occurred in events with depths less than 5 mm.

The rainfall depths were found to follow a log-normal distribution and treated as such in the statistical analysis. The 2007 and 2008 data was subjected to a correlation analysis which showed strong correlation among the gauges, and the correlation was found to decrease with increasing inter-gauge distance. In order to address the inter-event variability the data was transformed to be multivariate distributed. By doing so the standard deviation of the gauges was used to define the 95% prediction interval of a single gauge. All events having a rainfall depth larger than 15 mm were completely within $\pm 2\sigma_{min}$, while the majority of events having a rainfall depth less than 5 mm was within $\pm 2\sigma_{max}$. σ_{max} approximately corresponds to an uncertainty of ±12% and σ_{max} to ±23% of the rainfall depth. The 95% prediction interval provides the expected interval of the possible variability range of input from a single rain gauge and thereby the uncertainty that would have to be added to an application, e.g. a LAWR calibration, assuming that a single gauge is representative for a 500x500 meter area. The paper is submitted to the Journal of Atmospheric Research.

2.2 Paper B: Calibration of Local Area Weather Radar – Identifying Significant Factors Affecting the Calibration

Paper B analyses the Local Area Weather Radar (LAWR) calibration methodology. The output from a LAWR is energy backscattered from raindrops in the atmosphere denoted reflectivity. The reflectivity values must be converted into rainfall intensities by a calibration process which is normally done on the basis of ground based rain gauge observations.

The standard LAWR calibration is based on an assumed linear relationship between accumulated rainfall depths observed by a rain gauge and the accumulated reflectivity observed by the LAWR over the same duration. The 2008 data from the field experiment analyzed in Paper A is used together with data from the Aarhus LAWR located south of Aarhus, Denmark. Furthermore, data from three gauges part of the official Danish gauge network are included for validation of the methodology.

The Aarhus LAWR is the primary research radar, but unfortunately it is placed at a location resulting in beam shielding and blockage. Prior to the data analysis the LAWR data was therefore adjusted to compensate for these issues and for the underestimation as result of increasing beam volume with range by a new 2D volume correction approach. During the analysis it was discovered that when the reflectivity field from a LAWR is as inhomogeneous as in the case of the Aarhus LAWR, the location of rain gauges in relation to the accumulated reflectivity image for calibration and validation needs to be thoroughly evaluated. In this gauges located in blocked areas or in areas where the reflectivity level is not representative for the majority of the radar domain can be identified. The parameters identified to have the highest impact on the calibration were the time varying magnetron condition, proper volume correction and the gauge location in relation to the reflectivity level. Gauges located in non-representative areas should not be used for calibration.

The analysis was carried out on a total of 50 rain events where the gauges had recorded more than 1 mm and the LAWR had observed rainfall within the same time frame. The standard LAWR calibration method is based on a linear relationship between the rainfall depth of an event observed by gauge and the corresponding accumulated reflectivity observed by the LAWR. The linear relationship is a result of the LAWR having a logarithmic receiver, which is different from conventional weather radars having a linear receiver and using a power-law relationship calibration method.

As part of the analysis the calibration method was extended to include three parameters compared to the single parameter method normally used. In addition to reflectivity the duration (hour) and the intensity (reflectivity/hour) were included.

This new three parameter method improved the degree of explanation from 0.85 (the original method/Scheme 1) to 0.90 (Scheme 2).

The two calibration methods were evaluated with data from three independent gauges. The validation errors were within ± 7% when the total rainfall over 3 months estimated by the LAWR was compared to that observed with gauges. Both schemes were found to perform equally well when the validation gauge was located in an area with a reflectivity level equal to that of the calibration gauges. In cases where the validation gauges were located in an area with a higher or lower level of reflectivity than the calibration site, the new three parameter method (Scheme 2) outperformed the standard method (Scheme 1). The new calibration scheme is concluded to reduce the uncertainties of LAWR rainfall estimates, especially in cases where the reflectivity levels are strongly spatial inhomogeneous as those of the LAWR used here.

During this work it was discovered that the magnetron starts to decay more rapidly than assumed. This issue is to be corrected in the very near future eliminating the related uncertainties. The two dimensional volume correction method used here needs further development before operational implementation, however, it was concluded that it is a potential solution to the increasing beam volume issue. The paper is submitted to the Journal of Atmospheric Research.

2.3 Paper C: Estimation of Radar Calibration Uncertainties Related to the Spatial Variability of Rainfall within a Single Radar Pixel – Statistical Analysis of Rainfall Data from a Dense Network of Rain Gauges

Paper C contains the first results from the rainfall measuring campaign conducted from June 2006 to November 2008 as part of this PhD. Paper C presents the first results based on data from the summer and fall of 2007, since no usable data were collected in 2006 due to destroyed equipment. Nine rain gauges were placed in a three by three grid each representing one ninth of an area of 500x500 meter equal to a single Local Area Weather Radar (LAWR) pixel. The experiment was a continuation of an experiment conducted during the fall of 2003 which revealed that within such a small area rainfall depths could vary up to 100%. To verify the results from 2003 obtained using 0.01 optical drop counting gauges and extend the data foundation the experiment was recommenced as part of this PhD project using standard 0.2 mm tipping bucket gauges.

The characteristics of the new dataset from 2007 were found to vary significantly from the original dataset from 2003. The variability of rainfall depths was found to vary much less in 2007 than in 2003 based on coefficients of variation (CV) values.

The maximum variation within an event was estimated to 16% in 2007 compared to the original maximum value of 99% from 2003. The dataset from 2003 was subjected to further scrutiny resulting in omission of some dubious events which lead to a lower, but more reliable maximum CV of 77%. The 2007 dataset only contained shallow events (<10 mm) compared to the 2003 dataset which contained several events larger than 10 mm. The higher variability of rainfall depths in the 2003 dataset was concluded partly to be a result of a different gauge type and the presence of deep convective rainfall events which was lacking in the 2007 data set. The paper was presented by an oral presentation at the World Environmental & Water Resources Congress 2008 (EWRI 2008) and is the preliminary work leading to Paper A and Paper B.

2.4 Paper D: Application of Local Area Weather Radar (LAWR) in relations to Hydrological Modeling – Identification of the Pitfalls in using High Resolution Radar Rainfall Data

Paper D presents the first experiences of using LAWR data as input to a fully distributed MIKE URBAN (MU) model. The aim was to identify potential issues requiring adaption of either the LAWR and/or the MU software. A sub-model of an existing model used in operational context was provided for the analysis by the municipality of Vejle, Denmark, along with data from their LAWR. The LAWR was calibrated using the standard one parameter calibration method with data from the rain gauge located closest to the radar and the model area. The rain gauges normally providing the input data were included in the analysis and the result based on these was compared with results based on LAWR data.

The LAWR data was first applied as input to the existing model without any special considerations and modifications. This revealed that knowledge of local conditions affecting the LAWR data is of uttermost importance, and using LAWR data (weather radar data in general) requires new skills from the user to identify features in the LAWR data e.g. clutter affected areas. Furthermore, it was concluded that a model calibrated on the basis of rain gauges requires to be recalibrated when the input is changed from uniform rainfall to distributed rainfall since the missing spatial information is incorporated in the model calibration. When applying distributed input data to an urban drainage system it will respond as if it had a large capacity since it is not, as normally, affected over the full area simultaneously by a peak intensity.

The spatial resolution of the modeled catchments was found to be significant and should be in the same domain order as the pixels in order to utilize the spatial information of the radar rainfall input. The model used for the analysis applied one input boundary to each catchment, and in cases of multiple input boundaries with LAWR data each catchment was assigned the pixel which center coordinate being

closest to the center coordinate of the catchment. This approach was found to be problematic and causing inaccuracies when catchment areas and pixel areas differed significantly.

The work revealed that the current way of assigning rainfall boundaries to distributed catchments can be problematic when high resolution distributed rainfall is used. Furthermore, it was concluded that when transiting from uniform to distributed rainfall data the model has to be re-calibrated. The paper was presented by an oral presentation at the Fourth European Conference on Radar in Meteorology and Hydrology (ERAD06).

2.5 Paper E: Return Period for Radar Rainfall – Spatial Validity of Return Period

Urban drainage structures in Denmark and many other countries are designed based on a set of Intensity-Duration-Frequency (IDF) curves. The return period is the number of years between a given combination of duration and intensity statistically occurs. The system is designed to handle the volume of an event occurring with a statistical return period of e.g. 2 or 10 years. The IDF curves are derived based on statistical analysis of data from rain gauges that have been operating for many years. Since rain gauges only observe rainfall in a point, the probability of an extreme rainfall event passing right over a gauge is very low, and the spatial extent of the event is furthermore unknown. The work of Paper E focuses on estimating return periods based on LAWR data. Since the length of the time series from LAWR installations is still too short for ranking the data a different approach was tested. By assuming each pixel of an independent observation and having the same properties as a rain gauge the rain gauge derived IDF curves are used to link a LAWR estimated intensity of a given duration to a return period.

Each LAWR image consists of ~57,000 to 78,000 pixels depending on the spatial resolution of the Cartesian output image. The major challenge of the work was related to the vast amount of data required to be quality controlled and processed. The presentation of the results in a meaningful manner also proved to be challenging. A single event from 4th June 2005 was selected for detailed analysis. The event was recorded by the Aarhus LAWR and by a gauge part of the official Danish rain gauge network operated by the Danish Meteorological Institute. Based on the gauge estimate the event was estimated to have return periods for all durations less than one year. The LAWR estimated considerably higher return periods in an area less than 5 km to the east of the rain gauge. Within a 16.5x16.5 km area the maximum return period for 10, 30 and 60 minute maximum intensities was estimated to be 2.5 years, 18 years and 120 years respectively. The findings of LAWR return periods being higher than those estimated on the basis of gauges were consistent with a similar

Finnish study using Doppler C-band radars. The LAWR data furthermore revealed a strong correlation of the peak values which appeared in clusters having a spatial extent of 1-2 km. The spatial extent of high intense clusters could be a parameter in future design guidelines for urban drainage systems. The paper was presented by an oral presentation at the 7th International Workshop on Precipitation in Urban Areas.

2.6 Paper F: Extreme Rainfall Statistics Based on Rain Gauges and Radar Measurements

The work presented in Paper F builds on the methods used in Paper E for estimation of return periods based on high resolution distributed LAWR data. On 22nd August 2007 the city of Kolding, Denmark, was subject to surface flooding as result of intense rainfall exceeding the capacity of the urban drainage system. The official rain gauge located a few kilometers to the east of the city at the waste water treatment plant estimated the event to have a return period of 5 years for 5 and 10 minutes' duration and 10 years and 12 years for 30 and 60 minutes' duration, respectively. Data from the Vejle LAWR, located approximately 30 km north of Kolding, was analyzed with interest in estimating return periods. The area affected was on the far side of the 20 km range to which quantitative precipitation estimation normally is limited, and this was taken into consideration. The preliminary analysis revealed that Kolding had been hit by a series of convective events (thunder showers) dodging the rain gauges and thereby explaining the discrepancy of the observed flooding and the recorded rainfall a few kilometers away.

The Vejle LAWR covers five gauges all part of the official Danish rain gauge network operated by the Danish Meteorological Institute. The return periods estimated based on these gauges were compared to those of the corresponding LAWR pixels. The overall pattern was consistent except for one gauge where the LAWR estimate was significantly higher. The LAWR estimated return periods were, as expected, lower than the gauges estimated at locations more than 20 km from the LAWR which under normal conditions is the maximum range for quantitative precipitation estimation. The LAWR sampling volume increases rapidly with range, and since the rainfall estimate is an average over time and volume, there is an increasing risk of underestimating intensities at far ranges as observed here. The spatial structure of the return periods were, however, concluded to be well captured even at ranges further than 20 km.

The spatial structure of the LAWR estimated return periods was analyzed and the findings of Paper E were confirmed. The high return periods were clustered with a similar spatial extent of 1-2 km. Within a small area of 5x5 km the return periods were ranging from less than 10 years to more than 70 years. Based on the findings that return periods have a spatial extent of a few kilometers and that there is a

significant variability within even small areas, it is concluded that it can be very uncertain to estimate the return period of an event with a single gauge over an area a few kilometers away from the gauge. The paper was presented as a poster presentation at the International Symposium Weather Radar and Hydrology (WRaH 2008).

2.7 Paper G: Assessment of QPE results from 4 kW X-band Local Area Weather Radar (LAWR) Evaluated with S-band Radar Data

The data presented in Paper G was collected during a 3 months' research visit to the Department of Atmospheric and Oceanic Sciences at McGill University, Canada. During the visit a small down-scaled version of the Local Area Weather Radar (LAWR) was installed on the roof of the J. S. Marshall Radar Observatory only a few meters from the McGill S-band radar. The installed LAWR was a 4 kW down-scaled version of the standard 25 kW LAWR with a horizontal and vertical angular beam opening of 4° and 10°, respectively. The radar was operational from 10th October to 15th November 2007 and during this time a number of events were captured by both the LAWR and the S-band radar. For further analysis four events varying in character were selected. They varied from a convective event with a strong squall line (intensities > 50 mm/h) to more widespread light rain. One event was a mixture of light rain with cells of higher intensity.

The LAWR is based on a marine radar which is equipped with a range of facilities for suppressing rainfall detection. Due to limited experience with the 4 kW version which differs from the standard LAWR it was therefore of interest to establish whether the automatic built-in gain control was active and thereby affecting the data. An analysis based on clutter echoes in dry and rainy conditions revealed that it was properly disabled and not affecting the rainfall estimation. Unfortunately, it was not possible to calibrate the LAWR by means of rain gauge observations since only two of the four events were observed by a single gauge located more than 15 km from the LAWR. Instead a radar-radar calibration was attempted using the average reflectivity of a 2x2 km area five kilometers from the radar. By optimizing the RMSE of the fit between the two sources of reflectivity it became possible to estimate a satisfying calibration factor for the event of 19th-20th October (squall line event). The LAWR was concluded to detect high intense rainfall intensities and capture the spatial pattern of these well. In cases of light precipitation the LAWR underestimated the intensities as expected, since the beam volume is extremely large compared to the volume of the S-band and even larger compared to the standard LAWR. The high degree of underestimation of light precipitation is a result of the large beam of the 4 kW LAWR and would not be so dominant in case of the standard 25 kW LAWR.

One of the aims with the experiment was to assess the performance of the attenuation algorithm of LAWR. It was possible based on preliminary plots of data from both radars to verify that the LAWR signal was not extinct after passing through high intense rainfall and capable of capturing variations in the rainfall intensity afterwards. The timing issues due to the S-band radar operating with a significantly different scanning strategy than the LAWR resulted in comparison problems. The S-band scans 360° once before tilting the antenna to the next elevation angle (24 angles in total over 5 minutes), while the LAWR scans continuously at one elevation angle with 24 rounds per minute and an output frequency of 1 minute. It was not possible to make any final conclusion regarding the attenuation since timing issues turned out to be a very challenging task which was not overcome due to the deadline of this work. The paper was presented by an oral presentation at the Fifth European Conference on Radar in Meteorology and Hydrology (ERAD08).

2.8 Paper H: Network Architecture for Small X-band Weather Radars – Test Bed for Automatic Inter-Calibration and Nowcasting

In Paper H the prerequisite conditions for creating a network of small X-band weather radars were exploited. The intended network outlined here would consist of multiple Local Area Weather Radars (LAWR) operating with a maximum range of 20 km for quantitative precipitation estimation and 60 km range for nowcasting. One of the shortcomings of the X-band technology is the short range, however, by combining multiple LAWRs in a network this issue would be overcome. A network would furthermore provide observations of a rainfall event from more than one side and at different ranges providing new opportunities for attenuation correction. This is of special interest in connection with X-band since the 3 cm wavelength is sensitive towards rainfall attenuation.

The network architecture should facilitate online communication between the radars providing opportunity for inter-calibration and attenuation correction in real time. The following factors were identified as key parameters for the test-bed architecture: Physical geographical features, power availability, distances, existing radar and gauge installations, communication technology, bandwidth of communication channels and data formats. To test the proposed network architecture a test bed consisting of 3 LAWRs was to be implemented. The test bed LAWR is a down-scaled version (4 kW and 30 km range) of the standard LAWR (25 kW and 60 km range).

Note to Paper H:

Two out of the three LAWRs were installed at submission point of Paper H, but one was to be re-located due to beam shielding from nearby trees. The network was never fully implemented during this PhD since shortly after the submission of this paper it was concluded that in order to establish a network of LAWRs the calibration

methodology needed to be addressed more thoroughly in order to obtain reliable rainfall estimates, which is the number one prerequisite for a functioning LAWR network.

CHAPTER 3

Conclusions and Discussion

The aim of this Industrial PhD project was to improve and document the quality of Local Area Weather Radar (LAWR) rainfall estimates. The LAWR is a small scale weather radar capable of providing rainfall estimates with high temporal and spatial resolution for use in hydrological applications. The thesis integrates knowledge from the fields of hydrometeorology, radar meteorology and hydrology as rainfall estimation by LAWR and the use of the data are cross-disciplinary tasks. The assessment of the LAWR performance was evaluated on the basis of rainfall data collected during this project.

During the PhD-project an extensive amount of rainfall data was collected both by rain gauges and by LAWRs. The major field experiment included nine rain gauges placed in a three by three grid within a 500x500 meter area 10 km south of the primary LAWR used for this project and installed in Aarhus, Denmark. From the experiences gained from conducting the rainfall measuring campaign it can be concluded that placing the rain gauges in the waters of a shallow estuary cannot be recommended. The installation, maintenance and data collection proved to be very challenging and expensive, and the resting birds and their droppings were a major problem during the first season. During the two seasons a total number of 74 usable rainfall events with a total rainfall depth of 293 mm were registered by minimum three of the nine rain gauges.

In order quantify the accuracy of the LAWR rainfall estimate it is essential to identify the spatial variability of rainfall within a pixel since a single gauge is assumed representative for the whole pixel area in connection with the LAWR calibration. Based on analysis of the 2007 and 2008 data from the nine rain gauges it was concluded in Paper A that accumulated rainfall within a 500x500 meter area varies from 1-26% in a single event based on the coefficient of variation. The maximum coefficient of variation has been estimated with 95% confidence interval of ±0.2%. Furthermore, the 95% prediction interval of a single gauge was estimated to range from ~±12% to ~±23%, based on data from the nine gauges. This is consistent with the range of variability based on the coefficients of variation. The uncertainty related the scaling issue of comparing a point measurement (gauge) with a surface/volume measurement (radar) and thereby using a single gauge to represent the rainfall within a LAWR pixel is therefore concluded to range from 1 - ~26% and must always be taken into account when LAWR rainfall estimates are evaluated based on a single rain gauge.

The existing method for calibrating the LAWR was analyzed and the results were consistent with earlier findings both in terms of estimated calibration factor values and degree of explanation. The existing calibration method was concluded to provide satisfactory results when validated against rain gauge data from an area with equal level of reflectivity. A new three parameter calibration method was developed, tested and compared with the existing method (Paper B). The results showed an improvement in the degree of explanation (R-squared) from 0.85 to 0.90. The new calibration method is, besides reflectivity, conditioned on duration and intensity (reflectivity/hour). The validation of the two methods showed that in cases of spatial inhomogeneous reflectivity patterns the new calibration method outperformed the standard method, while in cases of homogenous conditions they performed almost equally well.

The Aarhus LAWR used for the calibration analysis has a spatial inhomogeneous reflectivity pattern due to beam shielding and blockage which invalidates the volume correction scheme normally applied to correct for the rapidly increasing beam volume prior to a calibration. Instead a new two dimensional volume correction approach was tested resulting in a satisfactory homogenous reflectivity pattern in the spatial domain.

In connection with the calibration analysis it was discovered that the magnetron starts to decay significantly after approximately three months. The magnetron continues to function throughout the full period (eight months), but the overall level of reflectivity becomes lower, thereby affecting the calibration. If a constant calibration factor is used the LAWR will underestimate rainfall intensities when the magnetron is older than three months. At the time of writing the magnetron signal time dependency

problem is planned to be solved by automatically compensating for the decreasing magnetron output based on clutter echoes in dry weather, thereby prolonging the duration of full signal to more than three months.

A point of great interest in connection with urban drainage are statistics of extreme rainfall as they are the foundation for IDF curves used for design of urban drainage systems. The statistics are also of interest in connection with flood damages as the liability for damages may depend on the return period of the given event. Based on the work presented in Paper E and F it can be concluded that return periods vary significantly even within areas as small as 5x5 km. In the context of urban drainage is this significant because the individual catchments are small and thereby sensitive to the large variability. Based on a limited data set the return periods were concluded to have a spatial extent of 1-2 km. This discovered spatial property of return periods of intense rainfall needs further analysis before anything can be finally concluded, however, if it proves to be a general characteristic it can be utilized in connection with design of local retention basins for sub-catchments. It should be noted that with the method used for linking LAWR rainfall intensities each pixel is treated as an independent observation which is an assumption since the data are correlated. Furthermore, the return periods are based on a model developed on basis of rain gauge data, but currently this is the most feasible solution due to the limited length of LAWR rainfall time series.

The probability of a single rain gauge observing an extreme event is extremely low compared to the probability of a weather radar observing it due to the large coverage area of a weather radar (20 km range ~ 1256 km^2). If extreme rainfall statistics are based on weather radar data there is a high probability that the return period of a given intensity-duration will decrease due to the higher detection rate.

Based on the conclusions from using LAWR data as rainfall boundary data in the MIKE URBAN model (Paper D) DHI has developed and incorporated a new method for assigning LAWR rainfall boundaries in MIKE URBAN. Today, each catchment is assigned a boundary based on the area weighted average of the all the pixels covering the catchment. Furthermore, it has become possible to visualize LAWR data in the model, thereby facilitating a more comprehensible way to evaluate LAWR data and identify possible flaws in the data.

The reluctance of using weather radar data in connection with hydrological applications is slowly starting to diminish in these years. There is no doubt that LAWR and weather radars in general offer unique information on the spatial properties of rainfall which is impossible to obtain with gauge observations. The hydrologists have never had any other sources of rainfall but gauges, which have resulted in models and applications being developed to handle the shortcomings of

gauge data and a strong belief in such data. The vast majority of research relating to using weather radars for rainfall estimation has been focused on correcting and fine-tune the radar data to resemble the properties of rainfall observed by gauges in order to meet the requirements of the hydrologist who considers a rain gauge the ”ground truth” when it comes to rainfall observations. The discussion is primarily on the uncertainties related to radar rainfall estimates which are of course important, but as with many other things it is a matter of weighing the uncertainties against the potential increased level of information and the potential effect on the performance. The question is what to use as source of rainfall data at an un-gauged location: Weather radar estimated rainfall or observation from a rain gauge many kilometers away. The answer depends on the type of information requested and the type of application. If yearly rainfall is of interest the gauge will provide a very reasonable estimate, but if a single convective event is of interest a gauge 20 km away would probably not even have recorded the rainfall. When it comes to providing forecast of coming rain the radar can provide information which it is not possible to obtain with a gauge network. A detailed high resolution forecast with a lead time of one hour can be of great value for many such as waste water treatment plant operators, Real Time Control (RTC) systems, flood warning systems and in principle any application affected by rainfall. Besides the mentioned urban related applications there are farmers, surfers and others who enjoy outdoor activities.

Based on the experiences gained through this PhD project it is believed that one of the most important future challenges is communication of knowledge across the involved science disciplines. If distributed rainfall data obtained by weather radars is to be widely used in hydrological applications it will require development of new tools for presenting the large and complex radar data in a more intuitive and feasible manner than available today. The transition from rain gauge data to radar data will require extra training and education as they are two completely different types of measurements. Quality index maps of radar data, GIS based analysis and visualization tools are examples of initiatives already being developed to meet these requirements.

PART II

Point of Departure

CHAPTER 4

Introduction to Radar Meteorology

The science of meteorology is spanning from the smallest atom to complex global circulations systems. In relation to weather radar meteorology which is the focus point of this thesis, the lower atmosphere is of interest with special focus on precipitation. This chapter is intended as a general introductory to radar meteorology focusing on precipitation characteristics and phenomena affecting precipitation measurements with weather radar.

Precipitation is a vital part of the complex global hydrological cycle as it transports the water vapor from the atmosphere back to the surface of the earth as illustrated in Figure 4.1. Precipitation is defined as any water, either solid (ice) or liquid (rain), that falls from clouds and reaches the ground (Ahrens, 2007).

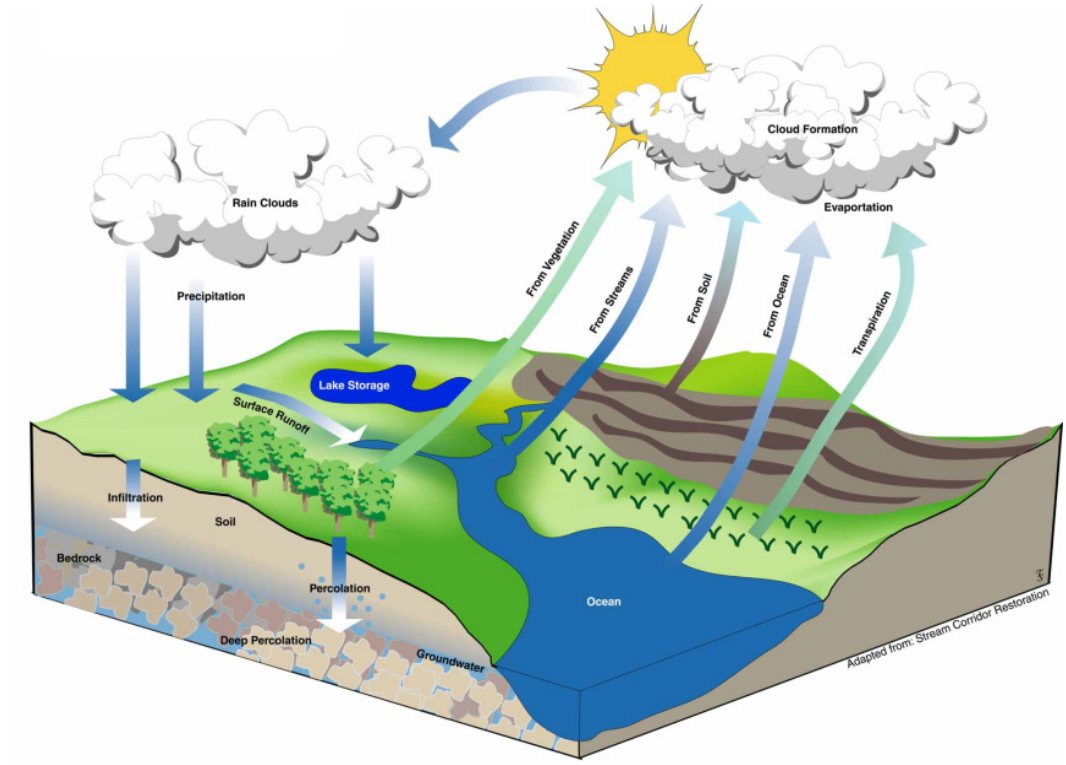

Figure 4.1The hydrological cycle. Illustration by Tom Schultz, Department of Natural Resource Ecology and Management" (NREM), Iowa State University.

Many methods exist for measuring how much precipitation falls at the surface, but the by far most common is some kind of container to collect the accumulated rainfall volume – a rain gauge. A variety of rain gauges exist – some automatic, some with heating for melting snow, some using tipping buckets, some weighing the water contents, etc., however, common for all of them is that they only observe rainfall in a point of a few hundred square centimeters. Precipitation is not confined to a point, but varies significantly over the area it falls on both in time and space. Weather radars, on the other hand, can provide spatially distributed measurements over a surface, which makes weather radars an interesting technique for rainfall measurements. Where a rain gauge observes the precipitation at the surface, the radar is observing the precipitation in the atmosphere.

4.1 Weather Radar Observation Domain of the Atmosphere

Many different types of radars are used as weather radars for various meteorological purposes. The most common radar type is C-band radar with a wavelength of 5 cm and a range of 240 km followed by S-band radar with a 10 cm wavelength and a range of 240-500 km. Today X-band radars with a 3 cm wavelength and a range of 30-120 km are starting to be used as weather radars. Until a few years ago X-band radars were considered inadequate for meteorological purposes as result of the 3 cm wavelength being affected by rain attenuation. The vertical range of the various radar types depends on antenna characteristics, scanning strategies and emitted power.

Most weather radars are operating with a dish antenna resulting in a pencil shaped beam with an angular width in the range of 0.5° to 2.9° (Rinehart, 2004). The radar used in connection with this thesis is a Local Area Weather Radar (X-band) which has a fan beam antenna resulting in a beam with a small horizontal angular opening (0.96°) and a wide vertical opening angle (±10° - effectively the opening angle is 10°). A thorough review of the LAWR system is found in Chapter 3.

The various types of antennas result in different beam patters. To illustrate the different types of beams, 1° pencil beams from a S-band radar scanning at 24 different elevation angles (tilting of the antenna) are shown in Figure 4.2 together with the beam of a LAWR. The beam center height, h is estimated on basis of (Doviak, et al., 2006) assuming standard propagation conditions (further described in Section 4.2):

$$h = [r^2 R_e^2 + 2rR_e \sin(\theta_e)]^{½} - R_e \tag{4.1}$$

where:

h: Center beam height above earth [km]
r: Range from radar [km]
R_e: Earths effective radius – 4/3 of earths radius[I] [km]
θ_e: Elevation angle [radians]

The wide vertical opening angle of the LAWR results in a beam reaching more than 10 km up in the atmosphere at full 60 km range, while the vertical span of conventional radars depends more on the elevation angles used in their scanning strategy as illustrated in Figure 4.2.

[I] Earth equatorial radius 6378.1 km (NASA, 2007)

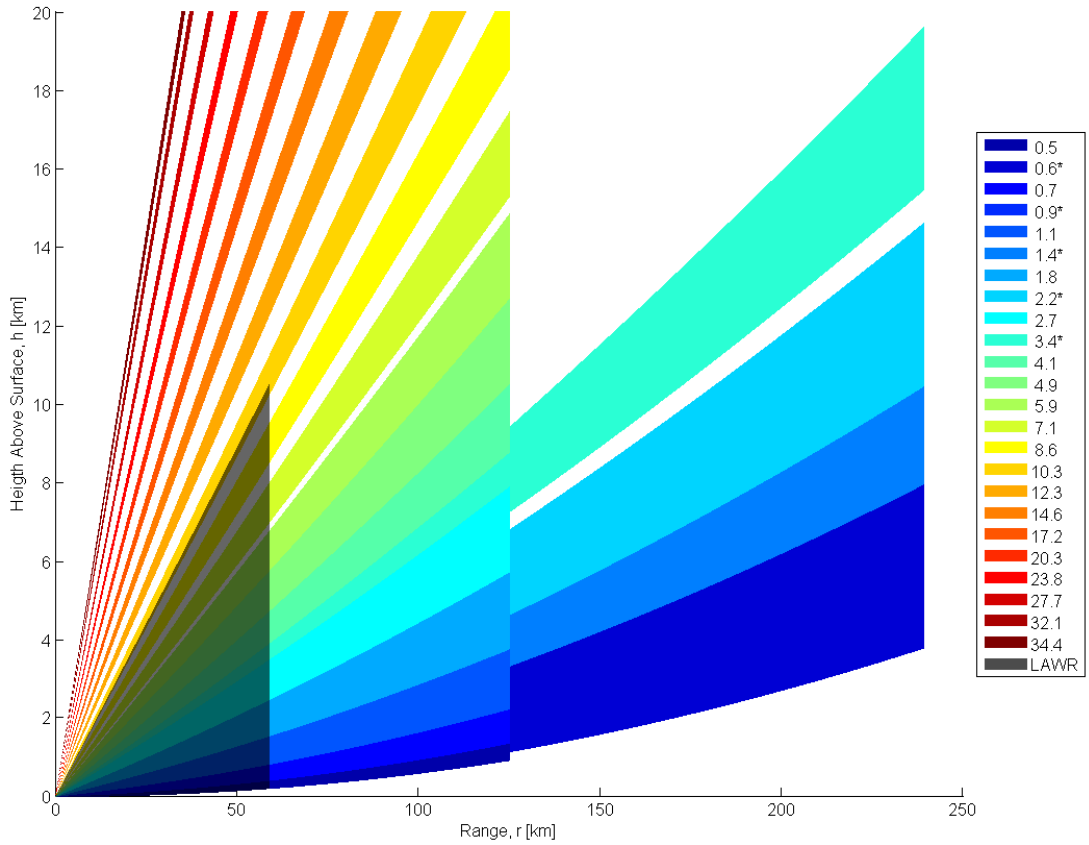

Figure 4.2 Approximation of the vertical extent of a 1° pencil beam at 24 different elevation angles compared to the vertical extension of the LAWR's fan beam antenna with 10° vertical opening angle (gray area). The height of the beam center is estimated by eq. 4.1, and the vertical extent is estimated by a tangential relation. Only S-band beams marked with * are of full range where the vertical extent is ~4 km, the rest has a range of 120 km. Only the lowest 20 km are shown. The elevation angles and ranges are based on the specification of the Canadian S-band radar located at J. S. Marshall Radar Observatory near Montreal, Canada. The beams from the lower elevation angles overlaps each other.

The beams from the highest elevation angles reach higher than 80 km up in the atmosphere, but only the lower part of the atmosphere is of interest in connection with precipitation measurements. The atmosphere is divided into four layers based on significant shift in the temperature gradient. The troposphere is the lowest part of the atmosphere followed by the stratosphere, mesosphere and the thermosphere. The troposphere is the part of the atmosphere where the weather affecting the earth is occurring since almost all the water vapor and aerosols of the atmosphere are found in the troposphere (Ahrens, 2007). The decreasing temperature gradient through the troposphere is also referred to as the lapse rate which is on average 6.4°C pr. 1000 meter (Ahrens, 2007). The majority of the radar sample volumes in Figure 4.2 are below 11 km altitude which is the average upper limit of the troposphere. The beams in Figure 4.2 are estimated assuming standard atmospheric conditions, but the atmospheric conditions may vary, thus having a strong impact on radar measurements.

4.2 Radar Beam Propagation in the Atmosphere

Radars transmit and receive electromagnetic radiation where path and speed depend on the medium travelled through. The refractivity is defined as the ratio between speed of light in vacuum and speed of light in the medium. In total vacuum electromagnetic radiation travels with the speed of light (299 792 458 m/s), while in air it travels slightly slower due to the presence of atmospheric gasses such as nitrogen, oxygen and water vapor. In the troposphere the refractivity depends on atmospheric pressure, temperature and vapor pressure, and hence it changes with height. It is not the refractivity itself that has the highest impact on weather radar observation, but the vertical gradient of the refractivity, since the vertical refractivity gradient affects bending of the radar waves. When assuming normal atmospheric conditions the refractivity decreases with height causing faster travel speed with increasing altitude which again results in downward bending of the waves relative to the earth's surface as illustrated in Figure 4.3.

Situations where the downward bending is stronger than normal is referred to as super refraction, while cases where the wave is bending less than normal or even bending upwards is sub refraction resulting in echoes being detected in "wrong" locations. The different types of wave propagation are illustrated in Figure 4.3.

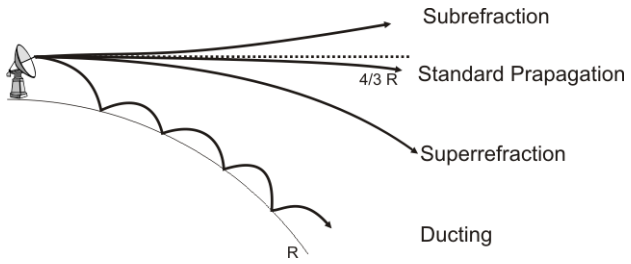

Figure 4.3 Illustration of different types of propagation of electromagnetic radiation in the atmosphere. The standard propagation follows the curvature of a sphere with radius 4/3R, where R is the radius of the earth (Doviak, et al., 2006).

Especially super-refraction can be problematic in connection with radar meteorology since the waves under this condition can detect ground targets at longer ranges than normal. It often occurs in connection with an inversion layer close to the ground (temperature increases with height) and is in radar terminology known as Anomalous Propagation- anaprop or AP for short. In cases of extreme refraction the wave can be trapped inside a layer (normally close to the ground) which acts as waveguide – this phenomenon is called ducting.

4.3 Cloud Formation Processes

Precipitation is coupled with clouds, which consist of ice crystals or water droplets or a combination suspended in the atmosphere. The water vapor of the troposphere condensates into ice crystals or water droplets when air expands as result of decreasing pressure with altitude and cools as it rises, cf. Figure 4.4. The creation of a

drop or a crystal requires the presence of a cloud condensation nucleus on which water vapor can condense. A condensation nucleus is a small particle suspended in the air and can origin from dust, pollution, volcano eruptions, ocean spray etc. Cloud condensation nuclei vary in diameter from less than 0.4 µm (Aitken nuclei) to more than 2 µm (giant condensation nuclei), but the optimum size for cloud formation is 0.2 µm or larger (Ahrens, 2007). Condensation occurs when the relative humidity[II] is 100% or just below, even though some types of nuclei are hygroscopic, thereby facilitating condensation at lower relative humidity, and others are hydrophobic, requiring more than 100% relative humidity.

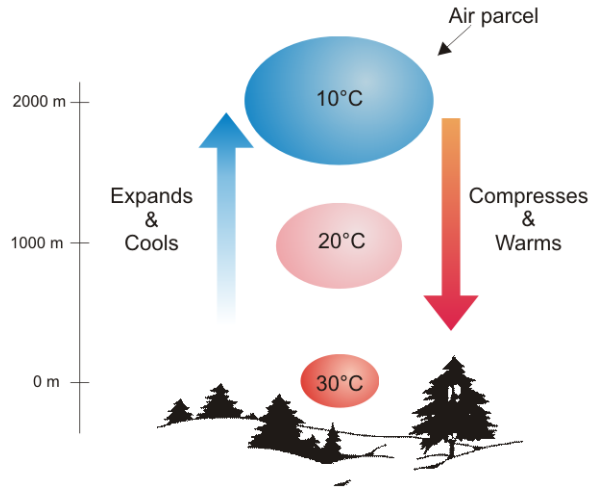

Figure 4.4 Illustration of rising and sinking of an unsaturated parcel of air defined by the dry adiabatic lapse rate of 10°C pr. 1000 m. Illustration adapted from (Ahrens, 2007).

The vast majority of clouds is a result of rising air cooling and thereby increasing the relative humidity of the air as illustrated in Figure 4.4 showing the dry adiabatic lapse rate for a parcel of unsaturated air. If the air parcel is cooled to the dew point or lower, the relative humidity exceeds 100%, condensation starts to occur and a cloud starts to form. The condensation releases latent heat inside the air parcel which causes the air inside the parcel to be cooled at a slower rate – denoted the moist adiabatic rate. The moist adiabatic rate describes the rising rate of saturated air and is not constant, but varies with temperature and therefore the moisture content.

The type of clouds formed in this process depends on the stability state of the atmosphere which again is determined by actual temperature profile at the location – the environmental lapse rate. A low environmental lapse rate will result in a lifting air parcel always being colder than the surrounding air and therefore it will tend to sink back down - the atmosphere is stable. When the

[II] Relative humidity is the ratio of air's water vapor content to the airs water vapor capacity

environmental lapse rate is larger than the dry adiabatic lapse rate, the air parcel is warmer than the air around it and it will continue to rise - the atmosphere is unstable. A stable atmosphere tends to result in layered clouds, while an instable atmosphere often results in cumuliform clouds. The different cloud types are illustrated in Figure 4.5. Most of the time the environmental lapse rate is between the dry and moist adiabatic lapse rates resulting in an atmospheric state of conditional stability. In case of conditional stability the atmosphere is stable if the rising air is unsaturated and unstable if the air is saturated.

4.3.1 Sources of Cloud Formation

As described in the previous section a cloud is formed when air rises, expands and cools, but there are several means for this to take place. The most common sources are surface heating and free convection, uplifting as result of topography, convergence of air and uplift as result of weather fronts (Ahrens, 2007). The geographical location has strong influence on which cloud formation type is the most dominant since temperature, mountains, proximity to the ocean and climate zones all affect the processes and they vary from location to location.

The different processes causing air to rise result in different types of clouds. Clouds formed as a result of air being lifted by weather fronts can extend over several hundred even thousand kilometers in the horizontal extent. Clouds created as result of convergence of air or topographic lifting extends from 150-500 km, while clouds as result of local convection may only be a few kilometers wide. Convection can occur very locally and often in the warm summer months where unstable air close to ground often results in a local parcel of air rising upwards.

4.3.2 Cloud Types

Clouds come in all sizes, shapes and color shades. Most common are white, gray and black, but sunsets can result in the most fantastic cloud colors. Clouds are classified into four overall groups based on their height of their cloud-base and these four groups can again be subdivided into a total of ten cloud types, cf. Table 1. The classification is based on Latin words for how the clouds appear when observed from the ground.

Table 1 Cloud classification (Ahrens, 2007). The Latin words translate into: Cirrus (curl of hair), stratus (layer), Cumulus (heap), nimbus (rain) and alto (middle). Precipitation yielding clouds are underlined.

Cloud Type	Height Group	Cloud base height*
Stratus	Low	0-2000 m
Stratocumulus	Low	0-2000 m
Nimbostratus	Low	0-2000 m
Altostratus	Middle	2000-7,000 m
Altocumulus	Middle	2000-7,000 m
Cirrus	High	5000-13,000 m
Cirrostratus	High	5000-13,000 m
Cirrocumulus	High	5000-13,000 m
Cumulus	Vertical development	1000
Cumulonimbus	Vertical Development	600-12,000**

* For middle latitude regions (Ahrens, 2007)
** Vertical extent

The classification system furthermore specifies precipitation yielding clouds with the pre-/suffix nimbus - nimbostratus clouds and cumulonimbus clouds. The vertical extent of the precipitation producing clouds is vital in connection with weather radar precipitation measurements, since they measures at different altitudes and with different beam volumes. The cloud height of the different cloud types listed in Table 1 in relation to the Local Area Weather Radar's beam height is illustrated in Figure 4.5.

At ranges further than 10-20 km precipitation from low level nimbostratus clouds is underestimated by the LAWR, hence only a fraction of the volume is filled as illustrated in Figure 4.5. Conventional weather radars instead overshoot low hanging precipitation at ranges further than 100-150 km due to the curvature of the earth, cf. Figure 4.2. In particular the detection of tornadoes at far ranges with a conventional weather radar is a problem. Tornadoes most often occur in connection with cumulonimbus clouds (especially on the Great Plains East of Rocky Mountains, USA) and can be observed by conventional weather radars and warnings can be sent out to the public. The problem is that this is only possible if they occur close to the radar, since tornadoes start to form at mid-level, but the funnel forms at the base of the cloud close to the ground which is not observed by conventional weather radars at far ranges.

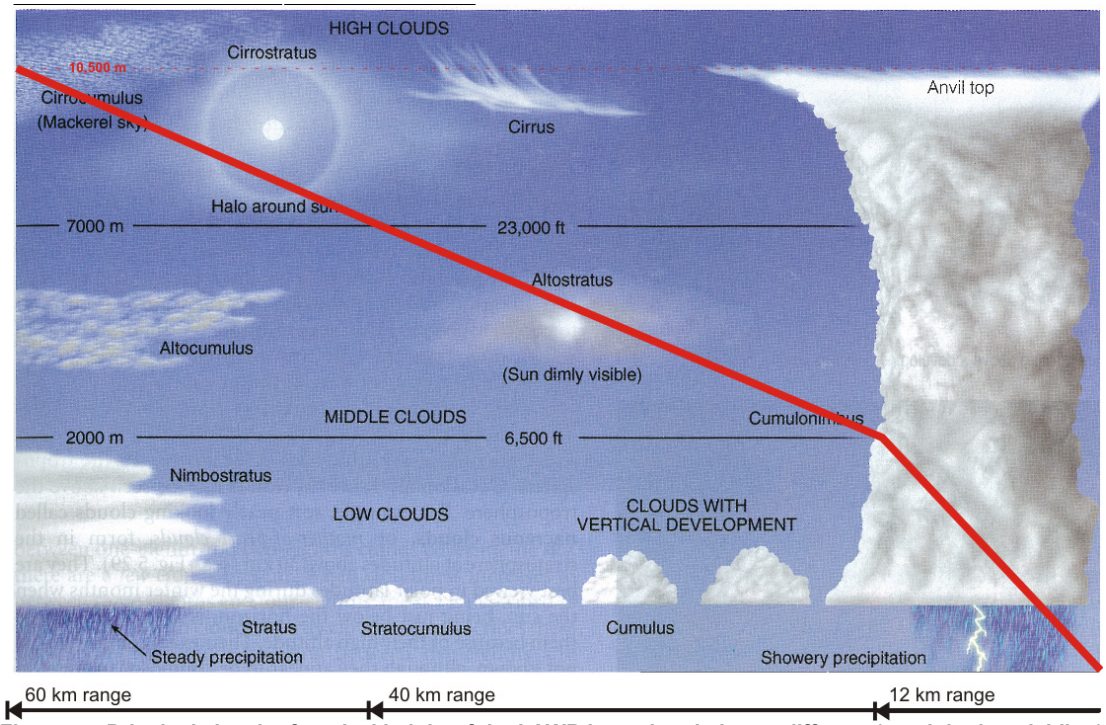

Figure 4.5 Principal sketch of vertical height of the LAWR beam in relation to different (precipitation yielding) cloud types. The bend at 2000 meter altitude is a result of the vertical scaling of the cloud image from (Ahrens, 2007). Lines and figures in red are added to the original and the LAWR is assumed located in lower right corner.

It should be noted that the LAWR only measures falling precipitation (rain, snow or hail), and not the droplets suspended in the clouds. Conventional weather radars can to some degree detect clouds at close range, but for cloud research vertical pointing K_a-band and W-band radars (clouds radars) are preferred for studying the microphysics of the clouds (Moran, et al., 1998).

4.4 Precipitation Processes

A cloud consists of an extreme number of droplets with an average diameter of 20 µm, while raindrop ranges from 200 µm (drizzle) to 5000-6000 µm (large raindrop) with an average of 2000 µm. The two primary processes describing cloud droplets transformation to raindrops are collision-coalescence and the ice-crystal (Bergeron) method (Ahrens, 2007).

The collision-coalescence process requires a range of droplet sizes to be present in the cloud and the cloud temperature must be above -15°C - a “warm” cloud. Large cloud droplets have a higher fall velocity than smaller drops due to their smaller surface-area-to-weight-ratio. The critical size when a drop starts to fall depends on the updraft within the cloud. As the drops fall down through the cloud they collide with other (smaller) drops and they merge by collision. Other small drops may be trapped in the wake of the large drop which is the coalescence process. The thickness of the cloud and thereby the fall length and duration of the droplet in combination with the updraft

speed determines the size which a cloud droplet can grow into. Raindrops reaching the ground are hardly ever larger than 5000 μm, since the collision process tends to break them up into smaller drops (Ahrens, 2007).

The collision-coalescence process is dominant in warm clouds, but in midlevel and high level clouds the ice-crystal (Bergeron) process is the dominant process. In mixed subfreezing conditions there will be a higher number of liquid droplets compared to ice crystals. Since the saturation vapor pressure is higher above a liquid surface than an ice surface the water vapor molecules will diffuse from the droplet towards the ice crystal. The reduced vapor pressure over the water droplet causes it to evaporate and thereby moisture is available for ice crystal which absorbs it and thereby grows rapidly. Most rain falling at middle latitudes is a result of the Bergeron process. (Ahrens, 2007)

A cumulonimbus cloud extends from low to high level (10-12 km), and as result the precipitation from such a cloud is a result of a combination of the two processes. The collision-coalescence process governs precipitation formation at the lower warm part of the cumulonimbus cloud. The lower part contains only water droplets, which continue to exist in liquid form well above the 0°C isotherm. This state is called super-cooled, and can exist up to altitudes where the temperature is above -4°C to -15°C - the critical temperature depends on the ratio between large and small cloud droplets. Between the 0°C isotherm and the -40°C isotherm the cloud droplets are a mix of water and ice with increasing ice content with height, and here precipitation is formed by the Bergeron process. Above the -40°C isotherm the cloud only consists of ice crystals.

4.5 Bright Band

The transition from ice crystal to water drops in the mixed phase at midlevel altitudes can have significant consequences for radar observations. In order to explain the consequence of this transition it is necessary to introduce the radar equation for meteorological targets for a unit pulse volume (Rinehart, 2004). The radar equation returns the received power p_r as function of radar parameters, range and the radar reflectivity factor.

$$p_r = \frac{\pi^3 p_t g^2 \theta \varphi h |K|^2 z}{1024 \ln(2) \lambda^2 r^2} \quad (4.2)$$

where:

p_r: Received Power [mW]
p_t: Transmitted Power [mW]
g: Antenna Gain [-]
θ: Horizontal antenna beam width [radians]
φ: Vertical antenna beam width [radians]
h: Pulse length [μs]
|K|: Dielectric constant [-]
z: Radar reflectivity factor [$mm^6\ m^{-3}$], $z = \sum_{vol} D^6$, where D is drop diameter
λ: Wavelength [m]
r: Range [m]

In connection with estimation of radar reflectivity factor z the drop backscattering cross sectional area is normally assumed to be proportional to the sixth power of the diameter which is defined by the Rayleigh approximation[III].

Most of the parameters in eq. 4.2 are radar specific and can therefore be combined into a constant and a simpler form and for a specific radar the received power, p_r can be written as:

$$p_r = \frac{C_1 |K|^2 z}{r^2} \Leftrightarrow z = C_1 |K|^2 p_r r^2 \quad (4.3)$$

From eq. 4.3 it becomes evident that the strength of echo from an object is proportional to the dielectric constant and the reflectivity factor, z[IV]. The dielectric constant[V] $|K|^2$ of ice is ~0.197 and ~0.93 for water. The reflectivity backscattered to the radar from ice/snow crystals is lower than that of raindrops as result of the lower dielectric constant.

While ice crystals are above the melting layer (0°C isotherm) they fall slowly as result of their mass and size and aggregate to snowflakes. As the snowflakes reach the melting layer they start to melt from the outside and inwards. For a period of time they will have an outer coating of liquid water, but the size of a snowflake as illustrated in Figure 4.6, until they collapse into water drops.

[III] Drops (spheres) falls within the Rayleigh region if they are small compared to the wavelength. Small is usually defined as $D/\lambda<0.1$. When $D/\lambda>10$ the backscattering area is equal to the geometric area. The intermediate region is described by the Mie theory (Rinehart, 2004).

[IV] z can span several orders or magnitude in value, and therefore is z often log-transformed to Z by $Z = 10log_{10}\left(\frac{z}{1\ mm^6\ m^{-3}}\right)$

[V] The dielectric constant varies slightly with radar type and/or temperature (Rinehart, 2004)

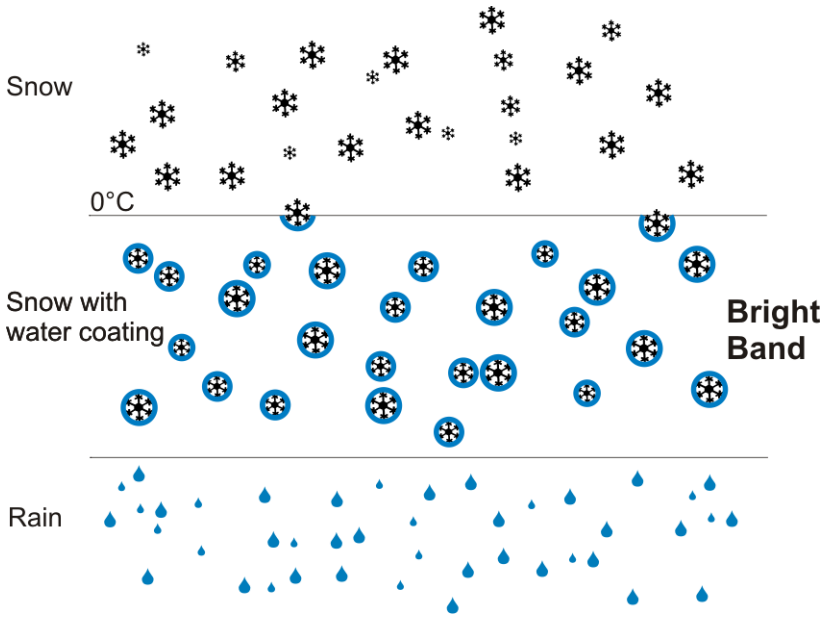

Figure 4.6 Illustration of the transition from ice/snowflakes to raindrops. The radar observes the water covered snowflakes as big raindrops resulting in a strong reflectivity echo. Rain drops are in fact not tear drop shaped, but spherical when smaller than 2 mm and oblate when larger.

The radar observes these water coated snowflakes as big rain drops and the result is a very strong echo since the echo received by the radar is proportional to dielectric constant as mentioned but also to the sixth power of the diameter. The height of the bright band varies since it depends on the location of the 0°C isotherm. Bright band is mostly found in stratiform precipitation (horizontal extent), and is providing information on the location of the boundary between the liquid phase and the mixed phase, which can be useful in connection with the conversion from reflectivity to rainfall intensities. Areas with bright band can lead to overestimation of rainfall intensities in connection with conventional radars, while it is hardly ever observed by LAWR due to the integration of the beam in the vertical direction smoothes out this feature which is normally a few hundred meters thick.

4.6 Precipitation Types

Precipitation is water originating for the atmosphere and reaching the earth, but is can be sub-divided into eight different precipitation types: Drizzle, rain, snow, sleet, freezing rain, snow grains, snow pellets and hail (Ahrens, 2007). In connection with using weather radar for precipitation estimation for use in hydrological applications rain is the primary objective. Drizzle consists of drops with diameters less than 0.5 mm and normally origins from stratus clouds, whereas rain is defined having drop sizes larger than 0.5 mm. The maximum diameter of rain drops reaching the surface is around 6 mm since collisions with other drops tend to break them up and at this diameter they furthermore become unstable and brake apart.

The amount of rain reaching the ground over an interval of time can vary significantly resulting in a wide range of intensities. (Ahrens, 2007) group them into three intensity levels: Light from 0.3-2.5 mm/h, moderate from 2.6-7.6 mm/h and intensities above 7.6 mm/h is heavy rainfall.

Besides difference in intensity rain also varies in duration and spatial extent. Rain originating from convective cumulonimbus clouds can be extremely local (e.g. it can be raining on one side of a house, but not on the other) and result in heavy rainfall intensities. This type of rainfall is commonly referred to as convective rainfall. Rain from layered nimbostratus clouds often covers large areas and has a longer duration than showers originating from cumulonimbus clouds – this type of rainfall is often referred to as stratiform rainfall. Stratiform rainfall can occur as result of frontal uplifting of the air masses resulting in frontal (stratiform) rain or more local as result of changes in topography resulting in orographic rainfall. Even small changes in topography can result in orographic rainfall it is e.g. raining more in the western part of the main Danish peninsula Jutland than in the Eastern part due to upward forcing caused by the "Jyske Højderyg" which is a ridge of less than 200 meters height.

4.7 Drop Size Distributions (DSD)

As shown in Section 4.5, eq. 2.1 the power received by the radar is proportional to the sixth power of the diameter – the radar reflectivity factor z. The radar reflectivity factor is the sum of all drop diameters within a unit volume. Under normal conditions only liquid drops are assumed present and the dielectric constant is fixed. Within a unit volume many different sizes of rain drops exist. This size distribution of the drops is denoted the drop size distribution (DSD) and is an essential issue in connection with calibration (from reflectivity to rainfall intensity) of conventional weather radars.

The first report of rainfall estimation using radar was by (Marshall, et al., 1947), followed by the findings of (Marshall, et al., 1948) which is the most well-known paper in the field of radar meteorology. (Marshall, et al., 1948) proposed a power-law relationship between reflectivity Z and rainfall rate R:

$$z = AR^b \tag{4.4}$$

where:

A: 220
B: 1.6

The A and b values vary and (Battan, 1973) lists more than 60 different sets of parameters and since then many more have been published. The parameters vary with precipitation type – e.g. from stratiform to convective and from climate regime to climate regime. Despite the knowledge of varying DSD the most common approach

in application context still is to apply a fixed set of A and b, and very often the values of the original Marshall-Palmer Z-R relations are used (Lee, et al., 2005). A review of the Z-R calibration used by conventional weather radars and the LAWR specific calibration method can be found in Paper B.

The reflectivity, Z and the rain rate R is related to each other by the DSD which is embedded in the power-law relationship in eq. 4.4. The first attempt to retrieve a DSD used paper sheets covered with flour exposed to the rainfall. By measuring the diameter of the marks left by the rain drops the distribution of the drop sizes were found. (Marshall, et al., 1948) found that except for small drop sizes the DSD could be described by an exponential distribution:

$$N_D = N_0 e^{-\Lambda D} \tag{4.5}$$

where:

N_D: Number of drops in a particular diameter interval in [mm^{-1} m^{-3}]
N_0: The value of N_D for D=0, N_0=8000 [m^{-3} mm^{-1}]
Λ: Slope parameter. $\Lambda = 4.1R^{-0.21}$, where R is rain rate [mm/h]
D: Drop diameter [mm]

DSD has been extensively pursued since those early days of radar meteorology, and today 3D video disdrometers are used to measure DSD. More recent research found that a three parameter Gamma distribution provides a better description of the DSD since it is capable of representing the smaller drops. It was found that in connection with dual-measurement techniques a Gamma DSD lead to significant improvements in the rainfall estimation (Ulbrich, 1983). The Gamma DSD as defined by (Ulbrich, 1983):

$$N_D = N_0 D^{\mu} e^{-\Lambda D} \quad (0 < D < D_{max}) \tag{4.6}$$

where:

N_D: Number of drops in a particular diameter interval in [mm^{-1} m^{-3}]
D: Drop diameter [mm]
N_0: Intercept parameter [m^{-3} $mm^{-1-\mu}$]
μ: Shape parameter [mm^{-1}]
Λ: slope parameter [mm^{-1}]

Many different approaches have been applied for estimating the DSD parameters of the two distribution types. For a detailed review of this work please see e.g. (Ulbrich, et al., 1998) and sources herein, and uncertainties related to DSD measurements with disdrometers can be found in (Lee, et al., 2005).

Since DSD is most often derived from disdrometer data there is a related scaling uncertainty which often is neglected. The Z-R relationship assumes that the estimated

DSD is representative for the whole radar domain and is constant over time. The disdrometer is as the rain gauge, a point measurement being assumed to be representative for a much larger spatial domain. Even if a vertical radar is used for DSD parameter retrieval, the spatial extent of the measurement is small compared to the rainfall field. Furthermore, the DSD is most often observed at ground, while the conventional weather radar observes at several different altitudes where the drop sizes change as function of altitude, temperature, pressure and cloud thickness.

The DSD estimation and uncertainties related to it is only of interest in connection with calibration of conventional weather radars, since the LAWR uses a different calibration approach without the assumption of the DSD as outlined in Chapter 5.

CHAPTER 5

Local Area Weather Radar

The Local Area Weather Radar (LAWR) is a small scale weather radar intended as supplement to rain gauges primarily in urban areas or ungauged catchments. The LAWR is developed and manufactured by DHI, and is also used for precipitation related research projects such as snowfall monitoring of the Klein Matterhorn glacier in Switzerland and the study of climate gradients and erosion processes in the Cordillera de San Francisco, Southern Ecuador. Lately, the LAWR technology is being used for studying bird migration patterns prior to off-shore wind farm installations and in the near future in connection with optimization of offshore wind mill operation.

The focal point of this PhD project has been rainfall estimation with LAWR and issues related to applying LAWR estimated rainfall to hydrological applications. This chapter provides background information on the LAWR system and the data processing methods.

5.1 The history of Local Area Weather Radar

The first Local Area Weather Radar was developed in 1999 as part of the EU Esprit 23475 project. The title of the project was *"High Performance Rainfall Radar Image Processing for Sewer Systems Control"* and the aim of the project was to *"provide short term rainfall prediction system optimally supporting decision makers operating sewage systems and wastewater treatment"*. The project involved 3 cities: Malmo

(Sweden), Paris (France) and Genova (Italy), and the original intent was to use radar data from the existing weather radars close to those cities. For Malmo and Paris there were no problems with data accessibility, but for Genova there was a problem. The radar to be used was located in Piedmont and owned and operated by the military and they would not release the radar images before they were cleared. It was not achievable to make a two hour precipitation forecast based on 24 hour old radar images, and therefore this radar was abandoned.

Instead the Danish Meteorological Institute and VKI (Danish Water Quality Institute), which was later merged with DHI, decided to develop a small weather radar based on a marine X-band radar. In 1999 the general opinion among researchers were that X-band technology was inadequate for precipitation measurements since the wavelength is heavily attenuated by precipitation. Only a few radar scientists were trying to use X-band for surface precipitation estimation, among those Geoff Austin and Isztar Zawadzki, however, it was not generally regarded as being a solution worth pursuing due to the limited range and the attenuation issue. X-band radars were mostly used as vertically pointing radars in atmospheric research projects focusing on drop size distributions.

In order to keep the development costs down it was decided to base the weather radar on an existing radar and only develop the necessary software and A/D converter. The system was designed as illustrated in Figure 5.1 with one PC handling the signal processing and another PC for the communication and data storage.

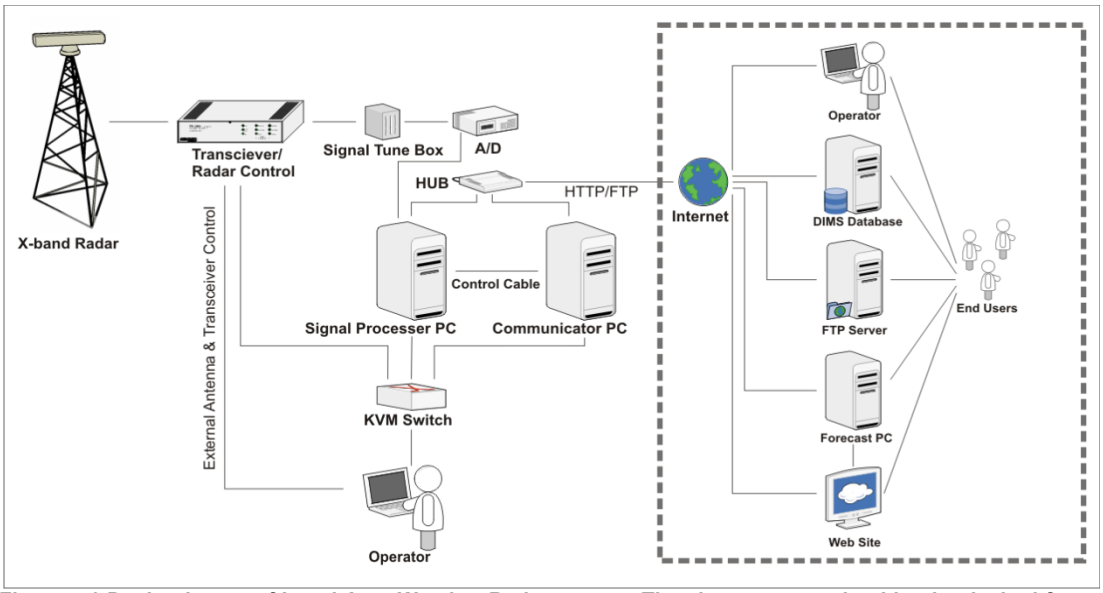

Figure 5.1 Design layout of Local Area Weather Radar system. The elements contained by the dashed frame are optional add-ons and all require an internet connection to the LAWR installation

The system can be operated remotely via an internet connection and the communication PC. The data format was based on the format of the data from the

Ericsson radars operated at that time by the Danish Meteorological Institute in order to facilitate use of existing software for data processing.

Signal processing algorithms were developed for attenuation correction along with general signal processing such as conversion from the raw data in volt to the Cartesian output files accessible to the user. The receiver in a LAWR is a logarithmic receiver, and thereby the received signal is already log-transformed prior to the signal processing. This is different from conventional weather radars which are equipped with linear receivers and therefore the signal is log-transformed afterwards from z to dBZ.

All hardware components used in the LAWR system are standard components except for the A/D converter which was designed and developed during this project. The signal is the raw video signal from the radar which is being processed by the signal processing PC (DOS operating system). The reason for using DOS was due to a high demand for speed since every 5 minutes 691 MB of data need to be processed before being pushed to the communication PC (Windows).

The first operating LAWR was installed in 1998 in Piedmont, Italy as part of the Esprit project after a test period in Aarhus, Denmark. The installation in Piedmont, where shortly after followed by a permanent LAWR installation in Aarhus, Denmark

Figure 5.2 The first LAWR installation in December 1999, Aarhus, Denmark

Since 1999 more than 25 LAWRs have been installed worldwide for various purposes ranging from precipitation related research to real time online warning system to citizens in cases with is risk of flooding. Others were installed in relation to high precision farming in Australia and Denmark and others again as supplement to rain gauges in urban areas. A short description of all LAWR installations can be found at http://radar.dhigroup.com. Since 2008 ten LAWRs for bird migration studies has been deployed in Denmark and of those ten there are four installations with both a horizontal and a vertical scanning radar operating simultaneously.

The LAWR system as it is today is illustrated in Figure 5.1. The overall structure today is identical to the original design, but several features have been added over the years, e.g. a scaling box which enables better use of the raw video signal and extra algorithms for handling beam filling issues. In the near future development of the next generation LAWR will start, enabling faster signal processing by use of FPGA (Field-programmable Array Gateway) and thereby reducing the number of PC's to one and enabling faster data processing.

In the past few years a paradigm shift has been ongoing since the large pixel sizes of S-band and C-band radars in connection with the lowest beam height being high above the surface causing problems with detection of near surface phenomena has increased the interest in using X-band radars as weather radars. Before 2005 only LAWR existed as an operational commercial X-band weather radar system. A few research institutions were using vertical pointing X-band radars for drop size distribution experiments, but only a couple was attempting to use X-band radars for rainfall estimation in the horizontal plane. The reason was that the attenuation at 3 cm wavelength caused by rain was considered to be too severe, completely ruining the opportunities to measure rainfall. By 2005 the Collaborative Adaptive Sensing of the Atmosphere (CASA) project was launched in USA and since then the interest towards using X-band radars for weather purposes has increased significantly. The CASA project aims at constructing distributed network of low-cost, low-power solid state radars with Doppler, dual-polarization and facilities for dedicated sector scanning. The goal is to construct a nationwide network covering the United States (Brotzge, et al., 2005), (Donovan, et al., 2006) among others. Beside the DHI LAWR several other commercial X-band weather radar systems exist today, e.g. the HYDRIX by Novimet (Bouar, et al., 2005) and the RainScanner from Germatronic (Gekat, et al., 2008). They overall share the X-band characteristics such as 3.2 cm wavelength, but differ on a range of specifications such as antenna type (dish vs. fan beam), receiver, Doppler, dual-polarization, spatial and temporal resolution of output, range and price. The Doppler and dual-polarization techniques used by conventional weather radars are thoroughly described in e.g. (Doviak, et al., 2006).

5.2 The LAWR system

There are presently two types of LAWR – a 4 kW and a 25 kW version. The 4 kW is only used for research projects whereas the 25 kW version is the standard version. For the future reference the 4 kW will be denoted 4 kW LAWR whereas the 25 kW just LAWR. The systems are almost identical – the City-LAWR is a downscaled version of the LAWR using the same signal processing software. Due to the reduced power the range is only 30 km, but as result of a shorter pulse length the spatial resolution of the output is a higher ranging from 50x50 to 250x250 meters.

The LAWR has two output parameters – reflectivity and variance. The most used of these are the reflectivity parameter. C-band or S-band weather radars can have a range of output parameters depending on of dual-polarization and Doppler techniques. The LAWR is not facilitating any of these features, however, the LAWR has never been intended to substitute these types of radars. The aim is to try to fill the huge spatial domain gap between a rain gauge (~200 cm^2) and conventional weather radar (1-4 km^2) a scale difference of several orders of magnitude. The LAWR provides output from 0.01 km^2 to 0.25 km^2.

5.2.1 System specifications

Examples of LAWR installations can be seen in Figure 5.3 and Figure 5.4 along with control equipment installed at ground in Figure 5.5. The system data are listed in Table 5.1.

Figure 5.3 City-LAWR installation. Temporary installation at J. S. Marshall Radar Observatory, McGill University in the fall of 2007.

Figure 5.4 LAWR installation at the Klein Matterhorn, Switzerland. The LAWR is used for research by ETH Zürich, Institute of Environmental Engineering (IfU)

Figure 5.5 Example of the equipment at ground. The radar monitor, 2 PC's, screen and keyboard are all fitted into a rack.

The LAWR is based on marine Furuno radars, which are designed to operate under harsh conditions on ships at sea making the LAWR system very robust and suitable for almost any climate. The full review of the antenna and other Furuno parts can be found in (Furuno, 2002).

Table 5.1 System data for the LAWR system

	City-LAWR	LAWR
Peak Power [kW]	4	25
Wave length [cm]	X-band 3.2	X-band 3.2
Pulse length [μs]	0.8	1.2
Antenna	0.61 m radome	2.5 m slotted waveguide array
Receiver	Logarithmic receiver	Logarithmic receiver
Vertical opening angle Horizontal opening angle	± 10° 3.9°	± 10° 0.95°
Samples pr. rotation	450	360
Range (forecast/QPE) [km]	30/15	60/20
Spatial resolution [m]	250x250 125x125 50x50	500x500 250x250 100x100
Temporal resolution [minutes]	1 or 5	1 or 5
Scanning strategy	Single layer and continuous scanning	Single layer and continuous scanning

5.2.2 Scanning Strategy and Beam Characteristics

Conventional weather radars are large infrastructural installations with a 5-8 meter diameter dish antenna covered by a radome mounted on a tower. The LAWR differs from conventional weather radar by a much smaller fan beam antenna, less peak power, receiver type, shorter range but higher temporal and spatial output resolution.

A LAWR scans continuously with a rotation speed of 24 rounds per minute at 0° elevation angle. The output is the integrated signal of the sampling period of either 1 or 5 minute. This differs significantly from the scanning strategy of conventional weather radars which normally scan 360° at one elevation angle and then the antenna is tilted to the next elevation for the next 360° scan and so forth. The full cycle takes between 5 and 15 minutes to complete and the number of elevations depends on the system and the operators behind it. The benefit of this method is discrete sampling in the vertical volume and thereby information about the location of the bright band, melting layers etc. The drawback is that a specific point of interest at the surface (e.g. over a rain gauge) is only sampled once at each elevation. If the scanning takes 15 minutes with 24 elevations it results in a time span between the samplings over the point. This can introduce large uncertainties since the precipitation may have moved up to 1 km[I] during the scanning cycle and thereby not equal to the precipitation at the surface observed by a rain gauge. Furthermore, the variability in the rainfall in both the vertical and horizontal plane will add to the uncertainty when creating 2D surface precipitation maps based on a multiple angle scanning strategy.

The vertical opening angle of ± 10° is large compared to traditional weather radars which normally have a pencil beam of ~1°, but they can vary from 0.5-2.9° (Rinehart, 2004). Effective is the vertical opening angle 10° since the lower 10° of the beam is

[I]E.g. if wind speed is 10 m s^{-1} which gives 900 m over 15 minutes.

cut-off either by use of natural blocking features such as walls or treetops in the intermediate vicinity of the radar or by a mechanical clutter fence. The principle of the effective vertical opening and the clutter fence is shown along with an example of such installation in Figure 5.6.

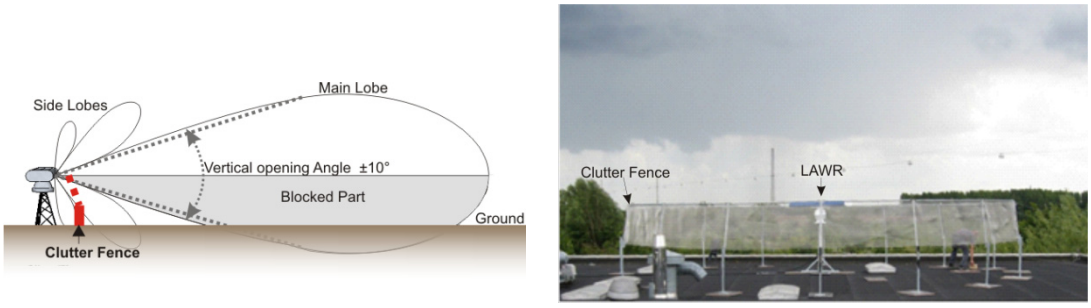

Figure 5.6 Clutter-fence design principle on the left and example from Hvidovre Denmark on the right. The mesh is tilted a few degrees towards the radar in order to avoid the signal to be mirrored back in the receiver.

The effect of the large vertical opening is illustrated in Figure 5.7 where the lowest beam height and the beam top are shown as function of range. The beam height, h above surface has been estimated by eq. 4.1 in Chapter 4 and the pulse volume, V in Figure 5.8 estimated by (Rinehart, 2004):

$$V = \frac{\pi r^2 \theta \phi h}{16 \ln(2)} \tag{5.1}$$

where:

V: Pulse Volume [m^3]
ϕ: Vertical opening angle [radians]
θ: Horizontal opening angle [radians]
h: Pulse length [m]

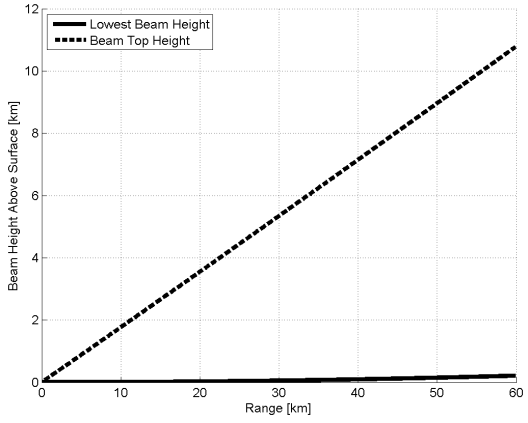

Figure 5.7 Lowest beam height (solid) and beam top (hatched) as function of range. The beam heights are the same for both City-LAWR and LAWR as they both have a ± 10° vertical opening angle.

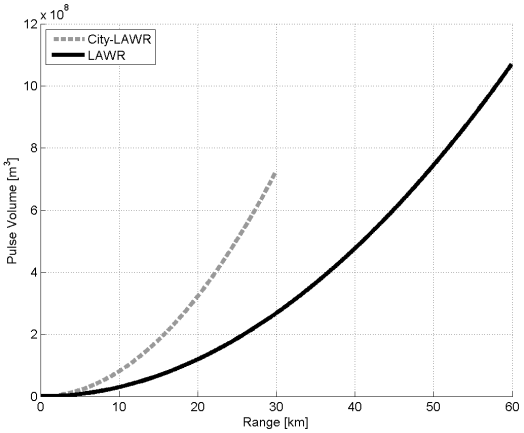

Figure 5.8 Pulse volume as function of range for both the 4 kW LAWR and the standard LAWR.

The rapidly increasing beam height is the weakness of the LAWR system since it results in large pulse volumes as illustrated in Figure 5.8. It results in risk of underestimating low hanging precipitation due to the fact that only a fraction of the beam is filled in the vertical extent as illustrated in Figure 5.9. The vertical extent of precipitation yielding clouds varies greatly and depends on the cloud types. Light precipitation is often from nimbostratus clouds extending from the surface and up to 3 km, while cumulonimbus clouds can reach a vertical extent of more than 20 km. Cumulonimbus also happens at lower altitudes such as 5 km. The beam filling percentage depends on the cloud top height, and in Figure 5.10 the filling degree as function of range is shown for three different cloud top altitudes.

The underestimation is a result of the LAWR integrating over the whole vertical extent of the beam, which means that a given number of raindrops will result in less echo at increasing range as illustrated in Figure 5.9. This problem is furthermore aggravated since light low hanging precipitation often consists of small drops, while strong convective rainfall is made up of larger drops. The reflectivity caused by a large number of small drops is smaller than that of a few large drops even though the water content is identical due to the reflectivity is proportional to the sixth power of the drop diameter.

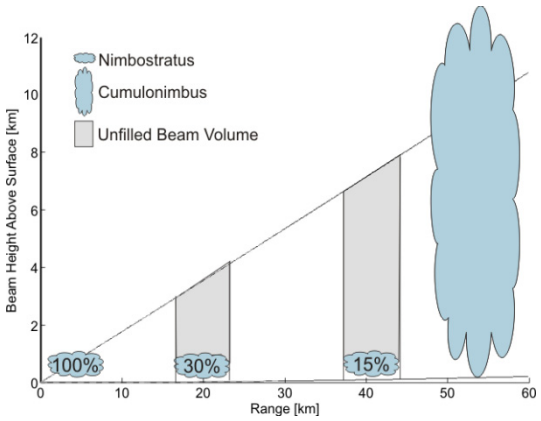

Figure 5.9 Illustration of LAWR beam filling issue in relation low hanging nimbostratus clouds (1000 m cloud top) and illustration of how a cumulonimbus cloud can fill the beam even at maximum range.

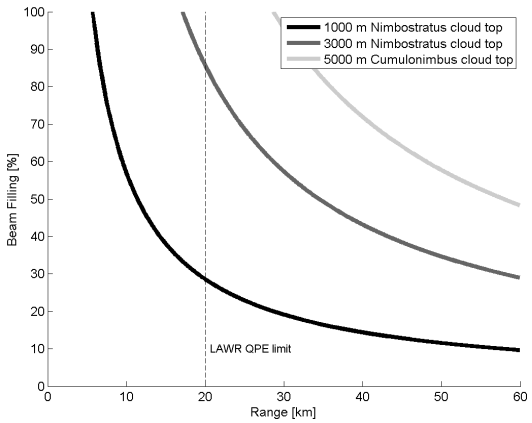

Figure 5.10 Beam filling degree in percent for different cloud types and with different cloud top heights. The 5000 m cumulonimbus cloud top is for a low cloud – they can reach up to more than 12,000 meter in altitude.

X-band radars are characterized by their short ranges which are normally considered a drawback, however, the benefit is that they observes near surface phenomena such as tornadoes very well, contrary to traditional weather radars which only can observe near surface phenomena's very close to the radar. At 240 km range the lowest beam height is approximately 3.4 km due to the curvature of the earth (at the lowest elevation angle).

The obvious solution to the limited range problem is to construct a network of multiple X-band radars with overlap at far ranges. The early phases of such network concept based on LAWRs have been exploited. The idea is to construct a network of LAWRs which allows for automatic real-time inter-communication in the network and from other types of sensors such as rain gauges or other radars. The first LAWR observing precipitation should then cascade the information to the other LAWRs in the network and thereby facilitate the selection of the appropriate calibration factors. Furthermore, the idea is to allow for inter-calibration and inter-attenuation correction parameters to be exchanged from LAWR to LAWR. The concept is described in more detail in Paper H. The implementation of such a network was discovered to be more time-consuming than first estimated and therefore only the concept has been addressed in this PhD project. Presently all LAWRs are operated as independent installations, but this could change in the future. One obstacle that would need to be overcome is ownership issues since the LAWRs in Denmark today are owned by different municipalities and operated by them on individual basis. A solution could be to let the municipalities be the purchaser and owner, but let a third party, e.g. Danish Meteorological Institute, handle the service, data storage and data quality control. Users can then get access to the data for a fee. The official Danish rain gauge network is operated in the same manner so the organization could be extended to include LAWR.

Some of the main principles of the network project has been taken over by a new Danish research project: The Storm and Wastewater Informatics Project. The overall aims of the project are: *"to close the knowledge gaps within prediction and control of current and future conditions in integrated urban wastewater systems, and major outputs will be components of an intelligent real-time decision support system, following a drop of water from the cloud, throughout the sewer–wastewater treatment system and into the receiving waters"* (SWI, 2008). The project is a joint research project between Aalborg University, Technical University of Denmark and The Danish Meteorological Institute and three partners from the industry (DHI, Krüger and PH-Consult). One of the subprojects is to create a nested forecast system based on a network of LAWRs combined with the existing network of C-band radars.

5.3 Installation and Operation

Prior to installation of a LAWR a few things need to be considered. First of all the necessary permits and licenses must be obtained. In most countries it is necessary to obtain a broadcasting license prior to installation of a LAWR. Under normal conditions this is not a problem since the LAWR broadcasting frequency is the same as most ship radars. If the LAWR is installed on a tall mast in an urbanized area it may be necessary to get an exemption from prospective zoning laws. It should furthermore be pointed out that good and clear communication to the public can be vital, since the same people happily sitting in a harbor a whole day surrounded by

ship radars may object to having a radar in their neighborhood. If the purpose of the LAWR is clearly communicated along with the fact that the LAWR only is a hazard if you are close enough to be hit by the rotating antenna it can prevent many potential problems. The installation process along with verification of the orientation is reviewed in the next sections along with the magnetron requirements.

5.3.1 LAWR Site Selection

The short range of the LAWR, 60 km for forecast and 20 km for quantitative precipitation estimation (QPE), requires that the LAWR is installed close to the area of interest, e.g. a city. The location most often suggested is on the highest building in the centre of the city. This is a poor solution for two reasons. First of all the rooftops of the surrounding buildings will cause massive ground clutter and thereby contaminate the signal over the area of interest. Secondly, the LAWR cannot observe rainfall right above itself and therefore the inner pixels will yield zero. The solution is therefore to find a site just outside the area of interest with an unobstructed view and as clutter free as possible. The LAWR can be placed on a mast, but a flat rooftop is preferred for several reasons. First of all the access to the antenna unit is easier and thereby the accessibility to the magnetron which requires replacement at regular intervals. A mast location requires a lift and most often the presence of two persons instead of just one which increases the maintenance costs. Secondly, it is easier to install a clutter fence, as illustrated in Figure 5.6, on a flat roof, and finally the building often provides suitable indoor facilities for the rack with the two PC's along with the required electrical power.

The site selection is a two step procedure where the first step is to look at geographical maps and aerial photographs (e.g. Google Earth) and locate potential sites. Next the selected sites normally are evaluated with the use of a 2 kW LAWR as illustrated in Figure 5.11 on a dry day. Besides the unit shown a portable installation exists, where everything is fitted into a large crate which can be carried as luggage on an airplane for site inspections abroad.

Figure 5.11 Example of site location test with use of a 2 kW X-band radar mounted on a mobile lift to the left. On the right a look at the mobile signal processing unit used for site locations.

The lift is extended at each potential site and the radar is left scanning for a short while. Based on the echoes observed in dry weather it is possible to determine the level of permanent clutter and blocked sectors. Besides clutter and beam blockage, access to a power outlet, internet accessibility and housing options for the cabinet with the two PC's (see Figure 5.5) also needs to be considered. The perfect site rarely exists, so the different drawbacks and virtues must be weighed against each other in each case in order to select a suitable location for the installation. In many cases the financial aspect related to setting up power, internet and housing facilities at an uncovered location is of such magnitude that such site would be rejected.

5.3.2 LAWR Installation: Procedure and Requirements

In principle the LAWR only requires three things for operation – power, a place to mount the antenna and an indoor room suitable for computers. The LAWR operates on the regular power-grid, but the antenna unit requires a ground connection. The cabinet must be placed in a location suitable for computer equipment with sufficient ventilation and relatively free of dust. It is possible to equip the cabinet with air-condition and particle filters, which is necessary if the cabinet is placed in locations where the temperature can be outside the +10°C to +35°C range.

The installation of a LAWR compared to that of a conventional weather radar is normally a simple job taking a single day. The exception is in cases where a mast or tower needs to be erected beforehand. Normally, the antenna unit is put in place first on a tripod as shown in Figure 5.6 followed by the clutter-fence if such is a part of the installation. The clutter-fence is assembled on site. Next step is to connect the antenna to the cabinet by the antenna cable. When the system is powered up and working an appropriate set of cluttermaps is collected and applied along with a general adjustment of the parameters.

A LAWR installation does not require an internet connection to work, but experience shows that in order to keep a LAWR running in a satisfying manner a daily inspection of the state of the systems is required. This is easily facilitated by remote access through an internet connection, and the latest version of the LAWR enables full accessibility to system components by remote access. The settings of the Furuno radar is accessed by the build-in panel, but it is possible to view the radar monitor remotely. An internet connection is furthermore required in order to utilize the optional add-ons in Figure 5.1.

In 2008 DHI had several LAWR installations running for consecutive months in remote locations not fulfilling the normal installation requirements outlined above. For instance a LAWR was installed on the stump of a not yet erected offshore windmill in the North Sea using a generator, special designed cabinet and wireless internet modem so it is possible, but also very demanding in terms of financial

resources for inspections and refueling. For a permanent LAWR installation this is not the optimum solution, but it can be done.

Orientation of LAWR

One of the most critical points in the installation is to get the physical orientation of the antenna unit correct. The antenna unit has a North indicator which determines the orientation of the radar in the sense that the first scan-line will be originating from here. The internal orientation of the antenna is often not precisely adjusted from Furuno so the first scan-line origins $\pm$ ~5° from the north arrow on the antenna unit. The LAWR software allows for a mathematical post-adjustment of the orientation so it can be adjusted if misaligned during the installation. If the misalignment is 90°, 180° or 270° the error is easily recognized since rainfall will be moving in the wrong direction and identifiable clutter would be in complete opposite directions of expected. It can be difficult though to identify a few degrees misalignment, but it will have a significant impact on data analysis results.

The ideal method would be to have a mobile transmitter/reflector e.g. a microlink which could be placed in a fixed location. It would thereby be possible to confirm the orientation or correct it in the software by locating the echo from the transmitter/reflector. This option is normally not available in connection with a LAWR installation, but there are other methods for verifying the orientation. At most locations there are objects causing clutter in fixed locations such as a tall/large construction, wind farms, shorelines or even the steam from a power plant can be seen as an echo in dry weather. By accumulating the observed values over 24 hours or more of dry weather the echoes from the clutter will be clearly evident. By correlating the dry-weather image with a background map containing the elements it is in most cases possible to verify the alignment. As illustration the orientation of the Aarhus LAWR is examined. First geographical coordinates of known clutter causing objects are indentified and converted to pixels as shown in Figure 5.12. The ridge on Samsø is here used for the correlation, while Tunø (small island with a rigde) and the wind farm are used for verification. The two other points Himmebjerget and Yding Skovhøj are used for verification of the process of converting the geographical coordinates. It should be noted that it is important to use objects some distance away from the radar in order to obtain a credible angle.

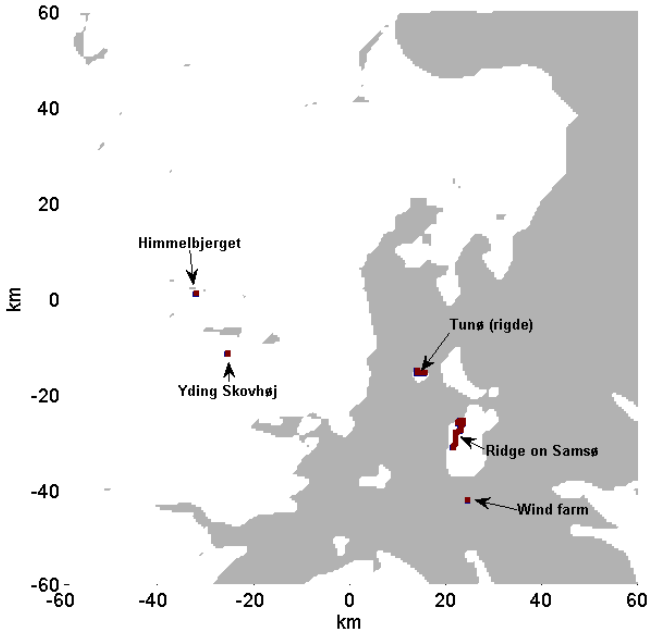

Figure 5.12 Clutter correlation map of the Aarhus LAWR coverage area. The background map is 0/1 values while the clutter areas is assigned a value corresponding to the accumulated clutter values.

When the accumulated dry-weather period echoes are overlaid the background image with clutter objects it becomes evident that the Aarhus LAWR was off in orientation. By rotating the dry-weather image one degree at the time counter-clockwise and each time computing the correlation of the clutter with the clutter objects on Samsø and verifying the results using the wind farm and Tunø it was found that the Aarhus LAWR data must be rotated 5 degrees counter-clockwise. The analysis was carried out on 2007 and 2008 data resulting in the same rotation.

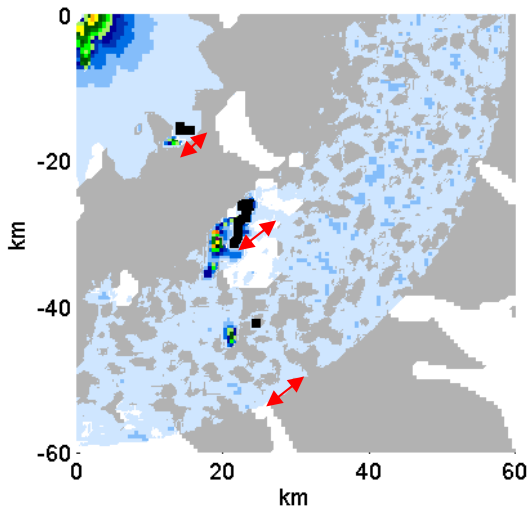

Figure 5.13 Accumulated echoes overlaid the background map with clutter objects. Only the fourth quadrant is shown.

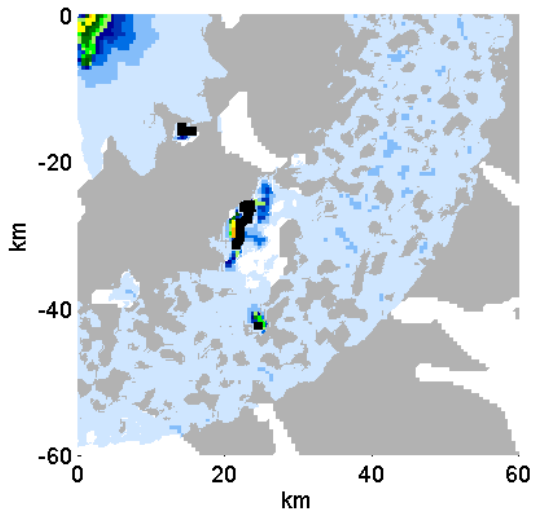

Figure 5.14 After 5 degrees counter clockwise rotation of the accumulated echoes.

The process outlined here is straightforward and an easy way to verify the LAWR installation. A misalignment error will have impact on calibration since the pixel being compared to the rain gauge is not on top of it, and if the distributed data is used as input to an application the results will be affected.

5.3.3 Magnetron replacement

The pulsed radio frequency being emitted from a radar is generated by the transmitter and then carried up to the antenna by the waveguide. The duplexer module switches from receiving mode to transmitting mode for the brief duration of the transmission and then back to the receiving mode. Most of the time the radar is listing for echoes being scattered back from the emitted pulses. If there was no duplexer in the system two antennas would be required as result of the orders of magnitude difference of the power in the transmitted signal versus the received signal. The general principle of a radar, including the LAWR is illustrated in Figure 5.15.

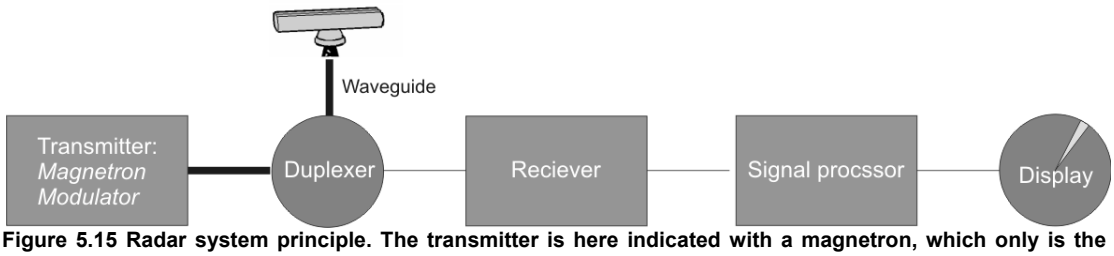

Figure 5.15 Radar system principle. The transmitter is here indicated with a magnetron, which only is the case in some systems (mostly marine radars). Conventional weather radars are most often using a klystron transmitter.

Being based on a marine radar the LAWR uses a magnetron for signal generation and the quality of the rainfall estimation strongly depends on the magnetron condition. The manufacturer of the radar guarantees a magnetron lifetime of 2,000-3,000 hours (83-125 days) (Furuno, 2002) since sporadically there is a magnetron with this lifetime, but according to Furuno the lifetime will in most cases be longer. During the development of the LAWR it was found that a magnetron lasted 8 months (~244 days) and this is the replacement interval normally used in connection with LAWR.

During the work presented in Paper B it was discovered that the magnetron decreases more rapidly than earlier believed. To illustrate the consequence of running the LAWR with a magnetron decreasing in effect, the accumulated reflectivity's from pixel 123,140 are compared (relatively) with the Aarhus regional rainfall depth in mm from (DMI, 2008). The months from January to November 2008 are plotted in Figure 5.16. Some months the LAWR and the regional estimate agree within the expected variations as result of comparing a single pixel with a multi gauge regional estimate, while in other cases the LAWR clearly underestimates. There is strong evidence of the magnetron being worn out from sometime in March until the magnetron replacement on 30th June.

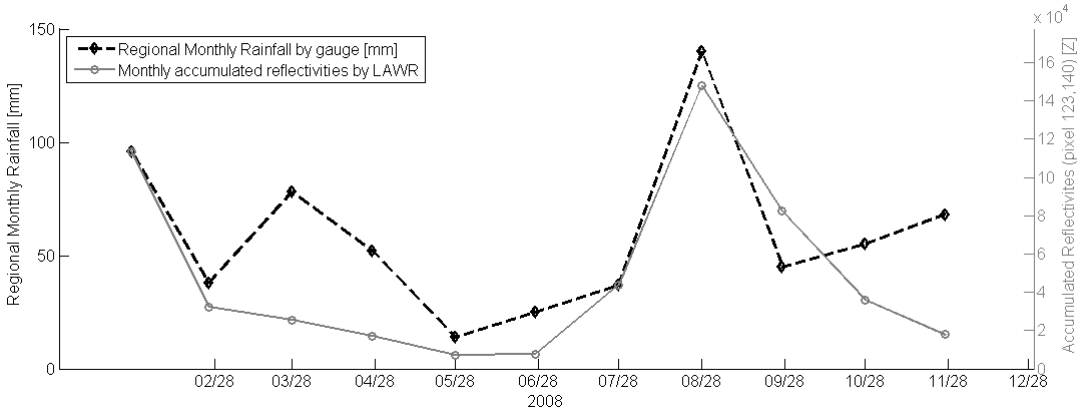

Figure 5.16 Accumulated regional rainfall for the Aarhus region on monthly basis reported by (DMI, 2008) compared to the monthly accumulated reflectivity's from pixel 123,140 (500x500 meter grid of Aarhus LAWR) on the right axis. The marker indicating the accumulation for a given month is placed at the last day of the month.

Unfortunately, there is no record of when the magnetron was changed prior to 2008, but a reasonable guess would be late November since the normal procedure is to replace the magnetron every 8 months. Based on Figure 5.17 there is evidence that the interval between magnetron replacing is too long since the Aarhus LAWR is relatively underestimating compared to the regional rainfall estimated by gauges in periods where the magnetron is more than 3 months old.

To confirm the above which is only based on the accumulations of a single pixel the accumulated reflectivity's for the months of June to November for the inner 20 km range of the Aarhus LAWR are shown in Figure 5.17. The corresponding regional rainfall depths reported by DMI is: June 25 mm, July 37 mm, August 140 mm, September 45 mm, October 55 mm and November 68 mm (DMI, 2008).

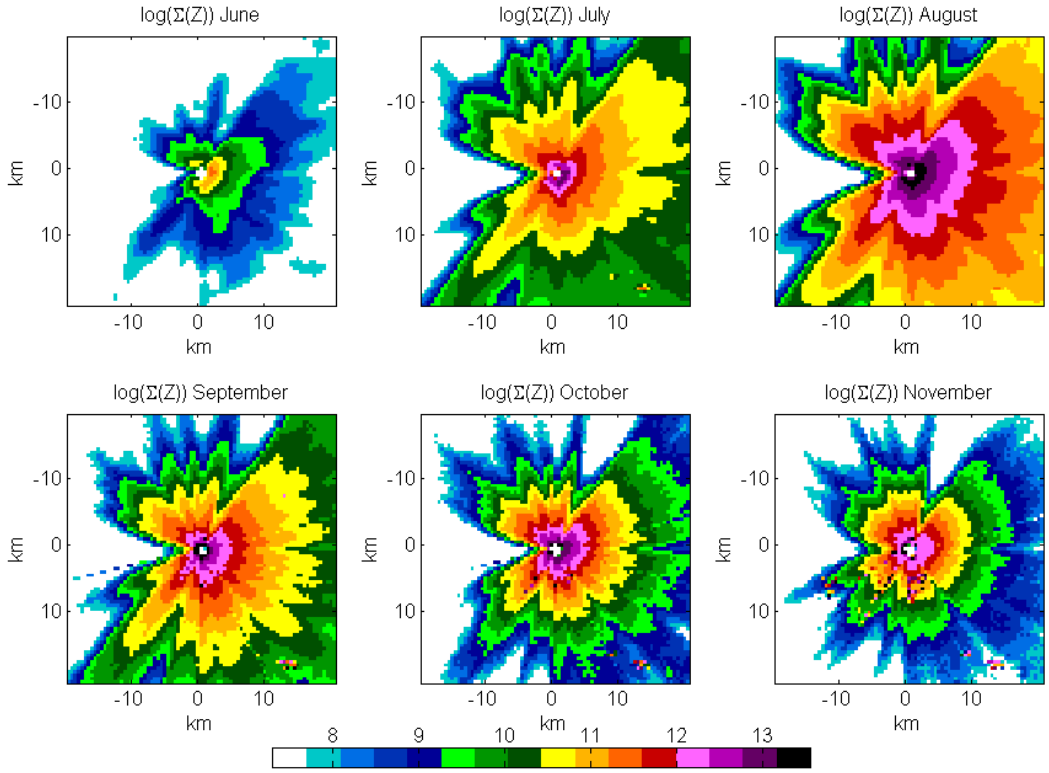

Figure 5.17 Accumulated reflectivity's for the months of June-November for the Aarhus LAWR at lat. 56° 5.790'N, long. 10° 12.317'E. Only the inner 20 km is shown. Please note the values have been log-transformed for plotting. The corresponding regional rainfall depths reported by DMI is: June 25 mm, July 37 mm, August 140 mm, September 45 mm, October 55 mm and November 68 mm (DMI, 2008).

For the month of June the LAWR only observes rainfall at short ranges and the level of reflectivity corresponding to a weak magnetron which is known to be the case. July has several orders of higher level of reflectivity at much further ranges even though the regional rainfall estimate is only 50% larger than that of June, but the magnetron is new. The months October and November have lower reflectivity level than September even though the regional rainfall estimates for October and November are higher than September. This furthermore indicates after 3 months' lifetime the magnetron output level starts to decrease more rapidly than during the first three months. The LAWR is still capable of detecting rainfall with a more than 3 month old magnetron, but the quantitative rainfall estimates will be affected. The magnetron condition is of utmost importance for the LAWR's ability to estimate rainfall. As result a given rainfall intensity from a period with a weak magnetron will be underestimated.

The decrease in magnetron effect can be handled by either changing the magnetron every 3 months or by amplifying the magnetron effect. The magnetron effect level can be monitored and thereby controlled. Currently a magnetron condition parameter based on the whole range is available, but it is not used for controlling the magnetron output level. By constantly monitoring the dry-weather echo of known ground clutter

at some distance – e.g. at the 20 km range used as QPE limit and comparing the level of echo with a reference value obtained with well functioning magnetron the magnetron intensity can be amplified as it starts to wear out, thereby increasing the lifetime to more than 3 months. This can furthermore be useful in connection with a brand new magnetron since the first few days it is extremely powerful and thereby emitting more than normal – this would also be possible to adjust for by the magnetron monitoring process outlined here. The automatic magnetron adjustment has not yet been implemented, but is in the pipeline for future installations.

5.4 LAWR Signal Processing

The signal processing converting backscattered energy to data files can be broken down into four parts: Reception, A/D converting, data processing and data storage. The primary part of the signal processing is done by the Signal Processor PC, cf. Figure 5.18 where the digitalized voltage signal is processed into reflectivity values. Every minute 120 mega byte of raw data is processed, and at the end of each scanning cycle (1 or 5 minutes) the 120/600 mega byte of data is pushed to the Communicator PC for final processing and data storage. During the signal processing the data is applied to a number of schemes in order to handle well-known radar obstacles, e.g. clutter and attenuation. The major processes will be reviewed in detail in Section 5.4.1 (attenuation), Section 5.4.2 (volume correction) and Section 5.4.3 (clutter removal).

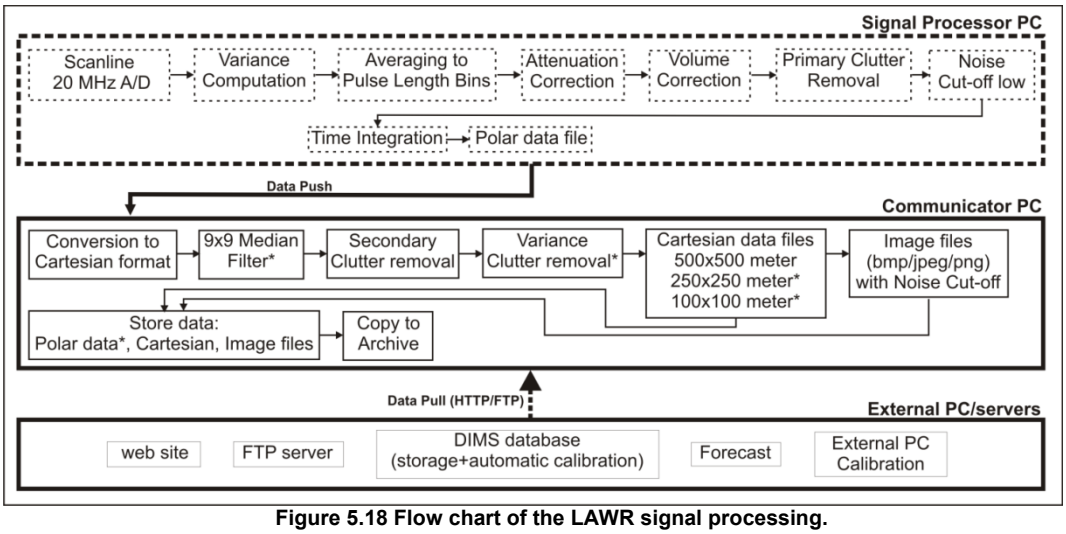

Figure 5.18 Flow chart of the LAWR signal processing.

The parameters used in the algorithms on the signal processing PC can be changed by the user via the Communicator PC. Some of the values are given in a txt file while others are controlled by the radar control software interface. The software interface provides the operator with a range of control options for the LAWR system such as start/stop the scanner, reload the Signal Processor PC, create new clutter-maps. Furthermore, the interface providing the operator with a series of data plots of

significant parameters such as the variance of the raw signal in each pixel, the primary and secondary clutter-maps, the raw image and the processed images for assessing the status of the system. In addition it is possible to see the magnetron condition as a function of time (based on the full range), a single user selected scan-line and the applied volume correction scheme.

5.4.1 Attenuation Correction

Any radar will be subject to attenuation since electromagnetic radiation passing through a medium will be reduced depending on the type of media. The attenuation depends on frequency, wavelength and medium travelled through. In connection with weather radars attenuation is caused by atmospheric gasses such a nitrogen, oxygen and water vapor in the atmosphere. The attenuation caused by atmospheric gases is not considered a significant problem for radar operating at frequencies less than around 10 GHz and can most often be neglected (Rinehart, 2004).

The attenuation by clouds varies a lot since clouds vary from thin to thick and can be made up of ice, water or mixture. (Rinehart, 2004) states that the cloud attenuation would be 10 dB for a one-way path of 25 km assuming a temperature of 20°C and a liquid water content of 4 g/m^3. The effect of cloud attenuation can be hard to address since the LAWR cannot detect clouds, but only falling raindrops, however, it will contribute to the overall loss of signal power as result of attenuation. The major attenuation source is rain, and especially X-band radars are affected as result of their wavelength and frequency, while S-band radars are normally considered unattenuated as result of a 10 cm wavelength. C-band radars operating at frequencies and wavelengths between the X-band and S-band is affected in some manners, but the lower cost of the C-band technology compared to S-band makes it the most favored weather radar choice.

Until a few years ago X-band radars were considered inadequate as weather radars as result of the attenuation problem. This attitude is changing and substantially amount of research regarding X-band radars are focused on the attenuation problem. Especially research conducted under the American CASA project is strongly focused on handling the X-band attenuation issue (Liu, et al., 2007). The approach used by the CASA project and the Hydrix system (Bouar, et al., 2005) is not feasible for the LAWR since it is not a dual-polarized Doppler radar. The LAWR attenuation algorithm was developed along with the LAWR and is enhancing the signal proportionally to the amount of power used at a given range without changing the properties of the rain event when observed from both sides as shown on Figure 5.19. If too much correction is applied the rainfall intensities will be over-enhanced with increasing range from the radar and vice versa in case of inadequate correction.

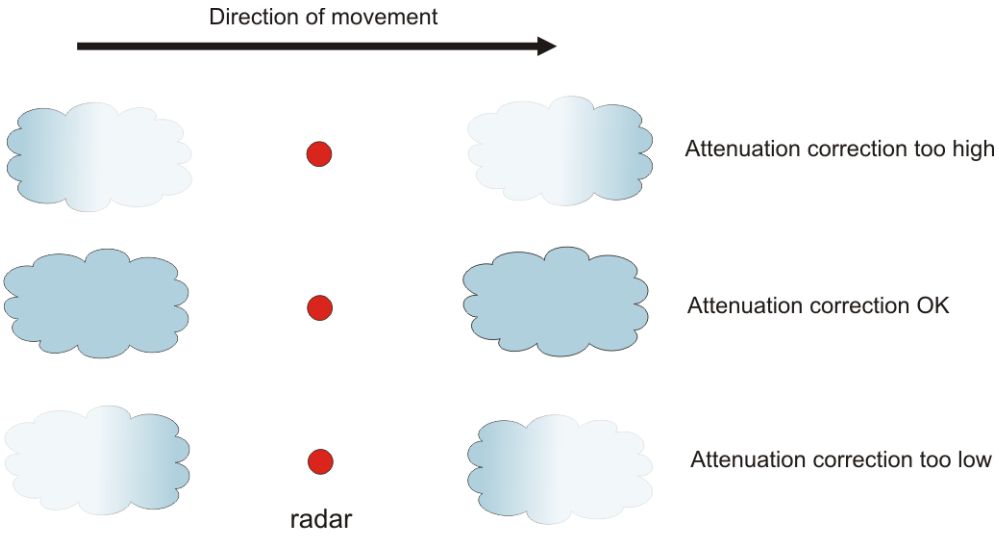

Figure 5.19 Illustration of LAWR attenuation correction principle. The cloud symbolizes a rainfall event observed at two different time steps – before and after passing over the radar.

The attenuation correction is applied en-route of each raw scan line.

$$Z_r = Z_{g,r}\left(1 + \frac{\alpha \sum_{i=0}^{r-1} Z_i}{C_1 \cdot n_{samples}}\right) \quad (5.2)$$

where:

Z_r: Adjusted reflectivity value at range r
$Z_{g,r}$: Uncorrected reflectivity at range r
$n_{samples}$: Number of samples in a single scan line, typical value is 8000
α, C_1: Empirical Constants where typical values are 1.5 and 200, respectively

The attenuation approach of the LAWR is very straightforward, but is working well taking all things into consideration. In Figure 5.21, Figure 5.22 and Figure 5.23 is an example of very strong rainfall occurring close to the J.S Marshall Radar Observatory, Montreal, on 19th October 2007 observed by a 4 kW LAWR temporarily installed just below the McGill S-band radar. The S-band radar has a 5 minutes' integration time while the LAWR has 1 minute which is the reason for the different locations of the high intensity areas as well as the larger extent of them in the S-band image. To illustrate the difference in the LAWR two formats the polar data is plotted in Figure 5.20 and the Cartesian data in Figure 5.21 and the S-band for comparison in Figure 5.22. The LAWR data is the raw reflectivity data and has been applied to a volume correction. The values of the polar data is in the range of 0-1024, but are here shown in the same intervals as those of the Cartesian (1-254). The white sector in the lower half was blocked on the LAWR during the experiment in order not to interfere with other research instruments at the observatory. Paper G contains the

preliminary result of comparing a 4 kW LAWR with the McGill S-band radar located in Montreal, Canada.

By comparing the LAWR data with the S-band it becomes evident that the 4 kW LAWR is not observing low intensities very well (blue and green areas) –it is assumed to be less of a problem with the 25 kW since the 4 kW LAWR has a horizontal opening angle 4 times that of the 25 kW LAWR, cf. Table 5.1. Regarding attenuation it can be seen that there is signal loss at the far ranges (>20 km), but the LAWR has detected the second row of clusters at azimuth 255-270 behind an area of very strong intensities. The attenuation algorithm is identical for both LAWR systems and the data presented here is obtained with the standard parameters.

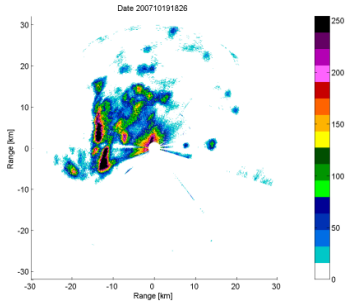

Figure 5.20 Polar image 19th of October 2007 18:26 from the 4 kW LAWR in Montreal. Image is 30x30 km and 1 minute integration time.

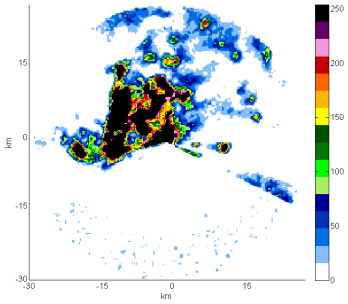

Figure 5.21 Cartesian image 19th of October 2007 18:26 from the 4 kW LAWR in Montreal. Image is 30x30 km, 1 minute integration time and 250x250 meter pixel resolution.

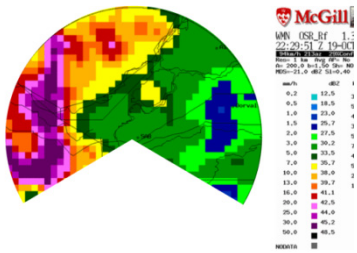

Figure 5.22 1.3 km CAPPI 19th of October 2007 18:29 from the McGill S-band radar. Image is 30x30 km, 5 minute integration time and 1000x1000 meter pixel resolution. The blocked area of the LAWR is white.

Attenuation is sometimes also referred to as extinction and if there is no more signal left after passing through a rain event it is of course not possible to restore it. A single case with total extinction of the signal was observed during the McGill experiment when a squall line with intensities above 50 mm/h passed over the radome of the 4 kW radar. The radome attenuation has not been observed to be a significant problem of the 25 kW LAWR probably as result of the difference in radome design. The 4 kW has a round radome with a large flat top surface while the 25 kW has a rotating fan beam antenna with a small constantly moving surface.

The effect of attenuation combined with the increasing beam volume is the major reasons for setting the maximum range for QPE to 20 km for the 25 kW LAWR.

5.4.2 Volume Correction

As previously shown the large vertical opening angle of the LAWR results in a rapid increasing beam volume with range, cf. Figure 5.8. The consequence of this is that a small number of drops in the sample volume at very close range, where the beam volume is very small, are most often observed, while the same number of drops at

further ranges will result in a value below the cut-off as result of the integration over a larger volume as illustrated in Figure 5.9. This is magnified by the side lobes which only exist close to the radar. This issue becomes evident when the reflectivities are accumulated over e.g. a month or longer. Figure 5.23 illustrates the problem where a cross section of the accumulated reflectivity's from the Aarhus LAWR is plotted. It is clear that the LAWR observes significantly more in the near vicinity of the LAWR installation than at further ranges. The drop to zero at range 0 km is because the radar does not observe the innermost pixel since the rainfall is right above the antenna. The difference in slope characteristics from West to East is a result of a hill to the west of the LAWR resulting in a shielded area where the radar beam is blocked and thereby not observing anything. The exact form of the curve shown in Figure 5.23 is installation specific, but the overall tendency with much higher values in the vicinity of the radar is shared by all installations.

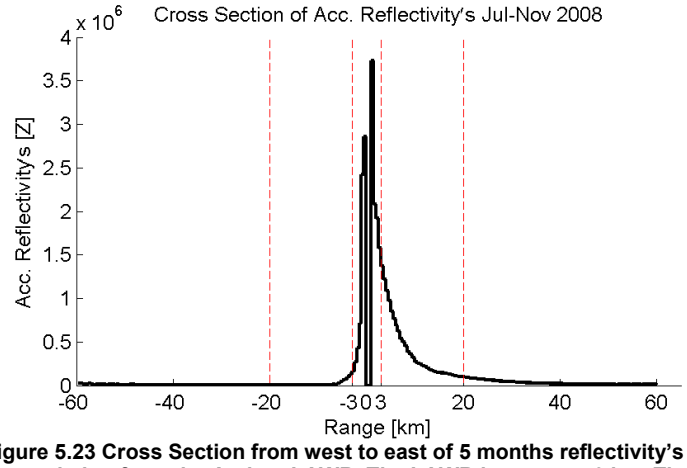

Figure 5.23 Cross Section from west to east of 5 months reflectivity's accumulation from the Aarhus LAWR. The LAWR is at range 0 km. The Aarhus LAWR is located south of Aarhus, Denmark at lat. 56° 5.790'N and long. 10° 12.317'E.

To adjust for this feature a volume correction scheme is applied to the data. The accumulated LAWR image is subdivided into a number of concentric circles, with the LAWR in the center, and an exponential function is fitted to the average of each circle. A number of different functions were tested, but it was found that the exponential function gave the best description. The function is forced to equal 1 at predefined reference distance so in principle values at ranges less than the reference distance are suppressed while at ranges further than the reference distance are magnified, cf. Figure 5.24. The suppression can be omitted by fixing the A-parameter to 1. The method assumes homogeneity of the rainfall over the radar coverage area over a 2 month accumulation period. The volume correction is applied the attenuation corrected signal Z_r in order to get the adjusted signal Z_{rv}:

$$Z_{rv} = Z_r \frac{1}{C_2 \cdot \exp(r \cdot C_3)} \quad (5.3)$$

where:

Z_{rv}: Volume corrected reflectivity at range r

Z_r: Adjusted reflectivity at range r from eq. 1

r: range

C_2, C_3: Empirical constants that are location dependent. Initial value guess: 1 and -0.03

The volume correction is only fitted to data between a minimum range and maximum range as result of the extreme high level of reflectivity's in the immediate vicinity of the radar and the risk of overestimating at far ranges as result of using a exponential function. Typically, the minimum range chosen is 3 km, maximum range 20 km and a reference distance of 5 km, as illustrated in Figure 5.23, corresponding to the range used for quantitative precipitation estimation (QPE). Furthermore, the volume correction is constraint to a maximum correction value of 4 as illustrated with the dashed lines in Figure 5.24 in order to avoid over-magnification.

The C_2 and C_3 values used in Figure 5.24 are examples of parameters used. The two parameter sets with C_2=1 and C_3=-0.003/-0.03 are typical parameters values implemented in the signal processing outlined in Figure 5.18, e.g. the Aarhus LAWR is running with C_2=1 and C_3= -0.003, while the Vejle LAWR[I] is using C_2=1 and C_3= --0.03. The volume correction for the Aarhus LAWR is less powerful than the one used on the Vejle LAWR. The result is that lighter rainfall intensities are better captured at far ranges by the Vejle LAWR since the signal is enhanced. The third set with C_2=2.2 and C_3=-0.12 is obtained based on a fit of 60 days of accumulated rainfall from the Vejle LAWR and is used in the post-processing of the Vejle LAWR data and applied prior to the calibration procedure.

[I] The Vejle LAWR is owned and operated by the Municipality of Vejle, Denmark and located at lat. 55° 43.842'N, long. 9° 33.345'E

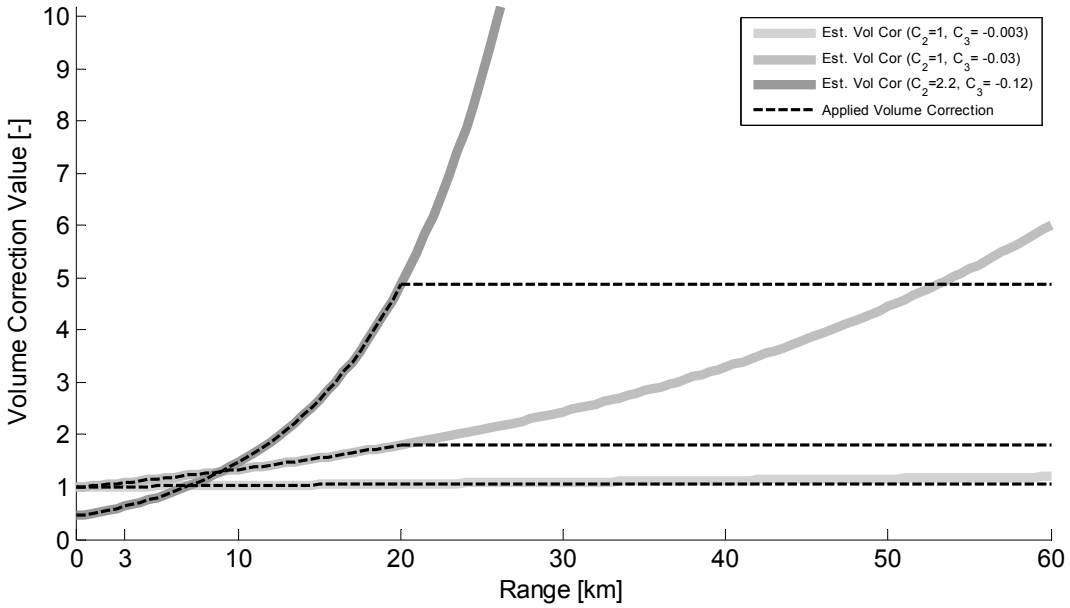

Figure 5.24 Example of volume correction with different C_2 and C_3 values. The dashed line indicates the applied version where values at ranges further than 20 km are not corrected more than the value estimated for the maximum range (here 20 km) or the correction exceeds a factor of 4. The curve as function of C_2=2.2 and C_3=0.12 exceeds 600 at 60 km range.

The volume correction is in practice a two step procedure. First step is a volume correction using a fixed set of C_2 and C_3 values and is a part of the initial signal processing performed by the Signal Processor PC. In order not to suppress data in the initial signal procession the C_2 value is fixed to 1 and the C_3 value should be approximately -0.03. The second volume correction is applied as part of post data processing carried out in connection with the calibration. The parameters used in the second volume correction are estimated on basis of the previous 60 days data by the method described above in this section. The 60 days is to avoid a single event resulting in doubling or tripling the accumulated reflectivity's which could be the case if a short time window of e.g. a week was used. The risk of this method is that if the data for some reason is flawed over a longer period it affects the volume correction for the next two months and thereby the rainfall estimate.

The C_2 parameter can be interpreted as an offset value primarily depending on the maximum values at the minimum distance, while the C_3 parameter is the shape.

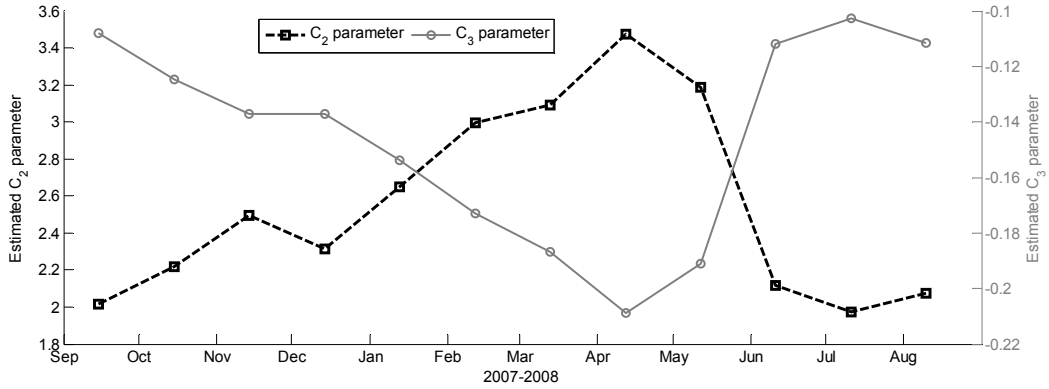

Figure 5.25 Example of estimated C_2 and C_3 values used in the second volume correction in connection with the calibration. The values are from the Vejle LAWR and are based on 100x100 meter resolution Cartesian data. Each parameter set is based on data from the previous 60 days. The magnetron was replaced on 17th of November 2007 and 10th of July 2008.

As shown in Figure 5.25 the estimated C_2 and C_3 parameters change over the year, but the variations are dampened due to the 60 day time window. The reason for the variation is due to changes in the amount of rainfall being detected since long periods with light rainfall will result in lower C_3 values while long periods with frequent rainfall will result in a higher accumulation value in the pixels close to the radar. The C_2 parameter varies opposite of the C_3 parameter, cf. Figure 5.17.

The volume correction scheme assumes homogeneity of the reflectivity at a given range (circular wise), but in some cases this requirement is not fulfilled. As example the accumulated reflectivity's over the months July-November 2008 from the Aarhus LAWR are shown in Figure 5.26. The basic assumption of a uniform rainfall used in the volume correction method is clearly not fulfilled very well in the case of the Aarhus LAWR. The accumulated reflectivity's show a very distinctive pattern and are clearly present even if only a single month is accumulated.

The Aarhus LAWR is DHI's main research LAWR and its location is resulting in some known artifacts and problems such as the blocked sectors evident in Figure 5.26. The Aarhus LAWR is placed underneath a four legged lattice antenna mast which results in both blockage and shielding, cf. Figure 5.27. The LAWR is closer to one of the legs which results in the blind sector to the west (left) in Figure 5.26. The blind sector is also due to a large hill to the west. The location of the Aarhus LAWR is far from ideal, but was chosen for its vicinity to DHI since regular visits were required in the development phase 10 years ago. Since then trees has grown up around the location adding more shielding effects. The Aarhus LAWR was dismantled in January 2009. The Municipality of Aarhus installed in 2008 their own LAWR installation in Aarhus at a much better location.

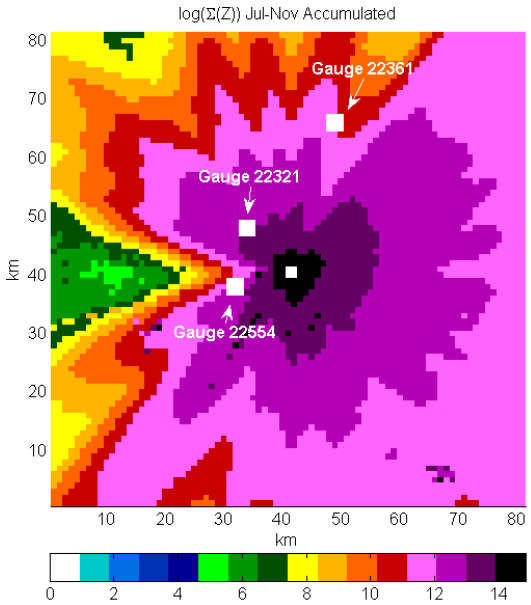

Figure 5.26 Accumulated reflectivities from the Aarhus LAWR (July-November). Only the inner 20 km is shown. The location of three gauges in the official Danish rain gauge network is marked. Please note the values has been log-transformed for plotting.

Figure 5.27 Picture of the Aarhus LAWR installed underneath a lattice mast surrounded by trees which have grown high enough to cause shielding

The reflectivity pattern is unique for each LAWR installation and is a result of local phenomena shielding or blocking the beam in combination with increasing beam volume. When the blocked area makes up such a large part of the whole area it is not possible to obtain valid volume correction parameters. The Aarhus LAWR data in Paper B has been corrected by a 2D approach which resulted in a more homogenous reflectivity level as shown in Figure 5.28.

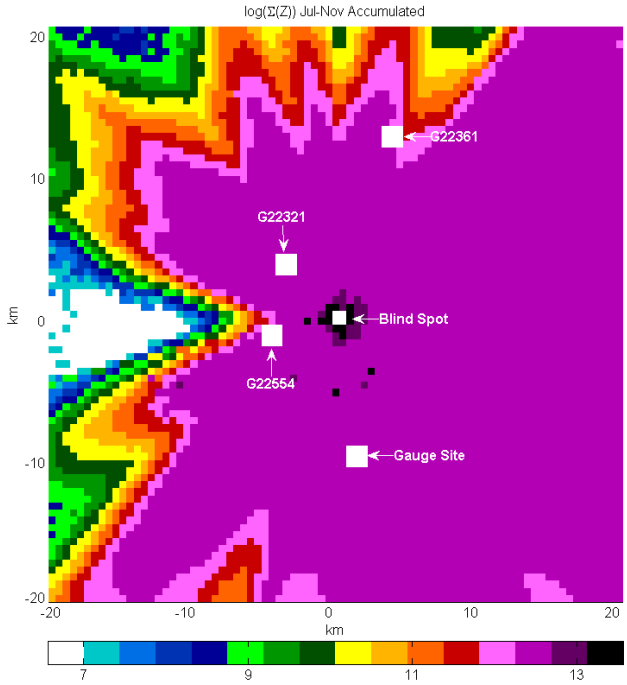

Figure 5.28 Volume corrected accumulated reflectivity's from the Aarhus LAWR (July-November) based on the 2D approach outlined in Paper B. Only the inner 20 km is shown. The location of three gauges in the official Danish rain gauge network is marked. Please note the values has been log-transformed for plotting.

The 2D approach has only been applied to data from the Aarhus LAWR and in order to create a robust method it would require data from several different LAWRs since the pattern differs from LAWR to LAWR and preferably from more than one year in order to establish a potential dependency of seasonal changes. This has not been a part of this PhD, but should be attempted in the nearest future in order to reduce some of the general uncertainties of LAWR.

The pattern or levels of reflectivity has a significant impact on the calibration since the calibration factor will depend on the location of the gauge(s) used for the calibration as outlined in Paper B. If the calibration gauge was to be located in a place with a given reflectivity level the calibration would in reality only be valid for areas with the same reflectivity level and thereby not be applicable to the whole rainfall field. In case of the Aarhus LAWR two out of the three potential gauges are available for calibration located in shielded areas or on the border (Gauge 22554 and Gauge 22361), while Gauge 22321 is not affected and thereby is the only one rational to use.

5.4.3 Clutter removal

Clutter can be a very obnoxious feature, but also an occasional useful feature. The most common source of clutter is from ground based targets, but in coastal regions sea-clutter can be a troubling issue. Temperature gradients (heat emitted from a cornfield for instance), passing ships, birds and other non-meteorological targets can

also result in clutter, but these are in particular hard to filter out as they are non stationary. One of the most used methods for detecting ground clutter is utilizing the Doppler velocity field – if an echo is persistently stationary it is classified as ground clutter. Sea clutter is more difficult to remove since it is not stationary, but the dual-polarization technology offers better solutions for this problem than Doppler alone. For more information on clutter removal techniques used by conventional weather radar please see (Bøvith, 2008) and sources herein.

The LAWR possesses neither Doppler nor dual-polarization facilities and is therefore using a two step stationary clutter removal approach – a primary and a secondary clutter map. The primary clutter map is subtracted in the signal processing after the attenuation correction and the volume correction, cf. Figure 5.18. At a dry clear day with no precipitation in the atmosphere the primary clutter map is obtained. The clutter map contains the permanent echoes caused by ground targets which needs to be subtracted from the signal as shown in Figure 5.29. The clutter map subtraction is dynamic in order to facilitate that the rainfall intensity is proportional to the whole signal range so when rain is present in bins with clutter the whole signal range is used and not only the difference between the clutter map and the signal in Figure 5.29.

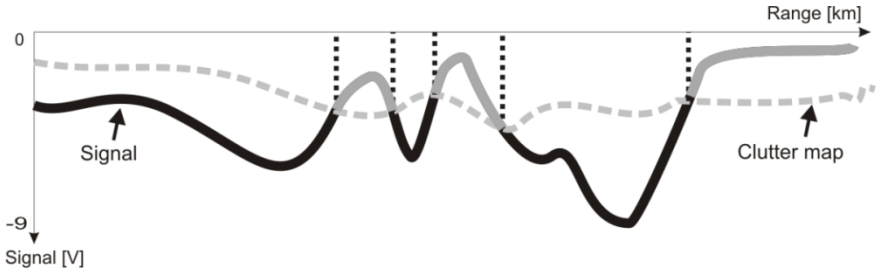

Figure 5.29 Principle of clutter map subtraction for a single scan line.

The secondary clutter removal is done prior to converting the data into the Cartesian format and is in principle identical to the primary, but there exists a separate clutter map for each Cartesian resolution. It should be noted that a regular update of the clutter maps is recommended since the clutter signature changes over time.

The variance parameter can be utilized in connection with clutter removal. A low total image variance is an indication of no rain and thereby false echoes caused by clutter can be identified during dry weather and removed.

5.4.4 External optional modules

A LAWR installation is providing reflectivity data stored locally on the Communicator PC. If an internet connection is available a number of additional modules can be added expanding the usage of the LAWR. The most used module is the web presentation module which pulls the radar data file from the Communicator

PC every 1 or 5 minutes and converts into a BMP/PNG file which can be shown on a website.

Data processing and storage

The data amount from a LAWR can be vast. If both the polar and three sets of Cartesian data files are stored every minute it results in more than 2 million files a year. The files are stored in a classical tree file structure with one folder for each day. In connection with data processing and calibration it can be convenient to use the facilities of a database – both for storing the LAWR data and for running scheduled automatic scripts for calibration and data quality control. An optional add-on module to the LAWR is the DIMS database (Dynamic Integrated Management System) which is a DHI system for handling large amounts of data offline as well as online and in real time. To handle the conversion from reflectivity values to rainfall intensities an automatic auto-calibration DIMS object has been developed pulling data from online rain gauges, websites and LAWR installations to perform an automated calibration. Such a system is not limited to DIMS, but could be developed for other systems as well.

Forecast

As earlier mentioned the LAWR was developed under the Esprit 23475 EU project, but in fact it was not the aim of the project which was to provide a short term rainfall prediction system. DHI's contribution to the project was a rainfall tracking algorithm providing a short term rainfall forecast, while the LAWR was a project spin-off as outlined in Chapter 4. The rain tracking algorithm can be used in connection with a LAWR providing a short term forecast of one hour of the rainfall. The system is denoted the "Auto-Forecaster" and requires an internet connection to the LAWR since it needs to be executed on a separate PC in order to avoid file addressing conflicts. The output is in the same format as the LAWR data, but is normally presented as series of BMP files for the future 70 minutes – one image pr. 5 minutes.

The forecast principle is based on an extrapolation of the derived movement vector field of the last two images at least 5 minutes apart. V_X and V_Y are estimated by dividing the $image_{t\text{-}5\ minutes}$ into nine sub-images and then estimating the correlation between each sub-images and the last valid $image_t$. This is done a number of times because the last valid $image_t$ is shifted 1-5 pixel in each direction in order to locate the highest correlation. The estimated vector between to echoes is a movement vector which can be translated to a velocity vector because the time difference between the two images is known. Only precipitation echoes are used to estimate the two velocity vectors V_X and V_Y – one for each direction for each pixel.

This type of forecast is straightforward and does not require input from other sources such as radio soundings of the atmosphere and so forth which are often a part of forecast provided by different weather services. The need for such additional

information is of less importance in a short term forecast, while the long term forecast of several hours is more complex. The downside of the forecast provided by the LAWR is that build-up and decomposition of rainfall is not incorporated. The forecast skills have so far only been evaluated by comparing the predicted reflectivity in a pixel with the observed reflectivity in rain/no rain evaluation method. The score was found to vary from location to location ranging from 64-80% and decreasing with increasing forecast time (Jensen, et al., 2005). The forecast has not been subject to in depth analysis in this PhD-project, but a new research project under the Storm and Waste Water Informatics program (SWI, 2008) is working towards a nested forecast combining the high resolution detailed forecast of the LAWR with the long term provided by the Danish Meteorological Institute and in that connection the skill of the LAWR forecast is to be evaluated.

5.5 LAWR Calibration

As with any weather radar a calibration is required in order to convert the indirect measurement of the rainfall denoted reflectivity's, Z, to rainfall intensities, R. Conventional weather radars use a power-law given by eq. 4.4 in Chapter 4. The power-law calibration approach was first proposed by (Marshall, et al., 1947) and shortly after by (Marshall, et al., 1948) who suggested an A value of 220 and B of 1.6. The values were based on experimental drops size distribution measurements. It was soon discovered that there does not exist a single set of A and B (Battan, 1973), but they depend on climatology and rainfall type. The values suggested by (Marshall, et al., 1948) are still widely used in operational context by the different meteorological services around the world (Lee, et al., 2005).

The calibration used by LAWR is different than the power-law relationship used by conventional weather radars. The power law relation used by conventional radars is a result of the linear receiver, but since the LAWR has a logarithmic receiver it uses the linear relationship between accumulated reflectivity's and rainfall depth observed by a gauge over the same time. The calibration gives a factor, denoted DHI CF, which applied to the LAWR output (Z) gives the radar rainfall intensity in mm/min (Pedersen, 2004):

$$\text{DHI CF} = \frac{\sum_{\text{Event Start}}^{\text{Event Stop}} \text{mm rain [gauge]}}{\sum_{\text{Event Start}}^{\text{Event Stop}} Z/\Delta t \text{ [LAWR]}} \tag{5.4}$$

Δt in eq. 5.4 is the time resolution of the radar data which either is 1 or 5 minutes. It should be noted that the calibration factor obtained by using eq. 5.4 is for an individual event which might not be representative for the whole pixel - yet less the whole area of rainfall as a result of significant inter-pixel variability of observed rainfall depths as outlined in Paper A and Paper C. To meet this problem and furthermore obtain a more robust calibration factor the LAWR calibration factor is

obtained by estimating the DHI CF parameter in eq. 5.5 by linear regression based on multiple LAWR and gauge rainfall observations.

$$Rainfall\ Depth\ = DHI\ CF \cdot \sum Z \qquad (5.5)$$

The method is thoroughly described in Paper B and an example from this paper is shown in Figure 5.30 using data from up to 9 rain gauges and the Aarhus LAWR.

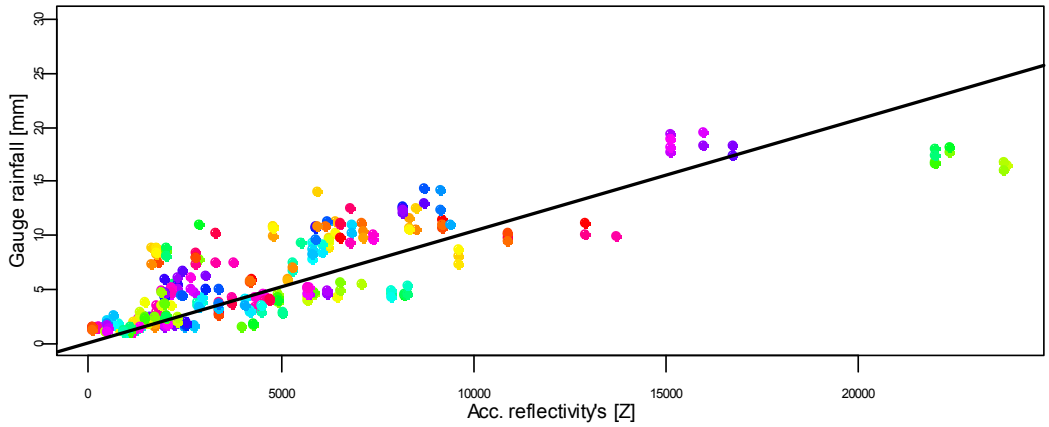

Figure 5.30 Estimation of LAWR calibration factor (DHI CF) based on more than 50 rainfall events. The DHI CF is for converting Z into mm/min.

The scatter in Figure 5.30 is a result of different rainfall types and inter-event variability. The variability in rainfall depths within a 500x500 meter area based on the 9 rain gauges was found to vary from 1-26% based on the coefficients of variation of. The variability is decreasing with rainfall depths and is independent of the mean event intensity. (Pedersen, et al., 2009)

As part of this PhD project the existing LAWR calibration has been attempted improved. By conditioning on the duration (h) and the intensity (Z/h) using multiple linear regression the LAWR calibration becomes:

$$Rainfall\ Depth\ = \varphi \cdot \sum Z + \phi \cdot Duration + \psi \cdot Intensity \qquad (5.6)$$

$$where \begin{cases} \hat{\varphi} = 5.96 \cdot 10^{-4}\ \ (0.40 \cdot 10^{-4}) & [Z] \\ \hat{\phi} = 0.60\ (0.05) & [h] \\ \hat{\psi} = 4.20 \cdot 10^{-4}\ \ (0.48) & [Z/h] \end{cases}$$

The figures in brackets are the standard deviation of the estimated parameter. The new calibration method (eq. 5.6) increases the degree of explanation from 0.85 to 0.90 for the data presented in Figure 5.30. Both calibration methods along with a detailed description of the data used for estimating the calibration factors are thoroughly addressed in Paper B. The estimated values listed here are not directly

transferable to other LAWR installations since they are estimated based on data from the Aarhus LAWR which as mentioned earlier is a research LAWR.

5.6 Examples of applications using LAWR data

To demonstrate the wide range of users/applications utilizing LAWR data a short overview over selected commercial and research projects are given here. Different international institutions are using LAWR for various research projects. The ETH in Zurich, Switzerland has installed a LAWR for snowfall monitoring over the Klein Matterhorn Glacier. Leuven University, Belgium is using LAWR rainfall estimates in connection with research on urban drainage modeling which also is being looked upon at Aalborg University, Denmark along with the vertical rainfall distribution with a mobile vertical pointing 4 kW LAWR.

www.regn.dk

This is a straightforward website presenting data from a number of LAWRs in Denmark and abroad. An animation of the past hour is presented followed by a forecast of the coming 70 minutes. The site has in the order of 60,000-70,000 visitors a year and the users are a wide range of people being outdoors such as people biking to work, kite surfers, amateur pilots, construction site managers and so forth.

FieldRain

FieldRain is a decision support system (DSS) web-application used for quantifying and visualizing the spatial and temporal extent of rainfall in relation to the farmer's fields. The idea is to provide the farmer with information about the quantity and the distribution of rainfall over the fields and thereby provide a better foundation for rainfall related topics such as irrigation, seeding and harvest planning. FieldRain uses the output from a LAWR and the facilities in the DIMS system and the latest version is presenting the data to the farmer in a web browser where rainfall from selected time periods is shown as animations over the fields in question. The farmer can furthermore get the accumulated rainfall over a defined period. A Danish version of the system can be viewed at http://markregn.dhigroup.com.

Real-time SMS Warnings on Expected Basement Flooding in Hvidovre, Denmark

As part of their strategic sewer management the municipality of Hvidovre, Denmark, has installed a real time warning system. The system sends a text message (SMS) to citizens who have chosen to subscribe to this service with a warning if their sub-catchment is of risk to be flooded by backwater from the sewers as result of intense rainfall. The warning is based on a decision support system using data from a LAWR – both the observed and the predicted reflectivity's are converted to rainfall intensities in a DIMS database and for each catchment the mean area rainfall intensity of 5, 10, 30 and 60 minutes duration is computed and the corresponding return period is obtained by using national IDF curves. The IDF curves are based on rain gauge measurements since the time series of LAWR data still is too short of long term

statics. The system was installed in 2008 and is in operation. Besides the SMS warnings data is collected and presented in a DSS web application available to the planning department of Hvidovre Municipality.

Integrated Real Time Control of Sewer Systems and Wastewater Treatment Plants combined with an Early Warning System for Water Quality in Lake, River and Harbour in the City of Aarhus, Denmark.

This project is working towards creating a real time control system for the sewer system and the waste water treatment plants based on LAWR data and forecast of rainfall over the city of Aarhus and its upstream rural catchments. The LAWR will provide data to an online numerical model of the sewer system which will be used to predict water levels at critical points in the sewer system along with a prediction of the inflow to the treatment plants and the E. Coli bacterial concentrations in the harbour. Every 5 minutes a new model simulation is performed using the latest data and thereby providing information to the decision makers. The system is currently being designed and is expected implemented during 2009 and 2010.

Bird Migration

In connection with large offshore construction projects, such as wind farms and bridges, it is often a requirement to document the influence on bird migration patterns. The normal approach is to have a number of ornithologists counting the birds which is an expensive solution and limited to daylight observations. As part of the baseline study in connection with an offshore wind farm at Rødsand, Denmark a modified version of the LAWR has been used to detect and quantify the migrating birds. A second system was deployed in connection with baseline studies of bird migration patterns on Horns Rev (off-shore wind farm). Both research projects were carried out during the fall of 2008 and the data processing and the final evaluation are being carried out presently. A bird tracking algorithm has been developed and an example of the identified track routes is shown in Figure 5.31.

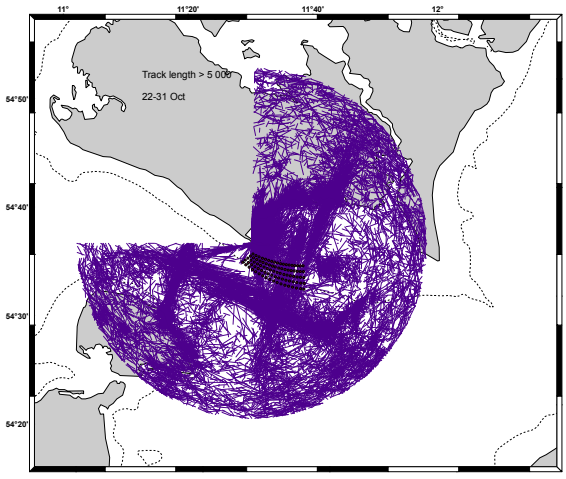

Figure 5.31 Example of bird migration patterns observed by a LAWR at Rødsand, Denmark

Radar@Sea

In connection with a large research project regarding development of new tools for wind power production management involving DTU Informatics, Dong Energy, Wattenfall and DHI the LAWR is to be used for predicting rainfall. Rainfall has been demonstrated to influence the potential magnitude of power fluctuations of wind mill power production (at a few minutes to few hours temporal scale). If heavy rainfall is present there is an increased chance of experiencing an episode of high wind variability. The LAWR is going to provide observations and forecast of the rainfall which is hoped to be utilized in connection with development and implementation of local forecasting models describing when and how fronts will hit the wind farm and thereby facilitate a more optimized operation.

CHAPTER 6

Weather Radar Data in Urban Drainage

Some of the first to construct sewage systems were the Romans who as early as 600 BC began the construction of the first know urban drainage system – the Cloaca Maxima meaning Greatest Sewer (Schladweiler, 2004). At that time Rome was a prosperous city with more than 100,000 inhabitants, and in order to avoid diseases the Romans realized that aqueducts leading clean water from the mountains and sewers to divert the polluted water from the city were vital for their health. An indication of the awareness of the important role of sewers can be found in the fact that the Romans had a goddess for the sewer system and particularly for the Cloaca Maxima. Her name was Cloacina and the Romans placed their faith/trust in the wellbeing of Rome's sewers in her. Their faith must have been strong because the Cloaca Maxima has been in function for more than 2400 years (Schladweiler, 2004). The drainage knowledge acquired by the Romans was lost with the fall of the Roman Empire around 500 AD, and the sanitation level of the European cities dropped dramatically and was followed by an increase in deadly diseases.

The main principle of urban sewer systems has not changed since the days of the Romans, however, the concept has been extended and improved since the re-discovery of the need for urban sanitation in the nineteenth century. The first large

scale sewer was constructed in Paris during the 1840's followed by London and other large cities in Europe. The implementation of Waste Water Treatment Plants (WWTP) came much later during the twentieth century, and today many cities around the world are in the process of implementing WWTPs.

Urban drainage systems in the western part of the world are often complex systems consisting of both combined sewers (waste water and surface water) and two-stringed separate systems where surface waters are lead untreated to the receiving waters and the waste water to a treatment facility as outlined in Figure 6.1. Urban drainage systems operate in two states: Dry and wet. In the dry state the system only needs to transport sanitary water and in some cases ground water leaking into the system, while in the wet state the system must handle rainfall reaching impervious surfaces connected to the drainage system, e.g. roads, roofs, driveways and squares.

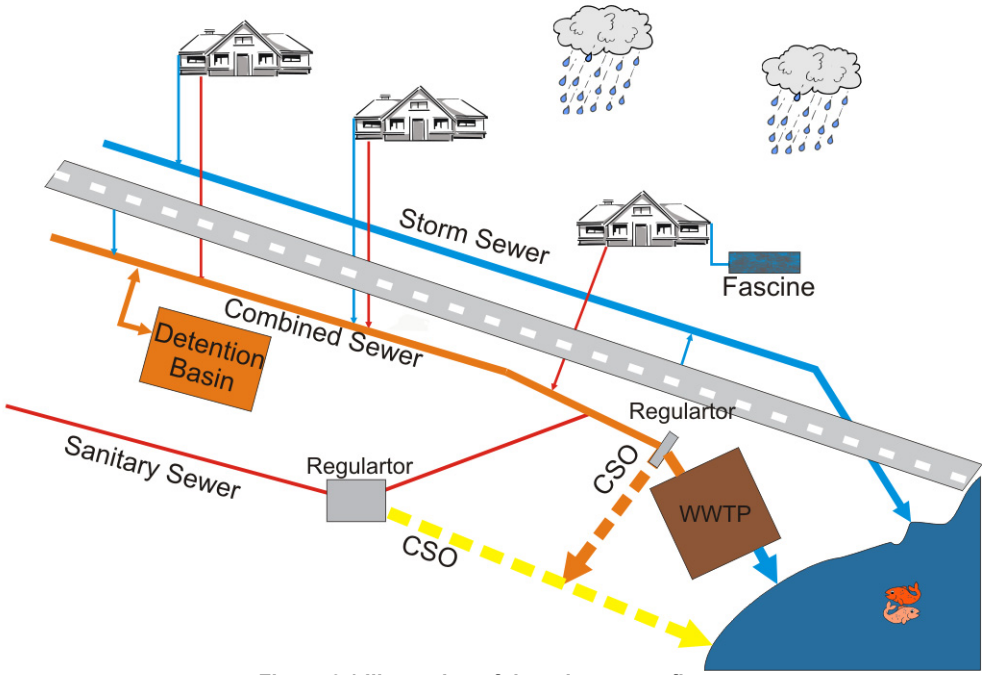

Figure 6.1 Illustration of the urban water flow

Besides the sewer pipes and the manholes an urban drainage system may have pressurized pipes, detention basins, combined sewer overflows (CSO), internal overflows, pumps, valves, water brakes and other types of regulators. Some of these features are passive elements such as most CSO structures discharging the water into receiving water at a given water level, while others are dynamic such as pumps and others again are controlled by Real Time Control (RTC). RTC can actively control regulators and pumps remotely based on online real-time information from sensors in the sewer system such as flow gauges, water level sensors and start and stop of pumps. RTC is becoming of more interest these years since the operation of urban sewer systems in large cities is a complex affair which is being challenged even

further in these years due to tighter discharge restrictions to improve the water quality of the receiving waters and as result of more frequent occurrence of large floods such as the large flood in Europe in 2002.

6.1 Rainfall Data in Urban Drainage Applications

In Chapter 4 precipitation was defined as liquid in any state reaching the surface, however, in connection with urban drainage rainfall is of primary interest. Rainfall varies from light drizzling rain hardly wetting the surface to extreme thundershowers relishing vast volumes of water over a short time. The run-off time and thereby the response time of the system can be very fast due to the high degree of impervious surfaces facilitating fast surface flows and providing no infiltration capacity.

Rain gauge data has been the sole source of rainfall data used in connection with hydrological applications. Multiple gauge designs exist, but the automatic tipping bucket rain gauge is probably the most common type of automatic recording gauges. A rain gauge observes rainfall in a point of a few hundred square centimeters, which is problematic since rainfall is highly variable in both time and space even at scales less than a few kilometers (Krajewski et al, 2003).

The obvious inadequacies of rain gauges in relation to representing the spatial characteristics of the rainfall field have lead to augmented interest in using observations from weather radars in connection with urban drainage applications. Weather radars are capable of providing distributed rainfall measurements over an area. Further information on rainfall estimation by weather radars and in particular the LAWR can be found in Chapter 5 and Paper B. The spatial resolution of weather radar data ranges from 0.1x0.1 km to typically 1x1 km – some even as large as 4x4 km. The temporal resolution ranges from 1 to 15 minutes depending on the radar system. Figure 6.2 illustrates various types of hydrological applications used in urban drainage context in connection with their temporal and spatial input scale requirements. A thorough review of the requirements for using radar data in urban drainage context can be found in (Einfalt et al, 2004).

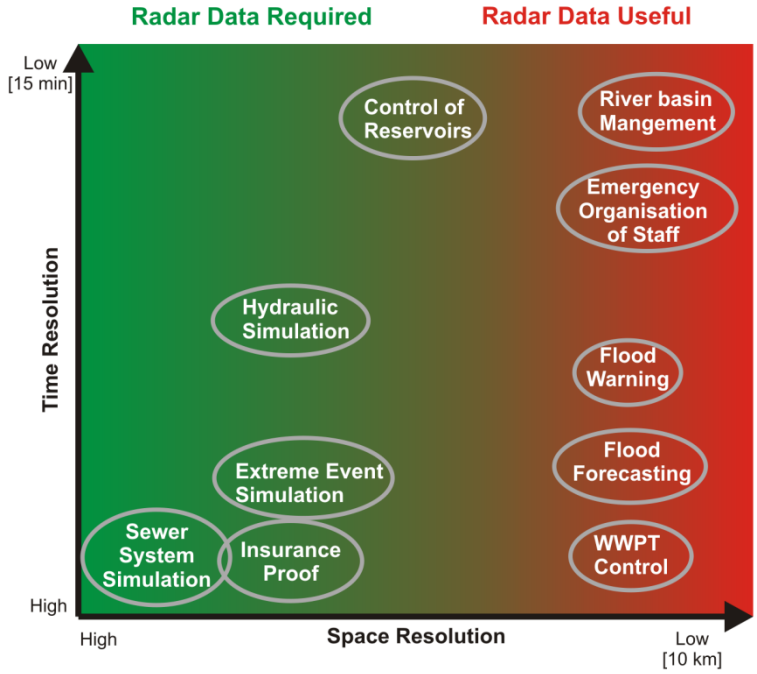

Figure 6.2 Spatial and temporal resolutions of applications in relation to radar data. Figure is by courtesy of Thomas Einfalt, hydro & meteo GmbH & Co. KG, Germany

Some urban drainage applications require input with high temporal resolution due to the fast response times of the system. Some radars still operate with 10 and even 15 minutes' output frequency which is low compared to the response times of a small steep catchment which may be as short as a few minutes. The LAWR described in Chapter 5 was developed to facilitate this problem. It is capable of providing rainfall estimates every minute with a spatial resolution ranging from 100x100 to 500x500 meter. Another example of tailoring weather radar measurements towards hydrological applications is the MARS radar – a low powered C-band weather radar developed by the University of Salford (UK) and McGill University (Ca) in 1990 and later on installed near the city of Manchester, UK for hydrological purposes (Cluckie et al, 1997). The HYDRIX system is yet another example of a weather radar developed specifically for hydrological purposes (Bouar et al, 2005).

Weather radars are furthermore capable of providing a nowcast of the next few hours' rainfall which can be of great benefit for optimizing the WWTP operation since it takes time to switch from dry weather to wet weather mode. Radar rainfall forecast combined with RTC furthermore facilitates routing of the water from areas with inadequate sewer volumes to areas less or not affected by the rainfall in question and thereby increasing the available storage volume in the drainage system.

Despite the obvious advantages provided by radar data they are still regarded with great disbelief by the majority of hydrologists around the world. Radar rainfall

estimates often are considered too uncertain and containing too many errors. When radar rainfall estimations are evaluated it is almost always based on rain gauge observations. The two types of observations rarely agree completely due to the nature of the observations. The radar is an indirect measure of a volume increasing with range, while the gauge is a point observation. (Sempere-Torres et al, 1999) states that thorough studies of the local conditions before adapting radar data to hydrological applications are important, since the area of interest may be poorly observed by the radar due to clutter, beam shielding or long range which would lead to poor results. The complexity of radar measurements and potential error sources are large compared to those of rain gauges, and as stated by (Einfalt et al, 2004) training of hydrologists in the background for radar data, interpreting and understanding the data along with the uncertainties is essential.

To complicate matters even further weather radars are operated by the meteorological services around the world. Their focus of operation is of meteorological character, while the hydrological community is interested in estimations of rainfall at the surface with highest possible accuracy. The two communities are starting to work together towards using radar data in hydrological applications, however, the difference in aim of the radar observations is a major obstacle for radar rainfall estimations being widely used as input to urban drainage applications. The use of radar data in urban drainage requires interdisciplinary action from meteorologist, hydrologist and computer scientist due to the many challenges and the vast amount of data (Einfalt et al, 2004).

It is, however, essential to remember that rain gauge data also contains errors and is known to underestimate high intense rainfall by up to 10% (Einfalt et al, 2004). So in order to provide usable data the rain gauges require regular maintenance and calibration along with careful data processing.

6.2 Weather Radar Data and Urban Drainage Modeling

In the field of urban drainage numerical models are frequently used to analyze the impact which a rainfall event has on a drainage system. Both historical rainfall events and design storm are used as input to these models. Today, many different models exist – some purely for research purposes, but there are also a number of commercially available models. The most utilized commercial models are probably the SWMM model (Storm Water Management Model) developed by the U.S. Environmental Protection Agency, the InfoWorks CS model from British Wallingford Software and the MOUSE/MIKE URBAN model from Danish DHI. Common for all these models is that they are developed on basis of rain gauge data and therefore tailored to meet the properties and compensate for the shortcomings of gauge data.

The standard approach today is still to assume a gauge representative for a large area, often the whole catchment, and thereby assuming uniform rainfall. It is also common to use data from a rain gauge several kilometers away if there is no gauge within the catchment assuming it to be representative. This may only lead to small errors in case of a large frontal rainfall system, but in cases of local convective rainfall (thundershowers) this approach is rarely providing good results.

Classification of rainfall into convective and stratiform rainfall is of interest in connection with e.g. artificial rainfall generators. Artificial rainfall time series are based on models containing the statistical properties of measured rainfall and can be used as input to urban drainage models in cases where the local rainfall time series are of insufficient length. There exist many such artificial rainfall generators and the field has been widely explored during the past 10-15 years. Examples of a rainfall generator based on a Markov chain model can be found in (Arnbjerg-Nielsen et al, 1998) and (Thyregod et al, 1998) who both found that the estimated parameters were related to the state of the rainfall. The state was found to be described by the duration between the last two gauge tips and the accumulated volume of the present event. Since the estimated parameters were found to vary according to the state and the physical properties of the rainfall, a classification of the present rainfall into convective or frontal rain based on the estimated model parameters was suggested. The classification is also an issue in relation to weather radars since the drop size distribution within the radar sample volume can vary depending on the rainfall type. It could be interesting in the future to explore the potentials of using he findings from (Arnbjerg-Nielsen et al, 1998) and (Thyregod et al, 1998) in connection with real time adaptive weather radar calibration.

In cases of more than one gauge within the catchment some models, e.g. the MOUSE model, can utilize the information from multiple gauges. In MOUSE each catchment is assigned the time series of the gauge located closest to the center coordinate of the catchment. This approach can be problematic in cases where the catchments are larger than the radar pixels, since only some of the pixels are applied and thereby the spatial distribution of the rainfall field is distorted. By the introduction of GIS tools for catchment delineation in urban models the catchment representation has improved dramatically from the simplified squared areas used before. Some models even facilitate the delineated catchments being combined with data from a high resolution digital terrain model. To facilitate and use the spatial information of radar data it is therefore important that the numerical model is able to handle and fully utilize distributed input data.

The high spatial resolution of catchment information as illustrated in Figure 6.3, which is being implanted in many models these years, is not completely utilized unless high resolution radar data are used as input. If rain gauge data is the input

source uniform rainfall is applied to all catchments. It is important to stress that model resolution and input data should be in the same spatial domain and the model performance can never be better than the quality of the input and boundary data. In the same way as a highly distributed model using lumped rainfall data is inaccurate, a lumped model applied to high resolution radar data is not utilizing the information correctly which can lead to errors.

One approach for integrating NEXRAD[I] data into PCSWMM.NET, which is a spatial decision support system for US EPA SWMM5 by Computational Hydraulics Int. (CHI)), is presented by (James et al, 2008) who, based on the radar data - calculates an area weighted hyetograph for each catchment based on the actual shape of the catchments. A similar approach is used when LAWR data is used as rainfall input in a MIKE URBAN model. Each catchment, represented by its actual form and extent, is assigned an individual LAWR rainfall input time series. In cases of more than one pixel covering a catchment as illustrated in Figure 6.3, the time series is created as an area weighted average of all the pixels covering the catchment.

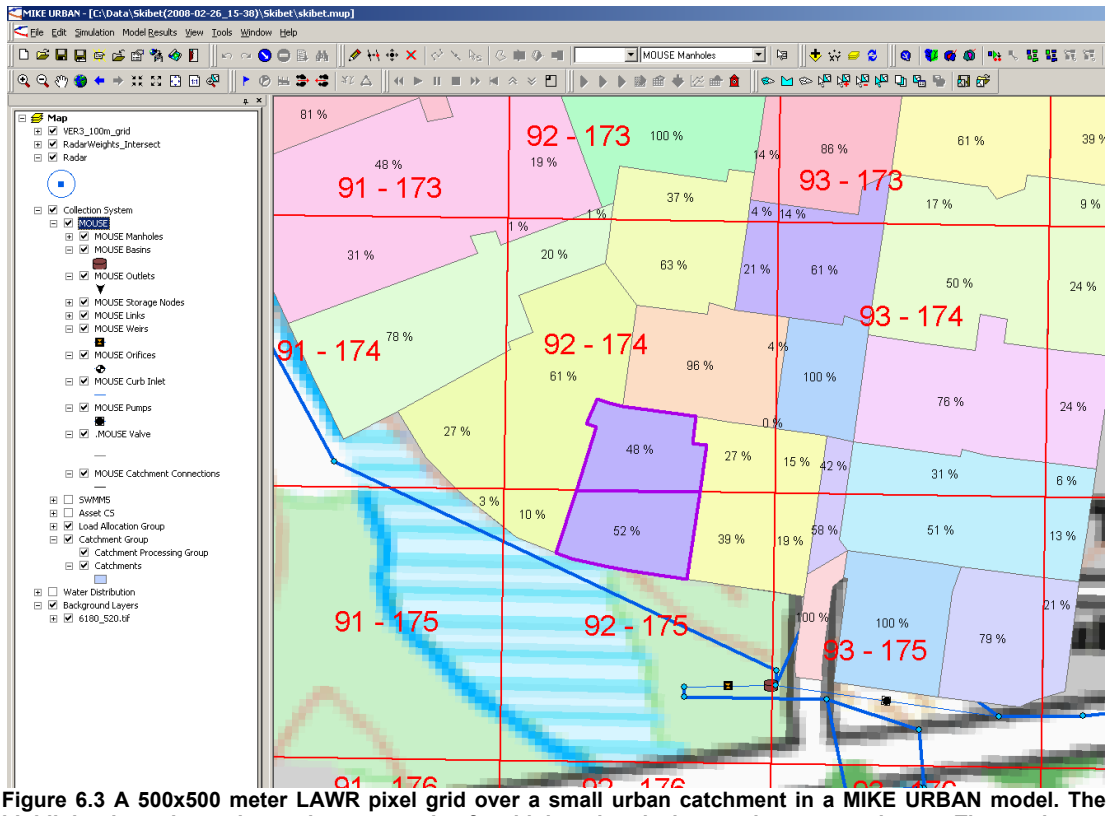

Figure 6.3 A 500x500 meter LAWR pixel grid over a small urban catchment in a MIKE URBAN model. The highlighted purple catchment is an example of multiple radar pixels covering one catchment. The catchment is applied a weighted time series from the two pixel 92,174 (48%) and 92,175 (52%).

[I] NEXRAD (Next-Generation Radar) is a network of 159 high-resolution Doppler weather radars operated by the National Weather Service covering the United States.

In connection with the discussion of catchment and radar data resolution of the catchments and the radar data it is important to keep in mind that radar data original are polar and during the conversion to a Cartesian format a lot of information is lost.

The potential benefit of high resolution radar rainfall data as provided by a LAWR in connection with urban drainage modeling is clearly illustrated in Figure 6.4. Here it is clearly evident that only lower parts of the drainage system are affected by rainfall while the upper part is completely dry. The area depicted in the figure is only approximately 7x5 km and as shown there is significant variability in the rainfall field.

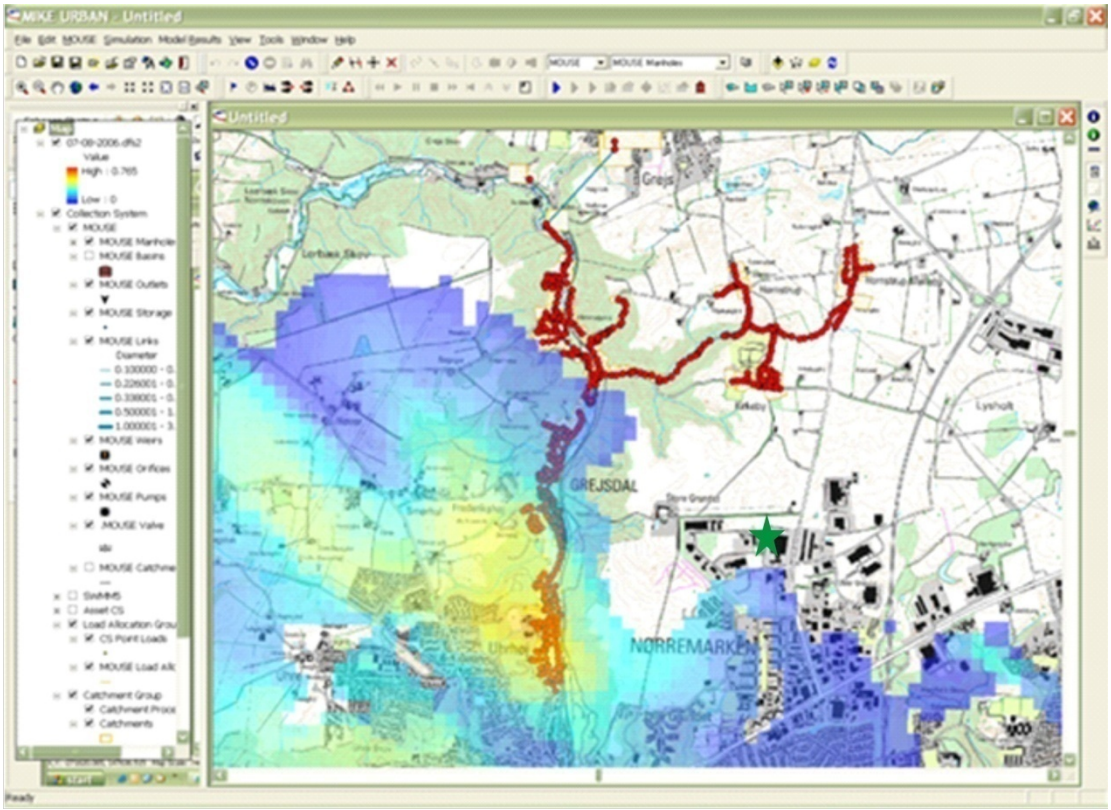

Figure 6.4 LAWR estimated rainfall from the Vejle LAWR in a MIKE URBAN model of Grejsdalen - a suburb to the city of Vejle, Denmark. The radar image has a 5 minute temporal resolution and pixels of 500x500 meters. The combined sewer system is outlined in red and the radar location is indicated by a green star. The image is approximately 7 km wide and 5 km high.

It is easy to comprehend the advantages which a rainfall forecast in such detail as the rainfall shown in Figure 6.4 could provide for authorities and drainage system operators. Especially in connection with RTC applications a detailed rainfall forecast is highly desired since it provides information about the rain beforehand which can be used to simulate the effects of the predicted rainfall and thereby support the decision making process. The LAWR can provide a forecast of the coming 1 hour for such purposes. The forecast is described in Chapter 5.

6.2.1 The transition from rain gauge data to radar data in urban drainage modeling

First of all it is important to understand and keep in mind that probably all available urban drainage models are developed based on rain gauge data and thereby developed to handle the shortcomings of rain gauge data. The non-uniformity of gauge rainfall is furthermore compensated for in the model calibration process where parameters are adjusted until simulated flows, levels and/or volumes are comparable to the observed values.

An example of how the models are developed to meet gauge properties is the default initial loss value ($6 \cdot 10^{-4}$ m) in the Time-Area model of the MOUSE/MIKE URBAN model equals to the volume of the first intensity value from a rain gauge from the official Danish gauge network[II]. The first 0.2 mm tip is assumed a duration of 1 minute equaling an intensity of 3.33 μm s^{-1}. This ensures that the significant, but artificial peak does not show up in the results.

For instance in the case of local orographic effects (please see Chapter 4) catchments located on top of a hill will receive more rainfall than catchments located at the bottom of the hill. Since many rain gauges are located adjacent to treatment plants which, due to the nature of things, are located at the lowest level of the catchment, the rainfall observed by the gauge would not be equal to the rainfall at the top of the hill. A way to compensate for this in connection with modeling is to adjust the hydrological reduction factor of the catchments on top of the hill to compensate for spatial variability in rainfall not observed by the gauge.

If radar data is to be used as input to an already existing numerical model, it is therefore important to re-calibrate the model. The model parameters should all be reset to physically based values before the re-calibration in order to obtain a rational model. If the radar data is applied to a model calibrated on basis of rain gauge data there is a high risk of poor results, which is often interpreted as erogenous/poor quality radar data leading to disbelief in the radar based on wrong prerequisites. Unfortunately, it seems that the recalibration is often neglected, maybe as a result of illiteracy of the physical process of rainfall in relation to measuring techniques or just overlooked. Paper D contains experiences and recommendations for using high resolution LAWR data in an urban drainage model with special focus on identifying pitfalls.

[II] Since 1979 the Danish Water Pollution Control Committee (Spildevandskomitéen) together with the Danish Meteorological Institute has been operating a national network of automatic recording tipping bucket rain gauges. Today more than 100 gauges are located in Denmark (43,000 km^2), with the densest networks around the city of Copenhagen.

There is no doubt that the transition process from a single or few rain gauges as input to the "2D" radar data will be challenging for both provider and user of the data (practitioners). It is fundamental that the users get further training in hydrometeorology and radar observations in order to understand, assess and use radar data in a hydrological context. The gap between researchers and practitioners is often large and an obstacle to be taken very seriously as pointed out by (Arnbjerg-Nielsen et al, 2002). Their experiences from transferring research knowledge regarding regional extreme precipitation in connection with urban drainage and the proper implementation of this knowledge should be used as a good example of how research knowledge can be transferred to application context and thereby used.

Yet another challenge is embedded in the fact that the provider of radar data (most often meteorological services) is different from the users (researchers, authorities and consultants), so in order to ensure compatible data formats, data transformations etc. communication, cooperation and training of people to acquire those inter-disciplinary skills are crucial.

6.2.2 Examples of Radar Data in Urban Drainage

Although the first attempts to use radar rainfall as urban drainage model input were taken more than 20 years ago it is scarcely used in operational context today. The reason for the little progress in this area is a combination of several things. One of the major reasons is the fact that for many years the hydrological community has been waiting for radar estimate to be sufficiently improved to resemble the gauge estimate as closely as possible – believing that ground base rain gauges are the so-called "ground truth" and thereby neglecting the fact that they are two different types of measurements. As result of this most studies have been towards radar-gauge comparisons and understanding of the uncertainty and errors related to radar rainfall estimates, however, some studies of application of radar data have been conducted and the number is increasing.

Quantitative rainfall estimation by radar has matured greatly over the past 20 years and the computational powers have increased dramatically facilitating more complex data processing, models and input. Furthermore, the introduction of GIS tools in connection with urban drainage modeling has facilitated better display options of distributed rainfall data along with the improved delineation of the catchments.

In 1999 a study using weather radar data to model combined sewer flows in Barcelona was carried out by the Universitat Politécnica de Catalunya, Barcelona. The study aimed at investigating the potential of using radar rainfall data in connection with the city of Barcelona's RTC system the primary objective of which is to reduce CSOs. An extreme rainfall event in September 2001 causing flooding and a single casualty formed the base of the analysis which also involved a calibrated

MOUSE model of the area being examined. Three rain gauges were situated inside the catchment, and a total of 18 1x1 km pixels from a Doppler C-band radar covered the area. The result showed that in a case like this with an extremely local strong convective event the spatial variability is of vital character for the result and such can only be provided in detail by radar. The radar data were found to provide better results than that of the rain gauges, despite the fact that no extra correction had been applied to resemble a real-time situation as much as possible. The study is reported in (Sempere-Torres et al, 1999).

As mentioned most studies of radar data in connection with urban hydrological models focus on the comparison of radar estimates with those from rain gauges. Only a few as the one by (Sempere-Torres et al, 1999) attempt to use the radar data in an operational model, and most of those are still carried out in a research context. (Hanson & Edwards, 2008) is one of the few reporting the results from utilizing radar in urban modeling tools carried out by authorities together with consulting engineers. They used radar data provided from the British MET office as input to hydrological models to model and predict CSO. They found that radar data provided acceptable results, but the radar data resolution was of vital character for the model performance. It does not appear from their paper if the model used was re-calibrated. The dataflow from the radar operator to the model operators along with conversion and data format was furthermore identified as a potential vulnerable point.

The use of radar data at larger scales where the surface flow and flooding are of interest is more often reported especially from the US using data from the NEXRAD network e.g. (Hoblit & Curtis, 2002) and (Vieux & Bedient, 2004). As a possible solution to the scaling issue related to the validation of weather radar performance based on rain gauges (Vieux & Bedient, 2004) suggest that evaluation by means of a stream gauge at the outlet of the catchment (here 260 km^2) is a more suitable solution. This is consistent with the work of (Sempere-Torres et al, 1999) where it was found that in a punctual radar and gauge varied significantly, but minimized when area based estimates were compared to the ones observed. The rainfall-runoff process in the catchment reduces the random errors measured by the radar-gauge comparison. This is an interesting new approach, which will hopefully be pursued further in the future since a catchment is much more of the same spatial domain order as that of a radar pixel.

6.3 Urban Drainage Design and Weather Radar Data

Urban drainage design practices vary from country to country, but a common practice is to use statistically derived Intensity-Duration-Frequency (IDF) curves as foundation for sewer system design. The IDF curves contain the statistical historic properties of rain gauge observed rainfall and can be used for deriving an IDF design storm with a constant intensity over time. The Chicago-Design-Storm (CDS) is

probably one the most used types of design storms and is an extended version of the IDF-design storm since a CDS storm can contain multiple intensities with the same return periods in a single event. CDS storms are frequently used as input to numerical models for simulating flows, surcharges and backwater effects of a given rainfall event in an urban drainage system. This is only possible if a general assumption of the return period of the intensity being equal to the return period of the water levels in the system is accepted. Historical rainfall time series are often used to estimate return periods of e.g. critical water flow which only can be obtained this way.

In connection with urban drainage design extreme value statistics are of special interest since it is affecting the design criteria. In the past decade extensive research on the spatial (regional scale) and temporal variations of rain gauge recorded rainfall has been carried out in Denmark and other countries (Madsen et al, 2009) and sources herein. In 1979 an official Danish rain gauge network was initiated and has been expanding ever since to consist of more than 100 gauges today, cf. Figure 6.5.

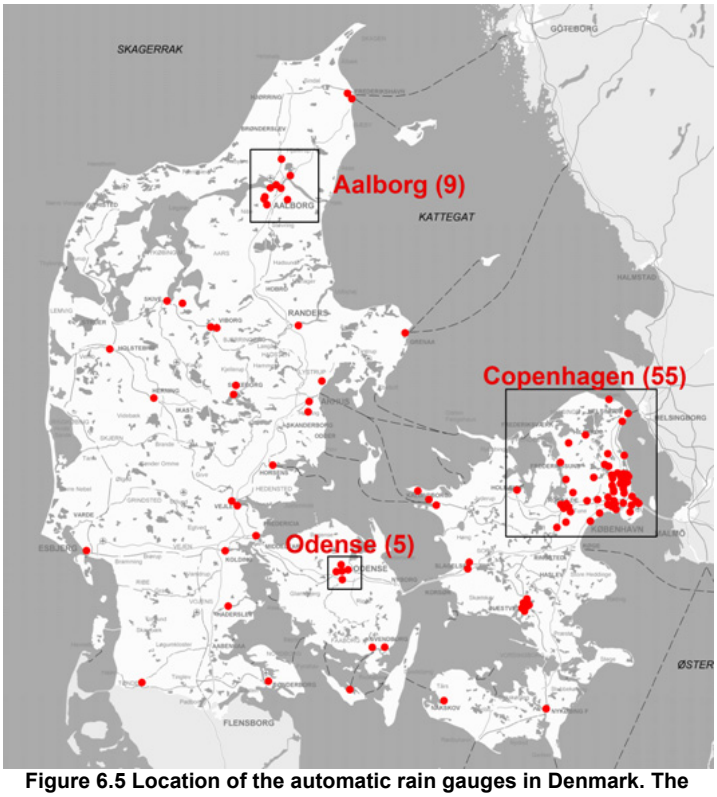

Figure 6.5 Location of the automatic rain gauges in Denmark. The number of gauges within a square is in the brackets after the city name.

The gauge data series has been subject to many research projects and is forming the base for the Danish sewer design guidelines published by the Danish Water Pollution Control Committee (Spildevandskomitéen). In 2006 a statistical study was carried out on data from 41 gauges, all with more than 20 years of recording. Based on this analysis it was concluded that for the 10 minute maximum intensity there was a

positive trend towards more extreme and more frequently occurring rain storms. Furthermore, it was concluded that based on this limited dataset the existing set of IDF curves were no longer valid without adjustment for climate change (Arnbjerg-Nielsen, 2006). Potential changes in the climate leading to more extreme rainfall events is not incorporated in the current IDF curves since they are derived based on historical rainfall data, the properties of which may not be consistent with those of future rainfall. Since urban drainage systems are designed to last a 100 years it is important to incorporate the newest data and constantly update the statistics behind the IDF curves.

One of the many outcomes of the Danish rainfall research has been a regional model for estimation of extreme rainfall characteristics in Denmark used in connection with estimation of IDF curves which again are the foundation for CDS design storms. The original analysis was carried out on data from 1979-1996, but in 2005 it was decided to update the work with data until 2005, a total of more than 1250 station years and thereby almost doubling the data foundation (Madsen et al, 2009). This study is a further elaboration on the findings from (Arnbjerg-Nielsen, 2006). Only stations with more than 10 years of recording were included in the analysis. The updated analysis confirmed what practitioners had believed for years – the frequency of extreme rainfall in Denmark had increased. For durations (30 min-3 h) and return periods (~10 years) the increase in intensity is in the order of 10% (Madsen et al, 2009). Furthermore, it was concluded that there exists a significant variability of extreme rainfall, which is partly related to the mean annual precipitation (MAP). Higher frequency of extreme events is observed in regions with higher mean annual precipitation (Madsen et al, 2009).

The Danish gauge network compared to many other networks is quite dense especially around the larger cities, but in some areas such as the western parts of the country there are large gaps in the network as shown in Figure 6.5. It can be argued that there are no large sewer systems in these blank areas and therefore there is less need for rainfall information, however, in connection with extreme value statistics this becomes an issue. Extreme events are most often connected to convective rainfall which occurs at very local scales. Often an event is less than 5 km across. The probability of a single gauge observing the peak intensity of such an event is therefore much higher in areas such as Copenhagen where there is a high density of gauges compared to the western parts of the country with only a few gauges. (Madsen et al, 2009) found that there was a tendency of larger extreme events in the Eastern part of Denmark, but whether this is a regional tendency or a result of the probability of an extreme event being intercepted by a gauge is much larger in an area with many gauges is still to be verified.

Weather radar data on the other hand provides spatial distributed rainfall measurements which in connection with extreme value statistics of rainfall data opens up for a whole new range of opportunities. The new opportunities are not without challenges. First and foremost the time series from radar data is only starting to be of a duration long enough for statistical analysis so only few studies exist on this topic. Linked with the duration problem is the issue of relating a radar observed rainfall intensity with a return period, which is the point of interest in this connection.

One of the major obstacles in connection with deriving extreme value statics on radar rainfall data is that a vast amount of data (tera-bytes) needs to be processed. Settings and properties are changed on weather radars over time which can have significant impact on the rainfall estimate, so the data scrutinizing prior to the statistical analysis is a huge and extremely important project in itself (Koistinen et al, 2006). Some of the first to attempt it was the Finish Meteorological Institute (FMI) which in 2006 analyzed data from seven Finish weather radars coving the time frame of six summers - a total of 10 TB data (Koistinen et al, 2006). The findings of 2006 suggested that the probability of high rainfall intensities (repeat time >50 years) from hydrological standard Finish gauge based figures has been underestimated with a factor of 2 compared to the result of the radar data. The work is still ongoing and no final conclusions are presented, however, the potential of extreme value statistics based on spatially distributed extreme rainfall is very motivating and of great importance in connection with the future design of urban drainage systems.

Paper E and F contains the first preliminary results of extreme value statistics based on LAWR data. Two general assumptions have been made in order to overcome the obstacle of the unknown radar IDF. Each pixel is assumed an independent sample of precipitation, an assumption also used in the work of (Koistinen et al, 2006). Secondly, the gauge based derived IDF-curves are used to relate a radar estimated rainfall intensity of a given duration to a frequency (return period). The spatial extent and structure of an extreme event is impossible to observe with a gauge network, but observed very well by a LAWR as illustrated in Figure 6.6.

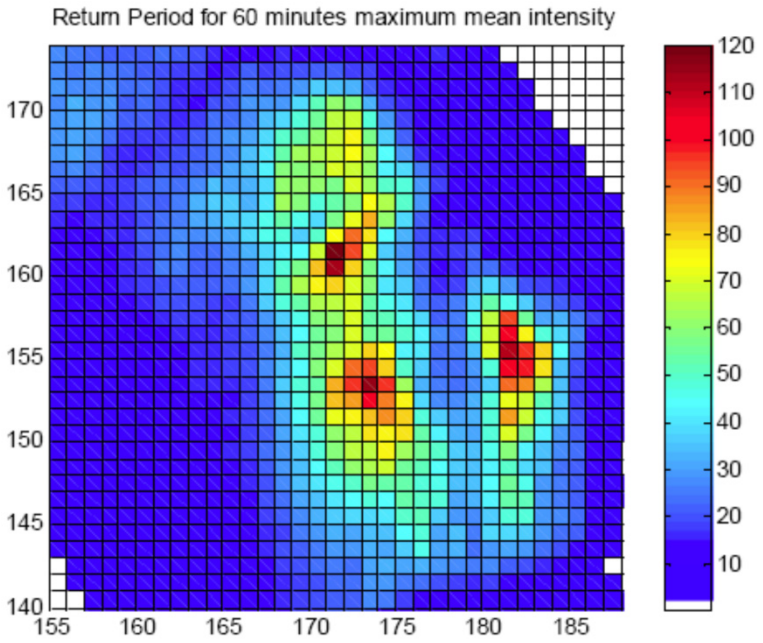

Figure 6.6 Example of estimated return periods from a LAWR. The return periods are estimated based on radar estimated rainfall intensity related to a return period by the Danish gauge derived IDF relationships. The area depicted is 16.5x16.5 km.

Today, drainage systems are designed based on a political selected combination of duration and intensity which a sewer system must be able to accommodate. The identification of the spatial structures of extreme events during this PhD project requires considerably more work before any conclusions can be made, however, it suggests that there could exist a characteristic "catchment space length" which is related to the return period and should be included in the future design practice of e.g. retention basins for individual catchments.

6.4 The Future of Weather Radar Data in Urban Drainage Applications

There is no doubt that in connection with urban drainage weather radars provide more knowledge of the spatial rainfall characteristics along with a much denser sampling of the rainfall. The combination of dense gauge networks and high resolution weather radars is a strong combination and the uncertainties related to both types of measurements must be evaluated relative to the potential gain of information.

Another issue solved by including weather radar measurements is the location of rain gauges. In Denmark many gauges are located at WWTP often for practical and administrative reasons, which means that there are more rainfall recordings in low altitude areas than in areas of higher altitude. Local terrain effects are known to influence rainfall patterns significantly which again means that the gauge data used today as foundation for drainage designed may to some (still unknown) degree be biased. Weather radars furthermore provide equally distributed sampling points over

an area with equal density, but it is important to keep in mind that the sample volume increases with range and thereby adds uncertainty to the estimate.

Up til now radar data in urban drainage context has mostly been in connection with research projects, however, over the past three years equal to the duration of this PhD project the interest from the urban drainage community has increased significantly. This is probably a combination of the fact that radar rainfall products have matured significantly and the meteorological services are starting to interact much more with the hydrological community. Another driving force has been the many servere flooding events over European cities since 2000, which have put increased and long needed political focus on the field of urban drainage boosting the general development of the field. It is the author's personal belief that weather radar data in the future will become a common data source in many types of hydrological applications, especially in connection with flood forecast and real-time control applications.

CHAPTER 7

References

Ahrens, C.D., 2007. *Meteorology Today - An Introduction to Weather, Climate, and the Environment*. 8th ed.: Thomson Brooks/Cole.

Arnbjerg-Nielsen, K., 2006. Significant climate change of extreme rainfall in Denmark. *Water Science and Technology*, 54(6-7), p. 1-8.

Arnbjerg-Nielsen, K., Harremoës, P. & Mikkelsen, P.S., 2002. Dissemination of regional rainfall analysis in design and analysis of urban drainage at un-gauged locations. *Water Sciense and Technology*, 45(2), p. 69-74.

Arnbjerg-Nielsen, K., Madsen, H. & Harremoës, P., 1998. Formulating and Testing a Rainfall Series Generator Based on Tipping Bucket Gauges. *Water Science and Technology*, 37(11), p. 47-55.

Battan, L.J., 1973. *Radar Observations of the Atmosphere*. The University of Chicago Press.

Bouar, E. et al., 2005. An Extensive Validation Experiment of Algorithm ZPHI. In *Proceeding from the 32nd Conference on Radar Meteorology*. Albuquerque, NM American Meteorological Society.

Brotzge, J., Droegemeier, K. & McLaughlin, D., 2006. Collaborative Adaptive Sensing of the Atmosphere (CASA): A New Radar System for Improving Analysis and Forecasting of Surface Weather Conditions. *Journal of the Transportation Research Board*, (1948), p. 145-151.

Bøvith, T., 2008. *Detection of Weather Radar Clutter*. PhD Thesis. Technical University of Denmark & Danish Meteorological Institute

Cluckie, I.D., Han, D., Austin, G.L. & Zawadzki, I., 1997. Operational Utilization of a High Resolution Hydrological C-band Radar. *Weather Technology for Water Resources Management (Chapter III Operational Systems)*. p. 455-467.

DMIa, 2008. *Måneden, sæsonen og årets vejr*. [Online]. Available at: http://www.dmi.dk/dmi/index/danmark/maanedens_vejr_-_oversigt.htm [accessed 15 October 2008]

DMIb, 2008. *Spildevandskomitéens regnmålersystem*. [Online]. Available at: http://www.dmi.dk/dmi/index/erhverv/spildevandskomiteens_regnmaalersystem.htm[accessed 12 January 2009]

Donovan, B. C., Hopf, A., Trabal, J. M., Roberts, B. J., McLaughlin, D. J., & Kuros, J., 2006. Off-the-grid radar networks for quantitative precipitation estimation. *Proceedings from Fourth European Conference on Radar in Meteorology and Hydrology (ERAD06)*. Barcelona.

Doviak, R.J. & Zrnic, D.S., 2006. *Doppler Radar and Weather Observations*. 2nd ed.: Dover Publications.

Einfalt, T., Arnbjerg-Nielsen, K., Golz, C., Jensen, N. E., Quirmbach, M., Vaes, G, & Vieux, b., 2004. Towards a roadmap for use of radar rainfall data in urban drainage. *Journal of Hydrology*, (299), p. 186-202.

Furuno, 2002. *Furuno Operator's Manual 15" MULTI-COLOR HIGH-PERFORMANCE SHIPBORNE RADAR AND ARPA, FR-1500 MARK-3 SERIES*.

Gekat, F., Pool, M. & Didszun, J., 2008. Performance comparison of a compact weather radar featuring different antennas. *Proceedings of the Fifth European Conference on Radar in Meteorology and Hydrology*. Helsinki.

Hanson, D.S. & Edwards, G., 2008. Integration of rainfall radar into near real-time information systems. *Proceedings of the 11th International Conference on Urban Drainage (ICUD)*. Edinburgh IWA.

Hoblit, B.C. & Curtis, D.D., 2002. Integration of Radar Rainfall into Hydrologic Models. *Proceedings of the Ninth International Conference on Urban Drainage*. Portland.

James, W.C., Heralall, M. & James, W., 2008. Integrated Web-Based Automated Radar Acquisition, Processing and Real-time Modeling for Flow/Flood Forecasting. *Proceedings of the 11th International Conference on Urban Drainage*. Edinburgh IWA.

Jensen, N. & Pedersen, L., 2005. Automated Short Term Forecast from LAWR X-band Radar. Proceedings *of World Weather Research Program Symposium on Nowcasting and Very Short Range Forecasting*. Toulouse, France.

Koistinen, J., Kuitunen, T. & Inkinen, M., 2006. Area-intensity probability distributions of rainfall based on a large sample of radar data. *Proceedings of European Radar Conference (ERAD06)*. Barcelona.

Krajewski, W.F., Ciach, G.J. & Habib, E., 2003. An analysis of small-scale rainfall variability in different climate regimes. *Hydrological Sciences*, 48(2), p. 151-162.

Langille, R.C. & McK., P.W., 1947. Measurements of Rainfall by Radar. *Journal of the Atmospheric Sciences*, 4(6), p. 186–192.

Lee, G., & Zawadzki, I. (2005). Variability of Drop Size Distributions: Time-Scale Dependence of the Variability and Its Effects on Rain Estimation. *Journal of Applied Meteorology , 44* (2), 241-255.

Lee, G.W. & Zawadzki, I., 2005. Variability of Drop Size Distributions: Noise and Noise Filtering in Disdrometric Data. *Journal of Applied Meteorology*, 44, p. 634-652.

Liu, Y.X. et al., 2007. Operational Evaluation of the Real-Time Attenuation Correction System for CASA IP1 Testbed. *Proceedings of 33rd Conference on Radar Meteorology*. Cairns, Australia.

Madsen, H., Arnbjerg-Nielsen, K. & Mikkelsen, P.S., 2009. Update of regional intensity-duration-frequency curves in Denmark: Tendency towards increased storm intensiteis. *Atmospheric Research*, Article in Press.

Marshall, J.S. & Palmer, W.M., 1948. The distribution of raindrops with size. *Journal of Meteorology*, 5, p. 165-166.

Marshall, J.S., Langille, R.C. & Palmer, W.M., 1947. Measurements of Rainfall by Radar. *Journal of the Atmospheric Sciences*, 4(6), p. 186–192.

Moran, K. P., Martner, B. E., Post, M. J., Kropfli, R. A., Welsh, D. C., & Widener, K. B, 1998. An Unattended Cloud-Profiling Radar for Use in Climate Research. *Bulletin of the American Meteorological Society*, 79(3), p. 443-455.

NASA, 2007. *Earth Fact Sheet*. [Online]. Available at: http://nssdc.gsfc.nasa.gov/planetary/factsheet/earthfact.html [accessed 22 January 2009]

Pedersen, L., 2004. *Scaling Properties of Precipitation - experimental study using weather radar and rain gauges*. M.Sc. Thesis. Aalborg University

Pedersen, L., Jensen, N.E., Christensen, L.E. & Madsen, H., Submitted to Atmospheric Research. Quantification of the spatial variability of rainfall based on a dense network of rain gauges. Submitted to Atmospheric Research

Rinehart, R.E., 2004. *Radar for Meteorologists*. 4th ed.: Rinehart Publications.

Schladweiler, J., 2004. *Tracking Down the Roots of Our Sanitary Sewers*. [Online]. Available at: www.sewerhistory.org [accessed 10 January 2009]

Sempere-Torres, D., Corral, C. & Raso, J., 1999. Use of Weather Radar for Combined Sewer Overflows Monitoring and Control. *Journal of Environmental Engineering* p. 372-380.

SWI, 2008. *Storm- and Wasterwater Informatics*. [Online]. Available at: "http://swi.er.dtu.dk" http://swi.er.dtu.dk [accessed 2 December 2008]

Thyregod, P., Arnbjerg-Nielsen, K., Madsen, H. & Carstensen, J., 1998. Modelling the Embedded Rainfall Process using Tipping Bucket Data. *Water Science and Technology*, 37(11), p. 57-64.

Ulbrich, C.W. & Atlas, D., 1998. Rainfall microphysics and radar properties: analysis methods for drop size spectra., 37(9), p. 912-923.

Ulbrich, W.C., 1983. Natural variations in the analytical form of the raindrop size distribution. *Journal of Climate and Applied Meteorology,* 22, p. 1764-1775.

UN, 2008. World Urbanization Prospects, The 2007 Revision - Highlights. United Nations, Department of Economic and Social Affairs.

Vieux, B. & Bedient, P.B., 2004. Assessing urban hydrologic prediction accuracy through event reconstruction. *Journal of Hydrology*, 299(3-4), p. 217-236.

PART III

Published Papers

PAPER A

Quantification of the Spatial Variability of Rainfall Based on a Dense Network of Rain Gauges

---

Submitted to *Journal of Atmospheric Research* December 2008

Quantification of the Spatial Variability of Rainfall Based on a Dense Network of Rain Gauges

Lisbeth Pedersen[a+bI], Niels Einar Jensen[a], Lasse Engbo Christensen[b] and Henrik Madsen[b]

[a]DHI, Gustav Wieds Vej 10, DK-8000 Aarhus, Denmark
[b]Institute for Informatics and Mathematical Modelling, Technical University, Denmark, Building 321, 2800 Lyngby, Denmark

Abstract: The spatial variability of rainfall within a single Local Area Weather Radar (LAWR) pixel of 500x500 meter is quantified based on data from two locations. The work was motivated by the need to quantify the variability at this scale in order to provide an estimate of the uncertainty of using a single rain gauge for calibrating the LAWR. A total of nine rain gauges was used, each representing one-ninth of the 500x500 meter area. The analysis is carried out on a dataset obtained using tipping bucket gauges during the summer and fall of 2007 and 2008, and the results are compared with results from an earlier campaign in 2003. The 2007-2008 dataset is almost four times larger than the original dataset from 2003 that motivated this extended study. Two methods have been used to describe the variability: The coefficient of variation and the spatial correlation structure of the rainfall field. Despite the small area of 0.25 km^2, accumulated rainfall was found to vary significantly within individual events with duration ranging from 5 minutes to 13 hours. The coefficient of variation was found to range from 1-26% in the 2007-2008 dataset and in some special cases even higher. The 95% prediction interval for a given rainfall depth is estimated and can be used to address the uncertainty of using a single rain gauge to represent the rainfall within a 500x500 meter area.

1 Introduction

Rainfall measurements are extensively required as input to a range of applications ranging from real time online warning systems in hydrology and meteorology to complex models for post analysis of critical events. These types of applications all require a precise and representative measurement of rainfall. The most common method of precipitation measurement has been, and still is, using gauges. However, gauges cannot provide information on the spatial variability of the rainfall, and this is required for most meteorological and hydrological applications. An obvious solution is to use radar for rainfall measurements, since a single radar can cover a large area, and sample the spatial as well as the temporal properties of rainfall. Weather radars have been used for precipitation measurements since just after World War II, when a relationship between the radar measurement of the energy backscattered from the hydrometeors in the atmosphere and the rain rate at ground – the Z-R relationship - was established (Marshall and Palmer, 1948). Despite more than half a century of dedicated research in the field of weather radars and major advancement in the field, radar measurements are still shrouded with distrust – especially by hydrologists. One of the major reasons for this distrust is that the most common approach to evaluating the radar performance is to compare the rainfall estimated by radar with that observed by a single rain gauge. Many consider the rain gauge to be the "ground

[I] Corresponding Author: DHI, Gustav Wieds Vej 10, DK-8000 Aarhus, Denmark, tel. +45 8620 5116, email: lpe@dhigroup.com

truth", despite the fact that it gives no information on the spatial patterns of the rainfall and also contains measurement uncertainties. When modeling hydrologic processes in urban areas in particular, the standard approach of assuming that a single gauge is representative for the whole catchment can lead to large errors, as the individual catchments may have different, and in some cases very rapid, run-off times. (Sempere-Torres et al., 1999) demonstrate that even raw radar data provides a better input to a distributed urban drainage model than data from a dense rain gauge network in cases of modeling combined sewer overflows resulting from strong local convective events.

Weather radars operate with pixel sizes from 0.1x0.1 to 2x2 km and provide output every 1-15 minutes, with 5-10 minutes being the most common. In reality the output is not a surface measure, but a volume measure at a given height, increasing with range. The quality of this measure is evaluated on the basis of a rain gauge, which is several orders of magnitude smaller and records every time a given volume is collected. In terms of addressing the accuracy of the radar it is therefore of great interest to examine the representativeness of the rain gauge within a single radar pixel, since the accuracy of radar precipitation estimation can only be as accurate as a single gauge representativeness of a pixel. (Einfalt et al. 2005) show that weather radars provide information on the spatial pattern of the rainfall that is often missed by rain gauges, and the peak intensities of an event are rarely captured by a gauge network.

Being a mechanical device, the rain gauge also suffers from uncertainties due to hardware and external forces, however, the primary issue is probably the representativeness of the measurement in the spatial domain. The catchment surface of a rain gauge is typically 0.02 - 0.04 m^2 and for this point the gauge can be assumed to yield a precise measurement, provided it is well maintained and wisely placed. The temporal resolution depends on the gauge type, but most automatic gauges today record every time a given volume of water is collected - often corresponding to a rainfall depth of 0.2 or 0.4 mm.

The spatial domain difference between rain gauges and conventional weather radars is one of the major obstacles to convincing hydrologists that weather radars can provide data equally good or equally uncertain to those of a rain gauge. To bridge this domain span and act as a supplement, not a substitution to rain gauges and conventional weather radars, a cost-efficient weather radar was developed in 1999 as part of the EP-23475 EU project to give sufficient information on rainfall for use in real time online warning systems for flash floods in urban areas. The radar system is called Local Area Weather Radar (LAWR) and it was developed and manufactured by DHI. The system is based on a 25 kW marine X-band radar and operates with pixels ranging from 100x100 up to 500x500 meters, a temporal resolution of 1 or 5 minutes and a maximum range of 60 km, of which the inner 20 km range is usable for quantitative precipitation estimation (DHI, 2009). Being based on X-band technology, the LAWR system is affected by attenuation as outlined in (Rahimi et al., 2006) and others, but the LAWR signal processing compensates for this issue so that extension due to attenuation has only been observed in a very limited number of situations during the 10 years of operation.

The LAWR is designed as a supplement to standard rain gauges, and requires the presence of rain gauges for calibration.

This paper focuses on the spatial variability of the rainfall within a single LAWR pixel and the uncertainties of representing the rainfall of a pixel by a single gauge.

2 Background and past experience

In order to evaluate the uncertainties of calibrating a LAWR with a single rain gauge, a field experiment was conducted during the fall of 2003 south of Aarhus, Denmark. Nine high resolution optical rain gauges were evenly distributed within an area of 500x500 meters, corresponding to a single pixel from the Aarhus LAWR. The purpose was to test the initial hypothesis: "On an individual event basis, rainfall within an area of 500x500 meters is uniform". If a single rain gauge is to be used for calibration of a LAWR, the hypothesis would have to be accepted, otherwise the calibration would vary in the same order as the rainfall within the pixel. An event had to contain a minimum of two gauge registrations less than 60 minutes apart. The event durations ranged from 5 minutes to 13 hours in the collected dataset. The analysis carried out in this work has not considered different aggregation times such as 5, 10, 15 or 60 minutes because the original focal point of the work was related to LAWR calibration. However, it is planned to consider these differences in future analyses.

Surprisingly, the results from the experiment showed high variability in the rainfall depths observed by the nine gauges within independent events. Expressed as coefficient of variation (CV), the variability ranged from 10% and up to 100%, and even if the most extreme of the gauges were omitted from the analysis, the variation was more than 50% in several events. (Jensen et al., 2005).

If the order of variability based on the 2003 dataset is representative, parts of the uncertainties related to radar rainfall estimation are not due to the radar, but a result of the variability of rainfall at very small scales influencing the calibration. The properties of rainfall at scales equal to or less than a single pixel is still more or less unknown, whether the pixel be 0.1x0.1 km or 2x2 km. Rainfall within areas of these scales is central for evaluation of radar performance as well as a range of hydrological applications, in particular urban hydrological applications.

Inter-gauge distances in operational gauge networks used for radar estimation evaluation and for hydrological modeling are often more than 20-30 km, and this yields no information on the spatial structure at small scales (Ciach et al., 2006). The definition of small-scale and network density varies from source to source, since small-scale is defined with inter-gauge distances ranging from 0.1 km to more than 10 km (Ciach et al., 2006), (Krajewski et al., 2003) and sources herein. There are many experimental gauge networks around the world, some of which are relatively dense, e.g. EVAC PicoNet (Oklahoma, USA) with 25 gauges spaced 0.6 km covering a 9 km^2 area (Ciach et al., 2006). Networks with such gauge density are unfortunately quite rare since they require a high number of gauges, frequent maintenance and calibration, as well as dedicated time for data quality control – all of which are expensive.

On the basis of five gauge networks of different densities and in different climate regimes (Krajewski et al., 2003) conclude that the small-scale variability of rainfall is significant, but state that their dataset is insufficient for final conclusions. The variability found by (Krajewski et al., 2003) is not as large as those found on the basis of the rain gauge experiment in 2003. There may be several reasons for this discrepancy, such as local orographic effects, climate zones, rainfall types, gauge types and gauge errors. The dataset from 2003 is limited to three months of sampling during the fall months of September to November (Denmark). During the experiment the optical drop-counting gauges were observed to vibrate due to wind, and low temperature caused ice to freeze in the funnel of the gauge, causing uncertainties in some events. The large variation in the 2003 dataset gave reason for concern, but a larger dataset is required to make a more final conclusion and therefore the experiment was recommenced in 2006 with minor alternations as part of a three-year field experiment.

This paper presents the results from the three-years measuring campaign from 2006 to 2008 with nine gauges equally spaced within a 500x500 meter area. In addition the dataset from 2003 is included for comparison. The intention of the experiment is to validate the results from 2003 by increasing the data foundation and more in-depth statistical analysis of the spatial variability. The paper is a further development of the work presented in (Pedersen et al., 2008) and it presents new data and methods.

3 Rain gauge setup 2006-2008

In order to validate previous results, the gauge experiment was recommenced in the spring of 2006. The gauges used in the original setup were optical drop-counting gauges with a resolution of 0.01 mm manufactured by Rosted DigiRain. The uncertainties observed during the experiment in 2003 have been confirmed by other internal DHI setups using this gauge type. As a result of this, and because of a desire for more comparable results with other studies of similar type, a standard 0.2 mm tipping bucket gauge from Pronamic was chosen for the 2006-2008 period. The gauges were all equipped with a data logger for data storage. For overview of different setups, cf. Table 1 and for illustrations Figure 1.

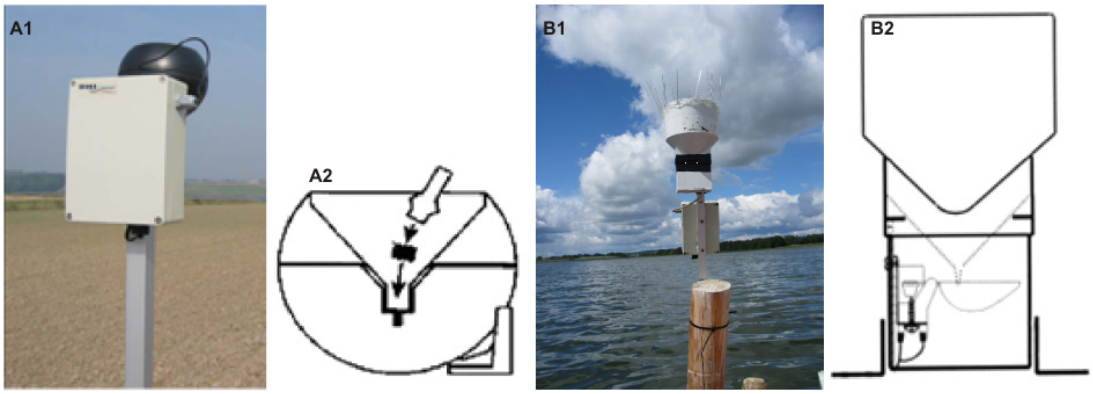

Figure 1 Gauge types used in field experiment. Left: the optical drop-counting gauge (marked A) based on a Rosted DigiRain gauge (2003) and a sketch of the gauge showing the sponge and funnel. Right: the tipping bucket gauge (marked B) by Pronamic (2006-2008) along with a sketch of the gauge illustrating the location of the tipping bucket. In 2008 the gauges where further more equipped with metal spikes on the rim of the gauge to avoid resting birds.

Table 1 Overview of gauge experiment. The data analyzed are from the years 2003, 2007 and 2008 since the gauges were damaged during the 2006 season. The different gauge types and locations along with calibration information are listed for each year.

	Measuring Time Frame	Gauge type	Location	Calibrated	In-situ calibration
2003	09.19.2003 11.25.2003	0.01 mm Optical drop counting gauges (Rosted DigiRain)	Open field	Yes	No
2006	No data	0.2 mm tipping bucket gauge (Pronamic)	Open field	Yes	No
2007	09.13.2007 11.07.2007	0.2 mm tipping bucket gauge (Pronamic)	Estuary	Yes	No
2008	06.17.2008 11.13.2008	0.2 mm tipping bucket gauge (Pronamic)	Estuary	Yes	Yes

In 2006 the gauges were installed at the same location as in 2003 (on land as illustrated in Figure 2), but unfortunately they were more or less all destroyed by farming equipment as a result of miscommunication with the landowners. After this the landowners would only allow the gauges to be sited from November to February, which in Denmark are winter months dominated by widespread frontal rain with occasional sleet and snow showers. Rainfall events with high intensities and large variability often occur during the summer and early fall, and a new location was therefore needed. The new location was selected based on the following requirements: undisturbed location, homogeneous conditions without terrain differences, and less than 15 km from the Aarhus LAWR. It proved hard to find such a location on land, and therefore the gauges were moved approximately 1 km north-east out into the shallow estuary “Norsminde Fjord”. The layout of the experiment is illustrated in Figure 2 and the inter-gauge distances are listed in Table 2.

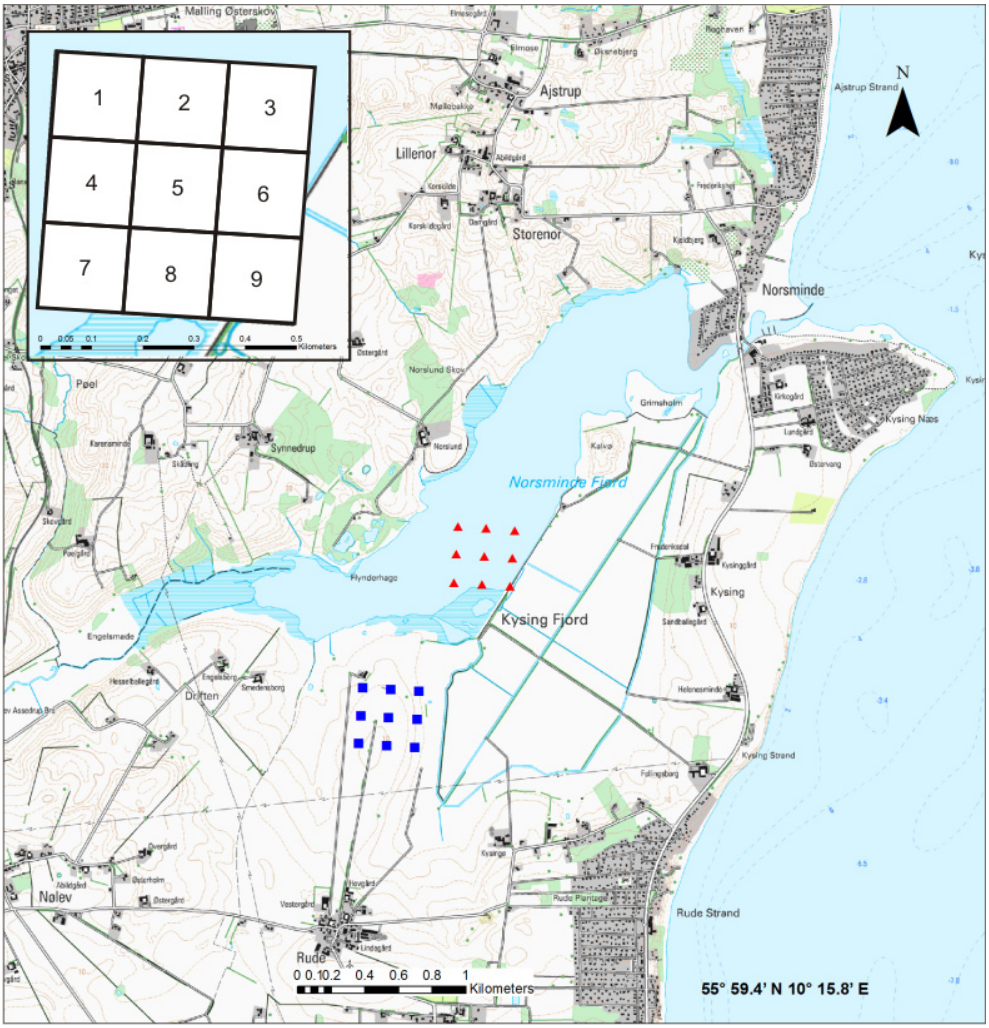

Figure 2 Location of the gauge sites. 2003 and 2006 site is on land marked with squares, while the 2007 and 2008 site is in the estuary (Norsminde Fjord) marked with triangles. Upper right corner: a close-up of the experiment layout and area represented by each gauge. The tilted orientation of the gauges grid corresponds to the radar grid of the Aarhus LAWR in 2006 which is located 10 km north of the gauge sites.

Table 2 Inter-gauge distances in field experiment

Possible inter-gauge distances [m]	
I (e.g. 1-2)	167
II (e.g. 1-3)	333
III (e.g. 1-5)	236
IV (e.g. 1-6)	373
V (e.g. 1-9)	472

The gauges were mounted on poles pounded down into the seabed of the estuary and because it was problematic to do this with a sledge hammer standing in a rubber dinghy, not all the poles were level. To alleviate this problem all the gauges were installed with an adjustable fitting allowing for adjustment of the gauge on site. During the fall of 2007 the poles holding the gauges were observed to be affected by the current, which may have caused the effective volume of the gauge bucket to be reduced or increased, due to tilting of the gauge bucket. If the gauge installation is tilted along the longitudinal axis of the bucket the bucket will be tilted upwards or downwards. As result it will tip at a different water volume since the point of gravity has been shifted. The gauge bucket is shown on Figure 2, marked as B2. As a result of this the gauges were in-situ calibrated throughout the measuring period in 2008, in order to establish the tipping volume as described in Section 3.1.

3.1 Calibration of gauges

All gauges were calibrated prior to deployment each year. A known water volume was poured into the gauge at different speeds to simulate a range of intensities. The observed number of tips was compared with the expected number. The dataset from the optical drop-counting gauges has been supplemented with a gauge-specific calibration factor based on the calibration prior to deployment. Unfortunately, the gauges were not recalibrated when dismantled. This would have provided information on possible drift of the gauge.

The calibration prior to installation in 2006 revealed that six of the gauge buckets did not tip at 0.2 mm, but at different volumes corresponding to rainfall depths ranging from 0.1-0.4 mm. All gauge buckets differing more than 2% in the calibration were replaced and the replacements were tested and accepted. During the calibration it was observed that this type of rain gauge is very sensitive to misalignment, since a slight tilting of the bucket around the longitudinal axis resulted in changed effective tipping volume and resulting in either over- or underestimation. If the degree of tilting is unknown or varying, this may corrupt data. Since the gauges were placed on a pole in an unstable environment, an in-situ calibration method was developed to facilitate this problem.

The challenge was to obtain a well-known volume of water and empty it down into the gauge at a controllable continuous speed in a manner reproducible within a 2% error margin; all at sea in a small dinghy. The method chosen used a 270 ml plastic wash bottle with a swan neck. The bottle was totally submerged under the water and filled to the rim (no air bubbles), then the spout was screwed on (still submerged) and the bottle was placed upside down in the gauge. The method was tested in the lab in order to determine the degree of error caused by excess water on the bottle and hands, the ability to fill the bottle with the exact same amount of water each time, and the drip rate of the spout. A total of 28 experiments resulted in a mean of 69.2 tips with a standard deviation of 0.74 tips. A one sided t-test gives 95%

confidence bounds of 68.9 and 69.5 and thereby the method is concluded to be reproducible within +/- 1 tip, which fulfills the 2% error margin requirement. The water used for the on-site calibration was brackish with a density of approximately 1.02 mg/l and the volume of the bottle would result in 69 tips if the gauge was level. At every visit to the gauge site each gauge was calibrated in-situ. The average number of recorded tips for each gauge per visit was interpolated to obtain a daily calibration factor reflecting changes over time, e.g. drift of the pole. Due to practical time limitations, only two in-situ calibrations were applied at each visit, which is less than desirable for making the calibration factor. Therefore a weight has been used in the estimation of the calibration factor. A factor of 1/3 has been assigned to each of the neighboring visits whereas the visit in question is assigned 3/5 and the actual value is the weighted average of the three visits. The calibration factor as a function of time is shown in Figure 3 for two selected gauges – gauge 3 and 7.

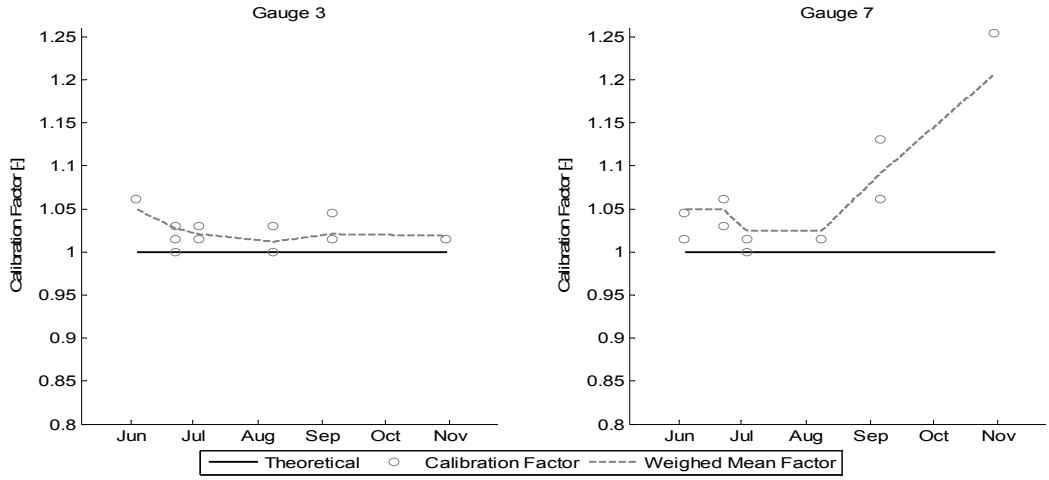

Figure 3 Calibration coefficients as a function of time for two of the nine gauges – gauge 3 and gauge 7. Circles mark the date of calibration. Gauge 3 is an example of a very stable gauge, while gauge 7 changed properties during the experiment. The rest of the calibration profiles lay between the two shown.

The calibration factor of gauge 7 increases significantly in the final two months, but the factors are consistent with an equal number of registrations on the respective days, so the increase is probably caused by the pole drifting or the adjustable fitting becoming dislodged.

3.2 Data quality control

As with any other field experiment, practical problems can cause data corruption. In relation to rain gauges clogging caused by debris collected in the orifice is probably one of the most frequent problems. In this experiment a whole range of debris types caused problems. On one occasion, a dead bee was found clogging the funnel and partly dissolved into the gauge bucket, decreasing the effective volume. However, the biggest practical problem was bird droppings resulting in clogging and reduced bucket volume. The latter was not observed to be a problem when the gauges where situated on land in 2003, but when they were moved to the estuary for the first period of sampling in 2007, the gauges were seriously affected. The reason for the difference is probably a different type of funnel, cf. Figure 1 and the change in location. The gauges were equipped with a crown of netting, but it became evident that the material used was too flexible because birds rested on the gauges anyway. Next the gauges were equipped with pigeon spikes glued to the rim as shown in Figure 1, and this turned out

to work well. Unfortunately, this means that there are few events with nine functioning rain gauges; most events have somewhere between three and nine gauges in working order.

Rain gauge measurements are known to be affected by wind, and a number of correction schemes have been developed to correct for the wind-induced loss. Studies carried out under the World Meteorological Organization (WMO) report of wind-induced losses in the range of 4-6% (Sevruk et al., 2009). It has not been possible to obtain reliable wind correction parameters for the site in question as no wind and temperature data were available. The potential error would be underestimation of the rainfall since the site is unsheltered (open waters). The underestimation would most likely be relative as all gauges would be affected equally due to the homogenous site conditions.

Another source of error causing data corruption was lightning. During the summer of 2008 several intense thunderstorms occurred over the site. On at least one occasion six out of the nine gauges were struck by lightning, causing them to stop recording. The data from this event has been split into two events in order to use both events in the analysis, since it was a large event with high intensities and large rainfall depths. The time of interruption occurred within a minute on all the affected gauges and the data from the working gauges were cut off at that time, cf. Figure 4. The full time series from gauges 4, 6, and 9, which were unaffected by the lightning, is illustrated in Figure 5.

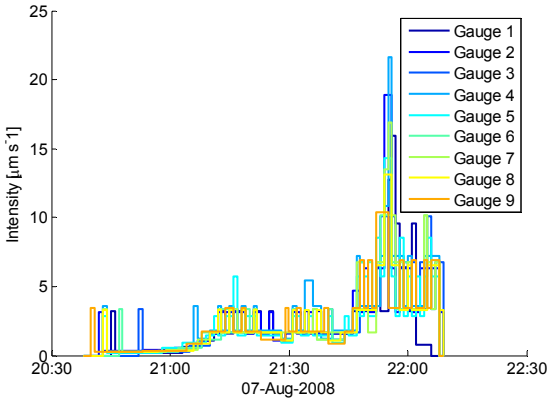

Figure 4 First part of intense rain event on 7th August 2008 with all nine gauges working. The gauges recorded between 11 and 14 mm of rainfall during 76-87 minutes (1.4 hours) until gauges 1, 2, 3, 5, 7 and 8 were struck by lightning

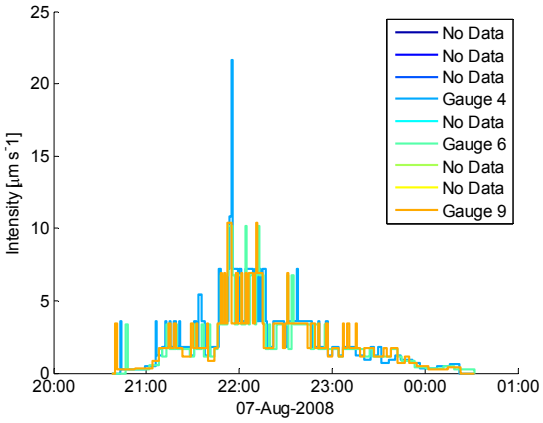

Figure 5 Full extent of rain event on 7th August 2008 based on gauges 4, 6 and 9 that survived the lightning. The gauges recorded between 38 and 30 mm of rainfall during 218-224 minutes (~3.7 hours)

In some cases short circuits in the electric system were observed. Whether this was a result of a previous lightning incident or malfunctioning hardware has not been established, but the data affected has been omitted from the analysis when detected.

A substantial amount of effort and time has been invested in scrutinizing the dataset before the analysis. Despite this there are cases where it has not been possible to determine whether suspiciously looking data are due to a gauge error or natural variability in the rainfall. This problem could have been alleviated by using a setup with multiple gauges in each point. On

the basis of their observations from various field experiments, (Krajewski et al., 2003) recommend a double gauge setup, since they observed difficulties in identifying error-affected data if only a single gauge was available. This has not been possible due to financial and practical reasons. The double gauge setup would furthermore have been useful since data were often missing due to malfunctioning gauges as a consequence of the problems accounted for above.

4 Data characteristics

The scrutinized data have been subdivided into events on the basis of the criteria applied to the Danish Water Pollution Control Committee network of rain gauges in Denmark operated by the Danish Meteorological Institute (Thomsen, 2006). An event must consist of at least two registrations and the time span between these registrations must be less than 60 minutes (Thomsen, 2006). An additional requirement of minimum rainfall depth of 1 mm has also been applied to the data in this analysis.

The characteristics of the dataset are listed in Table 3. Unfortunately, all three years had periods with one or multiple gauges malfunctioning, leaving 10 events in 2003 with all nine gauges functioning, five in 2007 and eight in 2008. The lower half of Table 3 gives the characteristics of events where a minimum of three gauges were functioning. By limiting the number of required gauges the dataset becomes significantly larger. Out of the 10 events with nine working gauges in 2003, only three events have rain depths larger than 5 mm, none in 2007 and five in 2008.

Table 3 Characteristics of the data samples from the three seasons of operation – 2003, 2007 and 2008.

	2003	2007	2008
Sample size [events >1 mm by 9 gauges]	10	5	8
Average total rainfall depth (mean of 9 gauges) [mm]	53	14	69
Range rainfall intensity [mm/h]	0.1-2.5	0.5-9.1	1.2-14.3
Mean rainfall intensity (mean of 9 gauges) [mm/h]	0.8	1.9	5.4
Sample size [events >1 mm by min. 3 gauges]	20	19	55
Average total rainfall (mean of 3-9 gauges) [mm]	89	71	222
Range rainfall intensity [mm/h]	0.1-3.4	0.5-11.5	0.3-32.5
Mean rainfall intensity (mean of 3-9 gauges) [mm/h]	0.9	2.4	3.6

2008 is characterized by a high number of events and a very large total rainfall depth of 222 mm, which is due to a large number of intensive convective events in August. The national average precipitation statistics for August 2008 confirm this with a recorded average regional rainfall depth of 146 mm compared to a normal of 67 mm for the month of August (DMI, 2008).

The aim of this work is to quantify the variability of rainfall at very small scales by means of descriptive statistical methods with focus on estimating the spatial correlation structure. Correlation is known to be an adequate measure of the relation between two variables, provided that the data are normally distributed. In hydrology and hydrometeorology correlation is widely used on rainfall data assuming they are normally distributed. This issue

motivated (Habib et al., 2001) to investigate this matter further, and they state that, among statisticians it is a well known fact that skewed data result in biased correlation results, but this is rarely taken into account in the communities using rainfall data in operational applications. Rainfall data at smaller spatial scales ranging from a few meters to 8 km are typical scales for radar products used in hydrological applications (Habib et al., 2001). At such local scales rainfall data can be considerably skewed and rainfall data should be log-transformed (Habib et al., 2001). The data in this study were therefore first tested to establish which type of distribution they follow.

The data analysis was carried out on the subset of the dataset corresponding to the lower half in Table 3 due to the very limited number of events where all nine gauges were recording properly. The rainfall events used in the analysis contain data from three to nine gauges.

If the data were normally distributed, the variance would be independent of the mean, but as Figure 6 clearly illustrates this was not the case. There is a clear tendency of increasing variance with increasing mean rainfall depth. For the cases of 2007 and 2008 the variance is lower compared to the 2003 data, where in some cases the variance is of the same order as the mean value. Common for all three datasets is an indication of a downward trend in the variance with increasing mean rainfall depth. As mentioned earlier, the dataset from 2003 is based on a different type of gauge at a different location and as illustrated in Figure 6 this set has a higher variability than 2007 and 2008.

There are outliers in the 2003, 2007 and the 2008 datasets, marked with a square in the plot. These events have been examined in detail and are considered dubious, so they have been omitted from the datasets.

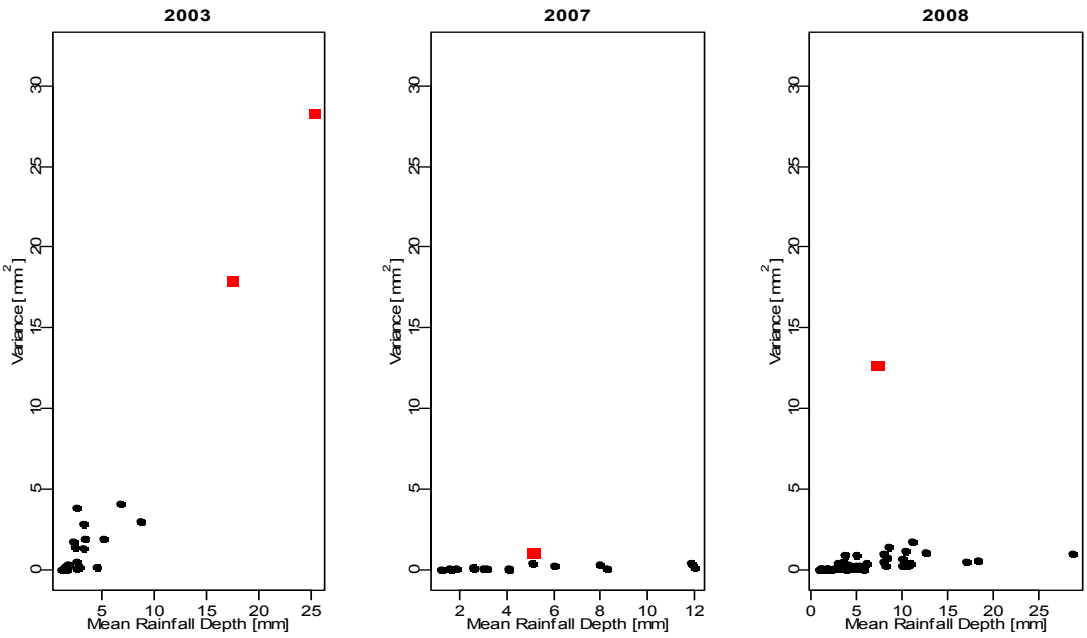

Figure 6 Variance of the rainfall depth as a function of the mean rainfall depth for each event – notice one graph per year. The events marked with a square are omitted from the dataset. The 2003 data are collected by optical drop-counting gauges, while the 2007 and 2008 data are obtained using 0.2 resolution tipping bucket gauges, cf. Section 3.

After log-transforming (natural logarithm) the data, the variance dependency of the mean rainfall depth is not as strong, cf. Figure 7.

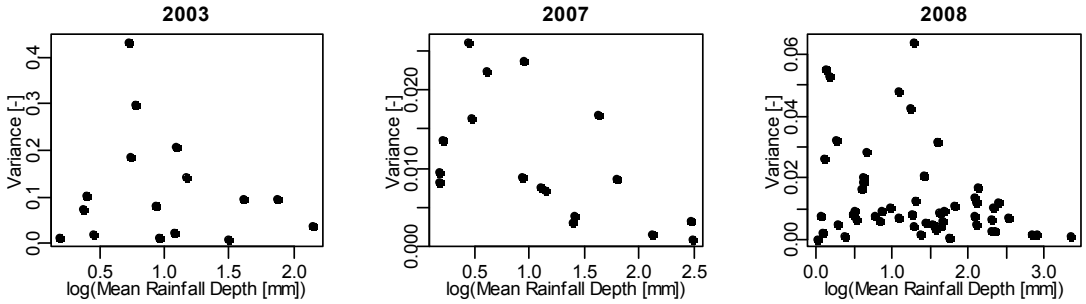

Figure 7 Variance of the rainfall depth as a function of the mean rainfall depth for each event based on natural logarithmic transformed data. The 2003 data are collected by optical drop-counting gauges, while the 2007 and 2008 data are obtained using 0.2 resolution tipping bucket gauges, cf. Section 3.

The Anderson-Darling test has been chosen for testing the hypothesis of normality of the log-transformed rainfall data. The obtained p-values from the Anderson-Darling test for each gauge in 2003, 2007 and 2008 are listed in Table 4 and there is no evidence to reject the null-hypothesis of normality. The Anderson-Darling test requires a minimum of seven samples, and since there only are five observed events at gauge 1 in the 2007 dataset, the Lilliefors test is used to test for normality. The strength of this p-value is less than that of the others, partly due to the low number of observations and partly due to the test type. The dataset is hereafter considered as being log-normally distributed.

Table 4 P-values from the Anderson-Darling test of normality. *P-value from Lilliefors test due to < 7 observations

	Gauge 1	Gauge 2	Gauge 3	Gauge 4	Gauge 5	Gauge 6	Gauge 7	Gauge 8	Gauge 9
2003	0.13	0.20	0.63	0.38	0.20	0.34	0.14	0.78	0.26
2007	0.06*	0.38	0.32	0.19	0.61	0.58	0.59	0.51	0.59
2008	0.28	0.12	0.09	0.62	0.26	0.34	0.06	0.11	0.44

5 Results

By adding the 2008 dataset using the same gauges and location as in 2007, the foundation for the conclusions is improved significantly compared to prior work reported in (Jensen et al., 2005) and (Pedersen et al., 2008). The 2008 dataset is larger than the 2003 and 2007 datasets together. The data from 2003 and 2007 has been scrutinized more extensively and more data have been omitted than in the prior work as a result of the information gained in the process.

To identify gauges with systematic errors, the non-parametric Kruskal-Wallis test was used to determine if the median of the observed rainfall depths (log transformed) for each year is constant across the nine gauges. If the median differs significantly, one or more gauge(s) have systematic errors under the assumption that over a period of several months the accumulated rainfall within such a small area is uniform. The null hypothesis of equal

population medians is accepted with p-values of 0.64 (2003), 0.98 (2007) and 0.95 (2008) and no gauge in any of the three datasets has been identified as containing systematic errors.

The distributions of rainfall depths observed for the three years are shown in Figure 8. For all three observation years the events with rainfall depths of less than 5 mm dominate the datasets. There are only a few events exceeding 15 mm in the 2008 datasets and none in 2003 and 2007.

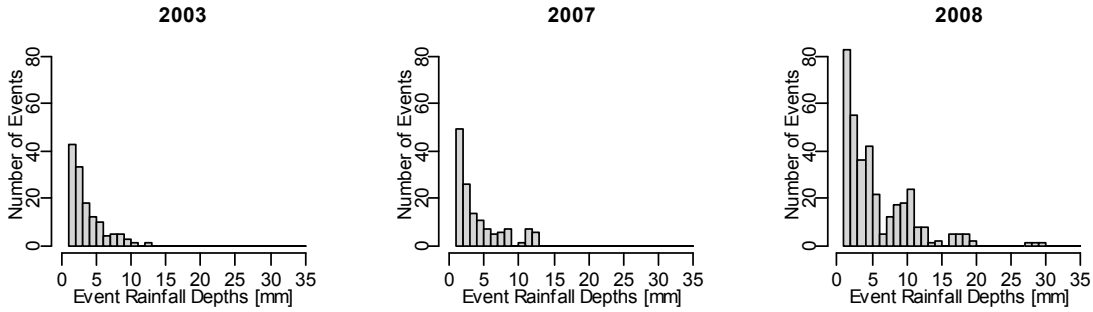

Figure 8 Histogram of rainfall event depths in mm for all functioning gauges. Each year is shown in an individual plot.

When the variability issue was addressed based on 2003 and 2007 data in (Pedersen et al., 2008) the smaller variability in the 2007 dataset was attributed to the limited dataset of 2007 and the lack of large events. The rainfall event depths of 2003 vary much more than those observed in 2007 and 2008, cf. Figure 7 where the variance is shown as a function of the mean depth (log-transformed). The dilemma is that the 2003 dataset was obtained with a different type of gauge and at a different location, and it is therefore difficult to directly compare the datasets, despite the identical layout. The variability of the 2008 dataset is larger than that of 2007 using the same location and gauge type, cf. Figure 6. The 2008 dataset also includes events with large rainfall depths of the same order as those observed in 2003. The large variation of the 2003 dataset cannot be recovered in the 2007 and 2008 dataset, and there could be several reasons for this. The mean rainfall intensity ranges from 0.1-5.4 mm/h for 2003 compared to 0.5-11.5 mm/h for 2007 and 0.3-32.5 mm/h for 2008, indicating that the large rainfall depths have occurred over a much longer time in 2003 than in 2008. The small mean event intensities in 2003 indicate that the large events are not of convective character, but more frontal, whereas the very high mean event intensities observed in 2008 are of convective character.

5.1 Spatial variability

The objective is to describe the variability of rainfall depths on the basis of events in order to quantify the uncertainty related to using data from a single gauge as input to a hydrological application or to calibrate a radar as defined in Section 4. The first approach is to analyze the variability expressed by the spatial Coefficient of Variation (CV) of the precipitation field, estimated as the ratio of the standard deviation to the arithmetic mean depth. The estimated CVs are shown in Figure 9 as a function of mean event depths, and in Figure 10 as a function of mean event intensities.

It is evident that the spatial variability is notably larger in 2003 than in 2007 and 2008. Figure 9 indicates correlation between rainfall depths and spatial coefficient of variation, since the CV is decreasing with increasing rainfall depths. The large variability represented with CV above 50% only occurs at depths of less than 5 mm and only in the 2003 dataset.

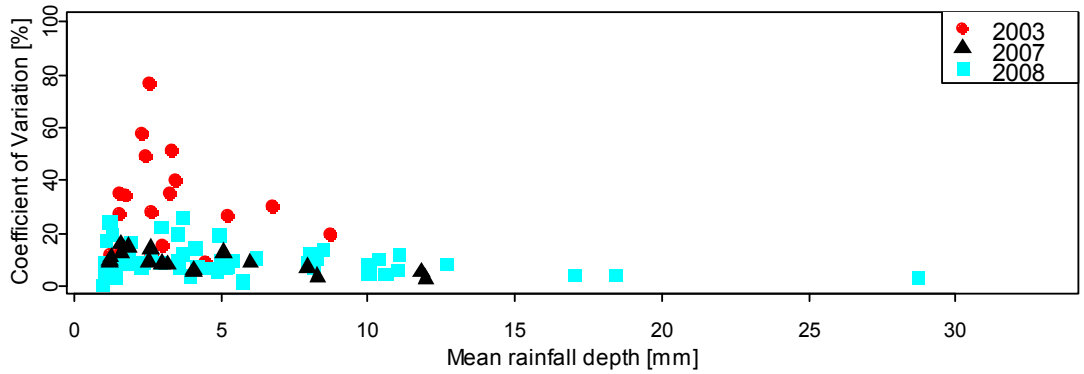

Figure 9 Coefficient of Variation (CV) as a function of the event-based mean rainfall depth in mm for all three datasets. 2003 (circles), 2007 (triangles) and 2008 (squares).

Generally, two types of rainfall occur in Denmark - widespread frontal rain with long duration and relatively small rainfall volumes, and convective events of short duration, but often releasing large volumes of water. As stated earlier the 2003 dataset only has low mean event intensities in contrast to 2008 and as shown in Figure 10, events with a high CV value are events with small event intensity and a low mean event depth.

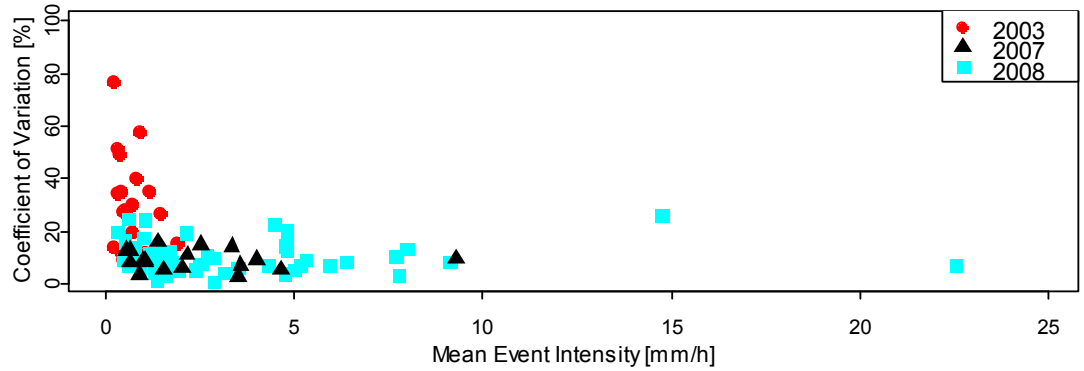

Figure 10 Coefficient of Variation (CV) as a function of the mean event intensity in mm/h for all three datasets. 2003 (circles), 2007 (triangles) and 2008 (squares).

Based on the CV values for the three datasets, the variability ranges from 1-77%, with a mean value of 14% variability. The CV values in the 2003 dataset are significantly larger compared to the 2008 dataset, and the most likely cause for this discrepancy is the gauge type. Past experience from other projects with optical drop-counting gauges confirms the suspected instability of this gauge type. Optical drop counting gauges have been observed to be unstable, e.g. recording continuously in known cases with no precipitation. If the variability is estimated based on 2007 and 2008 data, it ranges from 1-26% with a mean of 10%.

A coefficient of variation of up to 26% is lower than earlier reported, but nevertheless it is still quite large because the area of interest is only 0.25 km^2 and the inter-gauge distances, cf. Table 2, are very short. The upper value of 26% is based on the dataset in which the extreme event of 2008 has been omitted, cf. Figure 6. If the omitted event is taken into account, the range of the 2007 and 2008 dataset becomes 1-47%.

The event causing the rise in CV values has been omitted due to the extreme high variance, but there is a potential risk of omitting something that could be true. The rainfall depths of this event vary from 12.4 to 2.5 mm, with the largest depths in the north-west corner of the field, cf. Figure 11.

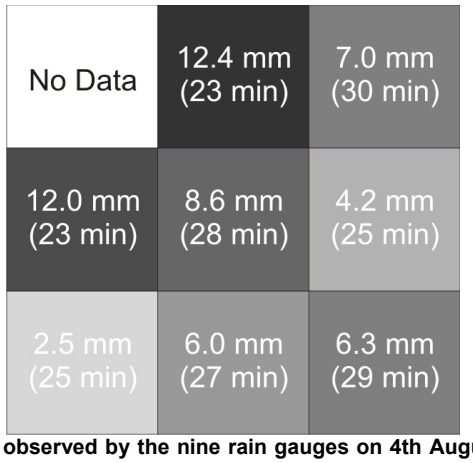

Figure 11 Accumulated rainfall observed by the nine rain gauges on 4th August 2008. Numbers in brackets are duration in minutes. This event has been omitted due to the large variance, but the variation could be because only a part of the area with the gauges was hit by the peak of the event and it cannot be ruled out that the coefficient of variation can be as high as 47%, as for this event.

Unfortunately, gauge 1 malfunctioned during this event, and without this gauge it is very difficult to determine whether this rain event only covered part of the gauge area, or whether there are errors on these gauges. The gauges agree on the duration of the event which suggests it is valid; furthermore the pattern of the rainfall depths is realistic, with a gradient over the field and no abrupt jumps. A single event is not enough to make any conclusions, but with rainfall depths potentially varying by up to 47% within an individual event, this may result in uncertainties of this order in output from applications which assume that rainfall is uniform within 500x500 meters. The effect is a potential difference of factor five in the radar calibration depending on the location of the gauge used in the pixel by gauge calibration.

5.2 Spatial correlation of rainfall data

So far, the variability has been quantified on the basis of the coefficient of variation of rainfall depths. To add more confidence to the findings, the inter-gauge correlation coefficient is estimated in the following section. The correlation coefficient gives a degree of linear decency between a pair of variables, and the key prerequisite is that the data are normal distributed. As described in Section 4, the dataset in question can be assumed to be log-normal distributed and is used as such in the following. Despite the very different behavior of the data, as well as the physical circumstances, it cannot be ruled out that the variability observed in the 2003 dataset is true, however, since other experience with the gauges has later

shown strong irregularities, the 2003 dataset has been omitted from the following analysis in order to get a more consistent result. The 2008 dataset covers the range of rainfall depths and intensities observed in 2003.

The traditional approach for estimating the correlation of a pair of rainfall processes observed by two gauges is by the population correlation coefficients ρ(X,Y), where (X,Y) is the pair of observed rainfall at two locations. To estimate ρ(X,Y) the Pearson sample correlation coefficient r, derived for N observations is used:

$$r(X,Y) = \frac{\overline{XY} - \overline{X}\,\overline{Y}}{\sqrt{\left(\overline{X^2} - X^2\right)\left(\overline{Y^2} - Y^2\right)}} \tag{2}$$

There are some problems in using the Pearson sample correlation coefficient as an estimation. (Habib et al., 2001) state that scatter in the correlation data became more evident when the sample size was reduced and the estimated values became more biased upwards. The Pearson sample correlation coefficient is furthermore limited to give a local correlation coefficient of two locations not taking the inter-gauge distances into account if a cluster of gauges are considered.

The Pearson sample correlation coefficients are estimated for all possible gauge combinations plotted as a function of the inter-gauge distance in Figure 12. The correlation coefficients are estimated for 2007 and 2008 separately, cf. Figure 12. Three correlation coefficients deviate significantly from the rest in the 2007 dataset, and these have been identified as being part of pairs including gauge 1. There are only five events where gauge 1 is functioning, so the foundation for the computation is very weak. The right part of Figure 12 shows the correlation coefficients without 2007 gauge 1 data. The estimated correlation coefficients are all very close to 1, indicating that over many events the gauges measure the same . It is therefore assumed they are working equally well and no gauge is biased. There is an indication of reduced correlation with increasing inter-gauge distance, which indicates that there is variability within the area. Unfortunately, there are only two gauge combinations with the highest inter-gauge distances because of the layout of the experiment.

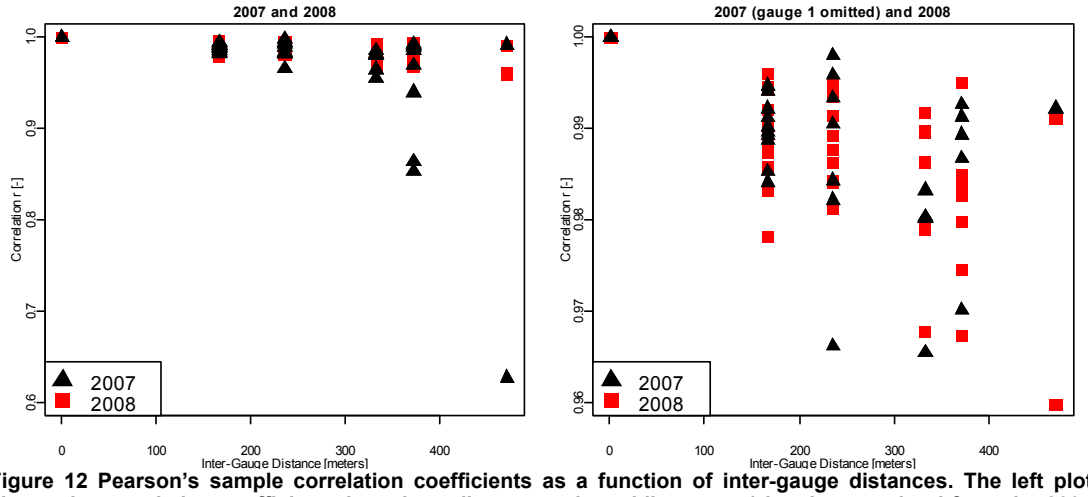

Figure 12 Pearson's sample correlation coefficients as a function of inter-gauge distances. The left plot shows the correlation coefficients based on all gauge pairs, while gauge 1 has been omitted from the 2007 dataset in the plot on the right since it results in the three significantly smallest correlation coefficients in the left plot.

The correlation in Figure 12 only provides limited information on the variability of individual event, which is of interest in this study. The correlation has therefore been determined based on an altered dataset where the event mean is subtracted from all observations in the corresponding event. By doing this it is assumed that each event can be considered multivariate normal distributed. This dataset will be referred to as multivariate normal distributed. With zero correlation in the multivariate normal distributed dataset there should only be white independent noise left, and each gauge can therefore be treated as an independent observation. Thereby it becomes possible to use the standard deviation of the individual gauges as a measure of variability.

The correlation coefficients estimated on the multivariate dataset are shown for each dataset separately in Figure 13.

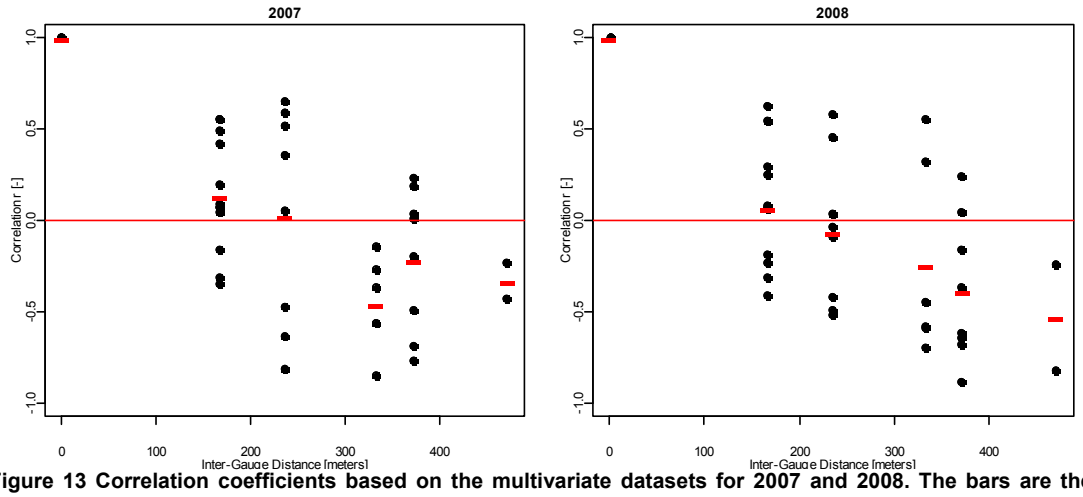

Figure 13 Correlation coefficients based on the multivariate datasets for 2007 and 2008. The bars are the average for the different inter-gauge distances. Gauge 1 is included in the 2007 dataset.

The average estimated correlation coefficient for the shorter inter-gauge distances (167 m and 236 m) is very close to 0, with a negative trend at the longer distances for 2007 and 2008, cf.

Figure 13. The increase in negative correlation can be caused by a gradient over the field, which can be physically explained by a dominant direction of the rainfall fields. The average correlation coefficients are not all zero, which makes the assumption of independent observations weaker. It cannot be rejected that in reality the correlation is zero, in particular because there are only very few observations contributing to correlation at far ranges. Due to the belief in the physical explanation of the gradient and the sparse dataset at the far ranges, in the following the standard deviations are used to describe the variability.

In order to estimate the standard deviations, the covariance matrices of the two multivariate normal distributed datasets are determined. The diagonal elements of the covariance matrix are the variance of the gauges, and by exploiting this property it becomes possible to use the variance as an expression for the variability between the gauge-observed rainfall depths. In order to aid interpretation, the standard deviations are shown. The estimated values for each gauge are listed in Table 5.

Table 5 Standard deviations for each gauge based on the covariance matrix of the multivariate normal distributed data. The standard deviations are estimated based on all events for the gauges separately.

	Gauge 1	Gauge 2	Gauge 3	Gauge 4	Gauge 5	Gauge 6	Gauge 7	Gauge 8	Gauge 9
σ(log(2007)) [-]	0.10	0.11	0.06	0.07	0.04	0.09	0.06	0.11	0.11
σ(log(2008)) [-]	0.13	0.08	0.06	0.10	0.07	0.10	0.11	0.07	0.09

A small standard deviation is interpreted as a well-functioning gauge, and gauges with a large standard deviation value are considered more uncertain. This is confirmed by the general observations in the field and the fact that gauge 1 and gauge 7 have been observed to be the most unstable and these yield the highest standard deviations. It should be remarked that gauge 1 has significantly less observations than any of the other gauges, but there is no apparent correlation between the number of observations and the standard deviations. The standard deviations vary from gauge to gauge, cf. Table 5.

To illustrate the uncertainty of using a single rain gauge for the minimum and maximum standard deviation of the rain gauges, the 2008 dataset from Table 5 has been chosen to calculate the 95% prediction intervals for a given rain depth. The 95% prediction interval for a given rainfall depth is defined as $\mu \pm 2 \cdot \sigma_{(\min \text{ or } \max)}$, and the increase in the band (interval) width is due the log transformation. The example is shown in Figure 14 using the rainfall data from 2008, where the narrow interval represents the scenario where the variability interval is predicted based on the gauge with less variability (σ_{min}), and the wide interval represents the scenario where the variability is predicted based on the gauge with most variability (σ_{max}). The prediction intervals are transformed from log-space to normal-space for the plot in Figure 14. In order to simplify the illustration, the prediction intervals shown in Figure 14 are estimated based on the mean event depth, but the uncertainty is for the separate observations.

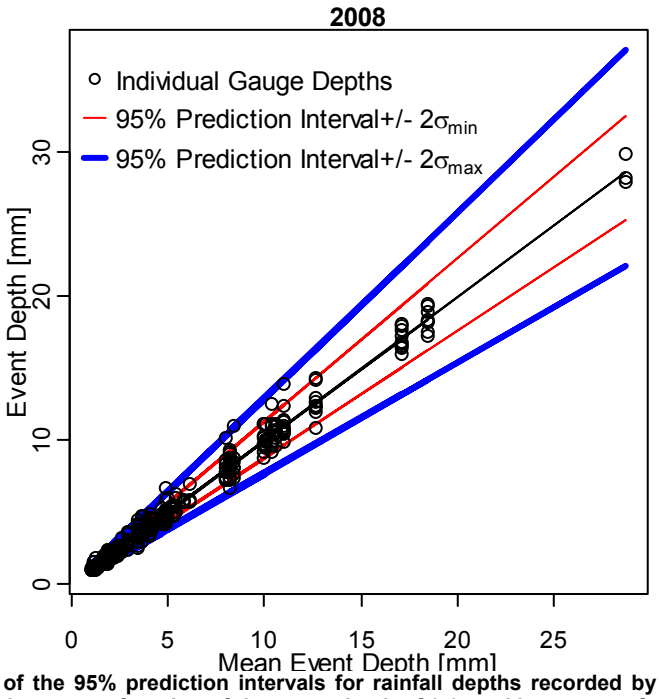

Figure 14 Illustration of the 95% prediction intervals for rainfall depths recorded by rain gauge. The 95% prediction interval is shown as a function of the mean depth of 3-9 working gauges for illustrative purposes – the prediction intervals are estimated based on the individual gauges. The minimum and maximum of σ(log(2008)) from Table 5 has been used.

To aid clarity, Figure 14 only contains 2008 data, but the range of the standard deviations of the two datasets is almost identical. A close-up of the 1-5 mm interval of the mean rainfall depths from Figure 14 is shown in Figure 15 to better illustrate the uncertainties related to small rainfall depths.

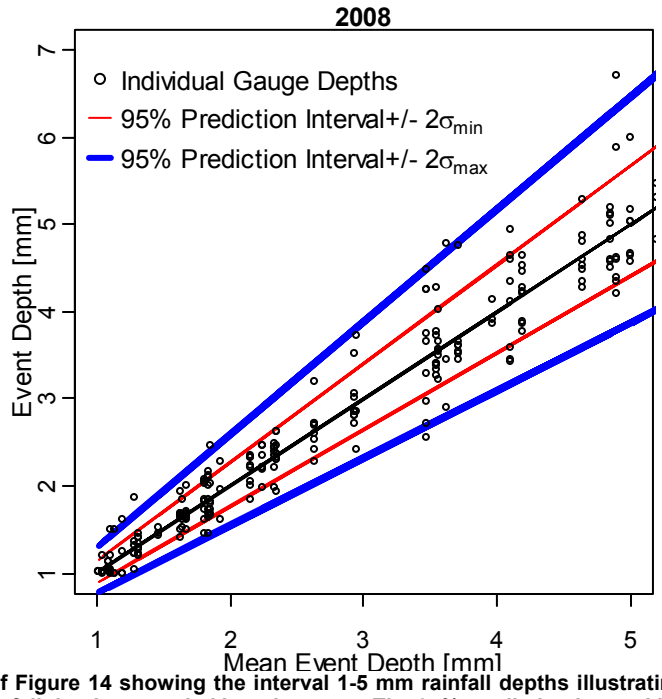

Figure 15 Close up of Figure 14 showing the interval 1-5 mm rainfall depths illustrating the 95% prediction intervals for small rainfall depths recorded by rain gauge. The 95% prediction interval is shown as a function of the mean depth of 3-9 working gauges for illustrative purposes – the prediction intervals are estimated based on the individual gauges. The minimum and maximum of σ(log(2008)) from Table 5 has been used.

As illustrated by Figure 14 and Figure 15 the uncertainty of using a single gauge as a representative measure of the mean rainfall depth over the 500x500 meter area is largest for events with depths smaller than 5 mm, since a higher number of the individual gauge depths are outside the 95% prediction interval.

The narrow interval ($\pm 2\sigma_{min}$) is approximately ±12% and the wide interval ($\pm 2\sigma_{max}$) is approximately ± 23%. Due to the transformation from the logarithmic values, the positive part is wider than the negative and therefore the approximate percentage value.

6 Conclusions

The aim of this paper was to quantify the uncertainties of using a single rain gauge to represent the rainfall falling over a 500x500 meter area corresponding to a single pixel of a Local Area Weather Radar (LAWR). The motivation for the work was the assumption of uniform rainfall used in connection with calibration of weather radars, where the rainfall measured by a single gauge is assumed representative for a pixel of sizes ranging from 0.25 km^2 to 16 km^2. The same assumption is used in connection with urban drainage modeling, where the rainfall measured by a single gauge is assumed uniform over a large catchment.

A field experiment placing nine rain gauges within an area of 500x500 meters, each representing one ninth of the area, was used to address the issue. The gauges were originally placed on an open field, but later moved out into a shallow estuary. It can be concluded that an offshore location is not recommendable for future gauge sites since although the inaccessibility of the site may be excellent for avoiding vandalism, it also complicates service

and maintenance of the gauges to a severe degree. Furthermore, resting birds and their droppings became a major problem, resulting in corrupted data.

2007 resulted in a total of 19 events with a total average rain depth over the 500x500 meter area of 71 mm. 2008 resulted in 55 events with a total average rain depth over the 500x500 meter area of 222 mm. The data from 2007 and 2008 were pooled with a previous dataset from a similar experiment in 2003 having 20 events and an average total of 69 mm to obtain the total dataset. The rainfall data were determined to be log-normal distributed; a property facilitating the use of standard statistic methods for estimating the variability.

The variability of accumulated rainfall within the 500x500 meter area has been estimated in different ways in order to obtain a robust estimate of the variability and thereby the uncertainty of using a single gauge to represent the rainfall over the area. The first and simplest approach uses the coefficient of variation (CV) as a measure of the variability on event basis. The CV values decrease with increasing rainfall depths, indicating that the largest variability is in events with an average rainfall depth of less than 5 mm. The CV values ranged from 1-77% for the complete dataset, and from 1-26% based on the 2007 and 2008 dataset alone. The large CV values for the 2003 dataset are to be considered keeping in mind the type of gauge used, since the optical drop-counting gauges have been found to be more unreliable than the tipping bucket type. It cannot, however, be concluded that the values are false, but the large CV values were all for events with a depth of less than 5 mm.

The correlation analysis of the data showed very strong correlation among the gauges, but decreasing somewhat with increasing inter-gauge distance, signifying variability over the area. The correlation analysis only provided an overall estimate of the variability among the gauges, whereas the focus of this work was on the inter-event variability. Therefore, the data were transformed to being multivariate normal distributed and thereby the standard deviation of the gauges can be used to express the variability as a function of rainfall depth. A 95% prediction interval based on the rainfall depth multiplied by $\pm 2\sigma$ of the gauges is used to give an estimate of the interval within which the observation from a single gauge would be. The standard deviations range from 0.4-0.11 mm for 2007 and 0.6-0.13 for 2008. For the events larger than 15 mm the standard deviations are all within $\pm 2\sigma_{min}$, whereas for the smaller events they are more scattered. However, most of the events with depths less than 5 mm are within $\pm 2\sigma_{max}$.

On the basis of the analysis of the coefficients of variation the conclusion is that the intra-event variability ranges from 1-26%, decreases with increasing rainfall depths and is independent of the mean event intensity. This is confirmed by the standard deviations estimated for each gauge separately. The standard deviations are used to defined the 95% prediction interval for a given rainfall depth using a single gauge. The narrow interval of the two estimated 95% prediction intervals ($\pm 2\sigma_{min}$) completely includes the large rainfall depth observations, whereas some of the smaller observations fall outside the 95% prediction interval determined by $\pm 2\sigma_{min}$. Whether to use σ_{min} or σ_{max} or an average of these depends on how much trust one wishes to place in the gauge used for the application in question. A conservative approach would be to use σ_{max} (the wide interval) to define the variability range

of input data and thereby the uncertainty that would have to be added to the output of an application, assuming rainfall is uniform within 500x500 meters.

7 References

Ciach, GG J., Krajewski, W. F., 2006. Analysis and modeling of spatial correlation structure in small-scale rainfall in Central Oklahoma. Advances in Water Resources, 29, 1450-1463.

DHI, 2009. DHI-Local Area Weather Radar – LAWR Documentation ver. 3.2.

DMI, 2008. Måneden, sæsonen og årets vejr [Online]. Danish Meteorological Institute, October 15, 2008. - http://www.dmi.dk/dmi/index/danmark/maanedens_vejr_-_oversigt.htm.

Einfalt, T., Jessen, M., Mehlig, B., 2005. Comparison of radar and raingauge measurements during heavy rainfall Water Science and Technology, 51, 195-201.

Habib, E., Krajewski W. F., Ciach, G.,2001. Estimation of Rainfall Interstation Correlation. Journal of Hydrometeorology, 2, 621-629.

Jensen, N. E., Pedersen, L., 2005. Spatial Variability of Rainfall. Variations Within a Single Radar Pixel Journal of Atmospheric Research, 77, 269-277.

Krajewski, W. F., Ciach, G. J.,Habib, E., 2003. An analysis of small-scale rainfall variability in different climate regimes. Hydrological Sciences, 2, 48, 151-162.

Marshall, J. S., Palmer, W. McK., 1948. The distribution of raindrops with size. Journal of Meteorology, 5, 165-166.

Pedersen, L., Jensen, N. E., Madsen, H., 2008. Estimation of radar calibration uncertainties related to the spatial variability of rainfall within a single radar pixel - Statistical analysis of rainfall data from a dense network of rain gauges, Preceedings from Environmental World Congress 2008, Honolulu.

Rahimi, A. R., Holt, A. R., Upton, G. J.G., Krämer, S., Redder, A., Verworn, H.R., 2006. Attenuation Calibration of an X-band Weather Radar Using a Microwave Link. Journal of Atmospheric and Oceanic Technology, 23, 395-405.

Sempere-Torres, D., Corral, C.,Raso, J., 1999. Use of Weather Radar for Combined Sewer Overflows Monitoring and Control. Journal of Environmental Engineering, 372-380.

Sevruk, B., Ondrás, M., Chvila, B., 2009. The WMO precipitation measurement intercomparisons. Jorunal of Atmospheric Research, 92, 376-380.

Thomsen, R. S., 2006. Drift af Spildevandskomitéens Regnmålersystem Årsnotat 2006. Danish Meteorological Institute.

PAPER B

Calibration of Local Area Weather Radar – Identifying Significant Factors Affecting the Calibration

---

Submitted to *Journal of Atmospheric Research* June 2009

Calibration of Local Area Weather Radar – Identifying Significant Factors Affecting the Calibration

Lisbeth Pedersen[a+bI], Niels Einar Jensen[a] and Henrik Madsen[b]

[a]DHI, Gustav Wieds Vej 10, DK-8000 Aarhus, Denmark
[b]Department of Informatics and Mathematical Modelling, Technical University, Denmark, Building 321, 2800 Lyngby, Denmark

Abstract: A Local Area Weather Radar (LAWR) is an X-band weather radar developed to meet the needs of high resolution rainfall data for hydrological applications. The LAWR system and data processing methods are reviewed in the first part of this paper, while the second part of the paper focuses on calibration. The data processing for handling the partial beam filling issue was found to be essential to the calibration. LAWR uses a different calibration process compared to conventional weather radars, which use a power-law relationship between reflectivity and rainfall rate. Instead LAWR uses a linear relationship of reflectivity and rainfall rate as result of the log transformation carried out by the logarithmic receiver as opposed to the linear receiver of conventional weather radars. Based on rain gauge data for a five month period from a dense network of nine gauges within a 500x500 m area and data from a nearby LAWR, the existing calibration method was tested and two new methods were developed. The three calibration methods were verified with three external gauges placed in different locations. It can be concluded that the LAWR calibration uncertainties can be reduced by 50 percent in two out of three cases when the calibration is based on a factorized 3 parameter linear model instead of a single parameter linear model.

Keywords: Local Area Weather Radar, calibration, Z-R relationship, spatial variability, precipitation, uncertainties, rainfall, weather radar

1 Introduction

Rainfall forecasting has always been strongly desired by hydrologists as it provides time for preparation, thereby facilitating damage control and making it possible to optimize treatments plants prior to an event. Hydrologists operate at a wide range of scales in time and space, from small urban catchments with a response time of minutes and hours, to large rural watersheds where the response scale is hours or even days. Today urban areas are spreading in most parts of the world. This leads to new challenges for urban drainage systems as new developments often have to be connected to the existing system of sewers and waste water treatment plants (WWTP). The design of the existing systems is most often based on a set of Intensity Duration Frequency (IDF) curves derived from regional historic rainfall records, i.e. based on rain gauge measurements. As result of the use of historic rainfall data for the design, existing sewer systems are not designed for a potential increase in rainfall resulting from climate changes in addition to the extra loads from new developments.

[I] Corresponding Author: DHI, Gustav Wieds Vej 10, DK-8000 Aarhus, Denmark,
tel. +45 8620 5116, email: lpe@dhigroup.com

The larger cities of Europe are all old and most often have combined sewer systems in the old part of the city making this part of the city especially prone to flooding of backwater due to insufficient sewer capacity in the event of heavy rainfall. Hydrologists, urban planners and scientists are working in a range of areas to meet the challenges. The simple approach is to increase the dimension of the pipes, but in most cases this is an extremely expensive solution and in some cases not a realistic one due to practical and economical reasons. Constructing detention basins, two-string sewer systems and local percolation facilities for surface water are all solutions being implemented in many places these years. The next step is to utilize the sewer system in a more optimal way by real time control (RTC), enabling water volumes to be detained in some areas or to be de-routed in order to increase the capacity in areas where needed in case of rainfall only occurring over a part of the total catchment it thereby becomes possible to increase the effective system volume, to reduce sewer overflows and to optimize the constituent part of water being treated by the WWTP.

RTC requires online information from sensors in the sewer system, e.g. water levels, pumping data or flow in critical points that is transmitted to a central place where either software or humans take action. The problem with this is that these sensor types only provide information on increased flow after the rainfall has reached the system, where the real advantage would be to get the information in advance so that the system could be optimized beforehand. This requires a detailed accurate forecast of the rainfall with a spatial and temporal resolution in the same domain as the sub catchments. Rain gauges are insufficient in this connection as they are point measurements. Furthermore there will often not be enough of them meaning that they often miss the peak intensities (Einfalt et al., 2005). Weather radars on the other hand are capable of providing spatially distributed information on rainfall over large areas. Radars can provide data for forecasting future rain over the catchments with up to a few hours of lead time. Like rain gauges, weather radars have shortcomings, since the radar rainfall estimate is an indirect measurement of the rainfall and requires input from a gauge or disdrometer for calibration and the uncertainty of the estimate is increasing with range.

In 1999 the EU project ESPRIT 23475 “High Performance Rainfall Radar Image Processing for Sewer Systems Control” was completed. The aim of the project was to utilize existing C-band radars to provide detailed forecasts for RTC of sewers. Since data from one of the pre-appointed existing radars were unavailable in real time, it was decided to develop a high resolution cost-efficient weather radar capable of providing detailed forecasts of rainfall for urban areas. The result was the Local Area Weather Radar (LAWR) based on an X-band marine radar. Partners in the LAWR development were DHI and the Danish Meteorological Institute (DMI), and today the LAWR is manufactured by DHI.

The LAWR differs in a number of areas compared to standard C-band and S-band weather radars, and it also uses a different calibration method. This paper focuses on evaluation of the LAWR calibration method and the uncertainty of LAWR rainfall estimation. Focus is on identification of parameters contributing to the calibration along with uncertainties related to the spatial variability of rainfall. The evaluation is based on experimental data. The uncertainties related to spatial variability of rainfall within a pixel will be present in any radar

calibration and are of great significance as these uncertainties will be added to those of the application using radar data as input.

Conventional weather radars such as S-band and C-band are poor at detecting near surface phenomena at long ranges due to the curvature of the earth. In addition to this the spatial resolution of conventional weather radars is often 1-16 km^2 which is high when compared to e.g. urban catchment sizes. The weaknesses mentioned here have resulted in strong focus on the use of X-band radars for meteorological purposes over the past few years. There are several groups around the world working on using X-band radars for meteorological applications both for research purposes and for commercial purposes. The Collaborative Adaptive Sensing of the Atmosphere (CASA) project is one of the largest of these groups working towards creating a distributed network of low-cost, low-power solid state radars with Doppler, dual-polarization capabilities covering the United States (Brotzge et al., 2006), (Donovan et al., 2006) and sources herein. Beside the LAWR made by DHI, several other commercial X-band weather radar systems exist, e.g. the HYDRIX by Novimet (Bouar et al., 2005) and the RainScanner from Germatronic (Gekat et al., 2008). Overall they share the X-band characteristic such as a 3.2 cm wavelength, but differ in a number of areas with regard to specifications such as antenna type (dish vs. fan beam), receiver, Doppler capability, spatial and temporal resolution of output, range and price.

2 Local Area Weather System

The LAWR is based on a 25 kW X-band marine radar manufactured by Furuno. The characteristics of the LAWR are listed in Table 1. The LAWR is not equipped with doppler or dual-polarization technologies.

Table 1 System data for the LAWR system

	City-LAWR	LAWR
Peak Power	4 kW	25 kW
Wave length	X-band 3.2 cm	
Pulse length	0.8 μs	1.2 μs
Antenna	0.61 m radome	2.5 m slotted waveguide array
Receiver	Logarithmic receiver	
Vertical opening angle Horizontal opening angle	± 10° 3.9°	± 10° 0.96°
Samples pr. rotation	450	360
Range (forecast/QPE)	30/15 km	60/20 km
Spatial resolution	250x250 m 125x125 m 50x50 m	500x500 m 250x250 m 100x100 m
Data output frequency	1 or 5 minutes	
Scanning strategy	Single layer and continuous scanning	

The marine radar is designed to operate continuously in harsh conditions at sea thereby reducing maintenance requirements. Only the magnetron needs to be changed every 8 months. The LAWR system is designed to use the raw video signal without any modifications of the original Furuno antenna unit thereby limiting vulnerability issues. The analog raw video signal ranges from 0 to -9 V and is converted to a 10 bit digital signal ranging from 0-1024 by the custom-made A/D converter sampling with 20 MHz. Originally the video signal was set to range from 0 to -6 V by the manufacturer, and the signal

processing was adapted to this range. It was later discovered that the signal range was wider, and subsequently an adjustment box tuning the signal to the range of the A/D converter was implemented in the system, cf. Figure 1. The system consists of the antenna unit, the transceiver, a custom-made 20 MHz A/D converter, two standard PCs and a monitor. The system is designed to run automatically and can be operated from afar. An overview of the system and optional features is shown in Figure 1.

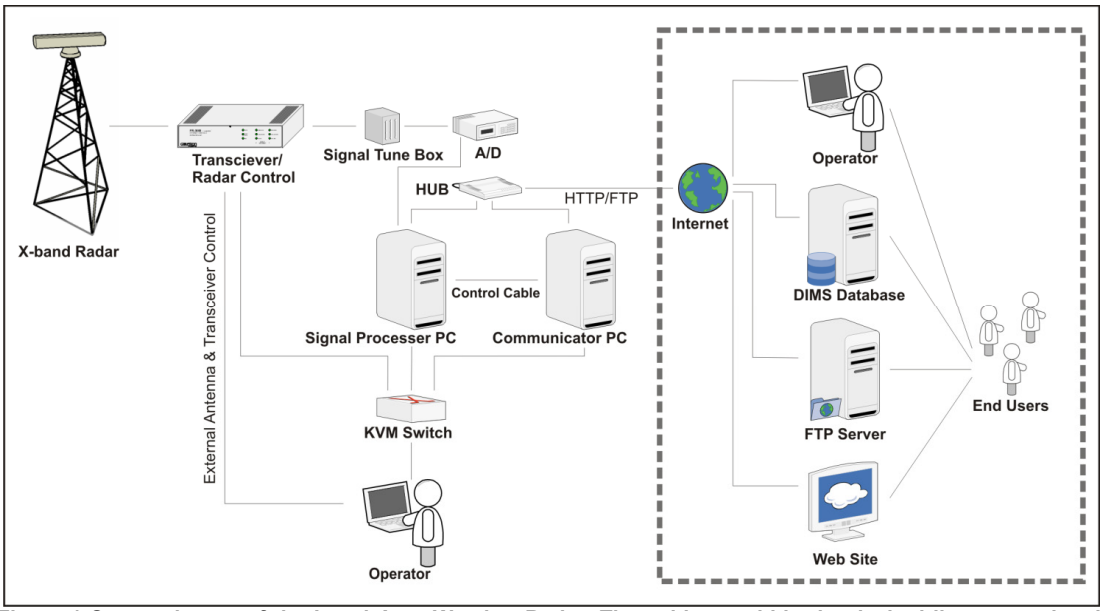

Figure 1 System layout of the Local Area Weather Radar. The subjects within the dashed line are optional features all requiring internet access to the LAWR installation. The radar is here illustrated on a mast, but is as often placed on an existing installation such as a rooftop.

2.1 Scanning strategy

Conventional weather radars operate with a range of scanning strategies depending on their type and on their operational purposes, however, the majority of radars share the feature that they scan at increasing elevation angles, visiting a given point only once in each elevation. The scanning cycle normally takes from 5 to 15 minutes, causing timing issues due to the velocity of the rainfall field combined with the spatial variability of the rainfall changing over time. This needs to be dealt with carefully when processing data, especially when creating 2D surface rainfall maps such as CAPPI (Constant-Altitude Plan Position Indicator) products in order to avoid timing issues when applications use the radar data as input.

The LAWR uses an alternative scanning strategy. It scans continuously with 24 rpm with a horizontal opening angle of 0.96° resulting in 360 scans in each rotation. The temporal resolution is chosen by the user to be either 1 or 5 minutes, so the estimation of rainfall at a given point at the surface is the average of 24 or 120 data samples of that point. The number one shortcoming of the LAWR is the large vertical opening angle of $\pm 10°$. Only the upper half of the $\pm 10°$ is used since the lower half is cut-off either by nearby obstacles or by a mechanical clutter fence. With a vertical opening angle of 10°, the sample volume increases rapidly with range, and at a range of 20 km the beam is 3.5 km high and at 60 km it is 10.5 km high. The maximum range of 60 km is limited compared to the maximum range of 240 km of conventional weather radars, however, the problems with

overshooting near surface phenomena at far ranges is eliminated as result of the short range. The cost of X-band technology compared to C-band, or the even more expensive S-band, is lower so it is possible to install a number of X-band radars to cover the same area covered by a C-/S-band radar for the price of one of these.

2.2 Signal processing

Signal processing from backscattered energy to data files can be broken down into four parts: Reception, A/D converting, data processing and data storage. The primary part of signal processing is done by the Signal Processor PC, cf. Figure 1 where the digitalized voltage signal is processed into reflectivity values. Every minute, 120 megabytes of raw data is processed by the Signal Processor PC, and at the end of each scanning cycle (1 or 5 minutes) the 120/600 megabytes of data is pushed to the Communicator PC for final processing and data storage. During the data collection, the data is applied to a number of schemes in order to handle well-known radar obstacles e.g. clutter and attenuation. Because it is an X-band radar, the LAWR is of course sensitive to attenuation due to the wavelength of 3.2 cm, but as part of the signal processing, the data is corrected for attenuation. The attenuation correction is applied along the path of each raw scan line. For each sample bin, the adjusted reflectivity, Z_r is estimated as follows:

$$Z_r = Z_{g,r}\left(1 + \frac{\alpha \sum_{i=0}^{r-1} Z_i}{C_1 \cdot n_{samples}}\right) \quad (1)$$

where:

Z_r: Adjusted reflectivity value at range r
$Z_{g,r}$: Uncorrected reflectivity at range r
$n_{samples}$: Number of samples in a single scan line, typical value is 8000
α, C_1: Empirical Constants where typical values are 1.5 and 200, respectively

The LAWR attenuation algorithm enhances the signal proportionally to the amount of power used at a given range without changing the properties of the rain event when observed from both sides as shown in Figure 2. If too much correction is applied, the rainfall intensities will be over-enhanced with increasing range from the radar and vice versa in the event of inadequate correction. The method was developed, tested and verified as part of the original LAWR development project.

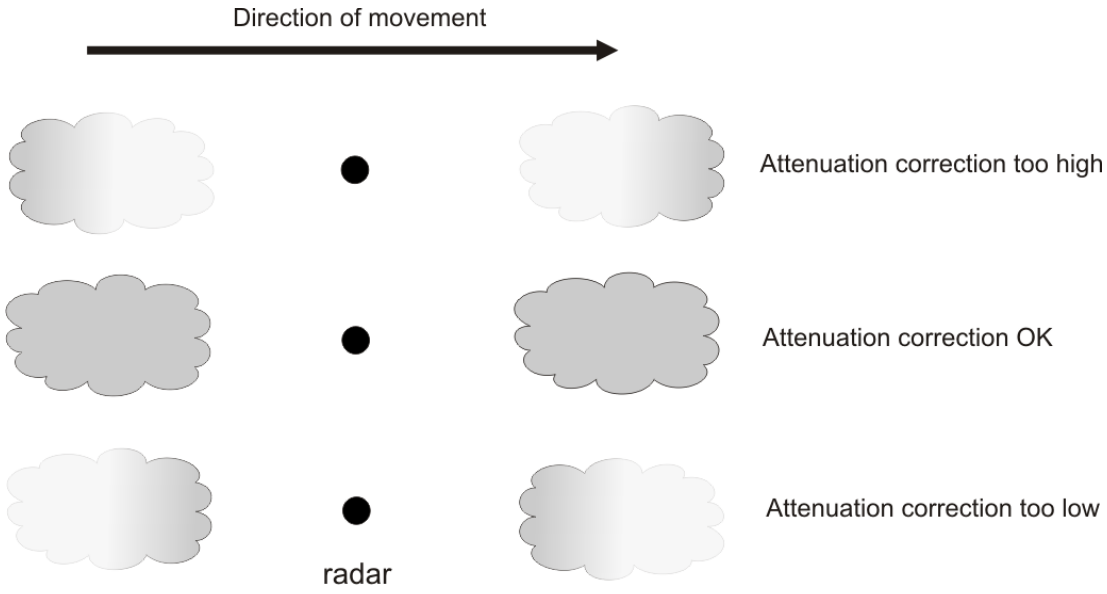

Figure 2 LAWR attenuation correction principle. The cloud symbolizes a rainfall event observed at two different time steps – before and after passing over the radar. If the applied correction is too powerful the remote part of an event (as observed from the radar) will be over-enhanced while inadequate correction will result in suppression of the remote areas of the event.

Furthermore, data is applied a volume correction scheme handling the rapidly increasing sampling volume with range due to the 10° vertical opening angle. If no volume correction scheme is applied, the LAWR will underestimate the rainfall with increasing range, which becomes evident if data is accumulated over a longer period e.g. more than two months. An accumulation period of two months is normally used in Denmark where rainfall is frequent, but in different climate regimes it may be necessary to adjust this period. The accumulated rainfall field is not homogeneous over the area; it peaks in the vicinity of the LAWR and decreases with range. This is due to the fact that at far ranges a higher quantity of rainfall is required in order to pass the noise cutoff threshold value, due to the greater vertical integration length. To compensate for the increasing beam, a volume correction algorithm was developed to compensate for this issue. The method assumes homogeneity of the radar coverage area over an accumulation period of two months. The accumulated LAWR image is subdivided into a number of concentric circles with the radar in the centre, and an exponential function is fitted to the average of each circle using a reference distance of e.g. 5 km. The reference distance is the point where the exponential function is forced to 1. The exponential function outperformed other function types (power law, linear and higher order polynomials) which were tested initially. In order to avoid extreme correction values, a constraint of a maximum correction of 4 is enforced. When the volume correction is applied to the data, the reciprocal of the function is used to adjust for the in-homogeneity as function of range. The applied volume-corrected reflectivity at range r, Z_{rv} is estimated by:

$$Z_{rv} = Z_r \frac{1}{C_2 \cdot \exp(r \cdot C_3)} \quad (2)$$

where:

Z_{rv}: Volume-corrected reflectivity at range r

Z_r: Adjusted reflectivity at range r from eq. 1

r: range

C_2, C_3: Empirical constants that are location dependent. Initial value estimate: 1 and -0.03

Until recently the only output format of the LAWR was data in Cartesian coordinates in the resolutions chosen by the user (Table 1), but raw polar data is also available today. The conversion from polar to Cartesian grid is by interpolation, and as a result some of the spatial information is lost. Furthermore, at ranges larger than 1 pixel width (6 km for 100x100 m pixels, 15 km for 250x250 m pixels, 30 km for 500x500 m pixels) the values are interpolated. The LAWR format and data processing was developed so it would be consistent with that used by the radars operated by the Danish Meteorological Institute at the time of development. Therefore a 9 by 9 pixel median filter for removing extreme abnormalities was implemented in the original data processing. Recently, this has become an optional feature in view of the fact that the work linking extreme value statistics and establishing IDF curves based on LAWR data are highly sensitive to this option since the median filter removes the peak values which are of interest in this context.

The output from any radar is not rainfall intensity, but reflectivity, representing the water content in a given radar bin. Radar reflectivity depends on the distribution of drops observed in the sample volume, and the same radar reflectivity value can therefore represent different water content. In order to use the radar data as a rainfall estimate in the same manner as that observed by a rain gauge, it is therefore necessary to apply a calibration. The LAWR calibration as well as the conventional radar calibration is outlined in the following section.

3 Weather Radar Calibration

One of the first reports of measuring rainfall using a radar was reported by (Marshall et al.,1947) who suggested that there is an empirical power law relationship between the reflectivity factor, Z and the rain rate R of the form $Z=AR^b$ - the so called Z-R relationship. (Marshall et al.,1947) suggested $Z=190R^{1.72}$ based on experiments with a military radar. One year later Marshall and Palmer published their famous paper "The distribution of raindrops with size" proposing a Z-R relationship of $Z=220R^{1.60}$ based on raindrop size distributions obtained experimentally (Marshall and Palmer, 1948). The constants of the power law express the distribution of drops in the volume sampled by the radar. The work of (Marshall and Palmer, 1948) formed the basis for research in the use of weather radars for estimating rainfall, and their approach is still widely used today in an operational context.

In the 60 years that have passed since the early days of weather radars, many things have improved. The introduction of computers for displaying and processing the data is probably the most significant change, but also hardware developments of antenna, transceiver and electrical components have led to significant improvements in terms of stability and accuracy.

The implementation of Doppler technology during the late 1980s and 1990s further improved the radar rainfall estimates. The latest addition is dual-polarization technology to the operational weather radar networks around the world. All these developments have reduced some of the uncertainties and added information to the meteorologists and researchers, but nevertheless the focus point is still the conversion from received power backscattered from the rain in the atmosphere to rainfall intensity. Despite enhanced equipment, 60 years of research in weather radars and atmospheric sciences, and new instruments such as the 3D Video disdrometer many still doubt the capabilities of weather radars for rainfall estimation at surface. The number one argument is that rainfall estimation by a weather radar is too uncertain because the comparison with the so-called ground truth, a single rain gauge, shows either over- or underestimation of both rainfall intensities and accumulated rainfall depths over a given area.

The reasons for the discrepancy between gauge and radar rainfall estimates have been widely addressed in the literature for the past 60 years, with primary focus on improving the radar calibration and understanding the uncertainties related to the Z-R relation. It was acknowledged early on that a unique global set of a and b constants does not exist and (Battan, 1973) summarizes 69 different Z-R relationship from various sources worldwide showing a wide range of constants. Since Battans study large research efforts have been put into understanding the physical properties of the processes of the drop size distribution (DSD), the variability of the DSD and uncertainties since they are related to the Z-R relationship by (Zawadzki,1975), (Ulbrich,1983), (Austin,1987), (Zawadzki,1984), (Ciach and Krajewski, 1999), (Jameson and Kostinski, 2001), (Uijlenhoet, 2001), (Lee and Zawadzki, 2004), (Fiser, 2004), (Lee and Zawadzki, 2005), (Lee et al., 2007) and (Uijlenhoet et al., 2008) among others. The research continues and the introduction of dual-polarized weather radars has facilitated new ways for estimating parameters describing the DSD (Lee et al., 2004). Depsite this, most operational systems use a simple Z-R relationship e.g. $Z=300R^{1.5}$ or the Marshall Palmer $Z=220R^{1.60}$ (Lee and Zawadzki, 2005).

The uncertainties related to the radar rainfall estimation are often focused around the DSD variability and the uncertainty related to choosing the right Z-R relation, however, there are several other contributing factors, e.g. hardware system calibration, meteorological phenomena (e.g. bright band), beam interception, timing of sampling just to mention a few. These factors can largely be divided into three groups: Sources of random errors, sources of systematic errors and sources of range dependent errors, even though some factors can be classified as belonging to more than one group (Zawadzki, 1984).

In an analysis comparing radar rainfall estimates with observed rainfall at a given rain gauge station, the uncertainties related to rain gauges are rarely mentioned and hardly ever quantified. The reason for this is probably the general perception of the rain gauge being the ground truth and the discussion of the related uncertainties is of the past. As rain gauges are mechanical devices, they can suffer from instabilities, errors and mis-calibration as any other instrument. On top of this are the uncertainties related to placement, sheltering (can change over time e.g. due to growing trees) and wind-induced errors. In order to obtain reliable rain gauge data, costly regular maintenance and meticulous data control are required in order to avoid flawed data (Krajewski et al., 2003).

In addition to all the uncertainties mentioned above there is the issue of scaling. The fact is that radar rainfall estimates are evaluated based on point measurements. The typical pixel size of conventional weather radars is 1x1 km or 2x2 km whereas the sample area of a rain gauge is typically 200-300 cm^2, which corresponds to comparing the continent of Europe with a radar pixel in terms of difference in the spatial domains. The variability of rainfall within an area as small as a single pixel can be significant and have impact on the radar calibration (Habib and Krajewski, 2001), (Krajewski et al., 2003) and (Pedersen et al., 2009). Furthermore, the radar samples a volume projected onto a 2D surface at a given height above the surface. The sample size increases with range and is an average over the duration of the scanning cycle, whereas the gauge measurement is a discrete measure defined by the gauge bucket volume. Another factor contributing to the discrepancy between radars and gauges are situations with partial pixel filling. When pixels are 1x1 km or even larger there will be cases where the gauge does not observe rain while the radar does and vice versa. (Habib and Krajewski, 2001) find that for a 5-minute timescale there is approximately 30% probability that a single gauge does not observe rainfall within an area of 1x1 km and the probability increases to about 50% when the area is 3x3 km. They furthermore state that these probabilities are likely to be conservative since a higher density of gauges could lead to higher values. This is an issue often overlooked in the discussion of radar performance.

3.1 Local Area Weather Radar Calibration

One of the objectives when the LAWR was developed was to make a cost-efficient supplement to rain gauges, and therefore an existing marine X-band radar was chosen. The drawback of this decision is a large vertical opening angle of the beam ($\pm 10°$) and a logarithmic receiver which is contrary to the linear receiver of conventional weather radars. The logarithmic receiver in combination with no available disdrometers for the first calibrations led to a search for an alternative method for calibrating the LAWR. The missing disdrometer data would constrain the calibration since it would only be possible to apply literature standard Z-R relations. This would result in added uncertainties in the calibration of the LAWR since the Z-R relationship would have been obtained by a different radar type in a different climate regime.

A preliminary experimental comparison of a LAWR and the Danish Meteorological Institute's C-band radar on Rømø was carried out in 2001 were it was concluded that the LAWR results appeared reasonable compared to those of a C-band radar. The spatial extent of the rainfall areas was well captured, but the intensities, especially the lower ones, were more uncertain (Overgaard, 2001). It should be noted that the comparison only used a very limited number of events and that the LAWR at that time used an early version of the A/D converter with less sensibility. A conversion curve from the LAWR reflectivity to dBZ was established by (Overgaard, 2001) which made it possible to convert the reflectivity value of the LAWR to a corresponding dBZ and thereby enable the use of a Z-R calibration. A description and example of such a conversion curve can be found in (Pedersen, 2004), however, a new conversion curve would need to be determined due to the different A/D converter used today.

Different calibration methods have been developed and tested, but common for them all is that they use a black box modeling approach. The output from the LAWR is related directly

to the rainfall observed at ground by a rain gauge without any attempt to include physical properties such as a drop size distribution of the rain drops in the sample volume. The reason for pursuing a different approach than the one outlined by (Overgaard, 2001) is to avoid dependency of a close-by C-band radar for creating the conversion curve required for this type of calibration. The conversion turned out to be a log-transfer function as expected taking the two types of receiver into consideration. The first initial attempts showed an obvious relationship between the LAWR reflectivity and 5 minute integrated rainfall intensities, however, it was found that the resolution of a 0.2 mm tipping bucket rain gauge (Rimco) was too coarse to establish a relationship between the reflectivity and gauge intensity when each five minute time step was used. Instead rainfall intensities obtained by an optical drop counting gauge (Pronamic) with a resolution of 0.01 mm were used and a second order polynomial was fitted to the data with a good result (Jensen, 2002).

To test the validity of the second order polynomial relationship and address the uncertainties of using a single gauge for calibrating the LAWR, a field experiment was carried out in 2003. Nine optical drop counting gauges were placed equally representing one ninth of a single LAWR pixel (500x500 m). On the basis of the data from this experiment it was concluded that accumulated rainfall as measured by rain gauges can vary significantly and thereby add uncertainty to the LAWR calibration despite the small pixel size (Pedersen, 2004) and (Jensen and Pedersen, 2005). The second order polynomial was based on a fit of 5 minute integrated values from both LAWR and gauge. An evaluation of the second order polynomial showed that the relationship was equally well described with a linear relationship, but the method required data from high resolution rain gauges (0.01 mm), which is a lot finer than that of standard tipping bucket rain gauges of 0.1, 0.2 and 0.4 mm, so gauges that were already installed could not be used to calibrate the LAWR. It was then discovered that a strong linear relationship existed between the total sum of LAWR reflectivity and the rainfall depth in mm resulting in the same slope coefficient (calibration factor) as when based on 5 minute values. This discovery facilitated the use of standard 0.2 mm tipping bucket gauges since the total rainfall depth is used instead of intensities. The calibration gives a factor, denoted DHI CF, which when applied to the LAWR output (Z) gives the radar rainfall intensity (Pedersen, 2004):

$$\text{DHI CF} = \frac{\sum_{\text{Event Start}}^{\text{Event Stop}} \text{mm rain [gauge]}}{\sum_{\text{Event Start}}^{\text{Event Stop}} Z/\Delta t \text{ [LAWR]}} \qquad (3)$$

Where $Z/\Delta t$ is the output from the LAWR per time step (Δt), which is either 1 or 5 minutes. The method is used as the standard LAWR calibration method today and is sometimes referred to as the "Sum Calibration Method".

As mentioned above the relationship between radar rainfall measurements and rainfall at ground is normally described by a power-law function. (Jameson and Kostinski, 2001) argue that when based on physical considerations, the relationship between Z and R should be linear. The linearity will appear in statistically homogeneous data (mean and variance are independent of the choice of origin), whereas non-linearity appears when statistically inhomogeneous (mean and variance depend on the origin and can thereby change throughout the dataset) data are used. The presence of power-laws is explained by the fact that almost all

Z-R relations are derived from statistically inhomogeneous dataset, since rainfall is not uniformly distributed but rather clustered (Jameson and Kostinski, 2001). The rainfall observed by the LAWR will in most cases be statistically inhomogeneous, but with the transformation carried out by the logarithmic receiver combined with the arguments from (Jameson and Kostinski, 2001) and the existing data analysis there seems reason to believe that the approach is reasonable.

4 Case study

The performance of the LAWR calibration method and the uncertainty of using a single rain gauge for the calibration are addressed with data from nine rain gauges placed within one LAWR pixel of 500x500 m. The rain gauges were set up to validate the finding based on a similar experiment in 2003 reported by (Jensen and Pedersen, 2005) and the new results are reported in (Pedersen et al., 2009). For the study data from the Aarhus LAWR has been used, cf. Table 1 for specifications, to assess the LAWR calibration method together with data from a dedicated rain gauge test site and three validation gauges. The nine gauges are placed so that they each represent one ninth of a LAWR pixel. An overview of the location is illustrated in Figure 3 along with a close-up of the rain gauge layout. The gauges are located in the water of Norsminde Fjord, a shallow estuary. The area of interest is located around the city of Aarhus, Denmark, and the rain gauge site is at latitude 55°59.4'N and longitude 10°15.8'E.

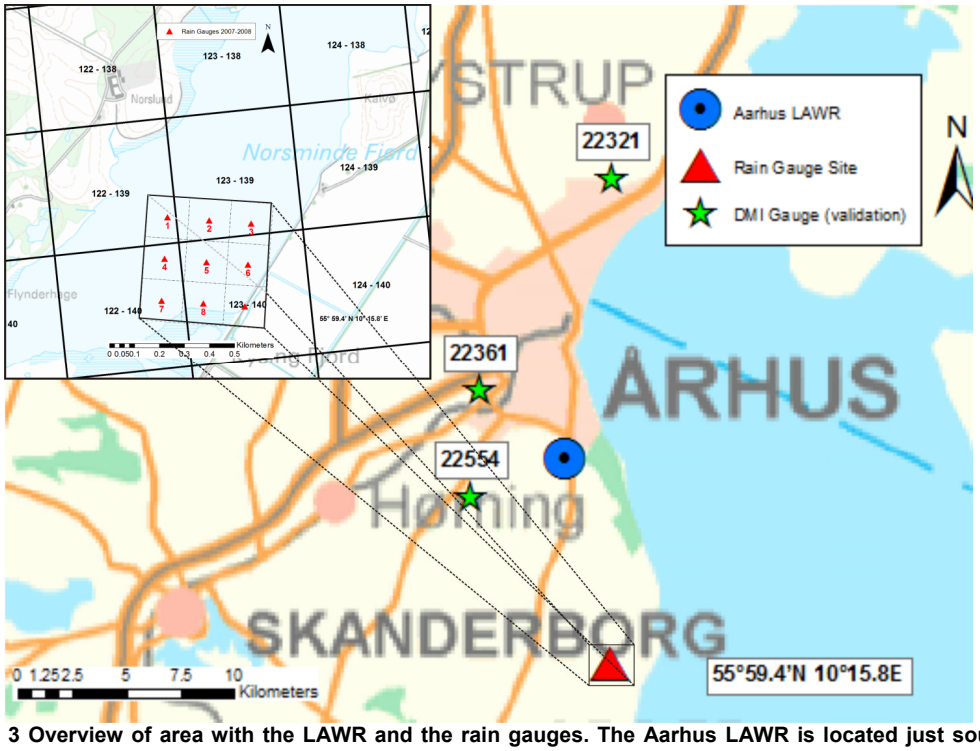

Figure 3 Overview of area with the LAWR and the rain gauges. The Aarhus LAWR is located just south of Aarhus, Denmark and the rain gauge test site is located at 55°59.4'N and 10°15.8'E. The gauges used for validation is marked with stars and are part of the official rain gauge network in Denmark managed by the Danish Waste Water Pollution Committee (SVK). The inserted picture is a close-up of the rain gauge test site shown in relation to the 500x500 meter grid of the Aarhus LAWR.

The misalignment between the gauges and the Aarhus LAWR 500x500 meter grid in Figure 3 is due to the fact that at the time when the gauges where commenced, it was believed that the

grid was rotated 6° clockwise, however, the grid rotated -5° counter-clockwise instead. The discrepancy was a result of different projections. The result is that all gauges are not within a single pixel in the Cartesian grid format as illustrated in Figure 3 and listed in Table 2.

Table 2 Gauges and corresponding pixels in the Cartesian grids of the Aarhus LAWR.

	Gauge Type	Distance to Aarhus LAWR [km]	Pixel (col,row) [500x500 m]	Pixel (col,row) [100x100 m]
1	Pronamic	9.3	122,139	160,244
2	Pronamic	9.3	123,139	162,245
3	Pronamic	9.3	123,139	163,245
4	Pronamic	9.8	122,140	160,246
5	Pronamic	9.8	123,140	162,246
6	Pronamic	9.8	123,140	163,247
7	Pronamic	9.8	122,140	160,248
8	Pronamic	9.8	123,140	161,248
9	Pronamic	9.6	123,140	163,248
22554	Rimco*	4.9	111,123**	105,163**
22361	Rimco*	5.3	113,113	115,115
22321	Rimco*	13.3	128,95	186,23

* Operated by the Danish Meteorological Institute. ** On the border to 112,123/106,163

4.1 Available Data

The gauge dataset consists of 2 seasons of measurements from September-November 2007 and June-November 2008. Only the 2008 dataset is used in the calibration analysis, since the 2007 gauge data was not calibrated in-situ as the 2008 gauge data, and the 2007 radar data was applied to the median filter. Detailed description of the rain gauge experiment, calibration procedures, data control and uncertainties can be found in (Pedersen et al., 2009).

During the 6 months of 2008 only 8 rainfall events were recorded by all 9 gauges simultaneously – the vast majority of events were observed by 3-9 gauges, cf. Table 3 for a summary of gauge data. The missing observations are a result of lightning, clogged gauges as result of bird droppings and brake-downs. Especially Gauge 1 suffered from malfunctioning and only observed 12 events in total.

Table 3 Gauge data summary.

Gauge	Number of events > 1mm	Total Rainfall Depth [mm]	Range rainfall Intensity [mm/h]
22554	80	273	0.5-21
22361	74	326	0.5-25
22321	80	242	0.7-42*
1	12	79	0.5-14.3**
2	34	202	0.3-26.9
3	26	149	0.6-26.5
4	50	297	0.3-28.5
5	40	220	0.3-10.8
6	52	286	0.3-28.3
7	41	248	0.4-32.5
8	43	226	0.3-28.1
9	55	295	0.3-26.2
Average of 1-9	*39*	*222*	*3.6*

* The maximum intensity is a single event where 1.4 mm fell over 2 minutes. The second largest is 20.3 mm/h.
** Gauge 1 suffered seriously from malfunctioning and only observed 12 events in total.

The data was collected over 6 months from 17 June to 13 November 2008 and has been divided into individual events inspired by a method used for the Danish Water Pollution Control Committees network of rain gauges in Denmark operated by the Danish Meteorological Institute (DMI). An event must consist of at least 2 registrations and the time span between these registrations must be less than 60 minutes (Thomsen, 2007). A requirement of minimum rainfall depth of 1 mm has furthermore been applied. The rainfall depths for the individual events (55 in total) and the average event intensity are shown in Figure 4.

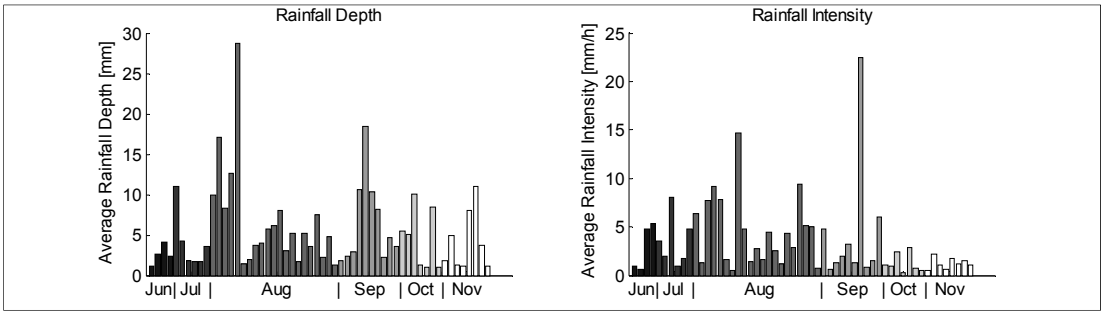

Figure 4 Rainfall depths and rainfall intensity for all events for the gauges used in the calibration analysis (1-9). The values are an average of the gauges functioning in the particular event – from 3-9.

If the reflectivity from a single pixel (number (123,140) – over 4 of the 9 rain gauges) is accumulated over a month and compared with the regional rainfall depths for the Aarhus region reported by the Danish Meteorological Institute based on interpolated rain gauge data from several gauges in the area (DMI, 2008), the overall agreement is good as seen in Figure 5.

The difference in the spring and early summer months is due to the fact that the magnetron was worn out and needed to be replaced, which was done on 30 June. The state of the magnetron is interpreted based on the average reflectivity value level over the full coverage area. The dry weather value drops when the magnetron is worn out. As result of this, all data prior to the magnetron change have been omitted from the analysis.

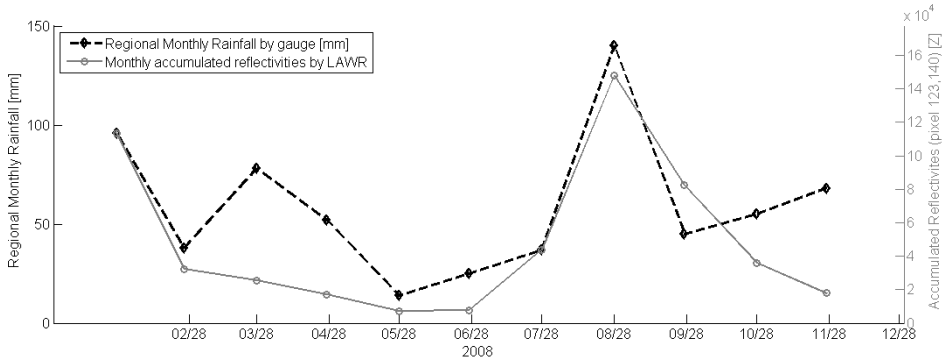

Figure 5 Accumulated regional rainfall for the Aarhus region on monthly basis reported by (DMI, 2008) compared to the monthly accumulated reflectivity's from pixel 123,140 (500x500 meter). The marker indicating the accumulation for a given month is placed at the last day of the month (last point is 30th November).

The discrepancy in November is probably due to the fact that the precipitation in this period was dominated by low-hanging light rainfall which is not very well observed by the LAWR due to the large beam. To illustrate the problem with shallow precipitation systems, the percentage a given cloud constitutes of the beam is plotted in Figure 6, where it is seen that low-hanging precipitation only fills a fraction of the beam even at short ranges and thereby results in underestimation of the rainfall intensity.

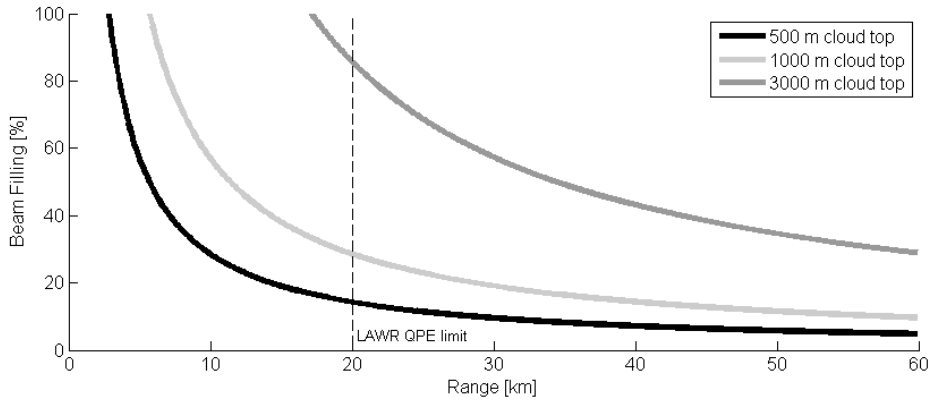

Figure 6 Beam filling degree for three different cloud top heights as function of range with vertical angular opening of 10°. The cloud top heights are typical for nimbostratus clouds.

4.2 Preparation of LAWR data

To compensate for underestimation as a result of increasing beam volume with range, a second volume correction (Eq. 2) is applied to the data prior to calibration. To accommodate for seasonal changes a new parameter set for the volume correction is estimated for every 10-15 days based on data from the previous 60 days, and a daily value is found by interpolation in cases of post-analysis. The process is part of the automatic calibration module running on some LAWR systems and here a new parameter set is estimated daily.

The LAWR used in this study is the Aarhus LAWR which is the primary research LAWR of DHI and the radar that has been in operation for the longest period at the same location. The location was chosen because of easy access, power, an internet connection and close proximity to the office. The drawback is that the LAWR is situated underneath a large four-

legged lattice antenna mast resulting in beam blockage and partial shielding. During the 10 years it has been in operation, the surrounding trees have grown and they now interfere with the beam path in some places. By accumulating reflectivity from the months July-November 2008, the blocked sector to the west is clearly evident in Figure 7. Figure 7 furthermore illustrates the effect of the increasing beam resulting in decreasing accumulations with increasing range, which are equalized by the volume correction. The data in Figure 7 has only been applied to the volume correction part of the signal processing, and in the case of the Aarhus LAWR the C_2-value was 1 and the C_3-value was -0.003. As result of the large blocked areas, the basic assumption of homogeneity used in estimation of the volume correction parameters does not hold. The second volume correction normally applied prior to the calibration is therefore not applied to the dataset used here, since the estimated C_2 and C_3 parameters would be skewed due to the large area that is blocked.

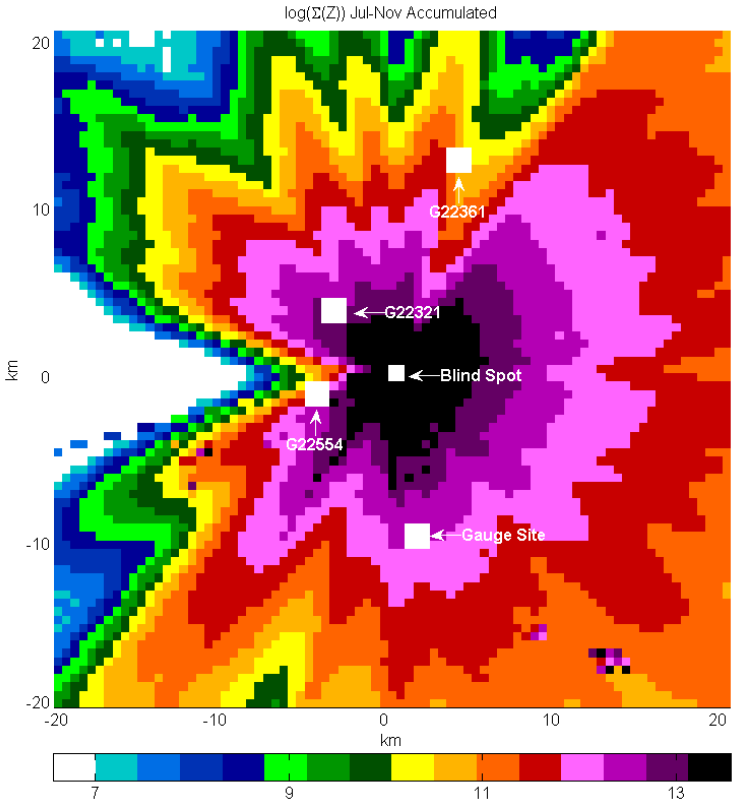

Figure 7 Accumulation over 5 months of 2008 for 0-20 km range. Please note that the data has been log transformed for plotting.

The accumulated reflectivity map of the inner 20 km in Figure 7 furthermore illustrates that in cases such as the Aarhus LAWR where beam blockage/shielding is present, the location of gauges used for calibration and validation is crucial. Figure 7 reveals that not all gauges available are equally suitable as they are placed in locations with beam shielding and thereby a general lower level of reflectivity. The gauges used for the calibration in calibration in Section 5 are located in the location marked Gauge Site in Figure 7 which is at an unobstructed location, and so is the location of G22331. Gauges G22554 and G22361 are both located in areas affected by shielding caused by the mast.

For this specific dataset from the Aarhus LAWR, a 2D volume correction has been applied adjusting the levels of reflectivity to match those of the area with the gauges used for calibration. The accumulated reflectivity has been discretized into 100 intervals linearly spaced, and the relation between a given pixel and the value of the pixel over the gauge site has been estimated. The result is a 2D image of volume correction factors ranging from a factor 0.29 to 4 – the maximum correction is limited to 4 as in the standard volume correction as shown in Figure 8. The adjusted reflectivity image is shown in Figure 9, where it can be seen that Gauges 22554 and 22321 now have the same reflectivity level, while Gauge 22361 still has a lower level.

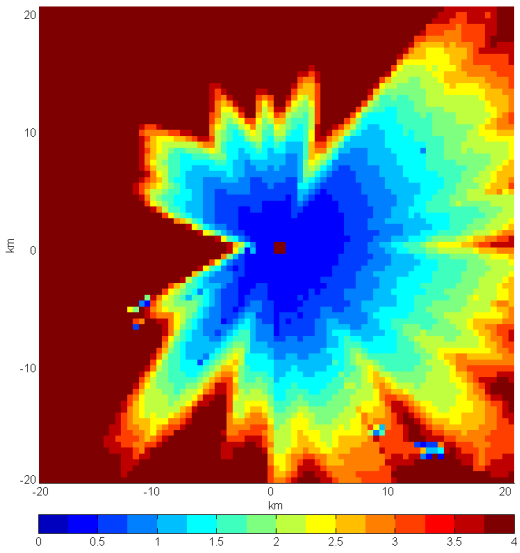

Figure 8 2D volume correction factors for adjusting reflectivity levels to match those of the gauge site. A maximum correction constraint of 4 is enforced.

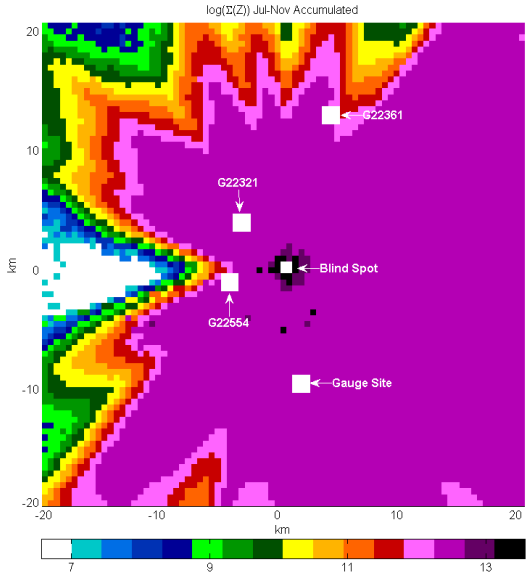

Figure 9 Accumulated reflectivity's from the Aarhus LAWR (July-November 2008) after the 2D adjustment from Figure 7 is applied.

5 Analysis of LAWR Calibration Methodology

The calibration analysis is carried out on events where both the radar and the gauges (>1 mm rainfall depth) have observed rainfall – a total of 50 events. One of the challenges is to define the appropriate time frame since the LAWR observes an area and records rainfall prior to and after the observations of the corresponding gauge. The analysis carried out here has been performed on LAWR accumulations over the timeframe defined by the gauge. This can result in underestimation of LAWR accumulations, however, when compared to extending the time frame by 10 minutes at the beginning and at the end of the event, in the majority of the events this is less than 5%.

The standard LAWR calibration, cf. eq. 3 is obtained by estimating the DHI CF parameter in eq. (4) by linear regression. The result is shown in Figure 10.

$$\text{Rainfall Depth} \;=\; \text{DHI CF} \cdot \sum_{\text{Event Start}}^{\text{Event Stop}} Z/\Delta t, \;\text{where}\; \widehat{\text{DHI CF}} \;=\; 1.04 \cdot 10^{-3} \qquad (4)$$

The estimated DHI CF of $1.04 \cdot 10^{-3}$ is used to convert Z values into rainfall intensities in mm/min – in order to get the LAWR rainfall estimates in e.g. µm/s, ordinary unit conversion

is applied and the DHI CF becomes 0.007. It should be noted that some precautions must be taken when applying unit conversion since the calibration depends on the temporal resolution of the LAWR data, which can be either 1 or 5 minutes – here 1 minute data is used.

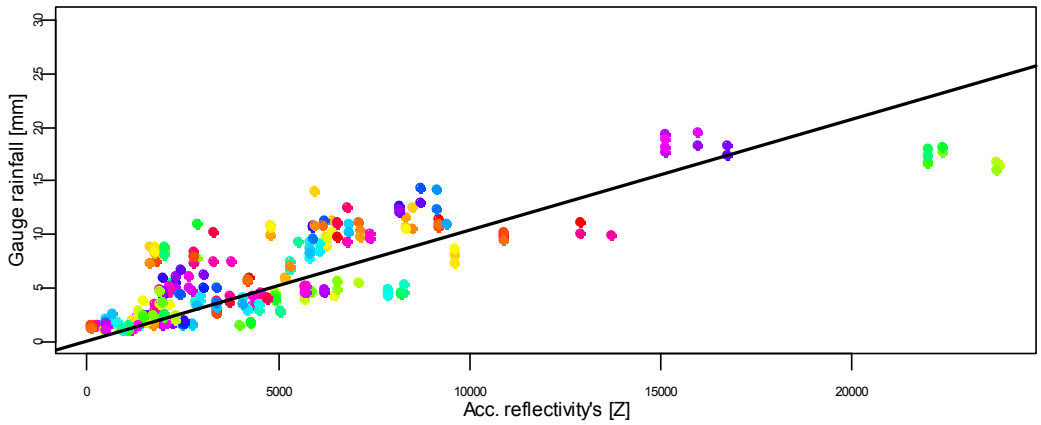

Figure 10 Estimation of LAWR calibration factor (DHI CF) as defined by Eq. 4. Data from are colored with respect to event and gauge number – same color range e.g. green for the event and different shades of green for each gauge.

The scatter of the data in Figure 10 is the result of comparing a surface measurement (0.25 km^2) with a point measurement (~200 cm^2) combined with the inter-event variability of the accumulated rainfall depths observed by the gauge. The variability in rainfall depths within a 500x500 meter area based on the 9 rain gauges was found to vary from 1-26% based on the coefficients of variation of the inter-event variability. The variability decreases with increasing rainfall depths and is independent of the mean event intensity (Pedersen et al., 2009). The accumulated reflectivity in Figure 10 originates from 4 different pixels, cf. Table 2, which is clearly evident in the two largest events where there is a relatively large difference in the accumulated reflectivity within the same event.

It is well known that different types of rainfall have different drop size distributions resulting in different Z-R relationships for stratiform rainfall and convective rainfall (Battan, 1973) and others. So far there has been no attempt to use rainfall type classifications in connection with the LAWR calibration.

The standard LAWR calibration only depends on the reflectivity (Z), but past experience shows that the calibration factor changes significantly from rainfall events with high intensity to long lasting events with low intensities. Inspired by this and the link between different Z-R relationships and different rainfall types, multiple linear regression analysis is used to evaluate which variables are significant in the calibration. Initially, the full model containing all variables: acc. reflectivity (ΣZ), duration (hour), intensity (ΣZ/hour), pixel number and gauge number are estimated, after which variables with an estimated p-value larger than 5% are removed in order to establish the most simple model. The simplest model where all variables are significant at the 5% level contains acc. reflectivity (ΣZ), duration (hour) and intensity (ΣZ/hour). The gauge number and pixel number were found to be insignificant which indicates that the calibration is not biased towards a specific gauge or pixel. In order to

determine if the simplified model is significantly poorer than the full model containing all five variables, the two models were compared by means of an ANOVA test (F-test). The conclusion of the test is that the simpler model with three parameters compared to the full model could not be rejected at a 1% significant level.

The estimated parameters for the chosen model:

$$\text{Rainfall Depth} = \varphi \cdot \sum Z + \phi \cdot \text{Duration} + \psi \cdot \text{Intensity}, \text{ where } \begin{cases} \hat{\varphi} = 5.96 \cdot 10^{-4} & [Z] \\ \hat{\phi} = 0.60 & [h] \\ \hat{\psi} = 4.20 \cdot 10^{-4} & [Z/h] \end{cases} \quad (5)$$

Table 4 summarizes the two different calibration schemes chosen for converting accumulated reflectivity into rainfall depth in mm. Scheme 1 is the standard calibration approach and Scheme 2 is the new approach as defined in Eq. 5. Duration and intensity have been removed individually from Scheme 2 and the degree of explanation is between Scheme 1 and Scheme 2.

Table 4 Summarized information on the LAWR calibration schemes. The parameters are estimated based on a total of 353 observations of 55 rain events. The figures in brackets are the standard deviation of the estimated parameter.

	Formulation	Estimated Parameters	R^2
Scheme 1	$\text{Rainfall Depth} = \text{DHI CF} \cdot \Sigma Z$	$\{\widehat{\text{DHI CF}} = 1.04 \cdot 10^{-3}\ (0.24)$ [Z]	0.85
Scheme 2	$\text{Rainfall Depth} = \varphi \cdot \Sigma Z + \phi \cdot \text{Duration} + \psi \cdot \text{Intensity}$	$\begin{cases} \hat{\varphi} = 5.96 \cdot 10^{-4}\ (0.40 \cdot 10^{-4})$ [Z] $\hat{\phi} = 0.60\ (0.05)$ [h] $\hat{\psi} = 4.20 \cdot 10^{-4}\ (0.48)$ [Z/h]	0.90

Scheme 2 provides a better degree of explanation than Scheme 1 (standard calibration) based on the increase in R-squared from 0.85 to 0.90. Of the parameters in Scheme 2, reflectivity is the most significant followed by duration and finally by intensity judged by the t-statistic values.

5.1 Validation of extended DHI LAWR calibration

Figure 11 shows the difference (percent) between the gauge observed rainfall depth and the LAWR estimated rainfall depth. The difference between observed and estimated rainfall is partly due to the natural scatter when comparing radar and gauge measurements and the uncertainty of the calibration method. The natural scatter contains the uncertainty related to representing the spatial variability of rainfall depths within a single LAWR pixel with a single gauge. The spatial variability expressed as coefficient of variation has in another connection been estimated from 1-26% for rainfall depths observed by gauge within an area corresponding to a single LAWR pixel and is marked in Figure 11 to illustrate the part of the uncertainty which may potentially be a result of a single gauge not being representative for the whole pixel. The validation data has been applied to the 2D volume correction outlined in Section 4.2.

For all gauges there are events where the LAWR overestimates more than 100%, but in most cases of events with depths between 1-1.4 mm and a duration of less than 1 hour. Especially light low-hanging frontal rainfall is difficult to estimate correctly by the LAWR due to the

rapidly increasing beam volume. At far ranges low-hanging light rain only fills a small fraction of the LAWR sample volume, and since the rainfall estimate is an integration of the full vertical, little rain will be under the cut-off value and therefore the estimate for that point is zero.

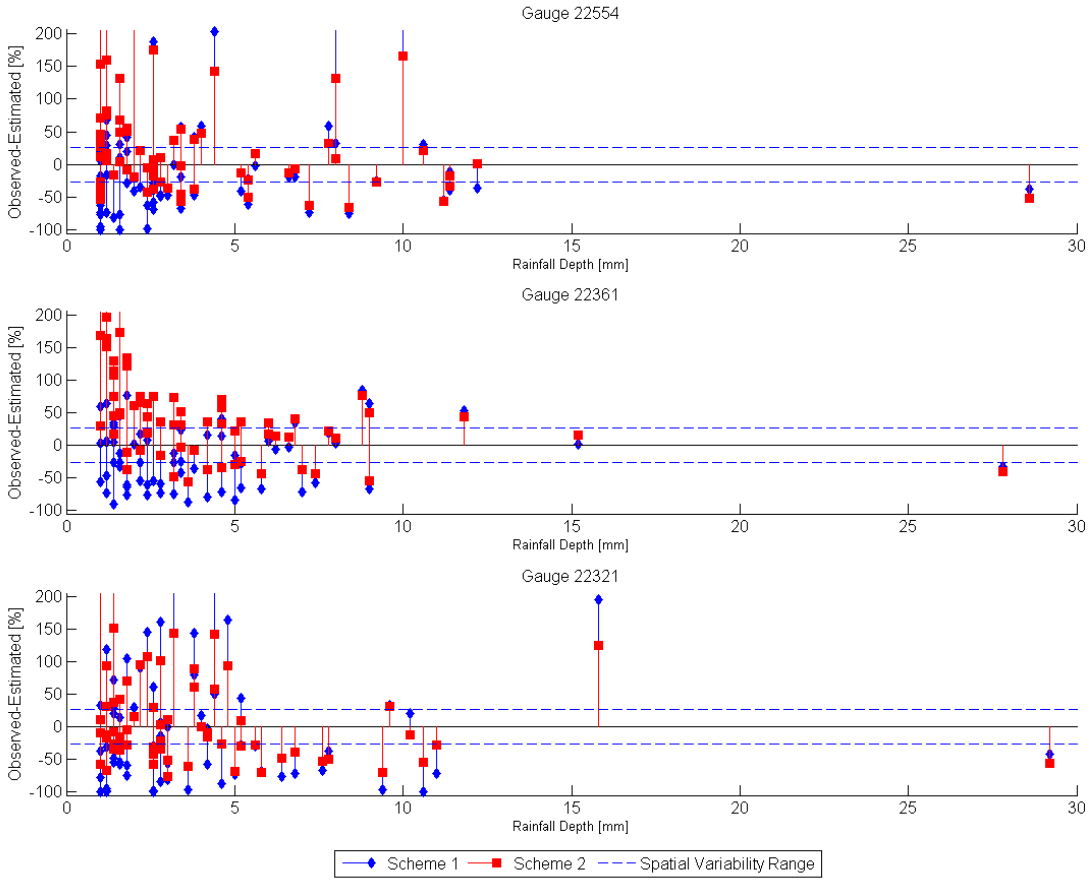

Figure 11 Difference in percent between observed rainfall depth (mm) and LAWR estimated rainfall depth (mm) for all valid validation events for the three different gauges as function of rainfall depth. Gauge 22554 and 22361 are both approximately 5 km from the Aarhus LAWR while gauge 22321 is 13 km away. Negative percentage figures indicate the LAWR estimate is smaller than the gauge observation. The LAWR data has been applied a 2D volume correction. The spatial variability range is the maximum coefficient of variation of rainfall depths within a single LAWR pixel based on rain gauge measurements from (Pedersen et al., 2009).

The two schemes are validated with 3 rain gauges operated by the Danish Meteorological Institute. Data from the corresponding LAWR pixels, cf. Table 2, is applied to the calibration schemes and the estimated rainfall depths are compared to those observed by the gauges. The location of the rain gauges in relation to the LAWR can be seen in Figure 7. The estimated accumulations for all valid events and the observations are listed in Table 5.

Table 5 Observed and LAWR estimated rainfall depths for the three different schemes in absolute values and percent deviation from the observed rainfall depth. The percentage values in brackets are the validation based on LAWR data without 2D volume correction.

	Gauge 22554	Gauge 22361	Gauge 22321
Number of events	68	66	64
Distance to LAWR [km]	4.9	5.3	13.3
Observed total rainfall depth [mm]	280 (σ=4.4 mm)	279 (σ=4.1 mm)	270 (σ=4.3 mm)
Scheme 1 total rainfall depth [mm]	285 (σ=5.9 mm)	241 (σ=4.3 mm)	257 (σ=6.6 mm)
Scheme 2 total rainfall depth [mm]	301 (σ=4.5 mm)	334 (σ=3.8 mm)	263 (σ=4.9 mm)
Scheme 1 obs-estimated [%]	2 (-30)	-13 (57)	-5 (-76)
Scheme 2 obs-estimated [%]	7 (-11)	20 (61)	-2 (-44)

Figure 11 and the values in Table 5 show that both schemes perform very well at locations where the reflectivity level is in the same order as where the calibration factors are estimated – up to 20 km range from the radar depending on the azimuth. This condition is not fulfilled for Gauge 22361 which is located in an area with servere beam shielding, and here the 2D volume correction is insufficient. As a result of this Scheme 1 underestimates the rainfall depths (as expected from previous experience) while Scheme 2 overestimates the rainfall depths. The validation based on Gauge 22361 is the worst with an underestimation of -13% (Scheme 1) and an overestimation of 20% (Scheme 2). This gauge is more than twice the distance from the LAWR than the two other gauges, but this is probably of less importance than the fact that the reflectivity level at this point is more than 4 times lower than that of the area used for the calibration parameter estimation. The lower reflectivity level at Gauge 22321 is a combination of beam filling effects and beam shielding as a result of the antenna mast. The data foundation is too weak for any final conclusions on the range effect of the calibration. Unfortunately, the number of validation gauges available was limited to 3 at only two different distances to the LAWR. In order to establish if there is a range dependency that needs to be implemented in the calibration schemes, a higher number of gauges at increasing distances from the LAWR is required.

If the validation is carried out over an inhomogeneous reflectivity field as in Figure 7 (without second step volume correction) the proposed new scheme has improved the LAWR calibration compared to the existing one. Both for Gauge 22554 and 22321, their estimate is in the order of twice as good as that of Scheme 1. The validation results of Gauge 22554 are the best with an average underestimation of -11% by Scheme 2. Generally, Scheme 2 outperforms Scheme 1 except for Gauge 22361, where Scheme 1 is slightly better, but both schemes overestimate the observed rainfall. The validation results without second step volume correction vary as expected when the location of the gauges relative to the accumulated reflectivity level is taken into account in Figure 7. The log(ΣZ) value of the gauge locations are: 12.3 (Gauge 22554), 13.1 (Gauge 22361) and 11.2 (Gauge 22321). When compared to the log(ΣZ) value of 12.6 from the Gauge Site where the calibration factors are estimated, it becomes evident that the variation of the validation results is a result of the different accumulation reflectivity levels which again are an expression of the general signal level in that point. The large variation in the signal level in Figure 7 would not be present under normal conditions, so the results would be in the same order as those obtained using the 2D volume corrected data.

Based on the validation results it is found that both schemes perform equally well if the reflectivity levels are homogenous over the area. In situations where this is not the case the new calibration method proposed denoted Scheme 2 is better than the original calibration method (Scheme 1). Scheme 2 provides the best rainfall estimation in such cases.

The gauges used for the calibration estimation are from a temporary installation dedicated to addressing LAWR calibration uncertainties related to spatial variability of rainfall. The LAWRs in Denmark normally use data from the official Danish rain gauges network (SVK), so in order to link the findings based on the temporary gauges, the three available official gauges have been used to estimate the calibration parameters. The estimated parameters based on the official gauges are listed in Table 6 and the tendency is the same with Scheme 2 resulting in the best results. As expected there is quite large variation in the estimated parameters due to the location of the gauges in relation to the general reflectivity level. It should be stressed that it is of utmost importance to identify the location of gauges used for calibration in relation to the overall reflectivity level as done in Figure 7 since the estimated calibration factors in principle are only valid for areas of equal reflectivity level to the calibration gauge(s).

Table 6 Calibration parameters estimated based on the three validation gauges all part of the official Danish rain gauge network. The LAWR data has been applied the 2D volume correction. The figures in brackets are the standard deviation of the estimate.

	Gauge 22554	Gauge 22361	Gauge 22321
Scheme 1	$\widehat{\text{DHI CF}} = 6.67 \cdot 10^{-4}$ (0.74) [Z], $R^2 = 0.60$	$\widehat{\text{DHI CF}} = 9.70 \cdot 10^{-4}$ (0.59) [Z], $R^2 = 0.81$	$\widehat{\text{DHI CF}} = 5.82 \cdot 10^{-4}$ (0.69) [Z], $R^2 = 0.57$
Scheme 2	$\begin{cases} \hat{\varphi} = 2.09 \cdot 10^{-4}\ (1.09)\ [\text{Z}] \\ \hat{\phi} = 0.98\ (0.23)\ [\text{h}] \\ \hat{\psi} = 4.74 \cdot 10^{-4}\ (1.82)\ [\text{Z/h}] \end{cases}$ R^2=0.72	$\begin{cases} \hat{\varphi} = 7.06 \cdot 10^{-4}\ (1.29)\ [\text{Z}] \\ \hat{\phi} = 0.27\ (0.20)\ [\text{h}] \\ \hat{\psi} = 4.80 \cdot 10^{-4}\ (1.46)\ [\text{Z/h}] \end{cases}$ R^2=0.84	$\begin{cases} \hat{\varphi} = 2.34 \cdot 10^{-4}\ (1.05)\ [\text{Z}] \\ \hat{\phi} = 0.96\ (0.24)\ [\text{h}] \\ \hat{\psi} = 0.89 \cdot 10^{-4}\ (0.55)\ [\text{Z/h}] \end{cases}$ R^2=0.68

To illustrate the LAWR's ability to estimate the rainfall, intensities from two events from Gauge 222554 have been shown in Figure 12 and Figure 13.

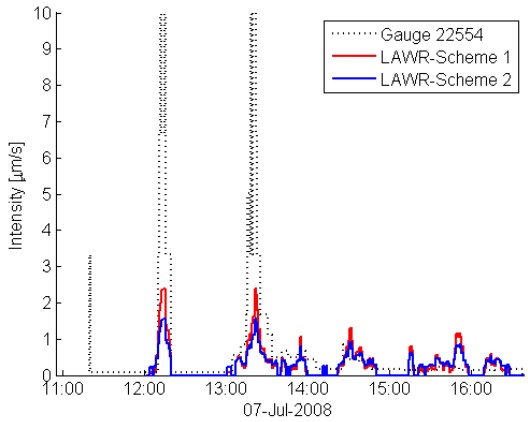

Figure 12 Intensities observed by DMI gauge and by LAWR the 7th of July. The event has two high peak intensities lasting only 1-2 minutes. The rainfall depth observed by the gauge was 11.4 mm, while the LAWR estimate was 7.0 mm (Scheme 1) and 7.6 mm (Scheme 2). The LAWR data has been applied the 2D volume correction.

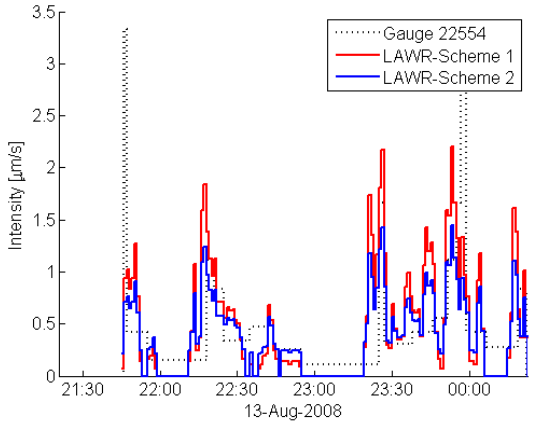

Figure 13 Intensities observed by DMI gauge and by LAWR the 13th of August. The event has 3 subparts which is captured by the LAWR but lost in the interpolation technique of the gauge. The rainfall depth observed by the gauge was 4.0 mm, while the LAWR estimate was 6.4 mm (Scheme 1) and 5.9 mm (Scheme 2). The LAWR data has been applied the 2D volume correction.

The event of 7 July (Figure 12) illustrates the effect of measuring rainfall with gauge and with radar. The gauge records some very short lasting peak intensities which are observed differently by the radar since the LAWR intensity sample is an average over a volume and over a time span, whereas the gauge is a discrete measurement in a small point. The key issue here is the scaling properties of the rainfall since the gauge estimate is only representative for a small area whereas the radar is an average of a volume over an area. Figure 13 shows an event where the LAWR correctly represents periods with no rain which are missed by the gauge due to the interpolation technique used, where the tip is divided by the minutes since the last tip and the mean value is used for all intermediate time steps. For both events there is good agreement of the timing between the gauge and the LAWR. The first peak (3.3 µm/s) in the gauge time series on both plots is an artifact from the gauge data processing. Since there is no way to know the time to fill the first gauge bucket, it is fixed to 1 minute and thus the significant peak.

6 Conclusions

The LAWR system and key data processing methods have been reviewed together with the existing calibration method. The focus point of the work has been to evaluate the performance of the LAWR and identify the significant factors affecting the calibration and thereby the uncertainty of the output. Based on a large dataset obtained during a field campaign in 2008 where 9 rain gauges where placed within a 500x500 meter area and three independent validation sets of data from the official Danish gauge network, the existing calibration method was evaluated. The existing calibration method for converting LAWR reflectivity into rainfall intensity is based on a linear relationship between the rainfall depth of an event observed by gauge and the corresponding amount of accumulated reflectivity. The linear relationship is a result of the logarithmic receiver, contrary to the linear receiver of conventional weather radars resulting in a power-law relationship between rainfall and

reflectivity. The standard one parameter LAWR calibration method has been observed to generally underestimate the LAWR rainfall. It was therefore of interest to search for a new calibration method which could reduce the uncertainties of the LAWR rainfall estimation. Based on the set of data from the 9 rain gauges, a new calibration scheme was developed. As the standard LAWR calibration, it uses the assumption of linear relationship between gauge rainfall and reflectivity, but it also includes the duration and the intensity observed by the LAWR. The new scheme improves the explanation degree of the calibration compared to the standard calibration with an increase in R^2 from 0.85 to 0.9 (Scheme 2).

The validation revealed that the location of the calibration gauge(s) is extremely important since the overall reflectivity level of the Aarhus LAWR is inhomogeneous as result of the location underneath an antenna mast causing beam blockage and shielding effects. Furthermore, growing trees result in signal absorption, and finally a hill to the west cause a large sector to be blocked. As a result of this, it was not possible to derive and apply the normal second step volume correction which aims at adjusting the reflectivity levels. Instead a 2D volume correction adjusting the reflectivity levels to match the level of the gauge site with the calibration gauges was applied to obtain homogenous conditions over the validation gauges. This method was found to result in a homogenous reflectivity field, but the method needs further development and testing before it is implemented in operational context. If the magnetron output level in the future is automatically adjusted to be constant over time, the 2D volume correction should be a constant filter, but individual for each radar.

The validation results showed very good agreement for gauges where the LAWR reflectivity level was in the same order as over the calibration gauges. If the reflectivity level is homogenous, both calibration methods perform equally well and the error is within $\pm$7%, while at locations affected by beam shielding, Scheme 1 results in underestimation and Scheme 2 in overestimation. If the reflectivity levels over the radar coverage areas are as inhomogeneous as those of the Aarhus LAWR used here (Figure 7), the new Scheme 2 calibration method outperforms the standard calibration.

The different uncertainties contributing to the total uncertainty are dominated by the range dependent uncertainties of a non-uniform rainfall field, increasing beam volume and attenuation. The random uncertainty as a result of spatial variability of rainfall depths within a single LAWR pixel ranges from 1-26% confines the accuracy limit of a calibration using a single gauge despite perfect radar data. The new calibration schemes can reduce the uncertainty level of the LAWR rainfall estimate, but in order to reduce the uncertainties more, the problem with different reflectivity levels needs to be addressed. A two dimensional mask as attempted here containing the level characteristics combined with the volume characteristics could be a solution to this issue.

The LAWR bridges the domain gap between rain gauge and conventional radars and provides information at the missing scales which is central in connection with urban drainage issues. Radars reveal the spatial structure of the rainfall in real time which is not possible to obtain by a few gauges, and furthermore they can provide forecast information. By combining information from gauge networks, LAWRs and conventional radars into a joint framework, it becomes possible to reduce some of the uncertainties at the different levels. The challenge is

to balance the potential gain in information level with the attached uncertainties originating from combining measurements at different spatial and temporal scales, which is also the core of comparing LAWR rainfall data with gauge data.

7 References

Austin, M., 1987. Relation between Measured Radar Reflectivity and Surface Rainfall. Monthly Weather Review, 115(5), 1053-1070.

Battan, L.J., 1973. Radar Observations of the Atmosphere. The University of Chicago Press

Bouar, E., Moreau, E., Testud, J., Poulima, H., Ney, R., Deudon, O., 2005. An Extensive Validation Experiment of Algorithm ZPHI. Proceeding from the 32nd Conference on Radar Meteorology. Albuquerque, American Meteorological Society.

Brotzge, J., Droegemeier, K., McLaughlin, D., 2006. Collaborative Adaptive Sensing of the Atmosphere (CASA): A New Radar System for Improving Analysis and Forecasting of Surface Weather Conditions. Journal of the Transportation Research Board, 1948, 145-151.

Ciach, G. J., Krajewski, W. F., 1999. Radar-Rain Gauge Comparisons under Observational Uncertainties. Journal of Applied Meteorology, 38, 1519-1525.

DMI, 2008. Måneden, sæsonen og årets vejr. [Online]: 15 October 2008, "http://www.dmi.dk/dmi/index/danmark/maanedens_vejr_-_oversigt.htm".

Donovan, B. C., Hopf, A., Trabal, J. M., Roberts, B. J., McLaughlin, D. J., Kuros, J., 2006. Off-the-grid radar networks for quantitative precipitation estimation. Proceedings from Fourth European Conference on Radar in Meteorology and Hydrology (ERAD06), Barcelona, Spain.

Einfalt, T., Jessen, M. & Mehlig, B., 2005. Comparison of radar and raingauge measurements during heavy rainfall. Water Science and Technology, 51(2), 195-201.

Fiser, O., 2004. Z-R (Radar Reflectivity-Rain rate) relationships derived from Czech Distrometer data, Proceedings from Third European Conference on Radar in Meteorology and Hydrology (ERAD04), Visby, Sweden.

Gekat, F., Pool, M., Didszun, J., 2008. Performance comparison of a compact weather radar featuring different antennas. Proceedings of the Fifth European Conference on Radar in Meteorology and Hydrology (ERAD08), Helsinki, Finland.

Habib, E. & Krajewski, W.F., 2001. Uncertainty Analysis of the TRMM Ground-Validation Radar-Rainfall Products: Application to the TEFLUN-B Field Campaign. Journal of Applied Meteorology, 41, 558-572.

Jameson, A.R., Kostinski, A.B., 2001. Reconsideration of the physical and empirical origins of Z-R relations in radar meteorology. Quarterly Journal of the Royal Meteorological Society, 127(517), 517-538.

Jensen, N.E., Pedersen, L., 2005. Spatial Variability of Rainfall. Variations Within a Single Radar Pixel, Atmospheric Research, 77, 269-277.

Jensen, N.E., 2002. X-Band local area weather radar - preliminary calibration results. Water Science and Technology, 45(2), 135-138.

Krajewski, W.F., Ciach, G.J., Habib, E., 2003. An analysis of small-scale rainfall variability in different climate regimes. Hydrological Sciences Journal, 48(2), 151-162.

Lee, G., Seed, A.W. & Zawadzki, I., 2007. Modeling the variability of drop size distributions in space and time. Journal of Climate and Applied Meteorology, 46(6), 742-756.

Lee, G., Zawadzki, I., 2004. Errors in Rain Measurements by Radar due to Variability of Drop Size Distributions. Proceedings of Sixth International Symposium on Hydrological Applications of Weather Radar, Melbourne, Australia.

Lee, G., Zawadzki, I., 2005. Variability of Drop Size Distributions: Time-Scale Dependence of the Variability and Its Effects on Rain Estimation, Journal of Applied Meteorology, 44(2), 241-255.

Marshall, J.S., Langille, R.C., Palmer, W.M., 1947. Measurements of Rainfall by Radar. Journal of the Atmospheric Sciences, 4(6), 186-192.

Marshall, J.S., Palmer, W.M., 1948. The distribution of raindrops with size. Journal of Meteorology, 5, 165-166.

Overgaard, S., 2001. Preliminary evaluation of the FUENEN LAWR WEATHER RADAR. Techinical Note, Danish Meteorological Institute

Pedersen, L., Jensen, N.E., Christensen, L.E., Madsen, H., 2009. Quantification of the spatial variability of rainfall based on a dense network of rain gauges. Submitted to Atmospheric Research.

Pedersen, L., 2004. Scaling Properties of Precipitation - experimental study using weather radar and rain gauges. M.Sc. Thesis. Aalborg University.

Thomsen, R. S., Drift af Spildevandskomitéens Regnmålersystem Årsnotat 2007. Teknisk rapport 08-06 (in Danish), Danish Meteorological Institute.

Uijlenhoet, R., Porra, J.M., Sempere Torres, D., Creutin, J.-D., 2008. Analytical solutions to sampling effects in drop size distribution measurements during stationary rainfall: Estimation of bulk rainfall variables. Journal of Hydrology, 328, 65- 82.

Uijlenhoet, R., 2001. Raindrop size distributions and radar reflectivity-rain rate relationships for radar hydrology. Hydrology and Earth System Sciences, 5(4), 615-627.

Ulbrich, W.C., 1983. Natural variations in the analytical form of the raindrop size distribution, Journal of Climate and Applied Meteorology, 22, 1764-1775.

Zawadzki, I., 1984. Factors Affecting the Precision of Radar Measurements of Rain. Proceedings of 22nd Conference on Radar Meteorology. The American Meteorological Society.

Zawadzki, I., 1975. On Radar-Raingauge Comparison. Journal of Applied Meteorology, 14, 1430 1436.

PAPER C

Estimation of Radar Calibration Uncertainties Related to the Spatial Variability of Rainfall within a Single Radar Pixel - Statistical Analysis of Rainfall Data from a Dense Network of Rain Gauges

---

Conference Proceedings: *World Environmental & Water Resources Congress 2008 (EWRI 2008*), May 12-16, 2008, Honolulu, Hawaii. (Oral Presentation)

Estimation of radar calibration uncertainties related to the spatial variability of rainfall within a single radar pixel - Statistical analysis of rainfall data from a dense network of rain gauges

Lisbeth Pedersen[(1+3)], Niels Einar Jensen[(2)] and Henrik Madsen[(3)]

[1]DHI, Gustav Wieds Vej 10, 8000 Aarhus, Denmark, PH +45 8620 5116, email: lpe@dhigroup.com (Corresponding author)
[2]DHI, Gustav Wieds Vej 10, 8000 Aarhus, Denmark, PH +45 8620 5122, email: nej@dhigroup.com
[3]Institute for Informatics and Mathematical Modelling, Technical University, Denmark, Bygning 321, 2800 Lyngby, Denmark, PH +45 4525 3408, email: hm@imm.dtu.dk

Abstract: A total of 6 months of rainfall data sampled with nine rain gauges on a 500 x500 meter area has been analysed in order to determine the variability of rainfall within such a small area. The area corresponds to that of a maximum pixel size of a Local Area Weather Radar (LAWR). To calibrate a LAWR, the rain depth from a number of events is used and the analysis is therefore carried out on a total of 29 events fulfilling certain criteria's. The variability is expressed with the coefficient of variation and found to vary from 3 % to 100 % depending on type of rainfall. This gives an uncertainty in that range if a post event specific calibration is performed with a single rain gauge.

1. Introduction

Representative rainfall measurements are of uttermost importance in many hydrological applications, e.g. real time control of water flows to avoid damages caused by flooding. Other area's is as input for hydrological models – especially when unique individual events are being analysed in order to establish how the system performed in a given situation.

Traditionally, rainfall for use in hydrological applications has been obtained with rain gauges and used under the assumption that rainfall could be considered uniform over an area, often of considerable size. This is highly problematic since rainfall is known to vary in both time and space. Especially convective events can be of limited spatial extent and duration and therefore be difficult to describe accurately with a single or few rain gauges. Goodrich et al. (1995) concludes, on the basis of a detailed analysis of relatively dense network of rain gauges within a small catchment of < 5 ha in Arizona, that the assumption of uniform rainfall is invalid at the 5 ha scale in regions with convective thunderstorms. Einfalt et al. (2005) states on the basis of radar observations that the spatial extent of heavy rainfall in several cases in northwest Germany was less than 15 km^2 and the maximum of the event was not observed by the rain gauge network in the area.

The obvious solution to this problem is to use distributed rainfall measurements from weather radars as input to hydrologic models. Today this is almost only attempted in research projects, but is becoming of more general interest in these years. The reasons for radar data not being widely used are many; some of practical nature such as computational requirements, availability and quantity of radar data, economical costs, while others is of a more conceptual nature. Weather radars are not measuring the actual amount of water at the ground, but are relating the signal backscattered from rain drops in a volume in the air to a rainfall intensity projected onto a surface at the ground. From a hydrologist's point of view the uncertainties of this are often regarded greater than the uncertainty of assuming uniformly distributed rainfall over a large area.

In order to relate the radar measurements to rainfall at the ground where it is of interest in relation to hydrological applications it is necessary to calibrate the radar with rain gauge measurements. The problem is that the gauge is a point measurements of a few hundred cm^2 whereas the radar is a volume sample projected to a surface ranging from 0.01 km^2 to most commonly 2-4 km^2. There are orders of magnitude between the two sample sizes and the problem of this in relation to radar gauge comparison/calibration as been addressed extensively in the literature among others by Zawadzki (1975) and Ciach and Krajewski (1999). Ciach and Krajewski (1999) suggest that a method to investigate the impact of small scale variability on remote sensing techniques is through analysis of very high resolution gauge networks in connection with radar data. An experiment designed to examine the impact of local variability of rainfall on radar calibration was conducted during the months of September through November 2003 and recommenced in January 2007 and is still running.

This paper is organized as follows: In the next section the two experiments are presented along with the background for the study. In Section 3 the analysis and results are presented followed by the quantification of the calibration uncertainty in Section 4. The conclusions and outlook close this paper.

2. Background and Experimental Setup

Since 1999 a cost-efficient type of weather radar has been available as a supplement to traditional rain gauges. The Local Area Weather Radar is based on a 25 kW X-band standard Furuno marine radar. The specifications are listed in Table 1. The LAWR is designed to deliver high resolution distributed rainfall data for hydrological applications such as urban drainage run-off models. In order to use the LAWR for this it needs to be calibrated on the basis of rain gauges. In order to know the uncertainty of the LAWR rainfall data it is necessary to quantify the limits of how precise a calibration can be based on the variation of rainfall within a single pixel.

The aim of this work is to quantify the spatial variability within a single pixel and thereby assess the uncertainty of a calibration based on a single gauge.

2.1 Background for experiment

In 2003 a rainfall measuring experiment was conducted. The aim was to verify the existing calibration method of the LAWR based on an experimental setup of 9 high resolution rain gauges. The initial assumption was that the LAWR pixel size of 500x500 meters was so small that rainfall could be considered uniform within and thereby a single gauge would be sufficient for calibration. The results showed up to more than 100% difference in accumulated rain depths between two neighbouring gauges less than 200 meters apart, Jensen and Pedersen (2005). Such large variability within an area of 500x500 meters which is a quarter of a normal radar pixel, indicates that some of the uncertainty in connection with radar rainfall intensities may not be due to errors in the radar but to variability in the rainfall which also is confirmed by Austin (1987). To verify and increase the data quantity for more reliable results, the experiment was recommenced in the spring of 2007.

Table 1 LAWR specifications

	LAWR 25 kW
Wave length	X-band, 3.2 cm
Antenna	8 (6) ft slotted waveguide array
Receiver	Logarithmic receiver
Vertical opening angle Horizontal opening angle	± 10° 0.95°
Range (forecast/QPE)	60/20 km
Spatial resolution	500x500/250x250/100x100 m.
Temporal resolution	1 or 5 minute image frequency
Scanning strategy	Single layer and continuous scanning

A LAWR differs in many ways from traditional weather radars based on C- or S-band technology which means that the prevailing methods for converting radar signal from backscattered rain does not hold. Since the LAWR is equipped with a logarithmic receiver the normal approach of using a Z-R relationship for converting radar reflectivities to rainfall intensities is not used. Originally, a second order polynomial was used to describe the relationship between Z and R, but based on experiments and experiences a different calibration method was established based on a linear relationship, cf. Eq. 1. The calibration factor denoted DHI CF in the following convert's radar reflectivity values to intensity in mm per time resolution of the radar which is either 5 or 1 minute.

$$\mathrm{DHI\,CF} = \frac{\sum_{\text{event start}}^{\text{event stop}} \text{mm rain (gauge)}}{\sum_{\text{event start}}^{\text{event stop}} \text{radar reflectivity}} \tag{1}$$

The performance of radars is often evaluated on the basis of how much the radar derived rainfall differs from those of a single rain gauge. The difference between gauge and radar is almost always put down to errors or in best cases uncertainty of the radar. The reason is probably more complex than that since studies have shown

that the A and B coefficients in the Z-R relation depends on the type of rainfall, e.g. convective vs. stratiform, Austin (1987), Atlas et al. (1999) and others. Another reason could be that rainfall within a single pixel varies significantly within an event.

2.2 Rain gauge setup

The 9 rain gauges were and are again placed in the central part of Denmark approx. 10 km south of Aarhus where a LAWR has been in operation since 1999. In 2003 the gauges were placed on an open field without any significant sheltering effects. The experiment was recommenced in January 2007 in the same location, but later moved approx. 1 km north and out in the shallow waters of a nearby estuary. The different locations are shown in Figure 1 in relation to Denmark.

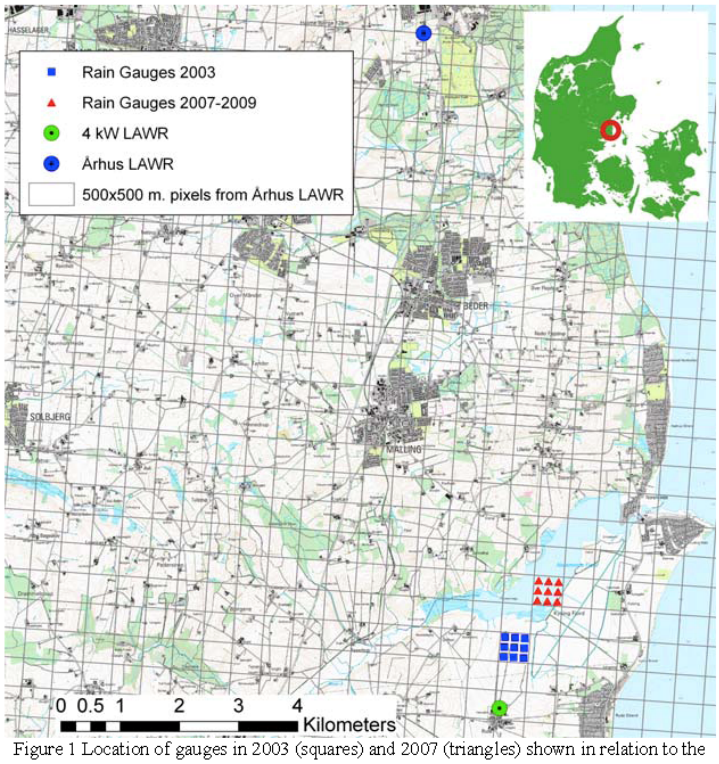

Figure 1 Location of gauges in 2003 (squares) and 2007 (triangles) shown in relation to the 500x500 meter grid from the Aarhus LAWR 10 km north of the gauges.

Both locations are overlooked by the Aarhus LAWR (blue circle) and in addition a small 4 kW experimental LAWR (green circle) has been installed south of the gauges as part of a LAWR network test bed.

The two experiments are identical in layout since the 9 gauges in both cases were placed representing 1/9 of a single pixel of 500x500 meters. In 2003 the experiment was conducted with high resolution optical drop counting gauges with a resolution of 0.01 mm. These were abandoned for the experiment in 2007 in favour of tipping

bucket gauges with a 0.2 mm resolution. The different types are illustrated in Figure 2 and Figure 3.

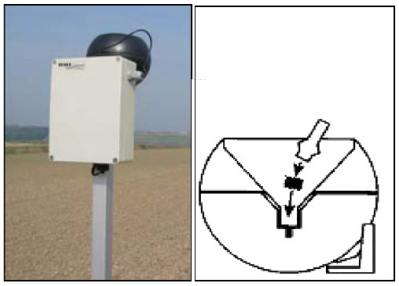

Figure 2 Optical drop counting gauge based on a Rosted Digirain gauge used in 2003. Pedersen (2004)

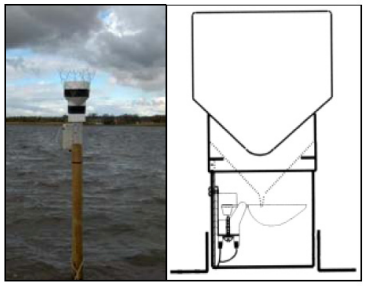

Figure 3 Tipping bucket gauge by Pronamic.

The gauge type was changed because the high resolution of 0.01 mm of the optical drop counting gauges were recognized not to be required and the tipping bucket gauges are less sensitive towards wind vibrations and more robust. Both times the gauges have been equipped with a data logger for storing the rainfall data. The data from 2003 was presented by Jensen and Pedersen (2005), but since different criterions were used for separating the rainfall into events they have been included in this study.

2.3 Data summary

Measurements were carried out from 21st September to 25th November in 2003 and from 17th January to 21st November 2007.

To separate the time series into individual rain events a separation criterion of maximum 60 minutes between two tips and a minimum of 1 mm rainfall to define an event has been applied. This results in a total of 36 events in 2003 where at least one gauge has fulfilled the criteria and a total of 23 events in 2007.

From January until June 2007 the gauges were located in the same location as in 2003. Due to communication problems with the land owners 6 of the 9 gauges were run over by farming equipment and ruined. As result of this it was decided to move the gauges to a new location in the estuary shown in Figure 1 where they would be undisturbed. As a result of this the data from January 2007 to June 2007 has been omitted from the analysis and only data from the new location has been used. The total amount of rainfall collected by the gauges is shown in Figure 4 along with box plots of the data.

Gauge no. 1 and 4 (2007) were observed in the field to be clogged by bird droppings. Until 09/23/07 all nine were functioning. In the period 09/23/07 to 10/18/07 gauge No. 1 and 4 were clogged. After the 10/18/07 only gauge No. 1 was clogged. For unknown reasons gauge No. 1 was not cleaned along with gauge No. 4.

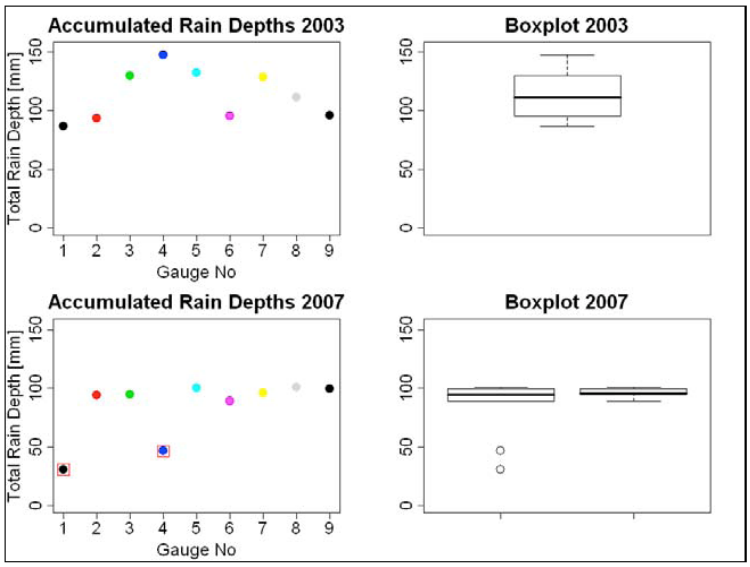

Figure 4 Total accumulated rainfall for 2003 and 2007 as function of gauge along with the corresponding box plot. The box plot for 2007 is shown for all data left, while gauge No. 1 and 4 are omitted on the box plot to the right.

3. Analysis of results

Initially it is seen that the accumulated depths for 2007 in general varies much less than those observed in 2003. This could indicate a higher quality of the data observed in 2007, but there is no presence of convective events in the 2007, which is the case of 2003. The variability of accumulated rainfall depth for individual events is shown in Figure 5 with a box plot and a histogram of the rainfall depths. In order to ensure a more robust analysis an additional selection criterion as been applied: only events where all possible gauges have recorded more than 1 mm have been selected. There are 13 events in 2003 where all gauges in an event are above 1 mm, whereas the number is 16 for 2007.

If only the box plots of the events are used to evaluate the data, events with large rain depths are classified as outliers since they exceed a value larger 1.5 times the interquartile range. The histogram of the data clearly shows that the dataset is dominated by events with a rain depth less than 3 mm.

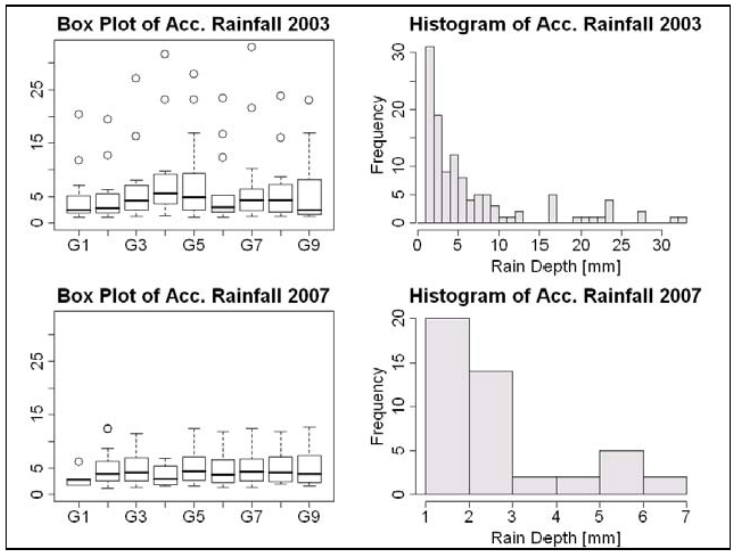

Figure 5 Accumulated rainfall for 2003 and 2007 for events where the rain depth in all gauges > 1 mm. Only valid events is used to compute the quartiles and median for gauge 1 and 4 in 2007, cf. Section 2.3.

Based on the non-parametric Kruskal-Wallis test it is concluded that the median is constant for each year (p=0.88 for 2003 and 0.94 for 2007). The large rainfall depths seen as outliers in Figure 5 are not unrealistic values and are probably caused by convective rainfall. Compared with the result of the Kruskal-Wallis test and the knowledge of convective events can occur in the fall in Denmark they are considered valid.

4. Quantification of the calibration uncertainty based on the variability of the rain fall in space

Before quantifying the variability the variance of the data is examined in order to see if there are any anomalies that have not yet been accounted for. The variance for the nine gauges of duration in minutes for the individual events is illustrated along with the variance of the rainfall depth in Figure 6.

By examining Figure 6 it is quite clear that there are two events (18 and 20) from the 2003 dataset where the duration is dubious. By manual examination of the data it appears to be a flaw in the initial data processing, but there is a risk of malfunctioning gauge since in both cases it is gauge No. 8. In the 2007 dataset event no. 4 has a relative large variance. The events in question have therefore been tagged in the following where the duration has been used as a parameter. If the variance of the accumulated depths is taken into consideration the 2003 dataset contains three events causing large variance: event No. 13, 18 and 35. These have been tagged in the same manner as the previous mentioned.

The reason for not omitting the events causing extreme variance is due to the fact that event no. 13 and 18 (2003) are the only two events above 10 mm rain depth in

all 9 gauges and the only event with convective characteristics, and at present it can not be ruled out the error is introduced in the initial data processing. The events detected in the variance analysis are in the following plots marked with a black circle.

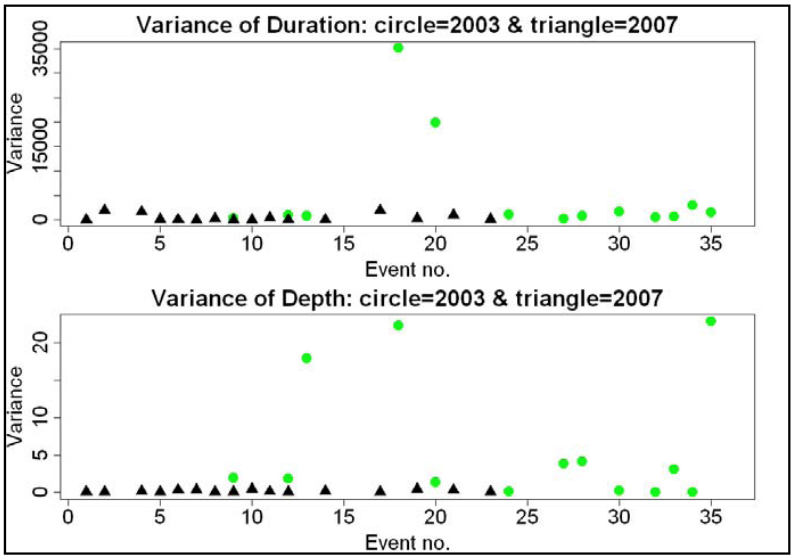

Figure 6 Variance of duration (top) and rainfall depth (bottom). Green circles are 2003 data, while black triangles are 2007.

To give a quantifiable measure of the variability within the individual events where all possible rain gauges have recorded minimum 1 mm the spatial variability is expressed with the coefficient of variation, δ. The results are illustrated in Figure 7.

$$\delta = \frac{S}{\overline{X}} = \frac{\sqrt{\frac{1}{n-1}\left[\sum_{i=1}^{n} x_i^2 - \frac{1}{n}\left(\sum_{i=1}^{n} x_i\right)^2\right]}}{\frac{1}{n}\sum_{i=1}^{n} x_i} \qquad (2)$$

The coefficients of variation for the data are shown in Figure 7 both as function of mean rainfall depth and as a function of the Mean Event Intensity (mean depth divided by mean duration). There is no clear evidence of correlation in the data, so at present it is not possible to determine whatever the variability depends on either depth or Mean Event Intensity. The variability expressed by the coefficient of variation is minimum 10 % (2003) and 3 % (2007) for the analysed events while the maximum is 99 % (2003) and 16 % (2007). If the events marked as dubious is removed the maximum values becomes 77 % (2003) and 16 % (2007). This gives average values of 29 % variation and 9 % for 2003 and 2007, respectively.

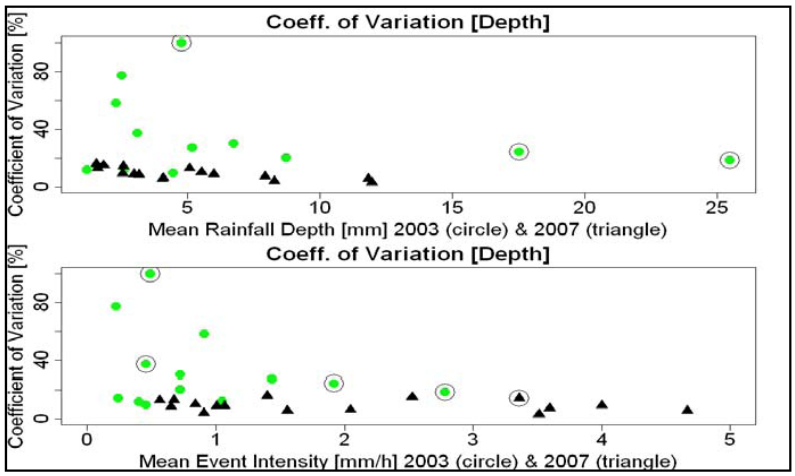

Figure 7 Variability within single events expressed by the coefficient of variation, δ as function of mean rainfall depth (top) and Mean Event Intensity in mm/h (bottom). Green circles are 2003 data. Black triangles are 2007. Events with an extra circle are dubious.

The largest variability is found in events with a low Mean Event Intensity and small rainfall depths. This indicates that only events above a certain minimum rainfall depth or Mean Event Intensity should be used for radar calibration purposes. An initial estimate of this value would be 3 mm or a Mean Event Intensity over 1 mm/h.

The major reason for the large difference in variability expressed by coefficient of variation between the two datasets is probably due to several things. There have been used two different types of gauges, which might explain some difference. This has not been examined any further in this work. Another issue was the 2007 gauges were observed to vibrate due to wind – it has not been able to determine the effect of this phenomena, but the gauges were all placed in the same way so it is assumed that the effect was the same on all of them. Another aspect besides different types of gauges is the fact that the gauges in the 2007 has been placed out in the water and the impact of this needs to examined closer in the future work.

5. Conclusion and future work

The conclusion on this initial statistical data analysis shows that even within a small area as 500x500 meters is there minimum a variability of 3 % when accumulated rainfall is considered on an individual event basis. With variability ranging from 3 to 77 (99) % there is great uncertainty related to use a single gauge for calibrating the radar in specific individual event. The original analysis of the 2003 dataset in Jensen and Pedersen (2005) showed coefficients of variation above 100 %, but in that analysis different event separation criteria's were used. First of all the dry period was set to 10 hours and secondly there were no criteria of all gauges exceeding a depth of 1 mm. This means that the results from the previous work can not be directly compared with the present work. The reason for using 1 hour in this work is that it corresponds to the normal criteria used by the Danish authorities in connection with the official net of rain gauges operated by the Danish Meteorological Institute.

If a calibration factor for the LAWR is obtained as an average over many primarily stratiform events there is a risk of this not being representative for an extreme convective event. In these cases it is normal to do a post event specific calibration, but it should not be done without taking the variability into consideration. Therefore the calibration should be followed by an estimate of the uncertainty. The analysed dataset only contains few events with large depths and/or high Mean Event Intensity, and it is therefore not yet possible to give a final estimate based on Mean Event Intensity. This is a problem since the variability of these often convective events are of most interest since it is those causing damages on infrastructure.

The dataset from 2007 does not contain any deep rainfalls and there is no evidence of any convective events, whereas the 2003 dataset contains several events with a rain depth above 10 mm, but is likely to less trustworthy, cf. Section 3. Furthermore there are at least 2 convective events in the 2003 dataset. The experiment is still running so the future datasets will hopefully contain more of both convective events and events with large amounts of rainfall. This is necessary in order to draw any final conclusions. Besides adding new data to the analysis the next step is to look at the variability of not only the accumulated rainfall depths but also on the variability of the intensities through out the event and compare those of the LAWR with those of rain gauges.

6. References

Atlas, D., Ulbrich, C. W., Marks Jr., F. D., Amitai, E., Williams, C. R. (1999), "Systematic variation of drop size and radar-rainfall relations", Journal of Geophysical Research, Vol. 104(6), 6155-6169

Austin, P. M. (1987). "Relation between Measured Radar Reflectivity and Surface Rainfall". Monthly Weather Review, Vol 15, 1053-1070

Ciach, G. J., Krajewski, W. F. (1999). "Radar-Rain Gauge Comparisons under Observational Uncertainties" Journal of Applied Meteorology, Vol. 38, 1519-1525.

Ciach, G. J., Krajewski, W. F. (1999). "On the estimation of radar rainfall error variance" Advances in Water Resources, Vol. 22(6), 585-595.

Einfalt, T., Jessen, M. and Mehlig, B (2005). "Comparison of radar and raingauge measurements during heavy rainfall" Water Science and Technology, Vol 51 no 2, 195-201

Goodrich, D. C., Faurés, J., Woolhiser, D. A., Lane, L. J., Sorooshian, S. (1995). "Measurements and analysis of small-scale convective storm rainfall Variability." Journal of Hydrology 173, 283-308

Jensen, N. E., Pedersen, L., (2005), "Spatial Variability of Rainfall. Variations Within a Single Radar Pixel", Atmospheric Research 77, 269-277

Pedersen, L. (2004) "Scaling Properties of Precipitation - experimental study using weather radar and rain gauges, M. Sc. Thesis from Aalborg University

Zawadzki, I. (1975). "On Radar-Raingage Comparison." Journal of Applied Meteorology, Vol. 14, 1430-1436

PAPER D

Application of Local Area Weather Radar (LAWR) in Relation to Hydrological Modeling – Identification of the Pitfalls in using High Resolution Radar Rainfall Data

---

Conference Proceedings: *Fourth European Conference on Radar in Meteorology and Hydrology (ERAD06)*, 18-22 September 2006, Barcelona, Spain. (Oral Presentation)

Proceedings of ERAD 2006

Application of Local Area Weather Radar (LAWR) in relation to hydrological modelling – Identification of the pitfalls in using high resolution radar rainfall data

Lisbeth Pedersen[1,2], Niels Einar Jensen[1], Henrik Madsen[2]

[1] DHI Water & Environment, Aarhus (Denmark).

[2] Institute for Informatics and Mathematical Modelling, Technical University, Copenhagen (Denmark).

1 Introduction

Recent analysis of spatial and temporal resolution of rainfall and the advent of small inexpensive rainfall radars has lead to increased use of radar estimated rainfall as input to hydrological models especially in urban areas. Detailed rainfall measurements have indicated a very high spatial variation of up to 100 % of a distance of less that 200 m over a 3 hour rainfall event [Jensen and Pedersen, 2005]. Modelling urban runoff using few rain-gauges may easily lead to very high uncertainty on the simulated flows.

By applying distributed rainfall data to an urban runoff model significant improvement in the model performance would be expected. This is not always the case and this paper analyses the pitfalls and benefits of using distributed rainfall data in relation to urban drainage modelling

The analysis is performed on basis of data from the Local Area Weather Radar (LAWR) owned by Municipality of Vejle, Denmark and the existing MIKE URBAN model for the city of Vejle. The drainage model has been calibrated against flow gauges in the system.

For use in the analysis a subpart of the MIKE URBAN model was selected. The subpart models the suburb Grejsdalen which is a narrow housing area along the stream Grejs Å. The drainage system is flat along the stream, but the system on the sides is very sloped with accordingly fast response times. The total catchment area is 118 ha has been divided into 344 sub-catchments.

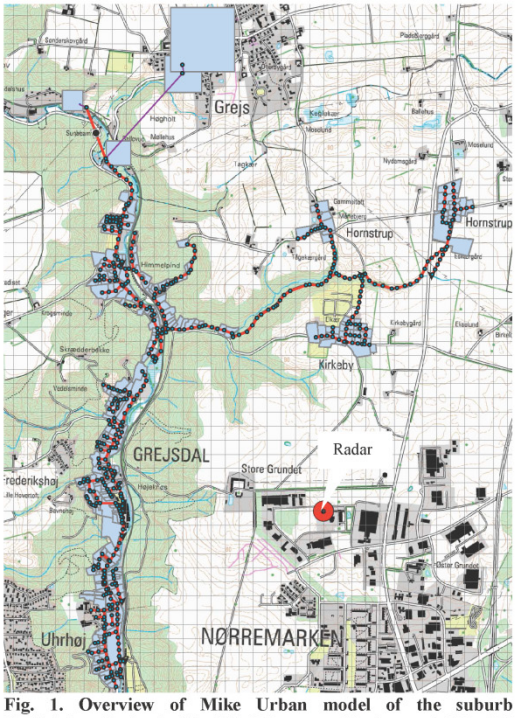

Fig. 1. Overview of Mike Urban model of the suburb Grejsdalen. Each pixel is 100x100 meter. The image is 3 by 7.5 km.

The radar used is a DHI Local Area Weather Radar (LAWR-25) X-band radar capable of measuring in very fine resolution from 500x500 meter pixel sizes and down to 100x100 meter. The temporal resolution of the radar is 5 min.

Besides the radar the municipality have two normal rain gauges operated by the Danish Meteorological Institute. The gauge stations are situated south and south east of the area shown on Fig. 1. Data from the gauges and the LAWR are both used in the analysis.

2 Method

The radar reflectivity has been calibrated against the rain-gauge nearest to the model area. Simulation has been performed using the rain-gauges individually and each of the radar resolutions. Since the model assigns rain-gauges on a proximity basis, the placement of the gauges in Vejle will not allow both gauges to be active in one simulation.

The Mike Urban model treats each radar pixel as an individual rain gauge and thereby as an individual boundary. Sub-catchments are connected to the pixel which centre coordinate is closest to the sub-catchments centre coordinate. If the catchments area is larger than one pixel only the pixel value closes to the catchments centre is applied. If a model consists of few large simplified catchments there is no benefit in using highly distributed data since the information is not used by the model.

A 7 day period from 15th to 22nd of May has been selected for use in this study since there fell 50 mm of rain in this one week period distributed on 4 events. In the Grejs Å area some CSO's are recorded automatically. The simulated discharges of the CSO's are compared to these.

3 Results

In order to verify the calibration the total rainfall recorded by the gauge and the corresponding two radar pixels are listed below in table 1.

Table 1. Rainfall in the period 15th to 22nd of May 2006

	Accumulated rainfall [mm]	Total Surface Runoff [m^3]
Rain Gauge Vejle Treatment Plant (WWTP)	50	10,600
Pixel no. (118,127)-500x500 meter resolution	51	10,800
Pixel no. (138,184)-100x100 meter resolution	47	10,100

The calibration results are satisfactory, and the small difference is due to the fact that the radar measures over the rainfall average over a surface. In situations with light precipitation the average value detected may not exceed a given threshold value and in these cases the precipitation is set equal to zero.

On Fig. 2 simulated run-off are shown as a function of rainfall measurement type.

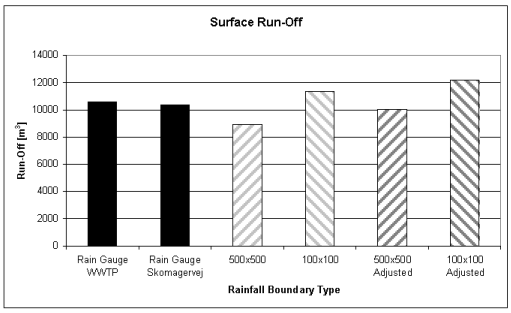

Fig. 2 Simulated surface run-off on basis of different rainfall measurement type. The adjusted data are using a reduced number of pixels.

Surprisingly, simulation based on radar input is less than on rain gauge basis. This is due to one of the major pitfall in using high resolution data – applying the radar data uncritical. In the vicinity of the radar it is not capable of detecting rain due to physical circumstances related to clutter. In these cases no run-off are generated from the influenced catchments. After sorting out the influenced pixels the run-off is increased to the expected level as show on Fig. 2 (marked adjusted). The simulation with 500x500 meter pixels applies a total number of 25 rainfall boundaries, when using 100x100 meter pixels a total number of 124 boundaries are applied.

The difference in run-off based on the two different radar resolutions is due to averring: in a 500 x 500 meter pixel the average value must exceed the noise level in order to be accepted as rain. Looking at the same pixel in 100x100 meter a fraction of the 25 pixels may indeed hold values exceeding the noise level and thus generating run-off.

The topography of the area causes increased rainfall on the hills while the lower part of the city receives less rain. Since the gauges both are located in the lower part they tend to underestimate the rainfall. The distribution of accumulated rainfall based on radar measurements is shown on Fig. 3.

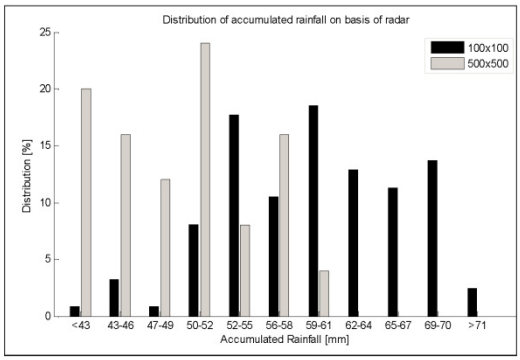

Fig. 3 The distribution of accumulated rainfall on basis of radar. For the 500x500 meter resolution is the mean rainfall 49 mm and correspondingly 60 mm for the 100x100 meter resolution.

Fig. 3 shows how distributed rainfall can be within an area of 2,250 hectares, and thereby indicates how random it is to use a single gauge (pixel) to represent the rainfall over a large area. From Jensen and Pedersen (2005) it is known that there can be more than 100 % difference in accumulated rainfall between two gauges less than 200 meters apart. If a drainage model consist of few simplified catchments representing large areas there is a great risk of either over estimating or underestimating the true run-off due to the fact that the model only apply one rainfall time series pr. catchment. This is one of the major pitfalls in using distributed rainfall data, since there is no gain in increasing the spatial distribution of the input data if the spatial resolution of the model data is of a much coarser scale since the information is not used by the model.

An example of this issue can be seen on Fig. 4 where the CSO's from a weir where all the upstream area is modeled as one single catchment are shown.

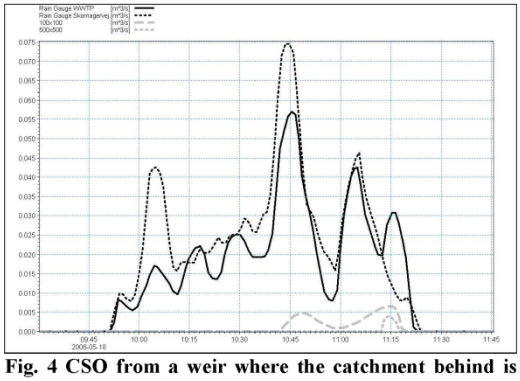

Fig. 4 CSO from a weir where the catchment behind is modeled as one simplified catchment.

As illustrated on Fig. 4 the CSO is varying very much depending on the type of rainfall used. Even with use of the two different radar resolutions there are significant differences which are caused by the fact that only one boundary time series is applied to the catchment.

If the effect of applying spatial distributed data are analysed in relation to CSO's the data in this case is a bit sparse. This is due to the fact that only two of the recordings of the CSO's in the model area were useable, and they were all of minor size e.g. less than 100 l/s for a few hours.

An example of a comparison can be seen on Fig. 5, where the model is doing a bad replication since none of the simulations are close to the measured CSO. The can have several reasons. First of all the model has been reduced in order to obtain a sub-model. In that relation the outflow has been set to a free outlet, which can cause the model to have a better capacity than it actually does and thereby not reacting correct in relation to CSO. Secondly the model is calibrated with use of rain gauges years ago, and since then the system has changed significantly both in physical geometry and in catchment characteristics.

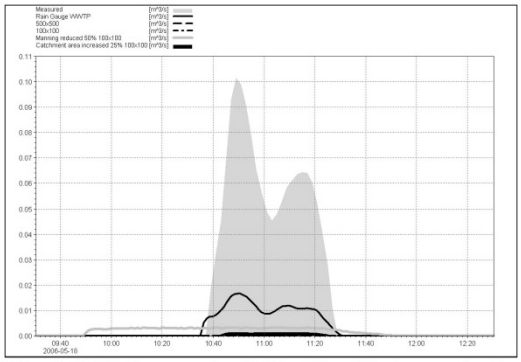

Fig. 5 CSO from weir OF34. The filled area is the measured CSO, while the lines are CSO based on simulations

To illustrate the consequences of manipulating with the normal calibration parameters all the areas has been increased with 25 % and simulated with 100x100 meter radar data. This causes some CSO, but not nearly in the range of what has been measured. Another common factor is to tweak the Manning number and here it was general reduced with 50%. This also causes some CSO but again not nearly in the order of the measured.

Since this paper is not about model calibration no further steps has been taken in order to tune the model to fit the measured data. But it should be stressed that when shifting from using point measurements to spatial distributed data a recalibration of the model is highly recommended. When applying distributed data the system is reacting by having a larger capacity than when applying point measured rain due to the fact that peak intensities are not applied to the whole catchment simultaneously.

4 Conclusions

Some of the most crucial elements to determine are how the urban drainage model handle distributed data. Since these models normally acquire their rainfall information from one or a few rain-gauges inside or in the vicinity of the model area, the delineation of sub-catchments boundaries inside the model area has not been very crucial, since the same "mean area precipitation" has been applied to the entire model area. Switching to distributed will in such cases have little or no effect if the sub-catchments do not have a similar spatial resolution as the radar rainfall data.

In Pedersen et al. (2005) an experiment using relocated radar rainfall on a small urban area indicated a significant dependency on the rainfall resolution. The results found here confirm this experiment.

When applying rainfall data measured by weather radar some of the temporal resolution is lost due to the fact that the intensity is an average intensity of 5 minutes. This means that there is a risk of losing some of the peak intensities and thereby causing some trouble in modeling the small CSO of short duration.

Acknowledgements: The authors would like to thank the Municipality of Vejle for the loan of the Mike Urban model and the data.

References

Pedersen, L., 2004: Scaling Properties of Precipitation – experimental study using weather radar and rain gauges. *M.Sc. Thesis from Aalborg University (can be downloaded from www.exigo.dk)*.

Pedersen, L; N. E. Jensen, M. G. Nicolajsen, M. Rasmussen, 2005: Urban run-off volumes dependency on rainfall measurement method - Scaling properties of precipitation within a 2x2 km radar pixel, Paper presented at the 10th International Conference on Urban Drainage, Copenhagen, Denmark, August 21-26, 2005

Jensen, N. E., L. Pedersen, 2005: Spatial variability of rainfall: Variations within a single radar pixel, Atmospheric Research 77, p. 269-277

PAPER E

Return Period for Radar Rainfall – Spatial Validity of Return Period

Conference Proceedings: *7th International Workshop on Precipitation in Urban Areas*, 7-10 December 2006, St. Moritz, Switzerland. (Oral Presentation)

7th INTERNATIONAL WORKSHOP on PRECIPITATION IN URBAN AREAS
Extreme Precipitation, Multisource Data Measurement and Uncertainty
7-10 December, 2006, St. Moritz, Switzerland

RETURN PERIOD FOR RADAR RAINFALL - SPATIAL VALIDITY OF RETURN PERIOD

by

L. Pedersen[(1+2)], N. E. Jensen[(1)], H. Madsen[(2)]

[(1)] *DHI Water & Environment, Gustav Wieds Vej 10, 8000 Aarhus, Denmark (lpe@dhigroup.com, nej@dhigroup.com)*

[(2)] *Institute for Informatics and Mathematical Modelling, Technical University, Copenhagen, Denmark (hm@imm.dtu.dk)*

ABSTRACT

In traditional urban run-off design, a politically selected return period for rainfall is used to select the combination of intensity and duration for which a given hydraulic structure must be designed.

As rainfall measurements are now being measured using high resolution radars like the LAWR (Local Area Weather Radar) the estimation of return period becomes more complicated. Using the findings of Jensen and Pedersen (2005) it is reasonable to assume that for any one-year-event, measured with a conventional rain-gauge, there may be a 2 or more year event somewhere in the immediate vicinity. Furthermore, the "point measurement" of the rain gauge may lead to one return period while the corresponding 100 x 100 m radar recording for the same point may represent a different period.

This paper presents the preliminary findings of return periods determined by the use of rain gauge and radar rainfall data and discusses the validity of a return period in context with the spatial distribution of rainfall and implication in terms of design criteria.

Keywords: radar, return period, design criteria, urban hydrology, X-band, variability, precipitation

1 INTRODUCTION

This paper contains the first preliminary results determining the return periods on the basis of rainfall measurements with an X-band radar of the type Local Area Weather Radar (LAWR). The return period of a rain event is often of great interest in relation to design and analysis of urban drainage systems. Urban drainage systems in Denmark have been and still are being designed on the basis of a politically selected return period based on rain gauge measurements. The return period is defined as the number of years between the occurrence of a given combination of duration and intensity of rainfall.

In Denmark rainfall data from rain gauges has been recorded since 1933, and since 1979 the Danish Meteorological Institute (DMI) and the Danish Waste Water Committee (SVK) have operated a large number of automatical high resolution rain gauges in more than 40 cities. Based on the recorded data the statistical properties of the rainfall were analysed by Mikkelsen et. al (1996) where, among other things, the return periods of mean maximum intensities were analysed in relation to extreme value statistics.

The findings in Mikkelsen et. al (1996) are all based on point measurements from rain gauges. Since rainfall is a spatially distributed dynamic phenomenon, a point measurement can be a very uncertain representation as discussed in Jensen and Pedersen (2005), where the accumulated rainfall of individual events was observed to vary by more than 100% within 200 metres. With such a large variation it seems reasonable to assume that a single event can yield many different return periods. In relation to deciding whether damages caused by rain were exceeding the design criteria or not, it becomes far more complicated since the rain may contain several different return periods depending on the location of the gauge.

As rainfall measured by radar has now been going on for some years, the available data are becoming still more interesting in relation to an analysis of the return periods based on radar data. Rainfall has been recorded with a range of radar types from S-Band and C-Band radars mainly operated by the meteorological services around the world to X-band radars. C and S-band radars have the advantage of very long range and thereby coverage of large areas. On the downside their spatial resolution are quite coarse, and normally they do not scan continuously. X-band radars, on the other hand, are capable of very fine spatial and temporal

7th INTERNATIONAL WORKSHOP on PRECIPITATION IN URBAN AREAS
Extreme Precipitation, Multisource Data Measurement and Uncertainty
7-10 December, 2006, St. Moritz, Switzerland

resolution and they scan continuously, but normally operate at ranges less than 60 km. Estimation of return periods based on radar data are complicated by the fact that the data processing must be done on a vast quantity of data. On top data are usually corrupted by all sorts of non rainfall detections, e.g. birds, airplanes, clutter, bright band etc., which have to be removed prior to estimation [Koistinen, 2006].

2 METHOD

At time of writing 15 LAWRs are installed and operating around the world. The radar which has operated for the longest period of time is the LAWR at Aarhus, Denmark, which has been in operation since 1999. Due to the large quantity of data the results presented here are the preliminary findings based on data recorded by the Aarhus LAWR from the four summer months June, July, August and September of 2005 and 2006. Since only rain is of interest in relation to return period for use in urban drainage context, the periods with potential snowfall is omitted.

2.1 Data

The LAWR is capable of measuring with spatial resolutions ranging from 500x500 metres down to 100x100 metres, and with these resolutions there are ~50,000 and ~78,000 individual pixels respectively. Each pixel is regarded as an individual observation. For comparison data from the tipping bucket rain gauge at "Egå Renseanlæg" operated by the Danish Meteorological Institute are included in the analysis.

2.2 Method for determining return periods

For each individual pixels the maximum mean intensity of 5, 10, 30 and 60 minutes is determined for every time step. The maximum mean intensity over a given period is the maximum intensity value after a moving average filter of the selected period, e.g. 10 minutes, has been applied. Since only a total of 8 months of data are analysed it does not make sense to rank the located maximum intensities in order to determine the return period (T). Instead the maximum mean intensities are related to a return period based on the relations shown in Figure 1. The figure shows the relation between return period and intensity modelled with a PDS model (Partial Duration Series Model) with Generalized Pareto distributed exceedings based on three model parameters for characterizing extreme events over a certain threshold level [Mikkelsen et. al., 1996].

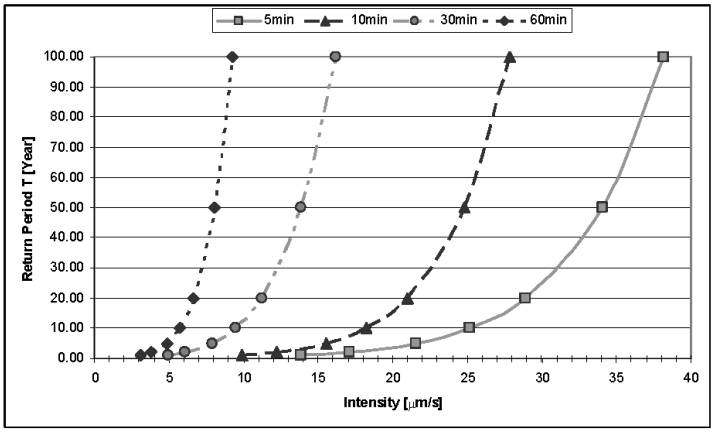

Figure 1 – T-year estimates based on subregion "Denmark outside Copenhagen" for 4 different intensities as function of intensity. Adapted from Mikkelsen et. al (1996).

7th INTERNATIONAL WORKSHOP on PRECIPITATION IN URBAN AREAS
Extreme Precipitation, Multisource Data Measurement and Uncertainty
7-10 December, 2006, St. Moritz, Switzerland

3 RESULTS

One of the challenges is to choose the appropriate way to present the results since the quantity of data are tremendous. To illustrate the large variability in return periods and the dependency on time window used, a 33 by 33 pixel subsection (16.5x16.5 km) of the total radar image is shown. The event illustrated is from 3rd and 4th June 2005. Only return periods larger than ½ year have been plotted.

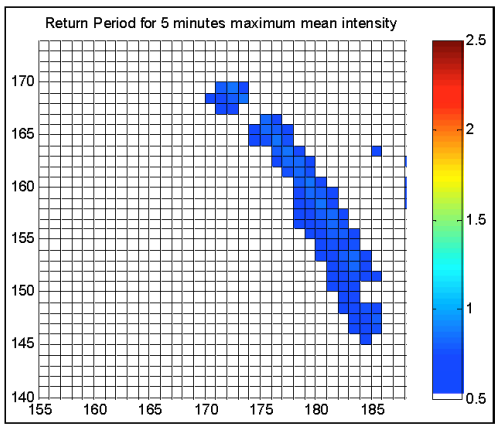

Figure 2 – T-year estimate for 5 minute maximum mean intensity.

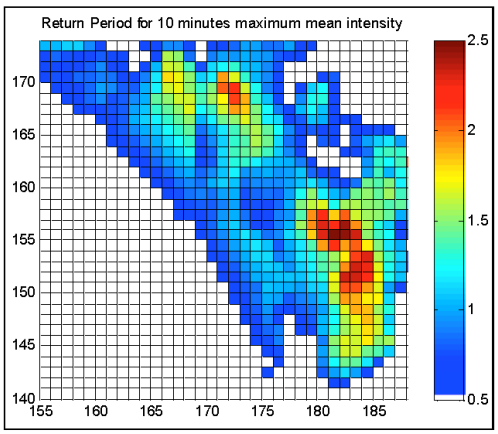

Figure 3 – T-year estimate for 10 minute maximum mean intensity.

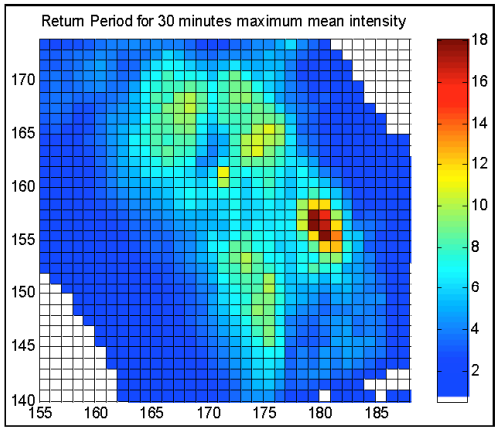

Figure 4 – T-year estimate for 30 minute maximum mean intensity.

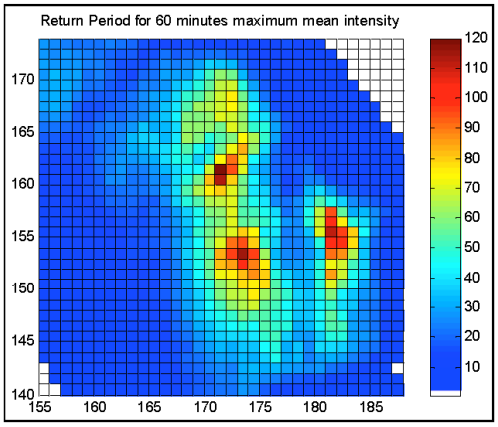

Figure 5 – T-year estimate for 60 minute maximum mean intensity.

The variability is much larger for the return periods based on 60 minutes' mean maximum intensity than for those based on 5 minutes. This indicates that the rain event is dominated by long duration, relatively widespread rainfall (the event lasted 3.2 hours with a accumulated value of 10.2 mm recorded at the official DMI rain-gauge west of the area shown on fig 4 (pixel 123, 146)). The return period for the rain gauge station was less than one year.

Similarly to the findings of [Koistinen, 2006] very high return periods were found, indicating that a return period determined on the basis of rain gauge data is higher that those determined on the basis of radar measurements.

One of the common properties of the maps is that the area having high return period is quite small. The +100 year return period recorded here has a spatial extent of 1-2 km.

The histogram of the return periods from Figure 5 is shown on Figure 6.

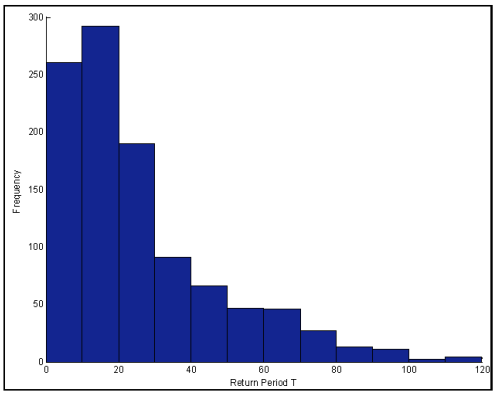

Figure 6 – Histogram of the return periods based on 60 minutes' mean maximum intensity

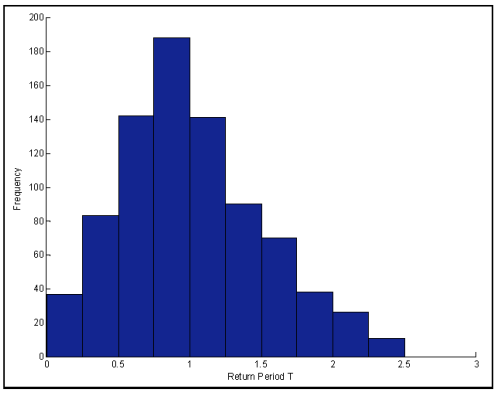

Figure 7 – Histogram of the return periods based on 10 minutes' mean maximum intensity

The shape of the histogram is varying depending on the time window used. The 60 and 30 minutes' window both have the same shape as on Figure 6, while the histogram on Figure 7 are clearly bell shaped. Due to the limited data it is not possible to draw any final conclusions on this issue, however, it will be further analysed in the future work.

4 CONCLUSION AND DISCUSSION

Establishing an N-year return period based on sparse point measurement may lead to an underestimation of the magnitude of the N-year intensity and duration. In this event less that 0.02% of the area monitored by the radar experienced a precipitation having a return period of more that 100 years.

Return periods are used to select the combination of duration and intensity which a given storm sewer system must be able to accommodate. Figures 2 to 5 indicate the existence of a spatial correlation in data. This suggests that a characteristic "catchment space length" should be included in the selection of return period.

In order to compare return period determined on the basis of rain gauge and radar measurement respectively, the next step is to establish the number of independent observations in the radar images.

The plot of the spatial return periods clearly illustrates the uncertainties in using point measurements of rainfall if short individual rain events are considered. Depending on the pixel the return period varies from less than ½ year to 118 years within a relatively small area of 16.5x16.5 km which is in the scale of hydrological catchments.

5 REFERENCES

Koistinen, J., T. Kuitunen and M. Inkinen, (2006) Area-In.tensity probability distributions of rainfall based a large sample of radar data, Proceeding of ERAD 2006, Barcelona, Spain

Jensen, N. E., L. Pedersen, (2005) Spatial Variability of rainfall: Variations within a single radar pixel, *Atmospheric Research* 77, 2005: 269-277.

Mikkelsen, P. S, H. Madsen, K. Arnbjerg-Nielsen, H. K. Jørgensen, D. Rosbjerg and P. Harremöes, (1996) Regional variation af ekstrem regn i Danmark, Spildevandskomiteens skrift 26, Ingeniørforeningen Danmark.

PAPER F

Extreme Rainfall Statistics Based on Rain Gauges and Radar

Conference Proceedings: *International Symposium Weather Radar and Hydrology (WRaH 2008)*, 10-12 March 2008, Grenoble, France. (Poster)

Extreme rainfall statistics based on rain gauges and radar measurements

Lisbeth Pedersen[1,2], Niels Einar Jensen[1] and Henrik Madsen[2]

[1] DHI, Aarhus (Denmark)
[2] Department of Informatics and Mathematical Modelling, Technical University of Denmark (Denmark).

1. Introduction

Flooding incidents caused by extreme rainfall events often have significant financial and sociological costs both for the people affected directly and for the community as a whole. Since rainfall and especially convective rainfall often has a limited spatial and temporal extent, it can be extremely difficult to get a representative recording of the event when only a few gauges are present. Einfalt et al. (2005) reports based on radar observations that the spatial extent of heavy rainfall in several cases in northwest Germany was less than 15 km^2 and the maximum of the event was not observed by the rain gauge network in the area. The combination of limited spatial extent and high temporal variability of convective rainfall makes it unlikely that a single gauge or a sparse network of gauges is able to sample a representative estimate of an extreme event.

A common way to establish the level of extreme of a given event is to determine the statistical return period of the intensity over a range of time frames. The return period of a given intensity is important, since it is one of the basis components of sewer system design. Up till now extreme value rainfall statistics have been based on rain gauge measurements, however, since a gauge only represents a few hundred square centimetres, the extreme value statistics obtained for this small area may not be representative for the whole catchment. To illustrate the problem and investigate the prospects of using Local Area Weather Radar (LAWR) for determining distributed return periods a series of thunder showers occurring on 22nd of August 2007 have benn analysed.

2. Analysed data

The event occurred on 22nd August 2007 over the southern part of Denmark. The event characteristics are listed in Table 1. It caused flooded streets and basements in the city of Kolding (5*) due to overloading of the sewer system. The extent of the area being analysed is show in Fig. 1 along with a single radar image.

Fig. 1 Area of interest. The circle is the maximum range of the Vejle LAWR (60 km). Rain gauges are marked with * and the LAWR with #.

There are five official rain gauges (tipping bucket - 0.2 mm resolution) in the area, all operated by the Danish Meteorological Institute (Bødtker, 2003).

Table 1. Event characteristics for 22nd August 2007

	Gauge	Start time	Duration [min]	Rain Depth [mm]
1	Horsens	22:52	284	20.8
2	Vejle I	22:13	262	32.2
3	Vejle II	22:05	258	35
4	Fredericia	22:52	284	20.8
5	Kolding	22:13	262	32.2

The area considered in the analysis is 11,310 km^2 corresponding to the radar coverage at maximum range, cf. Table 3. The area spanned by the rain gauges is smaller with the largest inter-distance being 48 km, cf. Table 2. The two Vejle gauges are located only 3.5 km apart and very close to the LAWR.

Table 2. Distance between gauges and LAWR in km.

	LAWR	Horsens	Vejle I	Vejle II	Fredericia	Kolding
LAWR	-					
Horsens	23	-				
Vejle I	3.5	26	-			
Vejle II	6	26	3.5	-		
Fredericia	22	36	20	17	-	
Kolding	29	48	26	23	13	-

The LAWR used in the study is owned and operated by the Municipality of Vejle and has the specifications listed in Table 3. The LAWR is equipped with attenuation correction, volume correction and is calibrated on the basis of the Vejle I gauge. Normally, the outer limit for QPE is 20 km due to risk of overestimation at further ranges due to the volume correction method. In this study data from the full range of 60 km has been used, but special care has been taken in order to minimize the uncertainties.

Table 3. Specifications of the Vejle LAWR.

	LAWR 25 kW
Wave length	X-band, 3.2 cm
Antenna	8 ft slotted waveguide array
Receiver	Logarithmic receiver
Vertical opening angle	± 10°
Horizontal Opening Angle	0.95°
Range	60 km
Spatial resolution	500x500/250x250/100x100
Temporal resolution	1 minute
Scanning strategy	Single layer and continuous scanning

3. Determination of return periods

The return periods for the 5 gauges are shown in Fig. 2. If only the data from the five gauges each measuring over a few hundred sq. centimetres is considered, the two gauges in Vejle have observed the most extreme rain.

The return periods estimated on basis of the Kolding gauge are not nearly as high and still the city of Kolding was affected the most. If the radar animation of the event is taken into consideration it can be seen that the event is not continuous rainfall, but a series of convective cells forming and vanishing in a band of 2-20 km in width, cf. Fig. 1. The majority of the event bypassed both the Kolding and the Fredericia gauge. The Kolding gauge is situated south of Kolding at the Waste Water Treatment Plant and did not observe the heavy rainfall that fell over the city.

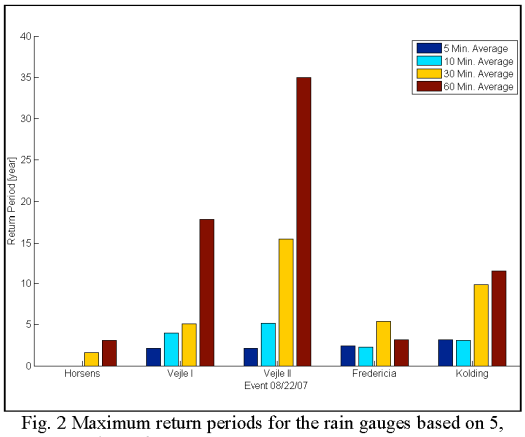

Fig. 2 Maximum return periods for the rain gauges based on 5, 10, 30 and 60 minutes average.

The relation between an average intensity and the corresponding return period in Fig. 2 is a result statistical analysis of many years of data from the Danish rain gauge network (e.g. Arnbjerg-Nielsen et al, 1996).

Since the number of years with LAWR data is limited it is still not possible to determine the return periods based on ranking the data. Instead the individual radar pixels have been assumed independent observations and equivalent to a rain gauge.

The intensities for each pixel over 5, 10, 30 and 60 minute average has been determined and the corresponding return period calculated. The maximum return periods exceeding 1 year for the event based on 57,600 radar pixels can be seen on Fig. 3 for the radar coverage area of 120x120 km. None of the calculated return periods for the 5 minute average exceeded one year and is therefore not shown.

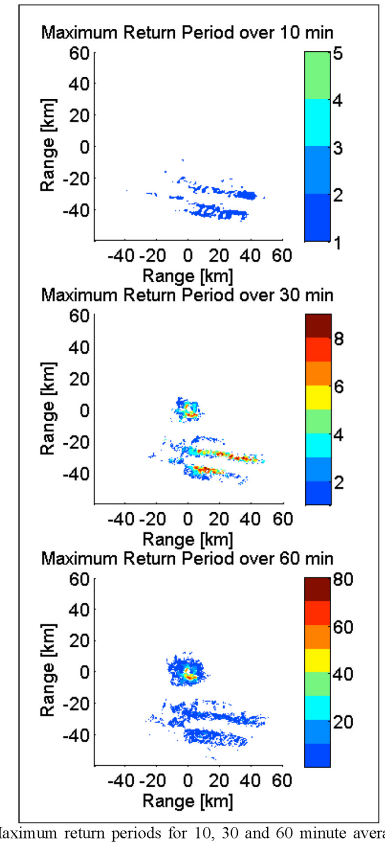

Fig. 3 Maximum return periods for 10, 30 and 60 minute average for the event of 22nd of August 2007 shown for the full 60 km range.

It should be noted that the return periods of the radar data seldom will yield the same high peak values as those found on basis of a rain gauge since the radar intensity is based of an average over both time and volume. Further more this effect will be increasing with range due to the volume increases rapidly with range, cf. the beam parameters in Table 3. This is seen on Fig. 3 where the high return periods only are found close to the radar.

The maximum return period for the radar pixels located over the 5 rain gauges is shown on Fig. 4. The overall pattern consist with that of Fig. 2, but the return period for the 60 minute average based on radar data is much higher for Vejle I than for Vejle II, which is opposite of those of Fig. 2.

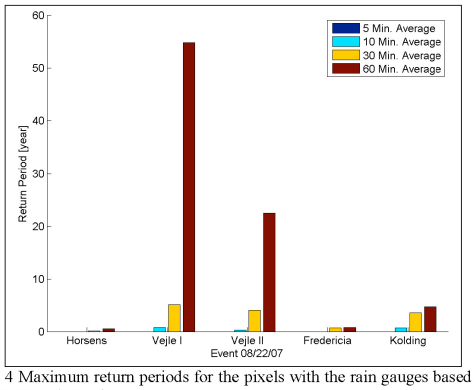

Fig. 4 Maximum return periods for the pixels with the rain gauges based on 5, 10, 30 and 60 minutes average.

If the return periods of a 5x5 km area around the rain gauges is taken into account it becomes evident that the variability of the return periods is very large. The return periods within a 5x5 km area around each of the two Vejle Gauges in Fig. 5 show large variability in the determined return periods. Within a distance less than 2 km the return period is varying from <10 year to more than 70 years. Both areas are very close to the radar so the sample volume is therefore very small. This means that there in this case is no problem with partial beam filling and the thereby following risk of underestimation.

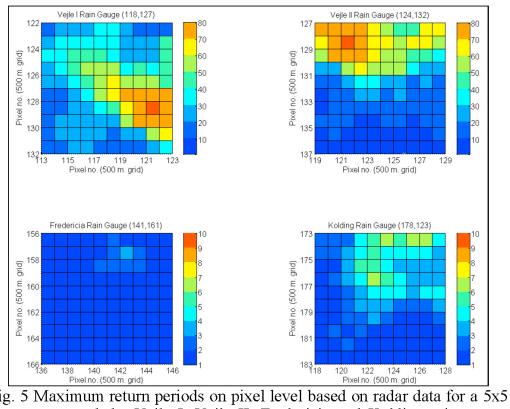

Fig. 5 Maximum return periods on pixel level based on radar data for a 5x5 km area around the Vejle I, Vejle II, Fredericia and Kolding rain gauge. (The radar is located at pixel 120,120)

On Fig. 3 there is a large area south – southeast of the radar with return periods exceeding 1 year. If the area is enlarged the spatial structure of the rainfall becomes evident. Unfortunately this area is up to 50 km away from the LAWR which normally is considered to far away for quantitative measurements, but the data is quite interesting and the Vejle LAWR is the closets radar. The spatial extent of the return periods seems to be in the same order as those found close to the radar, cf. Fig. 5.

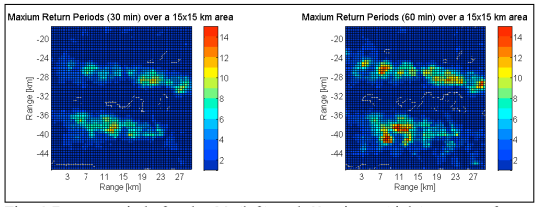

Fig. 6 Return periods for the 30 (left) and 60 minute (right) average for a 15x15 km area south east of the radar.

The return periods on Fig. 6 are ranging from 1 to 15 years, but due to the long range (> 20 km) the uncertainty of the estimate is very large. The spatial structure of the event is well observed by the LAWR even at this very long range.

4. Conclusions and future work

The event of 22nd of August 2007 was observed by 5 rain gauges within the Vejle LAWR coverage area. The statistical return period of the event based on rain gauge data was found to vary significantly. The Vejle I and Vejle II gauges is located less than 4 km apart and the return period for 60 minutes average was estimated to be 18 and 35 year respectively. If the LAWR data is taken into account it can be concluded that within a 2 km from the gauge a return periods ranging from 1 year to more than 70 years could be found. This indicates that within a small area of 5x5 km the return periods can vary in significantly.

Based on these data it can be concluded to be very uncertain to determine the statistical return period of a rain event based on a single, or as in this case on a few gauges. This is due to the large variability of the rainfall which also is found in the return periods – even when averring over 60 minutes. This is important since the performance of sewer systems normally is evaluated based on rainfall observed by a single or few gauges.

The spatial extent of return periods exceeding a given level seems to be of a limited area – in the order of a few kilometres. This needs to be examined further but is of great interest since the design and placement of local water retention facilities in the future can be optimized if the return periods can be coupled to a spatial extent.

These conclusions are based on a very sparse analysis. A much larger dataset is required to make any final conclusions and new design criteria's. The future work includes development of framework and methods for determining return periods based on large LAWR data sets.

References

*Arnbjerg-Nielsen, K.., Harremöes, P. Spliid, H., 1996: Interpretation of regional variation extreme values of point precipitation in Denmark, Amospheric Research **42** (1996) ,99 - 111.*

Bødtker, E. 2003: Observation Systems 2003, Technical Report 03-06, Danish Meteorological Institute

Einfalt, T., Jessen, M. and Mehlig, B ,2005: "Comparison of radar and raingauge measurements during heavy rainfall" Water Science and Technology, Vol 51, 2, 195-201

Thomsen, R,. S. 2007 Drift af Spildevandskomitéens Regnmålersystem Årsnotat 2006 no. 07-03

PAPER G

Assessment of QPE Results from 4 kW X-band Local Area Weather Radar (LAWR) Evaluated with S-band Radar Data

---

Conference Proceedings: *Fifth European Conference on Radar in Meteorology and Hydrology (ERAD08)*, June 30 - July 4, 2008, Helsinki, Finland. (Oral Presentation)

ERAD 2008 - THE FIFTH EUROPEAN CONFERENCE ON RADAR IN METEOROLOGY AND HYDROLOGY

Assessment of QPE results from 4 kW X-band Local Area Weather Radar (LAWR) evaluated with S-band radar data

Lisbeth Pedersen[1+3], Isztar. Zawadzki[2] , Niels Einar Jensen[1] and Henrik Madsen[3],
(1) DHI, (2) McGill University, (3) Technical University Denmark

1. Introduction

The Local Area Weather Radar (LAWR) is an X-band weather radar developed for quantitative precipitation measurements (QPE) and forecast (QPF) in connection with urban areas by DHI. The first radar was installed in 1998 and since then more than 23 radars have been installed worldwide.

The number one question is always how precise is a LAWR? Up till now this has been evaluated on the basis of LAWR-gauge comparison which is normally the only method for evaluating QPE results. The issue with this type of evaluation is that in principle it is a comparison of two very different measurements of the rain. A LAWR is measuring the backscattered energy from rain drops in a volume ranging from 0.1-700 m^3 up in the air, whereas a tipping bucket gauge is sampling the rain at ground over a surface of a few hundred cm^2. Field experiments have shown up to ~100 % variation in rain depths sampled with rain gauges within a distance of less than 200 meters [Pedersen et al., 2008].

In order to seek a better assessment of the LAWR's performance a field experiment was conducted during the months of October to December 2007. The main purpose of the experiment was to assess the performance of an experimental 4 kW LAWR by comparison with an S-band radar.

The experiment took place at the J. S. Marshall Radar Observatory where a 4 kW LAWR was temporarily installed less than 50 meters from the McGill S-band radar. The research and development of the LAWR is primarily carried out in Denmark, where there are no S-band radars, so this setup offered some new unique opportunities in the LAWR research.

The challenge is that the two systems differs on a range of parameters, e.g. sampling frequency, timing, range, bin size, horizontal and vertical opening angles, number of PPIs, wave length etc.

In the following the first result of this setup will be presented with focus on assessing the performance of the LAWR.

2. Experimental setup

The LAWR is based on a marine X-band radar which makes it a cost-efficient and robust solution, however, the price is a rapidly increasing beam volume due to a large vertical opening angle. The LAWR used in this study is a down-scaled version of the standard LAWR, cf. Table 1. The two LAWR types use the same AD converter, software and signal processing algorithms, however, the city-LAWR has a 4 times larger opening angle and 5 times less power than the standard LAWR. LAWR will be used throughout this paper for describing the 4 kW LAWR.

Corresponding address: Lisbeth Pedersen, DHI & DTU, lpe@dhigroup.com

Table 1 Specifications of the radars used in the setup. The specifications for the standard 25 kW LAWR is shown in grey for comparison.

	McGill	City-LAWR	LAWR
Peak Power	700 kW	4 kW	25 kW
Wave length	S-band 10.7 cm	X-band 3.2 cm	X-band 3.2 cm
Pulse length	1 µs	0.8 µs	1.2 µs
Antenna	9 m Dish	61 cm radome	2.5 m slotted waveguide array
Receiver	Linear receiver	Logarithmic receiver	Logarithmic receiver
Vertical opening angle Horizontal opening angle	0.89°	± 10° 3.9°	± 10° 0.95°
Range (forecast/QPE)	240/240	30/15 km	60/20 km
Spatial resolution	1x1 km	250x250 m 125x125 m 50x50 m	500x500 m 250x250 m 100x100 m
Temporal resolution	5 minutes	1 or 5 minutes	1 or 5 minute
Scanning strategy	24 PPI regular scanning strategy	Single layer and continuous scanning	Single layer and continuous scanning

The most significant difference of the two radars is their physical size as attempted illustrated below in Figure 1.

Figure 1 LAWR installed on the roof of the J.S. Marshal Radar Observatory next to the McGill S-band radar. Close up of the LAWR antenna unit on the right. The red circle shows the location of the LAWR.

The coverage area of the LAWR in relation to Montreal is illustrated on Figure 2 along with the placement of rain gauges within app. 15 km range from the LAWR.

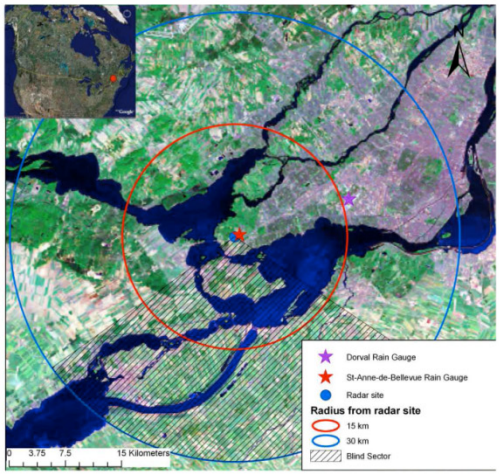

Figure 2 Coverage of the LAWR over Montreal and area. The hatched area is the blinded sector.

The LAWR was in operation from 10th October to 15th November with some interruptions due to testing of other research equipment at the site using the same frequency. During the period a number of rainfall events were captured with both systems. The events selected for further analysis is listed in Table 2. During the events I-III a sector ranging from azimuth 110 to 120 was blanked out on the LAWR due to other experiments.

Table 2 Events selected for further data processing

Event No.	Date	App. time (UTC)	Description	Max. intensity
I	19-20 Oct.	16:00-06:00	Heavy rain (squall line)	>50 mm/h
II	23 Oct.	06:00-24:00	Widespread rain	< 7 mm/h
III	27 Oct	02:00-24:00	Light widespread rain	< 7 mm/h
IV	6 Nov.	02:00-13:00	Widespread rain with cells of higher intensity	> 16 mm/h

In addition rain gauge data from the gauges St-Anne-de-Bellevue and Dorval from the Mesonet-Montreal has been collected for the four events. Unfortunately, the communication system of the mesonet was disrupted by lightning the 19-20 of October and therefore no data is available for this event. For odd reasons they are also missing for Event IV, which means that only Event I and II are supplemented by rain gauge data.

3. Basic adjustment of LAWR

The orientation of the radar is of uttermost importance and is far form trivia in the case of a LAWR. The normal approach of using the sun is not possible due to the antenna design and therefore is it necessary to orientate by use of ground clutter. Large buildings and dense city areas are normally used. If a power plant is present it is excellent due to steady transmission of vapor. The LAWR was initially orientated by use a compass and verified by the ground clutter. Later on in the data analysis it became evident that the LAWR was not orientated correctly and there were an offset of 1.5 km in the data. This in combination with the incorrect orientation caused some very strange initial results when LAWR-gauge comparison and radar-LAWR was compared. Eventually spatial matching between the two radars was done satisfactory.

3.1 Automatic Gain Control analysis

The signal used for QPE in the LAWR system is the raw video signal from the marine radar and one of the issues of interest was to determine if the automatic gain control function was acting an autonomous way and affecting the data.

An area with well know clutter was selected (1.5 to 2.4 km range in azimuth 56-65). The mean reflectivity of this area was calculated along with the mean of the full area (range 1.5 to 20 km) for complete dry days in order to establish a reference level of the clutter area. As shown on Figure 3 the mean reflectivity of the clutter area is relatively stable and the overall mean is very close to zero and stable. The fluctuations of the mean reflectivity over the clutter field are due to temperature changes in the air over the day.

If the automatic gain control was active it would turn down as soon as rain became within range. This is not the case as shown on Figure 4 marked with the blue arrows. The overall mean increases around 18:00 as rain is detected in the western part within the 20 km range, but the mean of the clutter field is not affected. When the area with clutter is affected by rain the mean level raises accordingly. It can therefore be concluded that the automatic gain control is properly disabled.

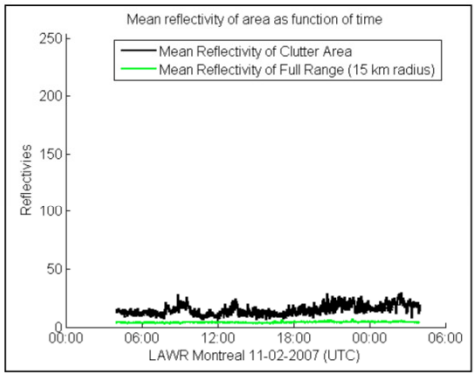

Figure 3 Mean reflectivity of area with clutter (black) compared with mean reflectivity of full range (15 km) (green) on a dry day.

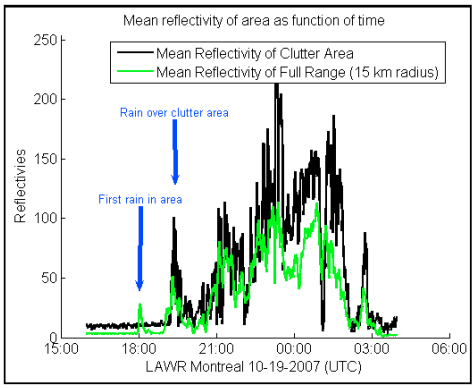

Figure 4 Mean reflectivity of area with clutter (black) compared with mean reflectivity of full range (15 km) (green) on a day with rain

4. Calibration

The LAWR is normally calibrated on the basis of traditional tipping bucket gauges (0.2 mm). The traditional radar calibration approach of using a Z-R relation is not used since a linear relationship between the accumulated rain depth in mm and the accumulated amount of reflectivity from the LAWR has been established experimentally [Jensen and Pedersen, 2004]. It is based on the ratio between the accumulated rainfall in mm and the accumulated reflectivities from the pixel over the gauge on individual rainfall event basis.

4.1 LAWR –Gauge calibration

It has not been possible to obtain a LAWR-gauge calibration in this setup due to fact that only two events were sampled with both gauge and LAWR and experience show that at least a couple of months data is required in order to obtain a stable calibration factor. Furthermore was the two available events dominated by light widespread rain which is not observed well by the LAWR due to the large vertical beam.

The large opening angles results in a large sampling volume at the 16 km range where the Dorval rain gauge is located. The radar pulse volume is calculated for the two radars in question using the sample volume equation [Rinehart, 2004]:

$$V = \frac{\pi \cdot r^2 \cdot \theta \cdot \varphi \cdot h}{16 \cdot \ln(2)} \qquad \text{eq. 1}$$

With the values listed in Table 1 the sample volume at 16 km range is 0.005 km^3 for the S-band, 0.079 km^3 for the 25 kW LAWR and 0.207 km^3 for the 4 kW LAWR. In addition is the peak power of the S-band 175 times larger than of the 4 kW LAWR. It is therefore not surprising that the LAWR does not observe light rain as good as the S-band. In case of convective events where the LAWR beam is filled there is no issue of underestimation as in the situation with light rain only partly filling the beam in the vertical direction. It should be noted that the LAWR only observe falling rain drops. Due to the TX delay offset it is unfortunately not possible to use the St-Anne-de-Bellevue gauge because it is located only 0.6 km from the radar and is therefore in the offset range.

A very initial estimation of the lowest detectable rainfall intensity of the 4 kW LAWR is in the order of 5-7 mm/h. In order to determine this conclusive further study is necessary with a larger data set. The lower limit would probably be different for the standard 25 kW LAWR, but it is at present not established.

4.2 S-band-LAWR calibration

In what follows a LAWR calibration by a radar-LAWR comparison is attempted.

Rainfall of the 19th of October at 22:55 (UTC) is shown as an example of how the precipitation was captured by the two radar systems. Figure 5 is the 1.3 km CAPPI from the McGill S-band radar over the area covered by the LAWR. The data is based on 5 minutes scanning in 24 different elevations. On Figure 6 the LAWR measurements of the same 5 minutes are shown. The values are the raw reflectivity's (0-255) and sampled with use of standard attenuation, en route and volume correction algorithms with standard parameters. Since the calibration is a factor and the data is linear it is just a scaling of the data.

It becomes evident that in the LAWR samples the high intensities very well and captures the pattern and extension of these even at ranges further than 20 km. Furthermore it is possible to see the movements and evolving of these due to the one minute image frequency of the LAWR, whereas the S-band is an average of the past 5 minutes.

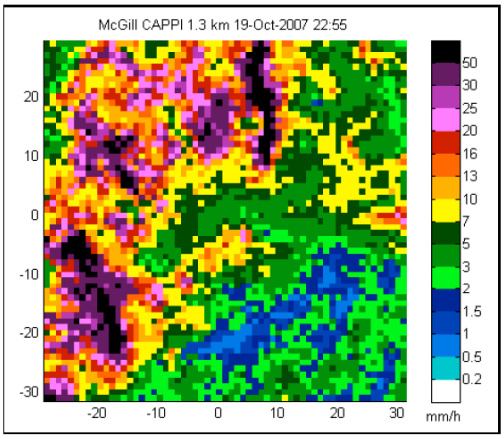

Figure 5 Intensities in mm/h based on the 1.3 km CAPPI from the McGill S-band radar at 22:55 the 19th of October 2007. The image is a 30x30 km sub image with the radar in the centre.

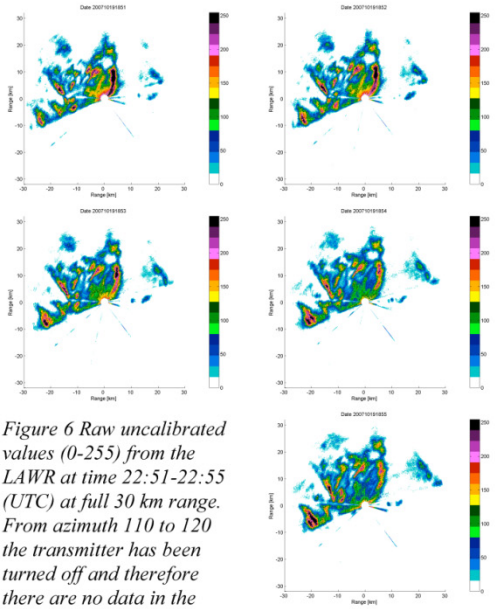

Figure 6 Raw uncalibrated values (0-255) from the LAWR at time 22:51-22:55 (UTC) at full 30 km range. From azimuth 110 to 120 the transmitter has been turned off and therefore there are no data in the major part of the bottom half of the images.

The lower intensities are not equally well captured due to the beam filling issues discussed in Section 4.1. From azimuth 110 to 120 the transmitter was turned off during this event and there are therefore no data in the major part of the bottom half of the images in Figure 6.

A subarea of 2x2 km has been selected for the radar-LAWR calibration 5 km from the radar centered in azimuth 315. For both systems the values has been averaged for this area and the 5 minute S-band data has been linear interpolated into 1 minute values.

The two time series representing the mean value of the area has been used to estimate a calibration factor for converting LAWR reflectivity's into intensities in mm/h by optimizing the RMSE of the fit between the two curves. The calibration factor is estimated to be 0.085 for this specific event. The result can be seen Figure 7.

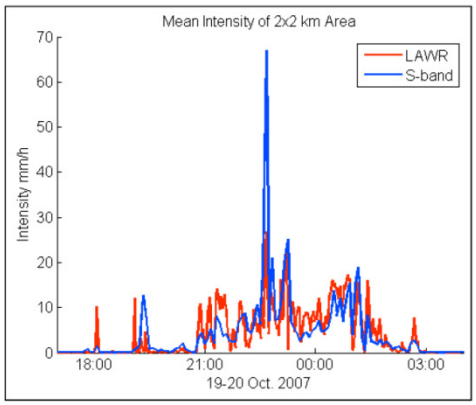

Figure 7 Mean intensity of the selected 2x2 km area as function of time with use of the estimated calibration factor of 0.085 for converting LAWR reflectivity's into mm/h.

The calibration factor is only valid for rain of this type and as mentioned previously the dataset available is too small to estimate a robust calibration factor, but it would have been possible if the number of intense rain events has been significantly larger. The next step is to do this for varying area sizes and different places in the image in order to establish if there are any intensity or range decencies.

5. Attenuation

The LAWR is an X-band radar and therefore affected by attenuation. The attenuation algorithm used by the LAWR is:

$$Z_r = Z_{g,r}\left(1 + \frac{\alpha \sum_{r=0}^{r-1} Z_{r-1}}{C_1}\right)\frac{1}{C_2 e^{rC_3}} \qquad \text{eq. 2}$$

Zr: Adjusted reflectivity value
$Z_{g,r}$: Measured value at range
α, C_1, C_2, C_3: Parameters

The LAWR used here has been operating with the standard parameter set used for the 25 kW LAWR since the experience of using the smaller type for QPE still is very limited.

The data used for this is the polar data from the LAWR consisting of 450 scan lines based on the average of 24 rounds pr. minute with a radial resolution of 60 m. The dataset is quite vast. For every 5 minutes there are 1.5552·106 (24·360·180) data points from the S-band and from the LAWR there are $1.1225 \cdot 10^6$ (450·500·5) data points – a total of $2.68 \cdot 10^6$ values every 5 minutes. To complicate matter further and this is probably the largest source of potential errors is the timing issue since the two radars operate with very different scanning strategies. It therefore becomes very challenging to find the right data points to compare in the attenuation analysis.

An example of the huge dataset is given in Figure 8 where data from the two systems are shown together. One of the issues in this analysis is the different format of the data. In this very first attempt the DVIP levels from the S-band radar

and the raw values from the LAWR are used for a single azimuth. Azimuth 315 has been chosen arbitrary for the illustration of this in Figure 8. The S-band DVIP values are reflectivity measurements collected at 8-bit intensity (0 to 255). The output from the LAWR was original designed to match the output from the radars (Ericsson) operated by the Danish Meteorological Institute and therefore is the raw output reflectivity values between 0 and 255.

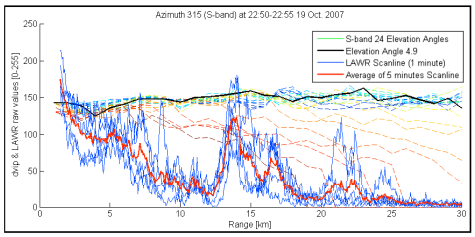

Figure 8 DVIP levels and raw LAWR values in azimuth 315 as function of range. S-band values for the 24 elevation angles (dashed curves in figure). The elevation at 4.9 degrees is app. in the centre of the LAWR beam and highlighted in bold black. The 5 scanlines from the LAWR in the same time is shown in blue and the average of these in red.

There is quite large variation in the radial direction in a single azimuth in both altitude (S-band) and time (LAWR). The second peak on the LAWR data at range 15 km shows that the signal is able to penetrate high intense rainfall without being absorbed. Furthermore is it possible to capture the decreasing and increasing intensities afterwards. The pattern can be seen on Figure 5 if the upper left quadrant is studied.

It should be noted that no attempt was made to calibrate the attenuation parameters for this LAWR installation.

The work of analyzing the effect of this method to handle attenuation is still only in its initial phase, but the opportunity of having data from S-band X-band at the same events gives some very unique possibilities that still have to be explored further. The problem with aligning the data in time is still not solved satisfactory and is ongoing. These first results are though encouraging and hopefully future work will reveal more.

6. Conclusion

The purpose of this field experiment was to gain more knowledge of using small scale LAWR's as supplement to traditional rain gauges and weather radars. The experiment used a relatively untested type of LAWR, primarily due to financial issues, but also to test if this type could be used for very small scale operations such as a farm or a small city. The physical setup and operation went as expected with some minor problems that were solved on the way and the data collection went well. Unfortunately, insufficient data did not allow a normal gauge-LAWR calibration, but the radar-LAWR calibration appears to work satisfactory. The uncertainties related with this type of calibration will need to be addressed in order to give a more robust estimate of the accuracy of the LAWR data.

The attenuation analysis has proven to be very challenging due to timing issues and data quantity and the work is still ongoing. Therefore it is not possible to give any conclusions on the performance of the LAWR's attenuation handling.

A LAWR is not and never will be a substitute for a C or S-band radar for metrological purposes, but as supplement to gauges or in a un-gauged catchments with requirement for high resolution rainfall measurements in real time it can add valuable information.

The LAWR underestimates light precipitation but in connection with floods of both rural and urban catchments it is not the light precipitation that is of concern but the slow moving convective cells that can dump huge water amounts very locally in short time that are important to capture correctly. For such thing at closer ranges (<20 km) the LAWR is providing useful results with a resolution as high as 100x100 meter every single minute.

Acknowledgment

The field experiment was part of a PhD student visit and would not have been possible without the enormous goodwill and help from the radar group at McGill University. In particular the author would like to thank Alamelu Kilambi, Aldo Bellon and Marc Berenguer for their help, guidance and encouragement.

References

Jensen, N. E., Pedersen, L., (2005), "Spatial Variability of Rainfall. Variations Within a Single Radar Pixel", Atmospheric Research 77, 269-277

Pedersen, L., Jensen. N. E .and Madsen, H. 2008, Estimation of radar calibration uncertainties related to the spatial variability of rainfall within a single radar pixel - Statistical analysis of rainfall data from a dense network of rain gauges, Accepted for presentation at: World Environmental & Water Resources Congress 2008, Hawaii

Rinehart, R. E., 2004, Radar for Meteorologist (4th Edition), Rinehart Publications

PAPER H

Network Architecture for Small X-band Weather Radars – Test Bed for Automatic Inter-Calibration and Nowcasting

---

Conference Proceedings: *The 33rd Conference on Radar Meteorology*, 6 – 10 August 2007, Cairns, Australia. (Oral Presentation)

12B.2

NETWORK ARCHITECTURE FOR SMALL X-BAND WEATHER RADARS – TEST BED FOR AUTOMATIC INTER-CALIBRATION AND NOWCASTING

Lisbeth Pedersen*[(1+2)], Niels Einar Jensen[(1)] and Henrik Madsen[(2)]
[(1)]DHI Water · Environment · Health, Aarhus, Denmark
[(2)]Technical University of Denmark, Copenhagen, Denmark

1. ABSTRACT

In recent years the use of small inexpensive X-band radars for meteorological and hydrological purposes has increased significantly.

Compared to the traditional C-band and S-band radars the X-band weather radar has the advantage of high temporal and spatial resolution and low financial cost; however, the trade off is attenuation due to X-band technology and short range due to the higher spatial resolution.

In relation to quantitative precipitation estimation (QPE) and forecasting (QPF) it is necessary to address the attenuation issue. Over the next two years a test bed with five X-band radars of the type Local Area Weather Radar (LAWR) will be set up south of Aarhus in Denmark. The three radars will be placed so that they overlook the same area and thereby are capable of intercepting a precipitation event from different angles, altitudes and ranges.

The overall aim is to construct a network of small X-band radars which are capable of automatic inter-calibrating and inter-correcting for attenuation on the fly by online communication. From the beginning the LAWR has been equipped with a set of attenuation corrections algorithms. However, verification of these algorithms has not been possible so far, due to lack of multi radar measurements of rainfall events. The prospects of verifying and possibly improving the method used for correction of attenuation using radar networks are promising.

The results from the test bed are expected to optimize attenuation handling and improve nowcasting capabilities.

2. INTRODUCTION

Rainfall measurements today are conducted with a variety of measuring equipment, the most common type still being rain gauges. They provide point measurement in contrast to weather radars which provide spatial distributed measurements. The two methods offer both advantages and disadvantages, however, the general opinion today is that they are both required in order to obtain reliable quantitative precipitation estimates (QPE). The predominant types of weather radars are based on either S or C-band technology, both of which facilitate long range measurements. However, due to the curvature of the earth the radar beam from these radars is often overshooting near surface phenomena at far ranges.

Lately, the focus has been drawn toward an approach of using a number of smaller radars instead and thereby overcoming these problems.

At present seven out of eight planned LAWRs are installed in Denmark – five LAWRs and three City LAWRs as illustrated in Figure 1. In addition four C-band radars are operated by the Danish Meteorological Institute, Gill et al. (2006).

Today, most LAWRs are operated individually, however, the process of generating a composite has begun, although it is complicated by the fact that they are owned and operated by different organizations with multiple interests.

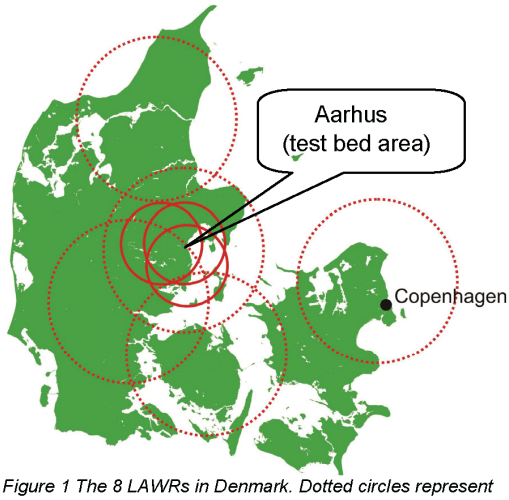

Figure 1 The 8 LAWRs in Denmark. Dotted circles represent LAWRs, while full circles represent City-LAWRs. It is one of the City-LAWRs that still remains to go up.

12B.2

When comparing X-band weather radars to the more traditional C- and S-band weather radars usually two limiting features are pointed out. First of all the X-band radars have a shorter range and they are more sensitive to attenuation caused by rain. The positive features are the high spatial and temporal resolution of this radar type along with the much smaller physical size. The last feature makes it much easier to find a suitable installation location. Furthermore, the X-band technology used in the test bed described here is very cost-efficient compared to traditional weather radars.

The short range problem can be solved by constructing a network of a number of X-band radars. As a result of the lower financial cost it makes sense to have a number of X-band radars in a network to cover the area spanned by a single S- or C-band radar.

The idea is to have several radars overlooking the same area and thereby observing a given event from different angles and ranges. The test bed layout provides opportunity to test and verify attenuation algorithms. The QPE and QPF based on different radars should coincide if the attenuation correction is done correctly.

2.1 Future advantages of LAWR network

Most of the more than 20 LAWRs installed today operate as individual installations providing QPE and QPF for their individual coverage area.

Many of the installed LAWRs are equipped with automatic forecast facility, Jensen and Pedersen (2005b). The forecast lead time is normally in the order of one hour. One of the great benefits from developing a network structure is for the users who get a larger coverage area and longer forecast lead time. The data quality will improve since rainfall at the outer range of one radar may be closer to another one in the network and thereby better.

By combining many radars into one network and thereby obtain a composite it will be possible to cascade the information obtained by one radar in the network to the others, and in this way the calibration and attenuation correction factors or parameters can be applied on the basis of actual measurements and not just on the basis of a set of standard values.

2.2 Test bed radars

The radars used in this specific test bed are of the type Local Area Weather Radars (LAWR). A LAWR is an X-band weather radar based on a standard Furuno marine radar. Signal handling is performed by a specially designed AD converter while the data processing and communication are performed by two standard PCs.

There are two variants of the LAWR – the standard LAWR is based on a 25 kW radar, whereas the smaller version named the City-LAWR is based on a 4 kW radar.

Examples of the two LAWR types can be found on Figure 2. Both LAWR types are included in the test bed.

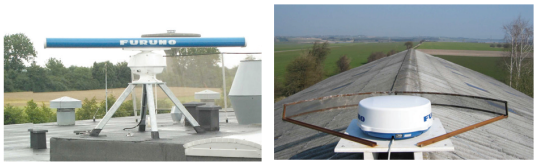

Figure 2 Example of LAWR installations. The LAWR on the left is a standard LAWR. The one on the right is a City-LAWR. Besides the antenna unit on the image there is a small cabinet with two PC's and the radar control unit.

The radars are calibrated on the basis on rain gauge data using the sum calibration method described in Pedersen (2004). The calibration can be performed either manually or set up to be automatical. The latter requires an internet connection to the radar as well as the gauge.

The technical details on both types of LAWRs are listed in Table 1.

12B.2

	LAWR	City-LAWR
Output power	25 kW	4 kW
Frequency	9410 ± 30 MHz	9410 ± 30 MHz
Image Frequency	5 or 1 minute	5 or 1 minute
Slotted Wave Guide Antenna	2.44 m	0.54 m
Horizontal beam width	0.95°	3.9°
Vertical beam width	±10°	±10°
Rotation speed	24 rpm	24 rpm
Pulse length	0.07-1.2 μs	0.08-0.8 μs
Number of vertical scans	1	1
Grid resolution (pixel size). All resolutions can be used simultaneously. The range in brackets is the maximum range.	500x500 *(60 km range)* 250x250 *(30 km range)* 300x300 *(15 km range)* 100x100 *(15 km range)*	250x250 *(30 km range)* 125x125 *(15 km range)* 150x150 *(7.5 km range)* 50x50 *(7.5 km range)*
Range for QPE	20-30 km	10-15 km
Range for forecast	60 km	30 km

Table 1 Technical specifications of the two LAWR types included in the test bed.

3. NETWORK ARCHITECTURE

The concept of a network of X-band radars is gaining a lot of interest these years, and in 2006 CASA presented their DCAS network (Distributed Collaborative Adaptive Sensing), Brotzge et al (2006) and McLaughlin et al (2006). Donnovan et al (2006) describes a variant of the DCAS network namely the Off-The-Grid radar network (OTG) which in its basic idea is identical, but operates at smaller ranges and is independent of external power supply. The latter is based on a Raymarine radar.

The most fundamental difference of LAWR network compared to the DCAS network is that the LAWR network is not aiming at distributing the calculation load in the network and it will depend on an external power supply which in this case is the ordinary power grid.

The key feature to be facilitated by the LAWR network is online inter-calibration and automatic attenuation correction of multiple radars in a network with overlapping coverage. At present the communication is handled by wired internet, however, part of the research will be directed towards wireless inter communication between the nodes. One option being considered is the use of radio modems, due to the low data rate required.

The layout for the network between the radars is illustrated in Figure 3. The present version of the test bed only consists of the network in Figure 3 which only is only a subpart of the full future network as shown on Figure 4.

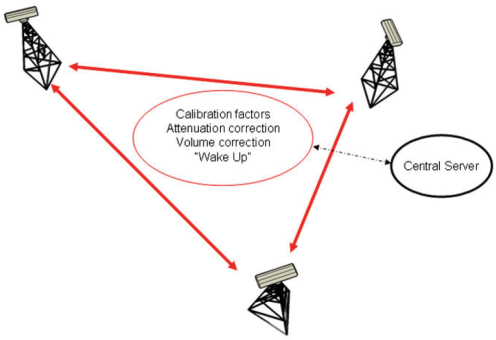

Figure 3 Network architecture.

Today each radar handles sensing, data storage and server facility. In the future the plan is to include a central server handling the composite image generation along with a range of other tasks including central data storage (backup) and interface between the users and the data. Furthermore, the idea is to facilitate other data sources, e.g. rain gauge data for calibration.

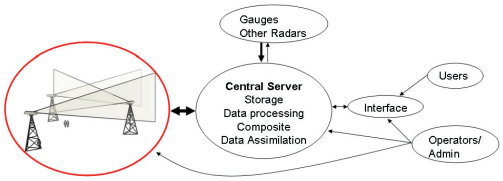

Figure 4 General LAWR network layout.

This work focuses on the layout of the LAWR network, marked with a red circle in Figure 4, in relation to installation of radars in the test bed.

3.1 Identification of key parameters in test bed layout

First step is to determine the key parameters to take into consideration. In this test bed the initial bounds are defined. First of all the radar technology is X-band and the radars used is of the

12B.2

type LAWR. Secondly, the aim is to use customary communication solutions in order to keep the network cost-efficient.

The test bed network architecture has been designed by taking the following factors into account in order of priority:

- Physical geographical features
- Power availability
- Distance requirements
- Existing radar and gauge installations
- Communication technology
- Bandwidth of communication channels
- Data formats.

The first four points all regard the location of the installation, while the latter three regard the communication. The focus of this paper is on the first four points, due to the current stage of the project. The wireless communication part of the network is still in the design phase and the first test bed will therefore be using wired communication.

Physical geographical features

One geographical feature to be concerned about in relation to the radar test bed was to find an area without interference from beam blockage. Fortunately, Denmark is a very flat country, so the issue of beam blockage is minor. The main issues in relation to geography have been to avoid areas massively affected by ground or sea clutter. This has been facilitated by choosing an area which has been covered by LAWR radars for almost 10 years and thus is well described in manner of clutter.

The location has also been selected so that the radars are relatively close to the office to facilitate regular inspections.

Power availability

Continuously scanning radars as the LAWR are quite power consuming and it has been opt out to make an off-the-grid solution for now. The locations chosen all have grid power.

Distance requirements

The characteristics of the three City-LAWRs can be found in Table 1, where it can be seen that especially the horizontal opening is large (3.9 degrees). This results in an increasing beam width distance as shown in Figure 5.

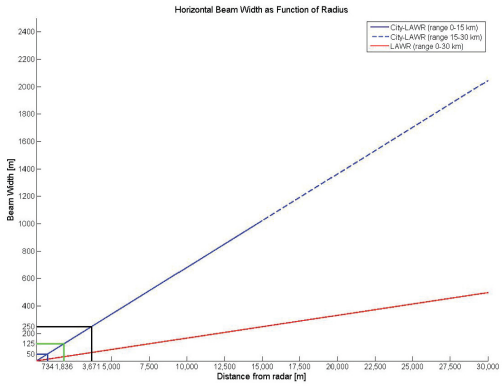

Figure 5 Beam width of City-LAWR and LAWR as function of radius. The radius at the pixel sizes given in Table 1 is marked.(blue=50 m, green=125 m and black=250 m).

The ranges where the beam width exceeds the given pixel width are illustrated. The consequences are only at very short distances the QPE/QPF in a pixel the average of a single pixel. At distances further away the QPE/QPF are based on weighed averages of pixels.

Part of this test bed setup is to evaluate the performance of both LAWR types. This is done by comparing the QPE to that found on the basis of a very dense network of rain gauges and the official rain gauge sites operated by the Danish Meteorological Institute in the area. The rain gauge setup is described later on in this section.

Vertically, the openings of the City-LAWR and the LAWR are identical. Only the upper part of the beam is used since the lower part is either cut off by the surroundings or a clutter fence. The vertical beam height reaches quite far, cf. Figure 6.

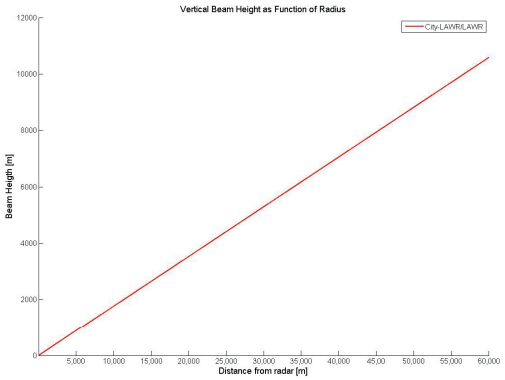

Figure 6 Vertical Beam Height based on the positive part of the vertical opening angle.

12B.2

At 60 km (maximum range) from the LAWR the top of the beam is reaching just above 10 km up in the atmosphere and the City-LAWR is reaching just above 5 km (shorter range). In relation to QPE and QPF this can be a problem due to the altitudes of different types of rain. The majority of cloud types causing rainfall such as the stratiform type are occurring in the lower part of the atmosphere usually below 2-3 km. A cumulonimbus cloud can fill the full vertical volume even at 60 km range.

This issue of different degrees of partially beam filling creates some challenges in order to obtain solid QPE/QPF. The setup of the test bed has been designed to facilitate further investigations of these issues.

By placing the radars relatively close together, but with varying distances between them, it becomes possible to have simultaneous radar measurements of the same rain event at different altitudes and on the basis of different degrees of beam filling. The overall idea of this problem is illustrated on Figure 7.

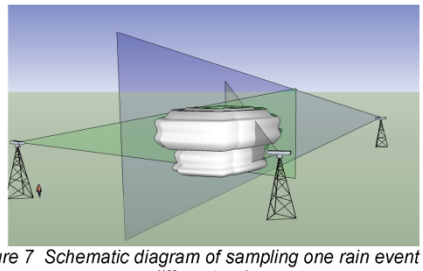

Figure 7 Schematic diagram of sampling one rain event from different radars.

Existing radar and gauge installations

As illustrated in Figure 1 there already exist 5 LAWR installations in Denmark, and it would be preferable to utilize as many of these as possible in the test bed layout.

In addition to the test bed of radar network a field campaign with nine rain gauges takes place within the same frame work. The field campaign is a reproduction of the one described by Jensen and Pedersen (2005a) and takes place 25 km south of Aarhus near the village of Rude. The field experiment aims at determining the spatial variability within one LAWR pixel of 500x500 meter based on nine tipping bucket gauges set up under identical conditions (no shelter effects and same elevation).

4. TEST BED PRESENTATION

Figure 9 contains a map of Denmark with the area of interest marked with red. If compared to the map in Figure 1 it can be seen that this area is the most LAWR covered area.

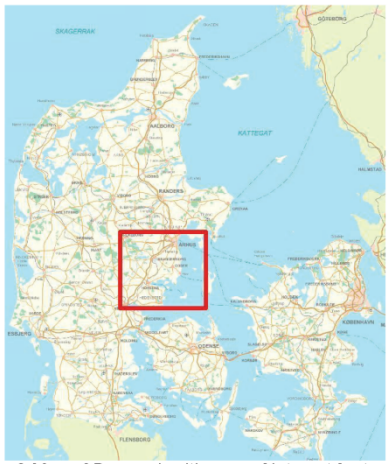

Figure 8 Map of Denmark with area of interest for test bed marked with red.

The field experiment with rain gauges also takes place within this area. A close up is shown on Figure 9 with the four radars already installed. The Vejle LAWR (red) and the Aarhus LAWR (green) are both permanent installations. The opportunity to use these as additional radars in the test bed has been one of the main reasons for choosing this specific area.

Figure 9 Overview of test bed area

12B.2

So far 2 of the 3 planned City-LAWRs have been set up – the location of the last one (Mårslet) has been determined, however, the final approval from the owners of the location has not yet been given. The Aarhus LAWR and the Aarhus City-LAWR are placed on the same location and thereby provide excellent opportunities for comparing the result of the different radar types.

The distances between the radars will then be 4 km, 8.5 km and 11.5 km as illustrated in Figure 10. Furthermore, the location of the rain gauge field experiment is shown. The distance from the Rude City-LAWR to the rain gauges is ranging from 600 to 1100 meters.

Figure 10 The distances between the three City-LAWRs in the testbed.

The Rude City-LAWR is installed on a barn rooftop on a simple wooden structure. The PCs are placed inside. The setup can be seen in Figure 11, where the field in the background is the location for the before-mentioned field experiment with nine rain gauges.

Figure 11 Rude City-LAWR. The rain gauge experiment take place in the field in the background.

5. CONCLUSIONS AND FUTURE WORK

The Rude and the Aarhus City-LAWR started operation early April 2007. The Aarhus City-LAWR is now being considered moved due to problems with blocking trees. At the time of installation the trees had no leaves, but after they have set leaves there seems to be some blocking issues. So either the radar is to be moved or the threes in front to be pollarded. Which step to be taken is still to be decided.

After these first months of operation it has become clear that it is very important to have a stable communication to the radars in order to monitor experiments closely. Another issue that was known, but which is still causing some challenges is the extreme amount of data to be handled. To illustrate this, the number of pixels within a 2x2 km area of the test bed is listed in Table 2.

	City-LAWR resolutions			LAWR resolutions			
	50 m	125	250	100	250	500	Sum
Aarhus LAWR	-	-	-	400	64	16	480
Vejle LAWR	-	-	-	-	-	16	16
Aarhus City-LAWR	1600	256	64	-		-	1920
Rude City-LAWR	1600	256	64	-		-	1920
Mårslet City-LAWR	1600	256	64	-		-	1920
Total no. of pixels							**6256**

Table 2 Number of pixels within a 2x2 km area within the test bed area per 5 minutes.

For a small sub area of 2x2 km there are 6256 individual pixel values to compare and inter relate per time sample.

The next step in the process is calibration of the radars and establishing the optimum way of handling the attenuation. Concurrent to this the plan is to develop the communication algorithms enabling the radars to exchange information.

6. REFERENCES

Brotzge, J., K.K. Droegemeier, and D.J. McLaughlin, 2006: Collaborative Adaptive Sensing of the Atmosphere (CASA): New radar system for improving analysis and forecasting of surface weather conditions. J. Transport. Res. Board, No. 1948, 145-151.

Donovan, B., A. Hopf, J. M. Trabal, B. J. Roberts, D. J. McLaughlin, J. Kurose, (2006), Off-the-grid radar networks for quantitative precipitation estimation, Proceedings of European Radar Conference 2006, Barcelona, Spain.

Gill, Rashpal S., Søren Overgaard and Thomas Bøvith, 2006, The Danish weather radar network, Proceedings of European Radar Conference 2006, Barcelona, Spain.

Jensen, N. E., L. Pedersen (2005a), Spatial Variability of Rainfall. Variations Within a Single Radar Pixel ,Atmospheric Research 77 (2005) pp. 269-277

Jensen, N. E. and L. Pedersen (2005b) Automated short term forecast from LAWR x-band radar systems. Results from the first three months of operation, World Weather Research Program Symposium on Nowcasting and very short range forecasting (WSN05), 5-9 September 2005, Toulouse, France.

McLaughlin, D., J. Brotzge, V. Chandresakar, K. Droegemeier, J. Kurose, B. Philips, M. Preston, and S. Sekelsky, 2004: Distributed Collaborative Adaptive Sensing for Hazardous Weather Detection, Tracking, and Predicting. Preprints, International Conference on Computational Science 2004, Krakow, Poland.

Pedersen, L. (2004) Scaling Properties of Precipitation - experimental study using weather radar and rain gauges, M. Sc. Thesis from Aalborg University, Department of Civil Engineering (can be downloaded from http://radar.dhigroup.com)